Universidade de Aveiro
2022

Daniel Blanco-Ward

A EXPOSIÇÃO DAS VINHAS MEDITERRÂNEAS AO OZONO TROPOSFÉRICO: UMA ABORDAGEM DE MODELAÇÃO

EXPOSURE OF MEDITERRANEAN VINEYARDS TO TROPOSPHERIC OZONE: A MODELLING APPROACH

Universidade de Aveiro
2022

Daniel Blanco-Ward

A EXPOSIÇÃO DAS VINHAS MEDITERRÂNEAS AO OZONO TROPOSFÉRICO: UMA ABORDAGEM DE MODELAÇÃO

EXPOSURE OF MEDITERRANEAN VINEYARDS TO TROPOSPHERIC OZONE: A MODELLING APPROACH

Tese apresentada à Universidade de Aveiro para cumprimento dos requisitos necessários à obtenção do grau de Doutor em Ciências e Engenharia do Ambiente, realizada sob a orientação científica da Doutora Ana Isabel Miranda, Professora Catedrática do Departamento de Ambiente e Ordenamento da Universidade de Aveiro, e coorientação científica da Doutora Elena Paoletti, Diretora de Pesquisa do Instituto de Pesquisa em Ecossistemas Terrestres – Centro de Pesquisa Nacional (IRET-CNR) em Florença na Itália.

Agradece-se o apoio financeiro ao CESAM por parte do FCT/MCTES (UIDP/50017/2020+UIDB/50017/ 2020+608 LA/P/0094/2020), através de fundos nacionais. Agradece-se também ao projeto DOUROZONE (PTDC/AAG-MAA/3335/2014; POCI-01-0145-FEDER-016778) pelo apoio financeiro através do Projeto 3599 – Promoção da Produção Científica e do Desenvolvimento Tecnológico e Redes Temáticas (3599-PPCDT) – e através do FEDER

Apoio Financeiro da Fundação para a Ciência e Tecnologia (FCT) e do Fundo Social Europeu (FSE) no âmbito do III Quadro Comunitário de Apoio pela Bolsa de Doutoramento com ref.ª SFRH/BD/139193/2018

To family and friends, both present and absent and both in prosperity and in difficulty, who have always relied on the value and guidance of contrasted study and objective reflection along these years so that men can lead a life of good.

o júri

Presidente

Doutor Delfim Fernando Marado Torres
Professor Catedrático, Universidade de Aveiro

Doutora Ana Isabel Couto Neto da Silva Miranda (orientadora)
Professora Catedrática, Universidade de Aveiro

Doutor António Castro Ribeiro
Professor Coordenador, Instituto Politécnico de Bragança

Doutora Myriam Alexandra dos Santos Batalha Dias Nunes Lopes
Professora Associada, Universidade de Aveiro

Doutor Nelson Augusto Cruz de Azevedo Barros
Professor Associado, Universidade Fernando Pessoa

Doutora Cristina da Conceição Ribeiro Carlos
Professora Auxiliar, Universidade de Trás- os-Montes e Alto Douro

Acknowledgement

First, I would like to thank Professor Ana Isabel Miranda from the Department of Environment and Planning of the University of Aveiro, Portugal, for her good academic guidance in supervising this work and the doctoral studies. During these years she has been for me an example of perseverance at work and good academic orientation, which has been a fundamental pillar for carrying out this work.

Likewise, I would like to thank Professor Elena Paoletti from the Institute for Research on Terrestrial Ecosystems of the Institute of the National Research Center at Florence (Italy), for her perseverance and scientific co-orientation, always seeking objective methods contrasted with the latest references in the field of research.

To the entire team of the Mountain Research Center of the Polytechnic Institute of Bragança (IPB) and, especially, to Professors António Castro Ribeiro and Manuel Feliciano, together with the doctoral candidate, David Barreales, for their help and good willingness to share the data from the field campaign associated with the DOUROZONE project, and their guidance regarding various agronomical aspects, such as the phenology and physiology of the grapevine in the Douro Demarcated Region, besides their collaboration in supervising the resulting co-authored works.

To the support of Professor Alfredo Rocha and Dr. Carolina Viceto, from the Department of Physics of the University of Aveiro, for sharing the climate simulations of the WRF model for the Douro Demarcated Region, and also for contributing to the orientation and supervision of aspects related to those GCM-RCM simulations along the resulting works in co-authorship.

To the Department of Environment and Planning of the University of Aveiro, for giving me the opportunity to start working during the first year and a half on the research subject of this doctoral thesis as a research assistant in the DOUROZONE project, especially to Professors Myriam Lopes and Carlos Borrego. Likewise, to all those who accompanied me in that first time, seeking a multidisciplinary experience: the group of emissions, modeling and climatic change (GEMAC) of the University of Aveiro, the professors, colleagues and University of Aveiro staff who accompanied me along the doctoral courses, and also professors João Verdial and João Castro from IPB and all the technical staff involved in the DOUROZONE field campaign from the Associação para o Desenvolvimento da Viticultura Duriense (ADVID), SOGRAPE VINHOS S.A. and Adriano Ramos Pinto Vinhos S.A..

Last but not least, to family and friends, both present and absent and both in prosperity and in difficulty, who have always relied on the value and guidance of contrasted study and objective reflection along these years so that men can lead a life of good.

palavras-chave

Ozono ambiental; Fitotoxicidade; Vinhas; Alterações climáticas; Condições mediterrâneas; Modelação numérica; Campanha de medição; Validação

Resumo

O principal objectivo desta Tese consiste no desenvolvimento e validação de um sistema de modelação capaz de simular em detalhe a exposição e a absorção do ozono (O_3) ambiental pelas vinhas em ambientes mediterrânicos. Visa também contribuir para o estado da arte sobre a influência do clima na viticultura no contexto das alterações climáticas. A área de estudo seleccionada foi a Região Demarcada do Douro (DDR), em Portugal. A avaliação do impacto potencial das alterações climáticas baseou-se no refinamento da resolução das simulações globais de ERA-Interim e MPI-ESM-LR, forçadas com um cenário de emissão de GEE RCP8.5 para períodos recentes (1986-2005) e futuros (2046-2065, 2081-2100), recorrendo ao modelo WRF. Para a avaliação do risco fitotóxico devido ao ozono, foi efetuada uma validação de uma simulação do sistema WRF-CHIMERE. Esta simulação abrangeu um período de crescimento para as vinhas entre Abril e Setembro de 2017. No mesmo período, foi realizada uma campanha experimental, incluindo medições do ozono ambiente, fenologia, troca de gases foliares e relações de água, ao longo de vinhas representativas da área de estudo. A campanha indicou que o limiar de fitotoxicidade para O_3 ambiental (40 ppb) foi atingido em todas as fases de desenvolvimento das vinhas, incluindo um período sensível como a floração. Em relação aos padrões de exposição ambiental ao O_3, o indicador AOT40 entre Maio-Junho, 8 ppm-h, excedeu o objetivo a longo prazo para a proteção da vegetação, 3 ppm-h, e aproximou-se do estabelecido como norma geral anual pelas Diretivas Europeias 2002/03 e 2008/50, 9 ppm-h. As simulações de ozono ambiente, validadas pelo sistema WRF-CHIMERE, também indicaram que os limiares específicos para as vinhas, para AOT40 entre Junho-Setembro, podiam ser excedidos, principalmente na sub-região mais seca e quente mais oriental da DDR, o Douro Superior. Por outro lado, o padrão baseado na dose de ozono fitotóxico introduzida na planta, POD, indicou também risco de fitotoxicidade, principalmente nas sub-regiões ocidentais da DDR, o Baixo Corgo e o Cima Corgo. O risco indicado pelo POD teve uma menor extensão quando ajustado ao comportamento fisiológico das castas de videira locais, sobretudo devido à inclusão do efeito de stress hídrico das plantas em toda a região. Os resultados das simulações climáticas WRF-ERA para o período recente revelaram também uma relação coerente com o rendimento e qualidade da vinha na DDR em clima presente. Os cenários climáticos de médio e longo prazo do WRF-MPI indicaram uma tendência para condições mais quentes e secas, que propiciarão valores de produção e de qualidade inferiores aos recomendados. Conclusões importantes deste trabalho são a relevância de incluir parametrizações fenológicas e fisiológicas das castas de videira locais para refinar as normas relacionadas com o risco fitotóxico do ozono e as alterações climáticas. Uma limitação atual é a falta de relações exposição ou dose-efeito válidas para o O_3 e as vinhas.

keywords

Ambient ozone; Phytotoxicity; Grapevine; Climate change; Mediterranean conditions; Numerical modeling; Measurement campaign; Validation

abstract

The main objective of this Thesis is to develop and evaluate a modeling system capable of simulating in detail the exposure and uptake of ambient ozone (O_3) by vineyards in Mediterranean environments. It also aims to contribute to the state of the art on the influence of climate in viticulture in the context of climate change. The selected study area was the Douro Demarcated Region (DDR) in Portugal. The assessment on climate change potential impact was based on WRF downscaled ERA-Interim and MPI-ESM-LR global simulations forced with a RCP8.5 GHG emission scenario, for recent-past (1986–2005) and future periods (2046–2065, 2081–2100). For the evaluation of phytotoxic risk due to ozone, a validation of a simulation with the WRF-CHIMERE system was carried out. This simulation covered a grapevine growing season from April to September 2017. In the same period, a field campaign was carried out, including measurements of ambient ozone, phenology, and leaf gas-exchange and water relations for the grapevine along representative vineyards of the study area. The field campaign indicated that the phytotoxicity threshold for ambient O_3 (40 ppb) was reached in all stages of grapevine development, including a sensitive period such as flowering. Regarding ambient O_3 exposure standards, the measured May-Jun AOT40, 8 ppm-h, exceeded the long-term objective for the protection of vegetation, 3 ppm-h, and was close to that established as a general annual standard by the 2002/03 and 2008/50 European Directives, 9 ppm-h. The validated ambient ozone simulations by the WRF-CHIMERE system also indicated that grapevine-specific thresholds for Jun-Sep AOT40 could be exceeded, mainly in the drier, warmer Douro Superior eastern subregion. On the other hand, the standard based on the phytotoxic ozone dose introduced into the plant, POD, also indicated risk of phytotoxicity, this time mostly located in the Baixo and Cima Corgo western DDR subregions. The POD risk had a lesser extension when adjusted to the physiological behavior of local grapevine varieties, mainly due to the inclusion of the plant water stress effect throughout the region. It has also been possible to relate the WRF-ERA recent-past climate simulations with vintage yield and quality in the DDR. The mid-term and long term WRF-MPI climate scenarios revealed shifts to warmer and drier conditions not remaining within the ranges for quality and production. Important conclusions of this work are the relevance of including phenological and physiological parametrizations of local grapevine varieties to refine standards related with ozone phytotoxic risk and climate change. A current limitation is the lack of valid O_3 exposure and dose-effect relationships for the grapevine.

TABLE OF CONTENTS

List of Figures

List of Tables

List of Abbreviations and Symbols

A/ci	Carboxylation efficiency.
A	Net CO_2 assimilation rate.
ABA	Abscisic acid.
ADVID	Associação para o Desenvolvemento da Viticultura Duriense.
AOT40	Accumulated O_3 concentration over a threshold of 40 ppb.
APA	Portuguese Environmental Sate Agency.
b subscript	Budburst to flowering phenological stage.
BBCH	Biologische Bundesanstalt, Bundessortenamt und CHemische Industrie phenological scale.
CDD	Maximum number of continuous dry days (P < 1 mm) per year.
CET	Central European Time.
CI	Cool night index (°C).
ci	Intercellular CO_2 partial pressure.
Clec	Cumulative exposure-based critical level.
Clef	Critical level based on stomatal flux.
CLRTAP	Convention on Long-Range Transboundary Air Pollution.
CMIP5	Coupled Model Intercomparison Project Phase 5.
CORR	Pearson's correlation coefficient.
CSDI	Cold spell duration index or total number of days being part of cool spells longer than 6 consecutive days in duration. A day is considered to belong to a cold spell if *Tmin* is less than the calendar-day *Tmin* 10th percentile centred on a 5-day window for the base period studied.
CSDI-3d	Cold spell index accounting for the total number of days per year with at least 3 continuous days with *Tmin* < 0 °C.
CSDI-6d	Cold spell index accounting for the total number of days per year with at least 6 continuous days with *Tmin* < 0 °C.

CTM	Chemistry Transport Model.
CWD	Maximum number of continuous wet days ($P \geq 1$ mm) per year.
DDR	Douro Demarcated Region.
DEM	Digital elevation model.
DI	Deficit irrigated (chapter 5).
DI	Dryness index (mm).
DO3SE	The deposition of O_3 for stomatal exchange model.
DOY	Day of year.
DPPD	Diphenyl-p-phenylenediamine.
DTR	Daily temperature range or annual mean difference between *Tmax* and *Tmin* (°C).
EC	European Community.
EDU	Ethylenediurea.
EEA	European Environment Agency.
EMEP	European Monitoring and Evaluation Programme.
EPA	Environmental Protection Agency.
ERA-Interim	European Reanalysis-Interim forcing.
ERDF	European Regional Development Fund.
ET_0	Daily reference evapotranspiration (mm).
ETCCDI	Expert Team on Climate Change Detection and Indices.
f subscript	Flowering to véraison phenological stage.
FACE system	Free-Air Controlled Exposure system.
FCT	Portuguese Science and Technology Foundation.
FD0	The number of frost days per year where *Tmin* < 0 °C.
fpaw	Plant available water factor (unitless, ranges from 0 to 1).

Fv/Fm	Photochemical capacity.
gage or *fphen*	Leaf age or phenological factor (unitless, ranges from 0 to 1).
GCM	Global climate model.
GDD	Growing degree days (°C units).
GHG	Greenhouse gas.
glwp	Leaf water potential factor (unitless, ranges from 0 to 1).
gmax	Maximum stomatal conductance (mmol m^{-2} s^{-1}).
GPM	Grape production model.
GSP	Growing-season total precipitation (mm).
GST	Growing-season mean temperature (°C).
gsto or *gs*	Stomatal conductance (mmol m^{-2} s^{-1}).
gswp	Soil water potential factor or plant available water (unitless, ranges from 0 to 1).
gtemp or *ftemp*	Leaf ambient temperature factor (unitless, ranges from 0 to 1).
gvpd or *fvpd*	Leaf vapour pressure deficit factor (unitless, ranges from 0 to 1).
HI	Huglin index (unitless).
ICP	International Cooperative Programme.
ILTER	International Long-Term Ecological Research.
INE	Portuguese Office for National Statistics.
IPCC	Intergovernmental Panel on Climate Change.
IPMA	Portuguese Institute for Sea and Atmosphere
IUFRO	International Union of Forest Research Organisations.
IVDP	Instituto dos Vinhos do Douro e Porto.
KS test	Kolmogorov-Smirnov test.

M12	The daily 12-h (08:00-19:00) average O_3 exposure metric (ppb).
MAE	Mean absolute error.
MAPE	Mean absolute percent error.
MCC	The multicriteria climatic classification system for grape-growing regions worldwide
MDA8	Maximum daily 8-h average O_3 concentrations.
MIA	Modified index of agreement.
MPI-EMS-LR	Max Plank Institute Earth System low-resolution model forcing.
NCLAN	National Crop Loss Assessment Network.
NECD	National Emissions Ceilings Directive.
NI	Non-irrigated
NOx	Nitrogen oxides.
OTC	Open-top-chamber.
P	Daily total precipitation (mm).
PAN	Peroxyacylnitrates.
paw	Plant available water.
PLA	Projected leaf area.
POD	Phytotoxic Ozone Dose (mmol m^{-2}).
PODY	Phytotoxic Ozone Dose above a treshold Y (mmol m^{-2}).
PODYAIM	Vegetation-type specific PODY (mmol m^{-2}).
PODYSPEC	Species or group of species-specific PODY (mmol m^{-2}).
PSII	Photosystem II.
QQ transform	Quantile-quantile transformation.
R10	Number of days with heavy precipitation per year (P > 10 mm).
R20	Number of days with very heavy precipitation per year (P > 20 mm).

Rad	Hourly mean global solar radiation (kJ m^{-2}).
Radmax	Daily maximum global solar radiation (kJ m^{-2}).
RCM	Regional climate model.
RCP	Representative Concentration Pathway.
RH	Hourly mean relative humidity (%).
RHmax	Daily maximum relative humidity (%).
RHmin	Daily minimum relative humidity (%).
RMSE	Root mean square error.
SWHC	Soil water holding capacity
STDE	Standard deviation of the errors.
SU25	Number of summer days per year.
SU35	Number of very hot days per year.
SU35-f	Yearly *SU35* from flowering to véraison (days).
SWC	Soil water content.
Tave	Daily mean temperature as (*Tmax* + *Tmin*)/2 (°C).
TF	Touriga Franca.
$Tmax_{Apr\text{-}May}$	Mean of daily maximum temperatures from April to May (°C).
Tmax	Daily maximum temperature (°C).
Tmax-f	Mean of daily maximum temperatures from the flowering to véraison phenological stage (°C).
Tmean	Hourly mean temperature (°C).
Tmin	Daily minimum temperature (°C).
TN	Touriga Nacional.
TOAR	Tropospheric Ozone Assessment Report.
TR20	The number of tropical nights per year where *Tmin* > 20 °C.

UNECE	The United Nations Economic Commission for Europe.
v subscript	Grape colour change onset to maturity phenological stage.
VOC	Volatile organic compounds.
VPD	Vapour pressure deficit.
W126	The sigmoidal weighted sum of all hourly O_3 values observed during a specified daily and seasonal time window, where each (ppb). hourly O_3 value is given a weigh that increases from zero to one with increasing O_3 value.
Wdmean	Daily mean wind direction (°).
WI	Winkler index (*GDD* or growing degree days, °C units).
WRF	Weather and Research Forecasting model.
Ws	Hourly mean wind speed (m/s).
WSDI	Warm spell index accounting for the total number of days being part of warm spells longer than 6 consecutive days in duration. A day is considered to belong to a warm spell if *Tmax* is greater than the calendar-day *Tmax* 90th percentile centred on a 5-day window for the base period studied.
WSDI-3d	Warm spell index accounting for the total number of days per year with at least 3 continuous days with *Tmax* > 35 °C.
WSDI-6d	Warm spell index accounting for the total number of days per year with at least 6 continuous days with *Tmax* > 35 °C.
Ψd	Predawn leaf water potential.

1 INTRODUCTION

1.1 FRAMEWORK

Tropospheric ozone (O_3) is by far the most important phytotoxic air pollutant worldwide (Krupa et al., 2000; Mills et al., 2018; Sicard et al., 2017; The Royal Society, 2008) causing foliar injury and reduction in growth, yield and quality of many agronomic and horticultural crops (Booker et al., 2009; Cho et al., 2011; Feng et al., 2022; Hayes et al., 2007; Rai and Agrawal, 2012), deciduous trees and conifers (Matyssek and Innes, 1999; Sacchelli et al., 2021; Watanabe et al., 2016), and seminatural and natural vegetation communities (Pfleeger et al., 2010; Volk et al., 2006). Global estimates of reduction in yield due to ozone exposure performed for the year 2000 are in the order of 8.5-14% for soybean, 3.9-15% for wheat and 2.2-5.5% for maize (Avnery et al., 2011a). As the global population is expected to grow from 6 to 9 billion between 2000 and 2050 and O_3-precursors are expected to increase in developing countries with a global impact due to transport between continents, tropospheric ozone could become a threat to global food security of the same order of magnitude as climate change (Fiore et al., 2009; Sicard et al., 2017; The Royal Society, 2008).

Ambient ozone levels in Mediterranean environments have been reported as much higher than in North-Central Europe (Guerreiro et al., 2014; Mills et al., 2018; Sicard et al., 2017). In European Mediterranean regions, in particular, weak levels of anti-cyclonic subsidence, low winds, and strong insulation with development of mesoscale processes and recirculation within air masses are frequent during the summer (Millan et al., 2000). These conditions favour the photochemical production of O_3, and ambient concentrations can be high enough to have phytotoxic effects. Field observations indicate that ozone injury is widespread on numerous crops grown in the Mediterranean region including wheat, maize and grapevine (Fumagalli et al., 2001; Mills et al., 2011a). As the levels of ambient ozone in Southern Europe could increase in association with a greater incidence of warm summers and heat waves under the worst emission trends and climate change scenarios (Fortems-Cheiney et al., 2017; Jacob and Winner, 2009; Katragkou et al., 2011; Lacressonnière et al., 2014; Meleux et al., 2007; Sicard et al., 2020, 2013), there is a need for consistent methods for risk assessment for these areas. A good number of studies have already addressed the possible impacts of different climate change scenarios on the suitability of different areas

to grow vineyards (Fraga et al., 2016; Malheiro et al., 2010; Santillán et al., 2019; van Leeuwen and Darriet, 2016). These studies also warn about the need to adapt to increased dryness for some areas whereas some other regions could benefit from gaining grape quality potential.

The United Nations Economic Commission for Europe (UNECE) Convention on Long-Range Transboundary Air Pollution (CLRTAP) has extensively used the accumulated ozone concentration over a threshold of 40 ppb parameter (*AOT40*) to support decision making on pollution abatement policies for ecosystems protection. However, this cumulative exposure approach has been extensively criticized, as it does not relate with the actual dose or flux of ozone entering the plant. To overcome this limitation, a flux-based approach was developed. This approach has a stronger biological basis as it estimates a Phytotoxic Ozone Dose (*POD*) or ozone stomatal uptake as a function of ambient ozone concentration and several other critical environmental parameters such as temperature, water vapour pressure, light, soil water content and plant growth (Emberson et al., 2000a; Massman, 2004; Musselman et al., 2006). The flux-based approach provides extremely useful information and it offers more realistic estimates of the actual O_3 risk in Mediterranean environments. However, it still has a considerable amount of uncertainty (Nussbaum et al., 2003), and it is not practical for routine monitoring (Ferretti et al., 2007; Paoletti and Manning, 2007). Studies on the effects of ozone on the grapevine are still relatively scarce (Pellegrini et al., 2015; Roper and Williams, 1989; Valletta et al., 2016), and, to date, still very few are addressed to set standards for regulatory purposes or to estimate reductions in productivity and quality under current or future air pollution and climate scenarios (Fumagalli et al., 2019; Miranda et al., 2020; Soja et al., 2004, 2003, 1997).

1.2 OBJECTIVES

The main objective of this Thesis is to develop and evaluate a modelling system able to comprehensively simulate exposure and ozone uptake for grapevines under Mediterranean conditions besides contributing to the current state of the art on the influence of climate in viticulture and wine production in the context of climate change. Thus, this study aims to advance knowledge on which key factors, model formulations and parameterizations should be considered in order to successfully assess potential climate

and phytotoxic O_3 risk under the local Demarcated Douro Region (DDR) Mediterranean conditions. In this context, five main research questions have been be investigated:

1. Can coupled Global Climate Model-Regional Climate Model (GCM-RCM) simulations be related to grapevine yield and quality in order to assess potential risks in the context of climate change?
2. Can the current European Monitoring and Evaluation Programme (EMEP) dry deposition model under CLRTAP adequately represent ozone uptake by local grapevine varieties in a Mediterranean area?
3. What are the most important variables affecting ozone uptake by grapevine in a Mediterranean area and how could they be taken into account by the modelling system?
4. What is the actual picture concerning ozone phytotoxic risk indicators once the dry deposition model is fitted to local observational data?

The final purpose of this Thesis is to support strategies aimed to preserve high-quality and sustainable wine production in the context of climate change.

1.3 METHODOLOGY

The proposed study area is the Portuguese Demarcated Douro Region. The DDR presents a warm Mediterranean climate with hot summers (Köppen Csa) (Andrade et al., 2021; Climaco et al., 2012). The area has already been subject of a research project funded by the Portuguese Science and Technology Foundation (FCT) and the European Regional Development Fund (ERDF) called DOUROZONE (PTDC/AAG-MAA/3335/2014; POCI-01-0145-ERDF-016778), which ended in June 2018. As such, there is access to a wealth of data and knowledge regarding the DDR that provide a suitable framework for this research. In the context of the DOUROZONE project and the subsequent development of this PhD Thesis dissertation, SOGRAPE VINHOS S.A. has also facilitated the collection of ambient O_3 data and shared meteorological data at one of its vineyard fields within the Douro Superior subregion and also shared meteorological data at one other location within the Baixo Corgo subregion. The Associação para o Desenvolvemento da Viticultura Duriense (ADVID) has also facilitated meteorological data for one representative location within the Cima Corgo subregion. Whereas the DOUROZONE project aimed to assess current and future exposure

scenarios for O_3, this research has its main focus on refining the ozone dry deposition model for grapevines under the local Mediterranean conditions.

To answer the identified research questions the following tasks have been addressed.

Task 1. Climate change potential impact

Concerning climate change impact assessment on the DDR, dynamical downscaling of European Reanalysis-Interim (ERA-Interim) and Max Planck Institute Earth System low-resolution (MPI-ESM-LR) global simulations forced with a Representative Concentration Pathway 8.5 (RCP8.5) greenhouse gas (GHG) emission scenario was performed with the Weather Research and Forecast (WRF) model to a regional scale including the Douro Valley of Portugal for recent-past (1986–2005) and future periods (2046–2065, 2081–2100). The number, duration and intensity of extreme climate events were superimposed over critical phenological phases estimated by using a specific local grapevine varietal phenological model in order to assess their positive or negative implications for wine production in the region. An assessment of the relevance of climate parameters and indices and their progression in recent-past and future climate scenarios with regard to the potential impact on wine production was performed.

Task 2. Modelling O_3 dry deposition

Concerning O_3 phytotoxic risk assessment for the DDR, a validation of a simulation with the WRF-CHIMERE modelling system was performed. The simulation covered a reference grapevine growing season in the Northern Hemisphere (from April to September 2017), during which a particular measuring campaign was also carried out. The validation of the meteorological simulations on a daily and hourly time resolution was performed based on data from three weather stations, namely on temperature, global solar radiation, relative humidity, wind speed and direction values. The ozone phytotoxicity was assessed with data from two measuring stations. A specific grapevine growth parameter based on monitored phenological observations was introduced for ozone stomatal uptake assessment.

Task 3. Model improvement

A specific parametrization was developed for autochthonous grape cultivars within a leaf-level stomatal flux model, the DO3SE model, which was coupled with the meteorological and atmospheric chemical transport modelling system, the WRF-CHIMERE. The DO3SE

model parametrization introduced in this study included phenology, photosynthetic active radiation, air temperature, air vapour pressure deficit, and leaf water potential as a proxy of soil water content. These modelling experiments included simulations with the current (default) Convention on Long-Range Transboundary Air Pollution DO3SE parametrization and with the proposed parametrization, and covered the reference grapevine growing season (from April to September 2017), during which a measuring campaign was carried out. A summary of the modelling procedure for the 2017 grapevine-growing season in the DDR can be found in Figure 1.1.

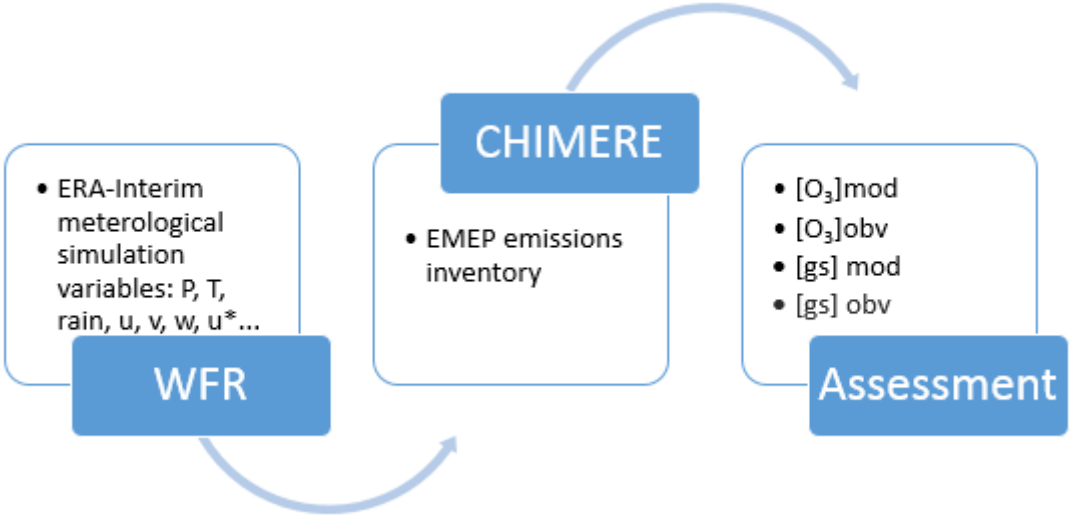

Figure 1-1. Schematic summary of the modelling procedure.

The ERA-Interim global simulations were dynamically downscaled using the WRF model. These downscaled simulations feed the atmospheric Chemistry Transport Model (CTM), CHIMERE, along with pre-processed emission data from EMEP. CHIMERE then models the sources (emission of anthropogenic and biogenic ozone precursors) and sinks (deposition) of ambient ozone. An assessment of the model was performed comparing ambient O_3 modelled data with observed one. The stomatal flux component (*gs*) is another key parameter to assess the model performance and the ambient ozone phytotoxic risk for the grapevine.

Task 4. Phytotoxic risk assessment indicators

Once the modelled grapevine ozone stomatal uptake was validated against the 2017 field observational and literature data, an analysis was performed to propose standards that could be used for regulatory purposes or to estimate changes in productivity and quality.

For this, the most critical situations (e.g. prevailing meteorological conditions, phenological stages, agricultural practices such as irrigation) regarding ozone phytotoxic risk have been identified. Moreover, specific ozone phytotoxicity standards for the grapevine in the DDR have been proposed considering the current air pollution and climate change abatement policies.

This work was also accompanied by an extensive review on the validity and limitations of the standards used for the protection of vegetation in relation to ambient O_3, the state-of the-art knowledge on O_3 phytotoxic effects on the grapevine and the available means to assess its impact.

1.4 STRUCTURE OF THE THESIS

This Thesis is divided into 6 chapters, where each of the principal objectives and tasks of the PhD work is addressed (Figure 1-2).

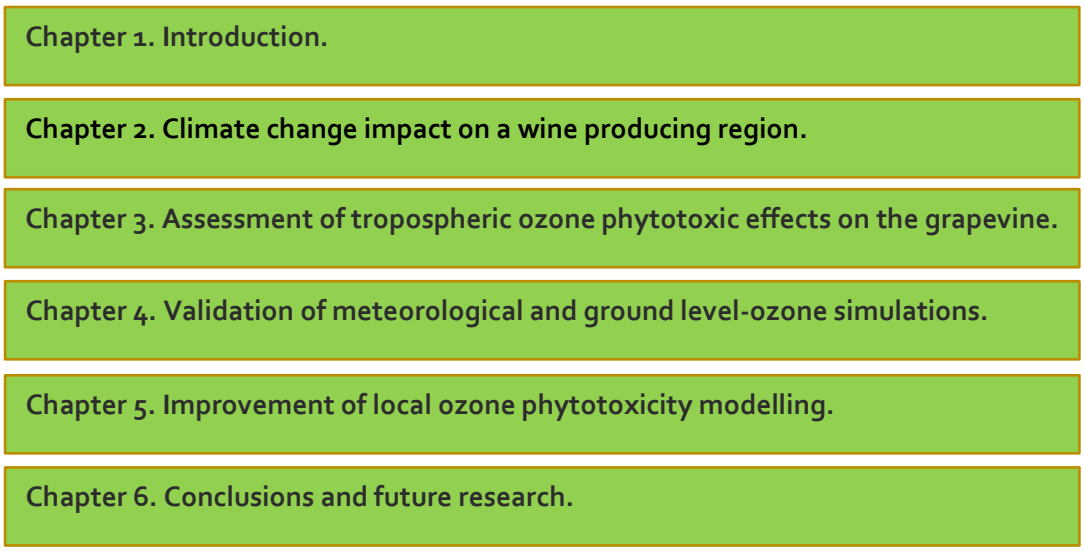

Figure 1-2. Structure of the Thesis.

Chapter 1 presents the general framework and objectives of the PhD work. Chapter 2 is concerned with the work performed in relation to climate change potential impact. The literature review performed to assess the validity and limitations of the standards used for the protection of vegetation in relation to ambient O_3, the state-of the-art knowledge on O_3 phytotoxic effects on the grapevine and the available means to assess its impact is presented in Chapter 3. Chapter 4 describes the modelling of O_3 dry deposition in the DDR with the WRF-CHIMERE modelling system and the default CLRTAP parametrization for the

grapevine. Chapter 5 presents the improvement of local ozone phytotoxicity modelling for the DDR by including specific autochthonous grape cultivars parametrization and a leaf water potential factor as a proxy for soil water potential factor. Finally, chapter 6 summarizes the main conclusions derived from this work and provides recommendations for future research.

For chapters 2 to 5, this Thesis comprises adapted versions of published or submitted papers to peer-reviewed Science Citation Index (SCI) journals. Both references and document formatting were altered, in order to make the text easier to read. In the papers, the author was responsible for the study design, the generation of the CHIMERE simulations covering the 2017 grapevine campaign in the DDR, the WRF and CHIMERE data postprocessing concerning climate parameters, bioclimatic and climate extreme indices, the statistical analyses, the analyses of results and the writing of the manuscripts. The co-authors were responsible for the critical revision of the manuscript, and, when applicable, for providing modelling simulations (i.e. WRF simulations for Chapters 2, 4 and 5) or field campaign data for validation purposes (Chapters 4 and 5).

2 CLIMATE CHANGE IMPACT ON A WINE-PRODUCING REGION USING A DYNAMICAL DOWNSCALING APPROACH: CLIMATE PARAMETERS, BIOCLIMATIC INDICES, AND EXTREME INDICES

This chapter was published as:

Blanco-Ward, D., Monteiro, A., Lopes, M., Borrego, C., Silveira, C., Viceto, C., Rocha, A., Ribeiro, A., Andrade, J., Feliciano, M., Castro, J., Barreales, D., Neto, J., Carlos, C., Peixoto, C., Miranda, A.I, 2019. Climate change impact on a wine-producing region using a dynamical downscaling approach: climate parameters, bioclimatic indices and extreme indices. Int. J. Climatol. 39, 5741–5760. https://doi.org/10.1002/joc.6185

I mainly contributed to the postprocessing of the WRF model simulations, the estimation of the climate parameters, bioclimatic indices and extreme indices, the grapevine phenological modelling, and the statistical analysis. I was also responsible for the writing of the paper.

Abstract

Climate change is of major relevance to wine production as most of the wine-growing regions of the world are located within relatively narrow latitudinal bands with average growing-season temperatures limited to 13–21 °C. This study focuses on the incidence of climate variables and indices that are relevant both for climate change assessment and for grape production, with emphasis on grapevine bioclimatic indices and extreme events (e.g. cold waves, storms, heatwaves). Dynamical downscaling of European Reanalysis-Interim (ERA-Interim) and Max Planck Institute Earth System low-resolution (MPI-ESM-LR) global simulations forced with a Representative Concentration Pathway 8.5 (RCP8.5) greenhouse gas (GHG) emission scenario was performed with the Weather Research and Forecast (WRF) model to a regional scale including the Douro Valley of Portugal for recent-past (1986–2005) and future periods (2046–2065, 2081–2100). The number, duration and intensity of events were superimposed over critical phenological phases estimated by using a specific local grapevine varietal phenological model in order to assess their positive or negative implications for wine production in the region. An assessment of the relevance of climate parameters and indices and their progression in recent-past and future climate scenarios with regard to the potential impact on wine production was performed. Results indicate a positive relation between higher growing-season heat accumulations and greater vintage yields. A moderate incidence of very hot days (daily maximum temperature above 35 °C) and drought from pre-véraison phenological conditions have a positive association

with vintage ratings. However, the mid- and long-term WRF-MPI RCP8.5 future climate scenarios reveal shifts to warmer and drier conditions, with the mean growing-season temperature (*GST*) not remaining within range for quality wine production in the long-term future climate scenario. These results indicate potential impacts that suggest a range of strategies to maintain wine production and quality in the region.

2.1 INTRODUCTION

There is a general acceptance by the scientific community of the contribution of anthropogenic greenhouse gas (GHG) emissions to climate change. Depending on the GHG emissions scenario, an increase in global mean surface temperature ranging from 1 °C to 3.7 °C is expected by the end of the century when compared to the reference period 1986–2005 (IPCC, 2014). These annual temperature increases along with higher atmospheric carbon dioxide (CO_2) may lead to longer growth seasons in Northern, Central and Eastern Europe, increasing the suitability of these areas for crops now prevalent in Southern Europe such as maize or sunflower. In an opposite way, productivity and suitability for energy crops and cereals is likely to decrease in Mediterranean Southern and South-Eastern Europe due to warmer and drier climate conditions (Falloon and Betts, 2009).

The influence of climate is also critical in viticulture and wine production (Jones et al., 2005; Pons et al., 2017; van Leeuwen and Darriet, 2016). Year-to-year meteorological variations affect the yield and optimal environmental conditions for grapes to ripen and, therefore, whether wine typicity for a given 'terroir' or grapevine-growing region will be correctly expressed to achieve its full potential. This influence is known as the 'vintage effect', with climate having a greater impact on yield and quality than other environmental factors such as soil type or grapevine variety. In this sense, it is already known that an increase of temperature produces an advance in phenology, which in turn could have advantageous effects in northern or Atlantic conditions but be detrimental under Mediterranean conditions (Fraga et al., 2016; Moriondo et al., 2013). As the grapes are exposed to higher temperatures due both to climate change and advanced phenology, the supply of metabolites to the grapes is altered, generally causing greater sugar accumulation and higher alcohol levels, lower acidity and variable effects on different aromas and secondary metabolites (Mira de Orduña, 2010; Teixeira et al., 2013).

Jones and Alves (2012) also emphasized that most of the wine-growing regions of the world, in particular the Douro region in Portugal, are located within relatively narrow latitudinal bands with average April to October growing-season temperatures limited to 13–21 °C. Therefore, small changes in temperature could affect the typicity and style of the wine produced, and if a climatic threshold is exceeded, balanced grape ripening becomes impaired.

The multicriteria climatic classification (MCC) system for grape-growing regions worldwide (Tonietto and Carbonneau, 2004) along with other bioclimatic indices (e.g. Winkler index, Branas hydrothermic index) have been commonly used to assess the impact of climate change on the suitability for wine production across Europe. For instance, Malheiro et al. (2010) calculated the indices from climate variables obtained from simulations with a 0.165° latitude–longitude resolution (grid size of about 18 km) performed with the regional climate model COSMO-CLM for the recent-past climate (1960–2000) and for the 21st century (2011–2040, 2041–2070 and 2071–2100 time periods). Their results indicated an increased soil water deficit and cumulative thermal effects during the growing season in Southern Europe, which could imply detrimental future conditions for wine production for this area unless suitable adaptation measures (e.g. rootstock and variety selection, training system and irrigation) are taken. In contrast, Western and Central Europe could benefit, with higher quality potential for grapes and even new potential areas for wine production.

In another study by Fraga et al. (2014), the atmospheric variables taken from coupled global climate–regional climate model (GCM-RCM) simulations in combination with the MCC system were used to assess present and future scenarios for the Portuguese grapevine-growing regions. An ensemble of 13 RCM simulations driven by three different GCMs produced by the ENSEMBLES project (van der Linden and Mitchell, 2009) was selected. The results illustrated relevant changes in the current bioclimatic Portuguese viticultural zones as they depict less bioclimatic diversity and a more homogenous warm and dry climate for most Portuguese wine regions.

Concerning particular studies for the Portuguese Douro Valley region, a multivariate linear regression analysis was performed by Santos et al. (2013) relating a long wine-production series (1932–2010) collected by the *Instituto dos Vinhos do Douro e Porto* (IVDP), and atmospheric variables (namely, temperature and precipitation) from a climatological

station available for the period 1941–2010. Results indicated that high rainfall and cool temperatures during budburst, shoot and inflorescence development (February–March) and warm temperatures during flowering and berry development (May) are generally favourable for high production. The regression approach was then applied to climate parameters computed from atmospheric variables provided by 16 RCM experiments for recent-past and future climate changes for the period 2001–2099. An overall positive impact was found, with an increase of 10% in production by the end of the 21st century and an increase of high-production years from 25% to over 60%. Corte-Real et al. (2015, 2016) developed another statistical work relating wine production to climate in the Portuguese Douro Demarcated Region (DDR). Series of climate parameters and bioclimatic indices derived from weather stations from the Portuguese National Meteorological Service present in the Douro Valley area were correlated with yield and Port wine vintage chart records used as a proxy for vintage quality. Temperature was introduced into the logistic model as the successive time periods required to reach a given threshold of heat accumulation to pass from a given grapevine phenological phase (e.g. budburst) to the next one (e.g. flowering). The results of this study illustrated that weather characteristics (e.g. growing-season temperatures above the mean, warm winters, cool temperatures during ripening) are strongly associated with better quality vintages.

Most recently, a grape production model (GPM) has been developed by Fraga and Santos (2017), relating daily historic temperature and precipitation from the E-OBS observational dataset with the grape production of three wineries within the Douro Valley region. The model compared thermal/hydric conditions each year with the average conditions for high- and low-yield vintages. Results indicated that relatively cool pre-flowering temperatures and relatively warm conditions during berry development favour higher yields. Higher production is also associated with years with precipitation above the mean before the flowering stage.

The present research aims to advance the current state of the art by using a dynamically downscaled GCM-RCM atmospheric modelling configuration. Based on the Representative Concentration Pathway (RCP) 8.5 emission scenario (Moss et al., 2008)), simulations were performed for 20-year periods as adopted by the IPCC 5th Assessment Report (IPCC, 2013), namely 1986–2005 for the recent past, 2046–2065 for the mid-future and 2081–2100 for the long-term future climate. The study first aims to find significant associations between

climate and key vintage production characteristics such as yield and quality in the Douro Demarcated Region (DDR) for the recent-past period using many of the pertinent climate extreme indices defined by the Expert Team on Climate Change Detection and Indices (ETCCDI) (Sillmann et al., 2013a, 2013b) besides the already commonly used atmospheric variables and the MCC system. It does so by using both a conventional approach based on Julian calendar dates and a phenological one based on thermal timings. Estimates of pertinent climate parameters and indices for both yield and vintage rating charts in the DDR as found in the first stage of this research are made thereafter for mid-term and long-term future climate scenarios. Therefore, this study offers a comprehensive analysis of 204 variables using state-of-the-art dynamically downscaled GCM-RCM high 9- and 1-km horizontal resolution climate simulations considering recent-past and future climate scenarios including key information for the DDR wine-producing area. According to the MCC system, the study area is currently representative of climatological conditions found in other renowned Mediterranean grape-growing regions such as the Napa Valley (USA), Mildura wine district (Australia) or Lujan de Cuyo (Argentina), making this study relevant for other areas besides the Portuguese DDR.

2.2 STUDY AREA

The Portuguese DDR is well known for the production of Port wine, a fortified type of wine with a long tradition produced only in Portugal and considered as one of the best wines in the world (Corte-Real et al., 2015; Fraga et al., 2017). The DDR runs along both margins of the Douro River from its midcourse in the west up to the border with Spain in the east. It extends along 50 km in the north–south direction and along 90 km in the west–east direction, with the westernmost area located 70 km from the Atlantic Ocean. The landscape is characterized by mountainous terrain, rising above the Douro River and its tributaries, with moderate to steep slopes and varying exposures. The average elevation over the entire region is 443 m, but it ranges from a low near 40 m to a high of just over 1400 m (Jones, 2013). The location of the study area is shown in Figure 2-1.

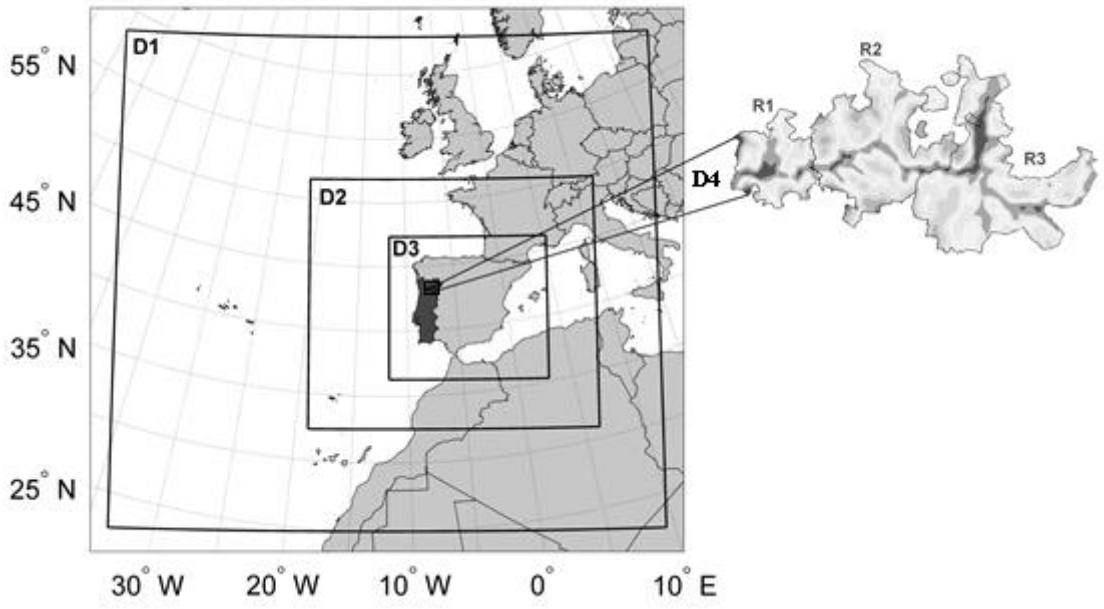

Figure 2-1. Map of the Douro demarcated region in Portugal. The map shows the location of the subregions "Baixo Corgo" (R1), "Cima Corgo" (R2) and "Douro superior" (R3). Nested domains used in the regional WRF model implementation are shown as squares. The domains have increasing horizontal resolution: 81 (D1), 27 (D2), 9 (D3) and 1 km (D4).

The region covers approximately 250,000 hectares, with sloping vineyard areas representing roughly 43,480 hectares (17.4% of the total land area) arranged in various terraced configurations. As observed in Figure 2-1, the DDR is divided into three subregions: Baixo Corgo, Cima Corgo and Douro Superior. Baixo Corgo covers the smallest area (45,000 ha), with Cima Corgo the next largest (95,000 ha) and Douro Superior the largest subregion (110,000 ha). The vineyard figures for these subregions are 13,368, 20,270 and 9,842 ha, respectively (IVDP, 2017a).

The DDR has a Mediterranean climate, with highly variable rainfall events concentrated in winter months, and hot summers. It is sheltered from Atlantic wet and cold winds by two mountain ranges, *Marão* and *Montemuro*, located at its western border. Temperature increases, and precipitation decreases from west to east. The westernmost subregion inside the Douro Valley (Baixo Corgo) is nearer to the Atlantic Ocean and therefore more affected by the moist maritime winds. The easternmost regions within the Douro Superior subarea are more distant from the Atlantic Ocean, therefore having a more continental climate influence. According to Corte-Real et al. (2014, 2016), the region is classified as having a warm temperate climate (cool summer type b Mediterranean climate,Csb, under the Köppen climate classification system), with average annual temperatures during 1980–

2009 of 15.4 °C, average daily minimum temperatures (*Tmin*) in the coldest month (January) dropping to 2.7 °C, and average daily maximum temperatures (*Tmax*) in the warmest month (August) reaching 32.1 °C. Mean growing-season temperature (*GST*) from April to September for the same climatological period is 20.6 °C. Growing-season precipitation (*GSP*) from April to September has a mean value of 193 mm, representing 30% of the annual total (624 mm). The average precipitation of the driest month (July) is just 11.2 mm. Jones and Alves (2012) emphasized that low precipitation values along with high temperatures and high radiation exposure give rise to situations of intense summer plant–soil–water stress, particularly in the Cima Corgo and Douro Superior subregions.

Based on data from three climatological stations representative of the three DDR subregions for the 1980–2009 period, the Huglin index (*HI*) averaged 2740 units whereas the cool night index (*CI*) was 13.6 °C and the dryness index (*DI*) was 126 mm. In the MCC system, the DDR climate is then classified as *HI*+2/*DI*+2/*CI*+1 (warm/very dry/cool nights) (Corte-Real, 2014). According to Tonietto and Carbonneau (2004), other renowned Mediterranean grape-growing regions falling under this classification are the Napa Valley (US) and the Mildura wine district (Australia). Although the MCC system is generally accepted as a useful tool to describe the climate of grape-growing regions globally, it is advisable to keep in mind that considerable variations at the mesoscale due to different factors such as topography or distance to the sea can exist (Blanco-Ward et al., 2007). In fact, values given for the Régua station within the Baixo Corgo subregion during 1951–1980, as reported by Climaco et al. (2012), were 2489 Huglin units – close to the *HI*+1 2400 *HI* limit of the temperate-warm class; 37 mm for *DI* –belonging to the *DI*+1 or moderately dry class; and 12.8 °C for *CI* – falling inside the same *CI*+1 category as the overall more recent classification. Those conditions would find an international match in the Lujan de Cuyo DO within the Mendoza province (Argentina). Regarding the grapevine varieties present in the DDR, Corte-Real (2014) mentioned that up to 50 are allowed by law and may be present in Port wine. Some of the most frequently used are 'Touriga Nacional', 'Touriga Francesa', 'Tinta Roriz' ('Tempranillo'), 'Tinta Barroca' and 'Tinto Cão'.

2.3 DATA AND METHODS

In this section, the datasets and methods used in this study are described. There are two main atmospheric datasets used in this work: the Weather Research and Forecast

European Reanalysis (WRF-ERA) dataset comprising daily records of atmospheric variables for the 1986–2005 recent-past climate simulation, and the Weather Research and Forecast Max Planck Institute (WRF-MPI) dataset also containing the 1986–2005 recent-past time span but also extending to the 2046–2065 mid-future and 2081–2100 long-term future climate scenarios. First, the WRF-ERA for the 1986–2005 recent-past simulations was validated using both a Julian calendar approach and a phenological thermal timing modelling approach. Once validated, the WRF-ERA dataset was used to estimate a group of 204 climate parameters and indices relevant for wine production in the DDR by using both the Julian calendar-based approach and the phenological approach. A statistical analysis was performed thereafter in order to find significant relations between the previously estimated climate parameters and indices and vintage yield and Port wine vintage rating records for the 1986–2005 recent-past simulation. Finally, a selected subset of indices and parameters found through the previous analysis was used to validate the WRF-MPI datasets and assess the possible impacts of climate change under the RCP8.5 GHG emission scenario for wine production in the DDR. Figure 2-2 displays a summary of the workflow followed in this research.

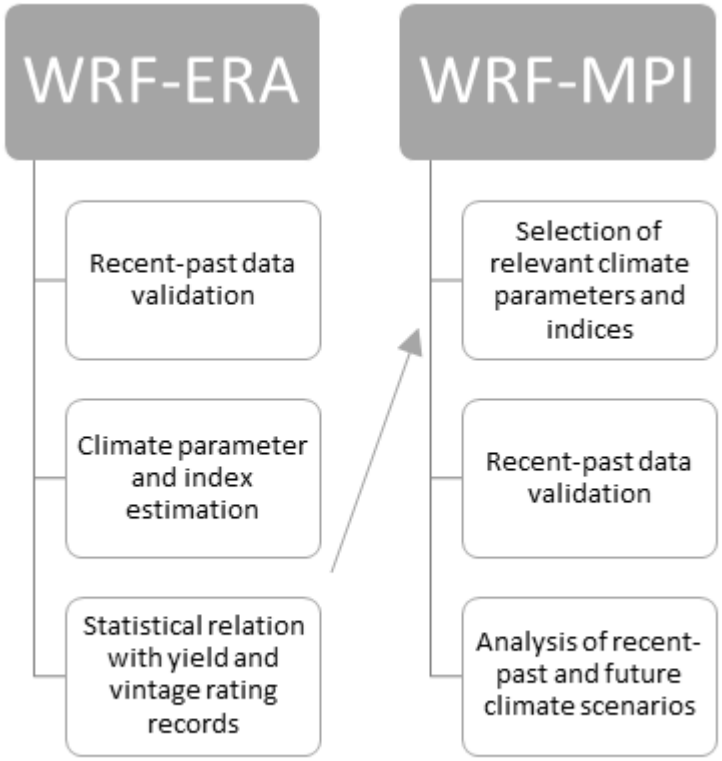

Figure 2-2. Summary of the workflow followed in this study. First, work was performed to validate the WRF-ERA recent-past data set. A correlation analysis was applied between climate parameters and indices and vintage yield and quality records in the DDR afterwards. Finally, the work progressed to analyse the WRF-MPI recent-past, midterm and long-term future data sets based on a selection of relevant climate parameters and indices found in the previous stage.

2.3.1 High-resolution WRF climate simulations

Two sets of GCM results were used to provide initial and boundary conditions for regional climate simulation, specifically the ERA-Interim reanalysis and the Max Planck Institute Earth System low-resolution model (MPI-ESM-LR). The reanalysis data were obtained from the European Centre for Medium-Range Weather Forecasts (ECMWF) through the ERA-Interim project, with a horizontal resolution of approximately 79 km (Dee et al., 2011). The MPI-ESM-LR is a global earth system model developed by the MPI with 1.9° horizontal resolution which corresponds to about 160 km horizontal resolution (Giorgetta et al., 2013). This model participated in the Coupled Model Intercomparison Project Phase 5 (CMIP5), which uses new emission scenarios, namely the RCPs (Andrews et al., 2012). In this study, RCP8.5, defined as a radiative forcing of 8.5 W m^{-2} by 2100 and a continuous increase after this year(Moss et al., 2008), was used. According to Riahi et al. (2011), the RCP8.5 provides an updated and revised quantification of the original IPCC A2 SRES scenario, representing a high business-as-usual GHG emission scenario assuming slow rates of economic development and technological change, and a rapidly growing population with associated high demand for food and corresponding high demand for fossil fuels. Compared to the total set of RCPs, it represents the highest GHG emissions scenario.

The WRF model was used as a dynamical downscaling tool to obtain regional climate information from the GCM simulations. WRF is a mesoscale numerical weather prediction system which can be used in a wide range of applications across scales ranging from tens to thousands of kilometres. A detailed description of the model can be found in Skamarock et al. (2008), and further information on parameterizations specifically suited for the Iberian Peninsula can be found in Marta-Almeida et al. (2016). The RCM WRF high-resolution climate simulations were performed for 20-year periods as adopted by the IPCC 5th Assessment Report (IPCC, 2013), namely 1986–2005 for the recent past, 2046–2065 for the mid-future and 2081–2100 for the long-term future climate. These simulations were implemented by Viceto et al. (2017) for three nested domains with increasing horizontal

resolution, namely 81 (D1), 27 (D2) and 9 km (D3). A fourth 1-km horizontal resolution domain (D4) was implemented for three years only (2000, 2049 and 2097) due to the intensive computer resources required by the dynamical downscaling WRF-MPI configuration (Figure 2-1). This study uses the 9- and 1-km horizontal resolution domains focusing on a confined area comprising the DDR, taking advantage of the WRF dynamical downscaling approach to include the effects of proximity to the Atlantic Ocean and the complex topography of the Douro Valley in the regional climate simulations.

2.3.2 Phenological modelling

It was Réaumur who first introduced in 1735 the concept of heat units or 'thermal time' and a relationship between the development rate of a crop and temperature as a sum of heat degrees (Bonhomme, 2000; Mcmaster and Wilhelm, 1997). Heat units are nowadays commonly measured as growing degree days (GDD, °C units) which are estimated as a daily temperature summation above a temperature base required for a given crop to complete a specific phenological stage:

$$\theta = \int (T - Tb)dt \qquad (1)$$

where θ (°C) represents the thermal duration of a specific phenological stage, *T* is the daily average temperature and *Tb* is a threshold above which there is plant development within that phenological stage. Models based on GDD have been used extensively to simulate the phenology of the grapevine (Carbonneau et al., 1992; Hidalgo, 1980) or as grapevine zoning bioclimatic indices (Huglin, 1986; Riou, 1994; Winkler et al., 1974).

A specific phenological scheme partitioning the annual development cycle of the grapevine into three major phases (*b* – budburst to flowering, *f* – flowering to *véraison*, and *v* – *véraison* to maturity) has been already proposed for the study area by Corte-Real et al. (2015, 2016). This phenological model used a mixed grapevine variety configuration as the Tinta Roriz variety was used to define the required GDD to reach budburst, flowering and *veraison*, and the Touriga Franca variety was used to estimate the required GDD to reach maturity in the DDR. This was done in order to simulate an intermediate varietal behaviour (neither an early nor a late grapevine variety class) for all those phenological stages, using two varieties present extensively in the Douro Valley region.

This work makes use of the mixed 'Tinta Roriz-Touriga Franca' local grapevine varietal phenological model to compute the timings of the key grapevine phenological timings (*b* –

budburst, *f* – flowering and *v* – *véraison* or ripening onset) for the four climate-modelling configurations presented in section 3.1 (WRF-ERA recent past, WRF-MPI recent past, WRF-MPI mid-future and WRF-MPI long-term future) based on the specific varietal GDD requirements as observed at the Portuguese National Ampelographic Collection (Lopes et al., 2008). In section 4, results are compared with specific phenological observations recently made available for the Douro Valley region (Alves et al., 2013).

2.3.3 Climate parameters and indices

Using the daily maximum and minimum temperatures and the daily total precipitation from the four different regional WRF modelling configurations (WRF-ERA recent past, WRF-MPI recent past, WRF-MPI mid-future and WRF-MPI long-term future), a total of 50 climate parameters, four grapevine bioclimatic indices and 150 climate extreme indices were calculated.

2.3.3.1 Climate parameters

The climate parameters resulted from computing the average of daily maximum temperatures, daily minimum temperatures and daily mean temperatures (as *Tmax* + *Tmin*/2), the total precipitation (*P*) for every month from April to September, and each one of the yearly phenological stages based on the conventional monthly scheme for the Northern Hemisphere (budburst usually occurs between March and April, flowering occurs more often in June and July, and *véraison* usually happens between August and September). Therefore, a set of 36 climatic parameters was calculated following the conventional Julian calendar scheme (e.g. *Tmax Apr-May*, *Tmin Apr-May*, *Tave Apr-May*, *P Apr-May* etc.). Another set of 12 climatic parameters was computed considering the thermal timings according to the phenological modelling (*Tmax-b*, *Tmin-b*, *Tave-b*, *P-b* etc.). Finally, two other climatic parameters were computed following the conventional scheme (months from April to October) to summarize information for intercomparison purposes: the growing-season average temperature (*GST*) and the growing-season total precipitation (*GSP*).

2.3.3.2 Bioclimatic indices

Four specific grapevine bioclimatic indices were selected: the Winkler index (*WI*), *HI*, *CI* and *DI*. These indices are commonly used to characterize grapevine-growing areas worldwide

in a standardized way and as an agronomic zoning tool (Anderson et al., 2012; Blanco-Ward et al., 2007; Jones et al., 2010; Tonietto and Carbonneau, 2004).

WI is the sum of the daily average temperatures above a threshold temperature of 10 °C considered the active grapevine temperature (the temperature above which its vegetative cycle is activated) during the growing season. This index is usually calculated from monthly data taking as growing season the months between April and October (Winkler et al., 1974):

$$WI = \sum_{April1st}^{October31st}(Tave - 10\,^{\circ}C), Tave \geq 10\,^{\circ}C$$

$$Tave = \frac{T\,max + Tmin}{2} \quad (2)$$

The *HI* provides information regarding heliothermal potential. According to Tonietto and Carbonneau (2004), this index is very much correlated with *WI* (r^2 = 0.98 over 97 grape-growing regions worldwide) but provides a better idea of qualitative factors such as berry sugar potential.

$$HI = \sum_{April1st}^{September30th} \frac{(T\,max - 10\,^{\circ}C) + (Tave - 10\,^{\circ}C)}{2} d$$

$$Tave = \frac{T\,max + Tmin}{2} \quad (3)$$

where, again, *Tave* is the mean air temperature (°C), *Tmax* is the maximum air temperature (°C), and *d* is a length of day coefficient ranging from 1.02 to 1.06 between 40° and 50° of latitude. A value of 1.02 was assumed for a latitude between 40°01' and 42°00'. This index is usually calculated from monthly climatic means, taking as growing season the April to September period.

The purpose of *CI* is to improve the assessment of grape qualitative potential, notably in relation to secondary metabolites (polyphenols, aromas) in grapes, and takes into account the minimum night temperatures during the usual ripening month (Tonietto and Carbonneau, 2004).

$$CI = \sum_{September\ 1st}^{September\ 30st} \frac{Tmin}{30} \quad (4)$$

Finally, *DI* indicates the potential water availability in the soil, related to the level of dryness in a region. It is also related to the level of grape ripening and wine quality:

$$W = W_o - P - T_v - E_v \quad (5)$$

where W is the estimated soil water reserve at the end of a given month, W_0 is the initial soil water reserve which can be accessed by the vine roots in that period, P is the total monthly precipitation, T_v the potential transpiration of the vineyard, and E_s the direct evaporation from the soil. To compute T_v and E_s, it is also necessary to compute the monthly total potential evapotranspiration. This is usually done by the Penman–Monteith method but, as we only work with temperature and precipitation records, it was approximated by the Hargreaves method, which produces comparable results in arid and semiarid environments (Hargreaves et al., 2003). For intercomparison reasons, W is also calculated sequentially on a monthly basis during the same period used for *HI* (April 1st to September 30th), which is acceptable for most grape-growing regions in the Northern Hemisphere. The result is expressed in millimetres of water in the soil. The initial W_0 is usually taken as 200 mm (Tonietto and Carbonneau, 2004). The classes of viticultural climate for the grapevine mean growing-season temperature, the Winkler index, the Huglin index, the cool night index and the dryness index can be found in Table A-1 (supplementary material).

2.3.3.3 Extreme climate indices

A group of fifteen climate extreme indices from the group of 27 core indices developed by ETCCDI (Sillmann et al., 2013a, 2013b) related to the incidence of cold waves, storms and heatwaves, which could be relevant for the grapevine, were calculated on a yearly basis first. Namely, these indices were:*FD0*, the number of frost days per year where *Tmin* < 0 °C.

SU25, the number of summer days per year where *Tmax* > 25 °C.

SU35, the number of very hot or stressful days per year where *Tmax* > 35 °C.

TR20, the number of tropical nights per year where *Tmin* > 20 °C.

CSDI, cool spell duration index or the total number of days being part of cool spells longer than 6 consecutive days in duration. A day is considered to belong to a cold spell if *Tmin* is less than the calendar-day *Tmin* 10th percentile centred on a 5-day window for the base period studied.

WSDI, warm spell duration index or heat wave index, or the total number of days being part of warm spells longer than 6 consecutive days in duration. A day is considered to

belong to a warm spell if *Tmax* is greater than the calendar-day *Tmax* 90th percentile centred on a 5-day window for the base period studied.

R10, the number of days per year with heavy precipitation (daily precipitation > 10 mm).

R20, the number of days per year with very heavy precipitation (daily precipitation > 20 mm).

CWD, the maximum number of consecutive wet days per year where daily precipitation > 1 mm.

CDD, the maximum number of consecutive dry days per year where precipitation < 1 mm.

DTR, daily temperature range or annual mean difference between *Tmax* and *Tmin*.

Warm spells accounting for the total number of days per year with at least 3 and 6 continuous days with *Tmax* greater than 35 °C were also computed and associated with indices named *WSDI-3d* and *WSDI-6d*, respectively. Cold spells accounting for the total number of days per year with at least 3 and 6 continuous days with *Tmin* less than 0 °C were also computed and associated with the variables *CSDI-3d* and *CSDI-6d*. The climate extreme indices were also computed for each phenological stage (budburst, flowering and *véraison*) based on the previously mentioned conventional Julian calendar monthly configuration and the mixed Tinta Roriz-Touriga Franca local grapevine varietal phenological model. The climate extreme indices related to cold surface atmospheric conditions were computed for the dormancy period (November to March) and extended only to the budburst stage during the grapevine-growing season. Overall, 150 variables related to climate extreme indices were computed at the annual scale and specific phenological-stage timings for the grapevine. A list of pertinent abbreviations is given in Table A-2 (supplementary material).

2.3.4 DDR yield and quality data

The average yield (hl/ha) of all types of wine produced in the DDR for the recent-past 1986–2005 period was considered. Data were available from Corte-Real (2014) consisting of a compilation of data from the Portuguese Office for National Statistics (INE), taking into account the increase in planted areas since 1982. Data on Port vintage ratings were selected from Corte-Real et al. (2016) and Corte-Real (2014), taking into account the scores of a set of eight renowned vintage charts and the IVDP regulating board ratings (Table A-3,

supplementary material) which classifies Port wines as Vintage Port wines only when very high standards of organoleptic quality are met. As Port wine makes up to 60.4% of the total production of wine in the DDR (IVDP, 2017b), it can be assumed that Port wine quality ratings are highly correlated with the overall vintage quality in the DDR. The original vintage scores for the recent-past period (1986–2005) can be found in Table A-4 (supplementary material) as compiled in Corte-Real et al. (2016).

2.3.5 WRF validation and statistics

The April to October *GST* values and the estimated dates for *véraison* from the mixed Tinta Roriz-Touriga Franca local grapevine varietal phenological model for the selected cells were used to validate the WRF-ERA recent-past modelling simulations against *GST* estimates from the 0.25° horizontal resolution E-OBS (Haylock et al., 2008) and data on grapevine phenology observations taken over 10 years in a vineyard within the DDR (Alves et al., 2013). As the maturity stage is highly dependent on the style of wine to be produced and cannot be defined with high precision, these records only report chronological duration up to the onset of the *véraison* phenological stage. Therefore, this phenological stage was chosen to evaluate the suitability of using the WRF-ERA recent-past simulations when the mixed Tinta Roriz-Touriga Franca local grapevine varietal phenological model is applied.

Once the WRF-ERA model outputs were validated, the data on standardized vintage yield and vintage rating scores, and the standardized climate parameters, bioclimatic and climate extreme indices estimated for the WRF-ERA 1986–2005 recent past were submitted to Spearman correlation tests to look for significant associations. For the case of the MB and IVDP vintage scoring systems, Mann–Whitney statistical tests were performed as they could be grouped into just two groups of vintages (IVDP 1 Vintage Port, IVDP 0 Non-Vintage Port, MB ≤ 3 Good/Very Good vintage, MB ≥ 4 Excellent/Award vintage). These tests were selected considering that many of the variable distributions analysed were non-normal as is often the case for climate extreme events (e.g. summer storms, warm or cold spells). Finally, based on the significant associations found for the WRF-ERA recent-past dataset, some representative climate parameters and indices were estimated by using the WRF-MPI simulations for the recent-past and future scenarios to assess their potential impact on wine production for the whole DDR and the grapevine-cultivated areas as derived from CORINE 2006 (Caetano et al., 2009).

2.4 RESULTS AND DISCUSSION

Results will be discussed in the same order as the workflow diagram (Figure 2-2) used in section 2.3. First, the quality of the WRF-ERA dataset for the DDR is introduced. A presentation and discussion of significant relations found between climate parameters, grapevine bioclimatic indices and climate extremes and vintage yield and Port wine rating scores in the study area follows. Finally, an assessment regarding the possible impacts of climate change in the DDR is performed by using WRF-MPI datasets for the recent-past and future RCP8.5 GHG emission climate scenarios.

2.4.1 WRF-ERA data validation

Due to the lack of detailed temperature records in the region covering the whole DDR area, E-OBS is considered here as the reference for validation purposes. The simulations used in this study, performed with the WRF forced by ERA (and also by MPI), were generally validated (at 9 km horizontal resolution) by Marta-Almeida et al. (2016) for the reference climate (1986-2005) by comparison with gridded temperature datasets derived from meteorological station records for Spain and Portugal. Marta-Almeida et al. (2016) reported an acceptable comparison of both model configurations applied in this work (WRF-ERA and WRF-MPI) when daily climatologies of temperature and precipitation were compared with observational datasets across coarse climatological subregions. Pereira et al. (2017) used the same simulations outputs and validated temperature (at 9 km horizontal resolution) and its extremes and other temperature-derived measures with those obtained from E-OBS.

Figure 2-3 shows the spatial pattern of the grapevine April to October *GST* over the Douro Valley as modelled for the D3 9 × 9-km WRF-ERA configuration.

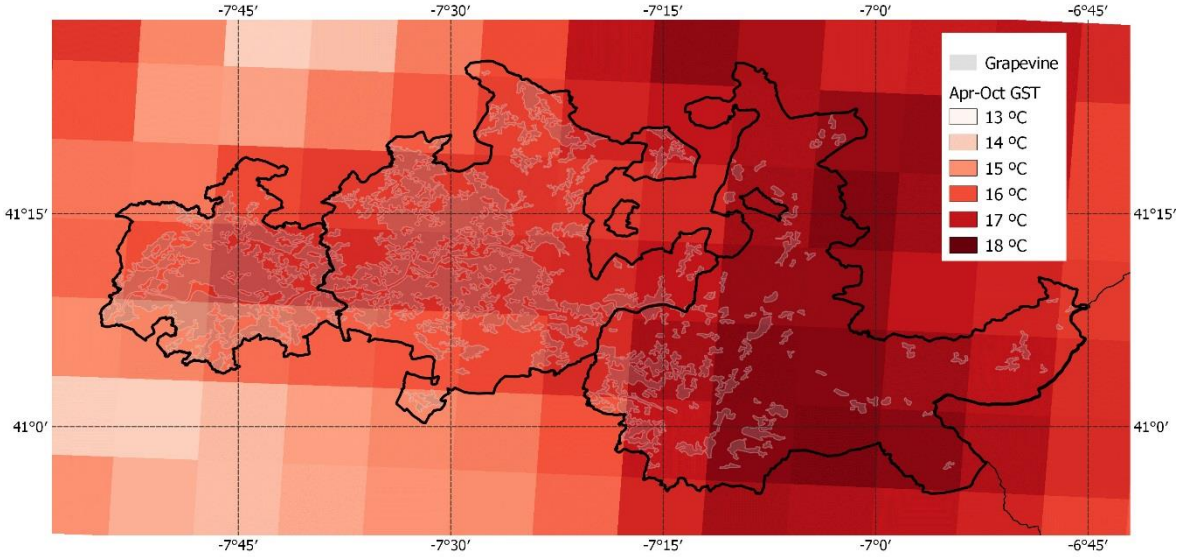

Figure 2-3. Mean April to October growing-season average temperature (*GST*, ˚C) as calculated from the 9 × 9-km 1986–2005 WRF-ERA simulations. The DDR limits are represented with its main subregions (Baixo Corgo, Cima Corgo and Douro superior), and grapevine-cultivated areas are derived from CORINE 2006.

The 9 × 9-km resolution WRF simulations forced by ERA-Interim reanalysis resulted in realistic patterns of surface atmospheric variables. Within the DDR, the *GST* values portray a west–east trend resulting from the orientation of the main valley itself and the increasing distance from the sea. Mean *GST* for the three DDR subregions are shown in Table 2-1 for WRF-ERA and E-OBS. Table 2-1 also portrays the resulting mean *véraison* dates along with the WRF-ERA April to October *GST* means obtained for each of the DDR subregions. The *GST* mean values are very close to those estimated based on the 0.25° horizontal resolution E-OBS dataset for the same years. Only the Douro Superior subregion presents an average *véraison* date within the 95% confidence limits of the timings reported for the area by Alves et al. (2013). These rather delayed phenological figures could be attributed to an important difference between the average height of the selected WRF-ERA cells (536 m for the Baixo Corgo subregion, 526 m for the Cima Corgo subregion and 452 m for the Douro Superior subregion) and that of the field plot where the phenological dates were observed (Quinta da Cavadinha, 205 m). Based on these results, only one WRF-ERA 9 × 9-km cell representative of the mean conditions of the Douro Superior subregion was used for the correlation analysis.

Table 2-1. Growing-season temperature (*GST*) and véraison statistics for the three DDR subregions.

1986–2005 recent-past period				
	GST means (°C)		*Véraison* date (Julian day)	
DDR subregion	WRF-ERA	E-OBS	Model	Field
Baixo Corgo	16.0	16.1	241	175–229*
Cima Corgo	16.4	16.8	237	
Douro Superior	17.4	17.4	224	

*The date range given represents the 95% confidence limits for the onset of *véraison* in a representative vineyard in the study area.

2.4.2 Vintage yield and quality in relation to climate

All of the rating charts have strong (>0.6) and significant Spearman's correlation coefficients with at least two other charts (Table 2-2). WA is the exception, not correlating significantly with any one of the others. As the number of Port vintages specifically evaluated was higher in IVDP (20), WE (19), MB (17) and DC (14) compared to the other charts, these were the final charts selected to analyse the relationship between Port wine vintage ratings and climate. It is worthwhile noticing that yield presented significant negative correlations with two of the rating charts (WS, VT). This suggests an inverse relationship between vintage yield and Port wine vintage ratings.

Table 2-2. Significant correlation coefficients among the different vintage rating charts.

	Yield	BBR	DC	IVDP	MB	SWE	VT	WE	WS
BBR	-0.075								
DC	-0.083	**0.939****							
IVDP	0.062	**0.642***	0.446						
MB	-0.227	0.626	**0.821****	0.447					
SWE	0.001	0.583	0.466	**0.749****	0.550				
VT	**–0.685***	0.671	0.316	0.570	0.474	**0.751****			
WE	-0.191	0.467	0.489	**0.607****	**0.751****	**0.632****	**0.673****		
WS	**–0.548***	0.772	0.830	0.412	**0.772***	0.482	**0.913****	**0.747****	
WA	-0.118	0.445	0.426	NaNNA	0.000	-0.031	-0.320	-0.061	0.088

Vintage rating charts acronyms: Berry Bros & Rudd (BBR), Decanter (DC), Instituto dos Vinhos do Douro e do Porto (IVDP), Michael Broadbent (MB), Sotheby's Wine Encyclopaedia (SWE), Vintages (VT), Wine Enthusiast (WE), Wine Spectator (WS), Wine Advocate (WA).

NaNNA – Not a number, not available. As it can be observed in Table A-4 (supplementary material), there are only 6 WA-rated vintages which were all qualified as top-vintage years with a value of 1 according to the IVDP vintage rating chart. Therefore, it is not possible to compute a Spearman's correlation coefficient for this case. * 95% significance level, ** 99% significance level.

Table 2-3 shows the significant moderate (> 0.5) and strong (> 0.6) associations found between the climate parameters and indices, as computed from the daily temperature and precipitation records from the Douro Superior subregion WRF-ERA cell, and the corresponding vintage yield and Port wine vintage rating records for the recent-past 1986–2005 time period. It is worth noticing that, within a viticulture context, correlation values as low as 0.54 have been considered highly relevant in a study relating water deficit to vintage quality (van Leeuwen and Darriet, 2016). These correlations are also similar in range to those found in another study at a close latitude (Galicia, north-west Spain) relating wine production to climate parameters (Lorenzo et al., 2012). Several correlations were found by using Mann–Whitney tests too. Some associations (e.g. *Tmax-b*, *Tmax-v*, *SU25-f*, *SU35-f*, *CDD-f*) were identified using the phenological modelling configuration, showing the benefit of using thermal timings based on accumulated heat rather than using only the conventional monthly schemes based on Julian calendar dates.

Table 2-3. Significant moderate (>0.5) to strong (0.6) correlations between vintage yield and quality rating charts and climate parameters and indices for the 1986-2005 recent-past period.

1986–2005 recent-past period					
	Yield	WE	DC	MB	IVDP
Statistical test	Spearman's correlation ρ			Mann–Whitney U	
Growing season					
Tave-AprSep (°C)	**0.519***				
GDD-AprSep	**0.575****				
HI (unitless)	**0.581***				
SU25 (days)	**0.555***				
Dormancy					
FD0-JanMar (days)			**0.580***	**0.038**	**0.025**
CSDI-3d-JanMar (days)				**0.048**	**0.037**
Budburst					
T max-b (°C)				**0.015**	
SU25-May (days)		**0.645****			**0.044**
P-May (mm)	**–0.538***				

Flowering					
SU35-f (days)		**0.723****			
CDD-f (days)	**–0.612****	**0.475****			
CDD-JunJul (days)		**0.592****	**0.678***		**0.069**
Véraison					
T max-v (°C)	**0.533***				
SU25-v (days)	**0.524***				
P-Aug (mm)		**0.423****			
R10-Aug (days)		**0.559****		**0.023**	**0.037**

Tave-AprSep (°C) – Growing-season April to September average temperature, *GDD-AprSep* – April to September growing-degree days, *HI* (unitless) – Huglin index, *SU25* (days) – number of summer days per year, *FD0-JanMar* (days) number of frost days from January to March, *CCDI-3d-JanMar* (days) – cold spell index accounting for the total number of days from January to March with at least three continuous days with *T min* < 0˚C, *T max*-b (°C) - mean of daily maximum temperatures from the budburst to the flowering stage, *SU25-May* (days) – number of summer days per year, P-May (mm) – May total precipitation, *SU35-f* (days) – number of very hot days from the flowering to the *véraison* stage, *CDD-f* (days) – maximum number of continuous dray days (*P* = 0 mm) from the flowering to the *véraison* stage, *CCD-JunJul* (days) - maximum number of continuous dray days (*P* = 0 mm) from June to July, *Tmax-v* (°C) - mean of daily maximum temperatures from the *véraison* stage to the end of September, *SU25-v* (days) - number of summer days from the véraison stage to the end of September, *P-Aug* (mm) – August total precipitation, *R10-Aug* (days) – number of days with heavy precipitation during August (P > 10 mm). * 95% significance level, ** 99% significance level.

Elevated growing-season April to September average temperatures (*Tave Apr-Sep*) and heat sums (*GDD-AprSep*, *HI*), lower rates of precipitation from May (*P-May*) accompanied by dry conditions during the flowering stage (*CDD-f*), and high daily maximum temperatures (*Tmax-v*) associated with a high frequency of summer days (*SU25-v*) from *véraison* to maturity time are related to high grapevine yields. These results are consistent with other studies performed in the area, such as those of Corte-Real (2014), Fraga and Santos (2017) and Santos et al. (2011, 2013).

Wine quality ratings relate differently to meteorological conditions than yield. Port wine vintage ratings appear to be positively associated with sufficient cold requirements during dormancy (*FD0-JanMar*, *CSDI-3d-JanMar*), elevated daily maximum temperatures during budburst followed by a high incidence of May summer days (*SU25-May*) and very hot days (*Tmax* > 35 °C) from flowering to *véraison* (*SU35-f*) associated with prolonged periods without rain (*CDD-f*, *CDD-JunJul*). Finally, moderate amounts of rain commonly associated with isolated summer storms (*P-Aug*, *R10-Aug*) help to relieve severe water stress and appear to be associated with good Port vintages too. According to van Leeuwen and Darriet

(2016), these conditions are favourable to a decrease in bud fertility and the development of a smaller berry size, which result in a smaller number of grapes developed per vine with a greater chance of a balanced supply of photoassimilates to them.

2.4.3 Climate change analysis: reference and future scenarios

2.4.3.1 Climate parameters and indices

GST, *véraison* onset and *SU25*, *SU35* and *FD0* climate extreme indices were selected as representative due to their simple definition and significant association with vintage yield and Port wine vintage ratings as found in the previous section. Table 2-4 shows the estimated climate-related parameters and indices based on the WRF-ERA and WRF-MPI simulations. The WRF-MPI 1986–2005 dataset manifests a cooler bias for *GST* (−1.1 °C), *véraison* (15-day delay), *SU25* (−12 days) and *SU35* (−3 days) but not for *FD0* where the figures are greater in WRF-ERA (+11 days). With respect to the bioclimatic indices, there is only agreement in the mean general Winkler class for the whole DDR (Ib) and *CI* (*CI*+2), with *HI* and *DI* having mean warmer and drier conditions, respectively, in WRF-ERA. Despite the differences found in means and bioclimatic class labels, the standard deviations are very close in most cases.

Table 2-4. Differences of means and standard deviations between WRF-ERA and WRF-MPI for some representative climate-related parameters and indices in the DDR.

1986–2005 recent-past climate scenario				
	WRF-ERA		WRF-MPI	
	$\bar{x}$	σ	$\bar{x}$	σ
April to October growing-season average temperature *GST* (°C)	16.7	0.38	15.6	0.37
Véraison onset (Julian day)	234	4	248	3
Number of summer days per year *SU25* (days)	77	6	63	6
Number of very hot days per year *SU35* (days)	4	1	1	0.3
Number of frost days per year *FD0* (days)	36	4	25	3
Winkler index *WI* (GDD)	Ib	75	Ib	70
Huglin index *HI* (unitless)	*HI*−1	85	*HI*−2	79
Dryness index *DI* (mm)	*DI*+1	14	*DI*−1	10
Cool night index CI (°C)	*CI*+2	0.2	*CI*+2	0.2

Performing a specific fit of the WRF-MPI dataset for the DDR is beyond the scope of this work. Instead, warm years offsetting the cooler bias during the April to October grapevine-

growing season of −1.1 °C detected in the 9 × 9-km MPI dataset in the DDR area when compared to the WRF-ERA dataset were selected to perform 1 × 1-km WRF-MPI D4 simulations that could be representative of extreme hot seasons for the recent-past and future climate conditions in the study area: namely, the years 2000, 2049 and 2097 were selected this way (highlighted in bold in Table A-5, supplementary material). Also, the maximum average temperature of the peak summer months (i.e. July to September) was considered to select 2097 instead of 2098 for the long-term future.

2.4.3.2 From reference to future climate scenarios

Results concerning *FD0*, *SU25* and *SU35* for the WRF-MPI 2000, 2049 and 2097 simulations are shown in Figure 2-4. *FD0* values are lower in the western subregion and could reach higher values close to 10–20 days per year at the highest elevations in the central and eastern subregions. The differences between the results obtained for 2049 and 2097 indicate rates of change between 0 and 10 fewer frost days per year for most of the DDR, with the greatest decrease in rates present at the highest elevations of the central and western subregions. The highest incidences for *SU25* with values greater than 100 days per year are found at the lowest elevations across the DDR, with greater extension in the eastern subregion. Rates of change range mostly between 10 and 20 *SU25* days more per year for 2049, and 30 and 40 more *SU25* days per year by 2097, with higher increases at higher elevations. With respect to *SU35*, higher values ranging between 20 and 40 *SU35* days per year are found across the valleys with the highest values found in the western subregion. There is no increasing tendency for the 2049 simulation but *SU35* numbers increase by 30 or even 50 days per year in the 2097 simulation.

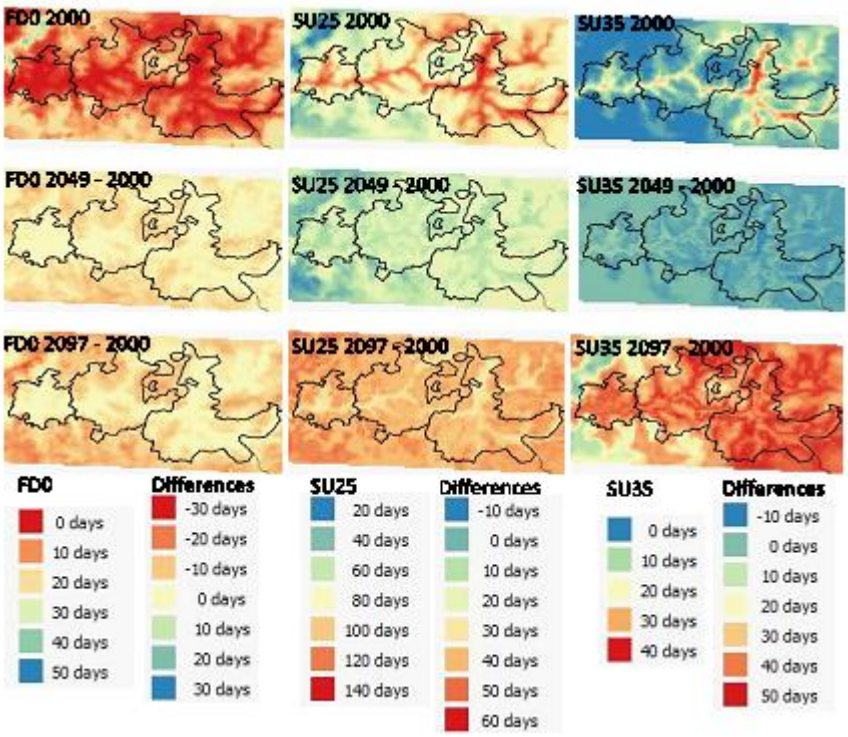

Figure 2-4. *D0*, *SU25* and *SU35* and associated rates of change thematic layers as derived from the very high-resolution 1 × 1-km WRFMPI RCP8.5 hourly simulations for selected representative recent-past (2000), mid-term future (2049) and long-term future (2097) years in the DDR.

Figure 2-5 shows the results after applying the local grapevine varietal phenological model to the WRF-MPI simulations. It can be observed that the earliest budburst dates, with values as low as 61 (March 1st) for the western subregion or 66 (March 6th) for the central and western regions, are associated with lower elevations with greater areal extension in the western subregion. The 2049 simulation shows a delay of the budburst reflecting less favourable conditions for this phenological stage than those present in the 2000 simulation. However, the 2097 simulation indicates advancements in the order of 10 or 20 days associated mostly with the higher elevations. *Véraison* has mean values of 206 (July 24th) for the western and eastern subregions and 210 (July 28th) for the central one. The 2049 simulation is associated with no or little advancement (up to 10 days) for this phenological stage. However, a clear advancement of between 10 and 30 days for *véraison* is observed in the 2097 simulation, with the highest advancement rates associated with the highest elevations. Finally, both the 2049 and the 2097 simulations indicate a shortening of the duration of the budburst to *véraison* growing cycle ranging between 5 and 25 fewer days across the DDR. The specific rates of change between the 2000 recent-past simulation and

the 2049 and the 2097 future ones for the grapevine areas present in the DDR as derived from the CORINE 2006 dataset for *FD0*, *SU25*, *SU35*, budburst, *véraison* and the length of the grapevine growing cycle between budburst and *véraison* can be found in Figure 2-6.

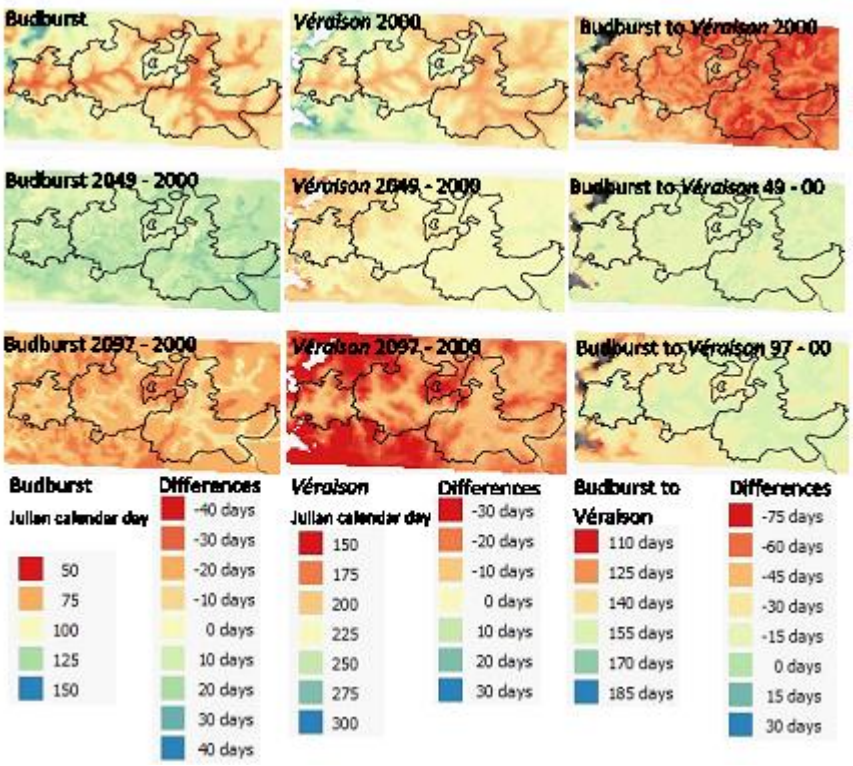

Figure 2-5. Budburst, véraison to véraison grapevine growing-season length and associated rates of change thematic layers as derived from the very high-resolution 1 × 1-km WRF-MPI RCP8.5 hourly simulations for selected representative recent-past (2000), mid-term future (2049) and long-term future (2097) years in the DDR.

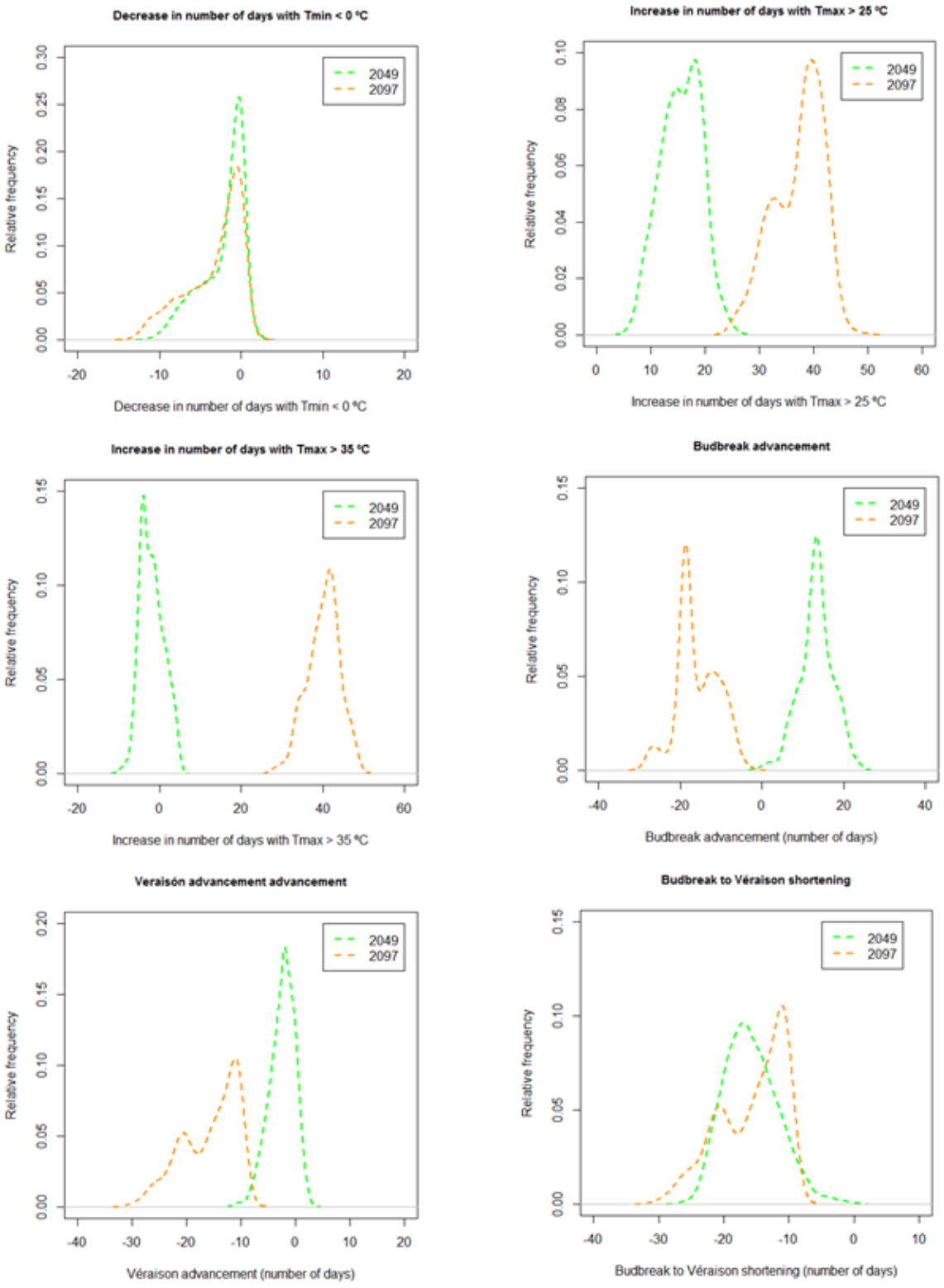

Figure 2-6. Probability distributions of changes in *FD0*, *SU25*, *SU35*, budburst, véraison and budburst to véraison period as derived for mapped CORINE 2006 vineyard areas in the DDR.

Figure 2-7 illustrates mean April to October *GST*, April to October *GSP* and *WI* thematic layers derived from the selected representative WRF-MPI recent-past (2000), mid-term future (2049) and long-term future (2097) simulations. For the year 2000 recent-past simulation, most cell values within the DDR are associated with the temperate and warm class, with some occurrence of the intermediate class for *GST*, rainfall values between 200 and 400 mm for *GSP*, and a diverse set of *WI* regions present ranging from Ib to V. The higher *GST* values and *WI* regions are associated with the lower elevations across the Douro River valley and its tributaries also increasing their presence as they are more distant from the Atlantic influence towards the east. The *GSP* spatial pattern results both from the yearly storm distribution and the variable topographical characteristics present in the area.

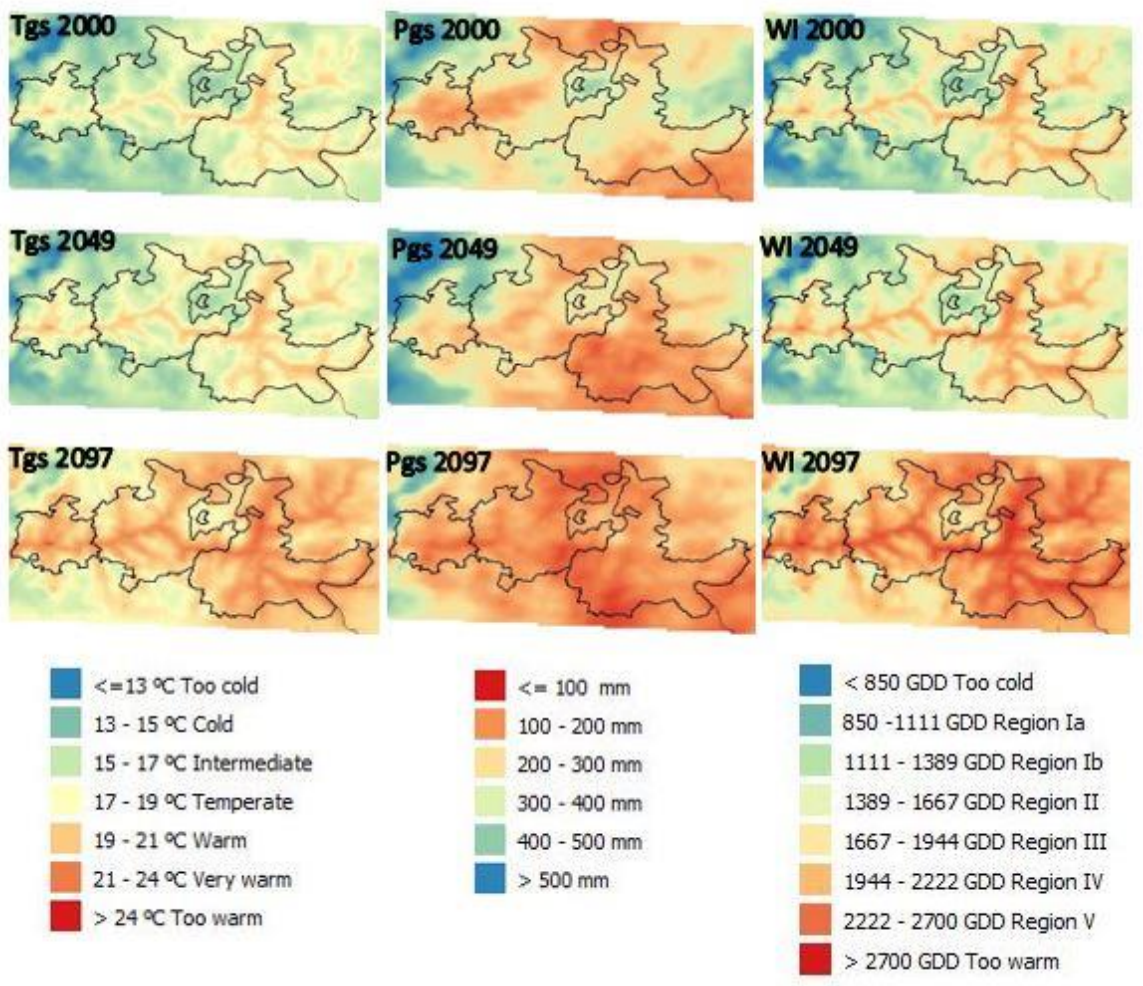

Figure 2-7. Grapevine mean *GST*, *GSP* and *WI* thematic layers derived from very high-resolution 1 × 1-km WRF-MPI RCP8.5 hourly simulations for selected representative recent-past (2000), mid-term future (2049) and long-term future (2097) years in the DDR.

For the year 2049 mid-term simulation, *GST* intermediate conditions decrease their presence whereas warm conditions become more frequent; there is an increase of cells with only 100–200 mm of *GSP*, and *WI* regions Ib and II reduce their area at the same time as IV and V increase their coverage.

Finally, the year 2097 long-term MPI-WRF future simulation indicates the disappearance of temperate conditions which are substituted either by warm or very warm areas; *GSP* values fall below 200 mm with about half of the cells having only 100 mm or less, and there is a continuation of *WI* diversity loss towards the warmer end, with only regions IV and V being present and extensive areas considered as too warm for wine production.

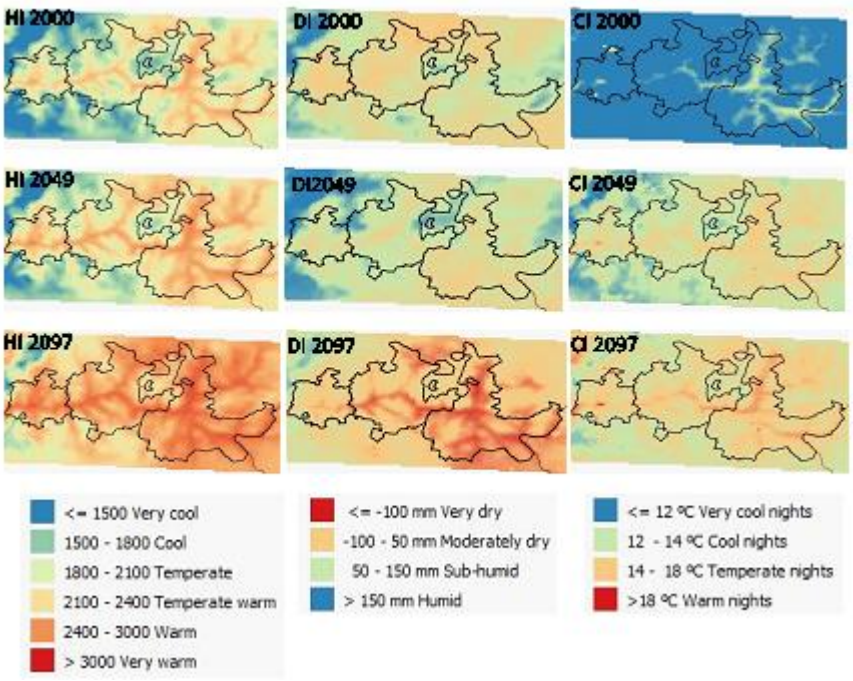

Figure 2-8. *HI*, *CI* and *DI* thematic layers derived from very high-resolution 1 × 1-km WRF-MPI RCP8.5 hourly simulations for selected representative recent-past (2000), mid-term future (2049) and long-term future (2097) years in the DDR.

Figure 2-8 illustrates the *HI*, *DI* and *CI* thematic layers derived from WRF-MPI simulations for recent-past (2000), mid-term future (2049) and long-term future (2097) years in the DDR. For the year 2000 recent-past simulation, most cell values within the DDR are associated with the temperate, temperate-warm and warm classes, with the presence of the cooler classes at higher elevations. *DI* ranges between the moderately dry and the sub-humid classes, with the drier areas associated with topographical valley lows and the

absence of storms. *CI* is also represented almost exclusively by the very cool and cool night classes, with higher values associated with lower elevations especially in the Douro Superior subregion. For the year 2049 mid-term future simulation, *HI* temperate conditions are reduced in area whereas the temperate-warm and warm classes become more frequent; *DI* continues to range between moderately dry and sub-humid classes depending on topography and annual storm coverage, and there is a marked shift in *CI* from very cool or cool night conditions to temperate or warm night conditions.

Finally, the year 2097 long-term MPI-WRF future simulation indicates the disappearance of the temperate and temperate-warm conditions which are substituted by either warm or very warm areas; *DI* undergoes a marked shift to very dry conditions at the lower elevations in the central and eastern subregions, and there is an increase of *CI* warm night areas mainly associated with topographical lows.

In Figure 2-9, sets of probability density function graphs for the grapevine mean *GST*, *GSP*, *WI*, *HI*, *DI* and *CI* are shown as derived for the mapped vineyard areas present in the DDR, which were identified by overlaying the Portuguese CORINE 2006 land-use map over the very high-resolution 1 × 1-km WRF-MPI-based thematic layers. Clear shifts towards warmer and drier conditions are observed, as previously commented on for all the land included within the DDR limits. These shifts become more pronounced from the mid-term 2049 simulation to the long-term future 2097, except for *CI* which changes abruptly in the mid-term future.

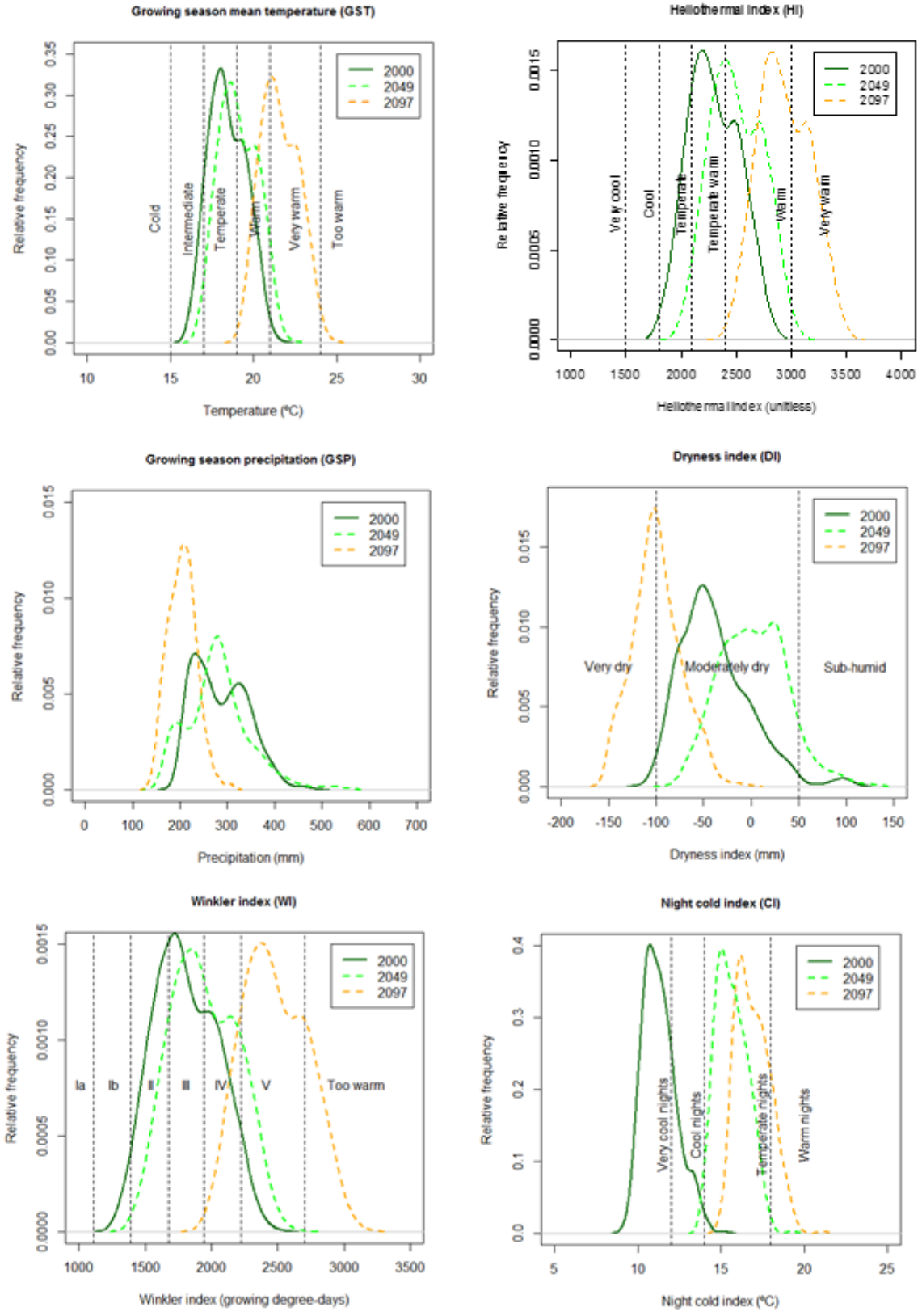

Figure 2-9. *GST*, *GSP*, *WI*, *HI*, *DI* and *CI* probability distributions as derived for mapped CORINE 2006 vineyard areas in the DDR.

2.5 CONCLUSIONS

The WRF-ERA 1986–2005 simulations for the DDR satisfactorily compare with April to October *GST* estimates based on the daily E-OBS dataset. The application of a specific local grapevine varietal phenological model to derive phenological stages from the WRF-ERA daily simulations also gives satisfactory results when the elevational differences between the WRF cells and the phenological observational site are also considered. When a 4D 1 × 1-km configuration is used for selected warm *GST* years, the simulated phenological dates closely resemble those reported in the DDR: a simulated mean value of the 83rd Julian calendar day for budburst, and the 207th Julian calendar day for *véraison* against observed values of 84th and 201st for budburst and *véraison*, respectively, for the specific Tinta Roriz-Touriga Franca thermal requirements adopted in this work. The year-2000 1 × 1-km dynamically downscaled WRF-MPI simulations also resulted in a closer agreement with the values of the viticultural bioclimatic indices and climate parameters estimated for the area by other studies such as those of Climaco et al. (2012) or Jones and Alves (2012).

Despite the limitations of the 9 × 9-km WRF-ERA simulations to reproduce the viticultural climate of an area of complex topography such as the DDR, it is still possible to select a representative cell or group of cells (e.g. the eastern subregion) to relate the 1986–2005 recent-past climate to vintage yield and Port wine vintage rating records in the area. Results confirm previous studies on the positive correlation between higher growing-season heat accumulation and greater vintage yields. Correlations found by using a thermal phenological model are often higher than those using conventional calendar-based monthly phenological divisions. Therefore, the phenological modelling also provided insight to understand the interactions between surface atmospheric conditions and vintage yield and quality in the DDR.

In general, the WRF-MPI very-high 1 × 1-km resolution simulations show an important increase in summer days (*SU25*) and very hot days (*SU35*) and an important reduction in frost days (*FD0*). These variations in climate extreme indices could relate to a higher incidence of heatwaves and fewer chilling units during dormancy and could pose a threat to maintenance of vintage quality. The simulations also illustrate an important advancement in phenology and shortening of the budburst to *véraison* period which could also expose the berries to warmer atmospheric conditions. Concerning bioclimatic parameters and indices, there is an increase in the average temperature during the

vegetative period of the grapevine, and a concurrent decrease in *GSP*, with the greatest changes taking place in the second half of the 21st century. *WI* is typical of values associated with the production of high-quality wines in the recent past. However, the future WRF-MPI climate scenarios show a decrease in the diversity of *WI* regions towards warm or very warm areas associated with the intensive production of wines of intermediate quality, especially by the end of the century. *HI* also exhibits a potential change from temperate or temperate-warm conditions to warm or very warm conditions although this transition is more gradual than in the *WI* case. In the recent past, *CI* was associated mainly with very cool night conditions which are commonly related to the production of quality wines, but from the mid-term future scenario there is also a marked shift to temperate night conditions, reaching even warm night conditions for several areas at the end of the century. Finally, *DI* associates with a similar range of values between the moderately dry and the sub-humid class during the recent-past and mid-term future simulations, with results apparently associated mainly with the varied topography of the DDR and storm coverage. However, there is a considerable increase in water stress, which is already considered high under the present climate, at the end of the century.

The used methodology provides evidence for future strategies aimed to preserve the high-quality wines in the region and their typicality as it presents the current and future broad picture for the selected climate parameters, bioclimatic and extreme indices in the DDR using conventional standards accepted worldwide. Coupling of climate simulations with dynamic crop models capable to simulate grapevine growth while integrating plant phenotype, soil profiles, weather data, CO_2 effects, and management options, has been applied at the European scale (Fraga et al., 2016). Other studies such as those of Santos et al. (2018) and Fraga et al. (2019) consider bioclimatic indices that incorporate non-linear plant-temperature relationships (e.g. chilling portions or growing degree hours). Whereas these methods have great potential to provide more physiologically consistent results, their application in viticulture is still relatively scarce, and there is still a considerable need to validate calibration data, assumptions and results concerning Portuguese grapevine varieties and their growing conditions.

These results do not necessarily imply a dramatic decrease of viticultural suitability in the DDR in the mid-term and long-term future scenarios, as adaptive measures can be taken and are already being taken by the grapevine growers in the area, and there is also a

constant evolution of wine consumer preferences (van Leeuwen et al., 2013). In this sense, several actions can be proposed to preserve as much as possible the DDR wine typicity, taking current state-of-the-art knowledge (Fraga et al., 2017; Hannah et al., 2013; van Leeuwen and Darriet, 2016) and previous works done in the study area (e.g. Jones and Alves, 2012) in a compromise to balance as much as possible economic, environmental and social costs. Short-term adaptations to increased temperatures and water deficits include the selection of suitable rootstocks, and late-ripening clones or varieties. Adapted training systems (e.g. *gobelet*), and canopy management (e.g. late pruning, reduced hedging and leaf pulling) can be applied to reduce water consumption, delay phenology or limit solar exposure too. Soil management can also be considered to increase the soil water holding capacity (SWHC) to promote a higher replenishment of the soil water storage by winter rains and growing-season storms. When there is need of irrigation, precise strategies such as deficit irrigation should be considered. It is also possible to relocate the vineyards in the long term to cooler sites such as higher elevations or areas with lower solar exposures or closer to the sea. These relocations should also be carefully planned in order to maintain as much as possible freshwater resources and natural habitats.

3 ASSESSMENT OF TROPOSPHERIC OZONE PHYTOTOXIC EFFECTS ON THE GRAPEVINE (*VITIS VINIFERA* L.): A REVIEW

This chapter was published as:

Blanco-Ward, D., Ribeiro, A., Paoletti, E., Miranda, A., 2021. Assessment of tropospheric ozone phytotoxic effects on the grapevine (*Vitis vinifer*a L.): a review. Atmos. Environ. 244. https://doi.org/https://doi.org/10.1016/j.atmosenv.2020.117924

I mainly contributed with the download and postprocessing of data from the Norwegian Meteorological Institute and the Tropospheric Ozone Assessment Report (TOAR) and the literature review. I was also responsible for the writing of the paper.

Abstract

The grapevine (*Vitis vinifera* L.) is a crop with great cultural, economic and ecological relevance for Mediterranean environments besides being the fruit crop with largest acreage and economic value at the global scale. Its exposure to high levels of tropospheric ozone (O_3) can result in phytotoxic effects and thus it is important to comprehensively re-evaluate these effects as well as related processes. A review of the validity and limitations of the standards used for the protection of vegetation in relation to ambient O_3, the state-of the-art knowledge on O_3 phytotoxic effects on the grapevine and the available means to assess its impact are presented and discussed. It is concluded that wide regions in the world, mainly between latitudes 30° and 50° N, where the grapevine has been traditionally cultivated, are exposed to O_3 concentrations that can affect both the yield and quality of the grape. Recently reported studies for global cultivars such as Cabernet Sauvignon or Merlot, along publicly available maps on O_3 standards to protect vegetation at the European and global scale, indicate potential yield reductions in the range of 20-31% and the quality of the grape can also be affected by reductions of total polyphenols in the range of 15-23% for these areas. Although a tendency to reduce ambient O_3 levels has been registered since 2000 in the western European Mediterranean basin, the flux of O_3 into the grapevine leaves could still exceed critical levels with phenological advancement driven by the increase of temperatures or interaction between O_3 and other climatic variables such as drought or high summer light intensities. Higher O_3 exposures are reported in western United States of America and eastern China, with this last region maintaining an increasing

tendency in summer ambient O_3 levels. It is still necessary to adopt common experimental and monitoring protocols to establish grapevine specific O_3 relationships and critical levels, as there is not yet a coherent and shared database for detailed risk assessment for this crop.

3.1 INTRODUCTION

Surface ozone (O_3) is produced in the troposphere by the catalytic reactions of nitrogen oxides (NO_x) with carbon monoxide (CO) and volatile organic compounds (VOC) in the presence of sunlight (Monks et al., 2015; Seinfeld and Pandis, 1998; The Royal Society, 2008). O_3 at low concentration is a normal component of the troposphere, but background levels have increased globally since pre-industrial times reaching current average concentrations ranging from 20 to 45 ppb (Booker et al., 2009; Krupa et al., 2000; Monks et al., 2015). Exposure to ambient O_3 can cause adverse effects corroding materials, damaging the respiratory systems of humans and animals and altering several physiological processes in vegetation (Mauzerall and Wang, 2001; The Royal Society, 2008). O_3 was first identified as a phytotoxic pollutant back in the late fifties in relation to foliar injury in vineyards and tobacco (Richards and Taylor, 1965). By the early sixties, O_3 was known as the main air pollutant affecting crops at some locations (Dairies et al., 1982). By the beginning of this century it became evident that O_3 is by far the most important phytotoxic air pollutant worldwide (Krupa et al., 2000) causing foliar injury and reduction in growth, yield and quality on many agronomic and horticultural crops (Booker et al., 2009), deciduous trees and conifers (Matyssek and Innes, 1999; Skarby et al., 1998), seminatural (Bassin et al., 2007; Volk et al., 2006) and natural vegetation communities (Pfleeger et al., 2010).

Yield loss due to ambient O_3 in the United States of America (USA) based on the large-scale experimental studies conducted in the 1980s at the National Crop Loss Assessment Network (NCLAN) was estimated to be about 10% for one third of the crops (EPA, 1996). In Europe, data driven from the European-Top Chamber Programme in the nineties suggested a reduction on wheat yield greater than 5% (Mauzerall and Wang, 2001). O_3 damage has also been observed in Asia across China, India and Pakistan for important crops such as wheat, rice and legumes with estimated yield losses ranging from 3% up to 65%, and the

scale of the problem in Asia could have been underestimated through the use of North American derived exposure-response relationships (Emberson et al., 2009). By using exposure-response relationships derived from open-top-chambers (OTC) in China, annual yield reductions for rice and wheat have been estimated to be in the order of 8% and 6% respectively (Feng et al., 2019). Global estimates of reduction in yield at the beginning of the century performed by means of modelling O_3 concentrations and concentration-response functions for three different staple crops were in the order of 8.5-14% for soybean, 3.9-15% for wheat and 2.2-5.5% for maize with total crop production losses between 79-121 million metric tons worth \$11-18 billion USD_{2000} (Avnery et al., 2011a).

A global study presented by the Tropospheric Ozone Assessment Report (TOAR) concerning present-day O_3 exposures and trends relevant to vegetation mentioned important reductions over 1995-2014 in North America and Europe and significant increases in East Asia, whereas Europe had the lower present summer ambient O_3 exposures and East Asia the highest (Mills et al., 2018). These figures are relevant as the global population is expected to grow from 6 to 9 billion between 2000 and 2050 and O_3-precursors are expected to increase in developing countries with a global impact due to transport between continents (Fiore et al., 2009). As surface O_3 concentrations are also expected to increase in many regions until 2050, even in the case that current legislation is implemented, O_3 could become a threat to global food security in the same order of magnitude as climate change (The Royal Society, 2008). Moreover, and despite a reduction on O_3 exposure under RCP2.6 and RCP4.5 scenarios, critical O_3 levels for the protection of forests and crops have been estimated to be exceeded in many areas of the northern hemisphere by 2100 and they could be much more exceeded under RCP8.5 (Sicard et al., 2017).

In European Mediterranean regions, in particular, weak levels of anti-cyclonic subsidence, low winds, and strong insulation with development of mesoscale processes and recirculation within air masses are frequent during the summer (Millan et al., 2000). These conditions favour the photochemical production of O_3, and ambient concentrations can be high enough to have phytotoxic effects. Several biomonitoring studies and field observations have indicated that O_3 injury is widespread on numerous crops (Hayes et al., 2007) and forests (Paoletti et al., 2019) grown in the European Mediterranean region. As such, visible injury has been reported on 24 agricultural and horticultural sensitive crops species in commercial fields with effects noticed on wide areas of thousands of square

kilometres during some O_3 episodes for crops, such as watermelon in north-eastern Spain or, on a more local scale, producing near 100% of crop loss for sensitive horticultural species such as lettuce or chicory (Fumagalli et al., 2001; Hayes et al., 2007; Pleijel, 2000). Wheat, maize and grapevine, which represent over one-third of the agricultural areas of Italy, Spain and Greece, are some of the crops where visible damage has been reported (Fumagalli et al., 2001).

A review study concerning tropospheric O_3 measurements representative of Mediterranean Southern Europe described an increasing trend in concentrations until the 1970s-1980s followed by a trend rate decrease since the 1990s, and identified that these concentrations were related with photochemical local production, transport of O_3 and its precursors, intrusion from the stratosphere and transport of mineral dust from the Saharan desert which could also be affected by climate change (Cristofanelli and Bonasoni, 2009). A later study based on hourly O_3 data from 214 stations from the Air quality database of the European Environment Agency (EEA) demonstrated that there has been an average decrease of 0.43% per year in rural stations in the Western European Mediterranean basin over the time period 2000-2010 and that this trend could be associated to O_3 precursor's emissions control measures, but it also warned that an increase of temperatures and dry weather could reduce the observed trend and that further studies are still required to take into account the role of climate change in the actual trends of ambient O_3 concentrations in this region (Sicard et al., 2013). An evaluation of the effects of climate and emission changes on air quality over Europe, for the 2030s and 2050s, pointed out that the levels of O_3 could decrease over the South of France, Italy, Spain and Greece in the 2030s benefiting from the European precursors' emission reduction policies. However, the changes in meteorological fields, as the increase in temperatures, and the influences of long-range transport, could significantly offset the benefits of reducing emissions in the 2050s (Lacressonnière et al., 2014). The impact of a +3°C increase of temperature under the RCP8.5 scenario, which would correspond to the intended nationally determined contributions to reduce greenhouse emissions before The Paris 2015 climate conference, could annihilate the benefits of emission reduction policies with a number of O_3 exceedance days over the World Health Organization threshold (maximum daily 8-h average O_3 concentrations - *MDA8* > 50 ppb) reaching 100 per year over the Mediterranean

Sea and adjacent areas along the 2040-2069 period and strongly affecting both human health and vegetation (Fortems-Cheiney et al., 2017).

The main purpose of this paper is to assess to what extent the current and future surface O_3 scenarios might be of relevance for a crop such as the grapevine, which has immense cultural, economic and ecological importance within the Mediterranean basin besides being the fruit crop with the largest acreage and highest economic value globally (Ponti et al., 2018). There is already a good number of studies in relation with climate change as a potential threat to wine production and typicity in these areas (e.g. Blanco-Ward et al., 2019; Fraga et al., 2016; Mira de Orduña, 2010; van Leeuwen and Darriet, 2016), but there is still a lack of studies addressing the potential effects of changes in the meteorological fields, drought or carbon dioxide (CO_2) atmospheric enrichment in relation to surface O_3 for this crop. To assess the relevance of ambient O_3 in the context of climate change for the grapevine, this work first presents the main exposure indicators commonly used as standards to support decision making on O_3 abatement policies against vegetation effects (Section 3.2). It continues reviewing what is the current knowledge concerning surface O_3 phytotoxic effects on the grapevine as noticed from observational or experimental studies including research gaps and prospects for future advancement (Section 3.3). Next, a section covering the modelling approaches that can be applied to assess the effects of O_3 on vineyards is presented (Section 3.4). Based on the state-of-the-art knowledge presented in the previous sections, the relevance of O_3 in the current and future surface O_3 scenarios for the grapevine and current assessment limitations are discussed (Section 3.5). Finally, the main conclusions from this work are highlighted (Section 3.6).

3.2 POLICY ORIENTED STANDARDS FOR VEGETATION

3.2.1 European and CLRTAP standards

The United Nations Economic Commission for Europe (UNECE) Convention on Long-Range Transboundary Air Pollution (CLRTAP) has extensively used the parameter *AOT40* (Accumulated O_3 concentration over a Threshold of 40 ppb) to support decision making on pollution abatement policies (CLRTAP, 2017a). Its mathematical expression follows:

$$AOT40 = \sum_{accumulation\ period} (0; C_c - 40)\Delta t \qquad (1)$$

C_c is the hourly mean O_3 concentration (in ppb) in a time interval, Δt, which is set to an hour. This parameter has also been adopted by the European legislation in the Directive 2008/50/EC although there are differences regarding its use. According to this directive, the *AOT40* is estimated using hourly O_3 concentrations values measured or modelled between 8:00 and 20:00 CET (Central European Time). The accumulation period is different for crops (May 1st – July 31st) and forests (April 1st – September 30th). According to the CLRATP, the index should be calculated for daylight hours (global radiation > 50 W m^{-2}) during the growth season of the vegetation species studied at canopy height (De Andrés et al., 2012).

Cumulative exposure-based critical levels (CL_{ec}) were first defined in the CLRTAP Gothenburg protocol, which came into force in 1997, as "the atmospheric concentrations of pollutants in the atmosphere above which adverse effects on receptors, such as human beings, plants, ecosystems or materials, may occur according to present knowledge" (The Royal Society, 2008). Extensive research was performed in the following years to set exposure-based critical levels (CL_{ec}) following the AOT40 exposure-based or level I approach for agricultural and horticultural crops (e.g. Fagnano et al., 2009; González-Fernández et al., 2014; Mills et al., 2007), trees (e.g. Karlsson et al., 2003), and (semi-) natural vegetation. The effect to be considered on vegetation ranges from a 5% grain yield reduction for agricultural and horticultural crops to a 10% above-ground biomass reduction for annual dominated (semi-) natural vegetation. Whereas the European Union established an *AOT40* target value of 9 ppm-h from May to July as a result of averaging five or three years of available data for all vegetation species and a stricter long-term *AOT40* target value of 3 ppm-h, the UNECE CLRTAP distinguished different thresholds depending on vegetation type and observed effect on a yearly basis. Table 3.1 shows the different O_3 critical levels considered for vegetation in Europe. Since 2005, only the critical level for horticultural crops has been revised (CLRTAP, 2017b).

Table 3-1. Current exposure O_3 standards for vegetation in Europe.

Source	Vegetation type	Accumulation period	Effect	CL_{ec} (ppm-h)
Directives 2002/03/EC 2008/50/EC	Any type	May-July 8:00 – 20:00 CET	Any	9 (5 - 3 years) 3 (long-term target value)

UNECE CLRTAP, 2017	Agricultural	3 months, daytime hours > 50 W m^{-2}	5% grain yield (based on wheat)	3 (in a year)
	Horticultural	3-5 months, daytime hours > 50 W m^{-2}	5% fruit yield (based on tomato)	8 (in a year)
	Annual-dominated (semi) –natural vegetation	3 months (or growing season if shorter), daytime hours > 50 W m^{-2}	10% above-ground biomass	3 (in a year)
	Perennial-dominated (semi) –natural vegetation	6 months, daytime hours > 50 W m^{-2}	5% total biomass	5 (in a year)
	Trees	Growing season (default: 6 months), daytime hours > 50 W m^{-2}	5% total biomass (based on beech and birch)	5 (in a year)

The cumulative exposure of level-I approach has been criticized, as it does not relate with the actual dose or flux of O_3 entering the plant (Mills et al., 2011b). Moreover, in Mediterranean environments, it often overestimates the risk as the recommended thresholds are exceeded in these areas without proportional evidence of damaging effects on vegetation as one would expect of such exceedances (Cieslik, 2009; Ferretti et al., 2007). Reasons for this might include the avoidance/tolerance strategies and mechanisms/traits present in the Mediterranean vegetation, such as sclerophylly which promotes better stomatal control, low gas exchange rates, strong emission of volatile organic compounds (VOC) and capacity to minimize oxidative stress through primary antioxidants (Ferretti et al., 2007; Nali et al., 2004; Paoletti, 2006).

To overcome these limitations, a flux-based or level-II approach was recommended as the preferred tool for risk assessment by the CLRTAP Convention since 2010 (Mills et al., 2011b). This approach has a stronger biological basis as it estimates a Phytotoxic Ozone Dose (*PODY*) using the O_3 stomatal uptake: the amount of O_3 molecules that penetrate the leaf tissue through the stomata as a function of ambient O_3 concentration and several other critical environmental parameters, such as temperature, vapour pressure deficit (*VPD*),

light, soil water potential and plant growth (phenological) stage (CLRTAP, 2017a).The *PODY* is defined as:

$$PODY = \sum_{accumulation\ period} (0; Fst - Y)\Delta t \qquad (2)$$

Fst is the instantaneous flux of O_3 through the stomatal pores per unit of projected leaf area (PLA). It refers specifically to the sunlit leaves at the top of the canopy. It is regarded as the hourly mean flux of O_3 into the stomata. *Y* is the threshold stomatal flux per PLA. Both parameters have units of nmol m^2 s^{-1}. Critical levels based on stomatal flux (Cl_{ef}) are then cumulative stomatal fluxes above which adverse effects may occur according to present knowledge. Therefore critical levels are currently defined in relation to vegetation as the "concentration, cumulative exposure or cumulative stomatal flux of atmospheric pollutants above which direct adverse effects on sensitive vegetation may occur to present knowledge" (CLRTAP, 2017b).

Some examples of Cl_{ef} can be found in Table 3.2. In this table, the term PODYAIM refers to a vegetation-type specific *PODY* requiring less input data and suitable for large-scale modelling, including integrated assessment modelling whereas *PODYSPEC* is a species or group of species-specific *PODY* requiring comprehensive input data and suitable for detailed risk assessment at any geographical scale up to the climatic or biogeographical region (CLRTAP, 2017a). As it happened with the exposure-based critical levels, stomatal flux-based O_3 standards also vary depending on vegetation type, associated accumulation period, observed effect and assessment purpose (large-scale AIM or detailed SPEC assessment). For instance, it can be observed that a wheat *POD6SPEC* standard which has been derived for 4 wheat cultivars has a lower Cl_{ef} value than a wheat based *POD3AIM* for the same observed effect (i.e. a 5% reduction in grain yield). The first standard is based on many specific observed stomatal flux dose-effect relationships (i.e. 36 data or points) observed within a given climate or biogeographical area (i.e. experiments which took place in Belgium, Italy, Finland and Sweden) whereas the second standard is based on simplified generic crop dose-effect accommodating for a lower *Y* threshold value being better suited for large-scale studies. In contrast with exposure based critical levels, there is a clearer distinction between specific crops (i.e. wheat, potato, tomato), with higher *Y* thresholds and lower flux-based critical levels, and semi-natural grasses or trees with lower thresholds

and larger flux-based critical values. AIM flux-based standards also involve lower Y thresholds and larger flux-based critical values than specific crop standards.

Table 3-2. Current stomatal uptake O_3 standards for vegetation in Europe (CLRTAP, 2017).

Vegetation type	Standard	Accumulation period	Effect	Cl_{ef} (mmol m^{-2})
Wheat	*POD6SPEC*	200 °C days before anthesis to 700 °C days after Anthesis	5% grain yield reduction	1.3
			5% 1000 grain weight reduction	1.5
			5% protein yield reduction	2.0
Potato	*POD6SPEC*	1130 °C days starting at plant emergence	5% tuber yield reduction	3.8
Tomato	*POD6SPEC*	250 to 1500 °C days starting at planting in the field (at 4th true leaf stage)	5% fruit yield reduction	2.0
			5% fruit quality reduction	3.8
Temperate perennial grassland	*POD1SPEC*	3 months from April 1st to Sept 30th	10% above-ground biomass reduction	10.2
			10% total biomass reduction	16.2
			10% flower number reduction	6.6
Mediterranean annual pasture	*POD1SPEC*	1.5 months from February 1st to June 30th	10% above-ground biomass reduction	16.9
			10% seed/flower biomass reduction	10.8
Beech and Birch	*POD1SPEC*	Growing season	4% whole tree biomass reduction	5.2
Norway spruce	*POD1SPEC*	Growing season	2% whole tree biomass reduction	9.2
Mediterranean deciduous oak trees	*POD1SPEC*	Growing season	4% whole tree biomass reduction	14.0

			4% root biomass reduction	10.3
Mediterranean evergreen trees	*POD1SPEC*	Growing season	4% above-ground biomass reduction	47.3
Crops (Based on wheat)	*POD3IAM*	90 days centred on the timing of mid-anthesis (flowering) in wheat	5% grain yield reduction	7.9
Non-Mediterranean broadleaf trees	*POD1IAM*	The start and the end of the accumulation period is determined by a latitude model.	4% whole tree biomass reduction	5.7
Mediterranean broadleaf trees	*POD1IAM*			13.7

From a research perspective, the Cl_{ef} provides extremely useful information and it offers more realistic estimates of the actual O_3 risk in Mediterranean environments at large scales under different scenarios. However, the Cl_{ef} approach implies the estimation of several variables (related to meteorology, atmospheric chemistry, canopy geometry, soil and plant physiology), which make difficult to quantify the total amount of error that propagates up to the final stomatal flux estimates, and therefore the uncertainty of the final value is considerable (Gerosa and Anfodillo, 2003). Moreover, it does not usually take into consideration yet detoxification processes (Musselman et al., 2006) nor the non-stomatal uptake, which accounts for 30-70% of the total O_3 flux in Mediterranean environments leading to an overestimation of *PODY* (Gerosa et al., 2005). Another important disadvantage of using a Cl_{ef} methodology concerns its complexity to be used for setting standards accessible to environmental agencies for regulatory purposes. These agencies would take more benefit of a more practical concentration-based approach and better suited for routine monitoring at national and/or sub-national scale if suitable experimental data, field assessment and monitoring data are available for different CL_{ec} for distinct parts of Europe (Ferretti et al., 2007; Paoletti and Manning, 2007).

There is also a need of gaining consistency by linking different investigation levels (from the cell to the plant and the ecosystem level) and approaches (large-scale monitoring to chamber and free-air fumigation experiments) (Ferretti et al., 2007). In this regard, the

International Union of Forest Research Organisations (IUFRO), through its series of biennial conferences on Air Pollution and Forest Ecosystems, has also emphasized the relevance of performing multi-factorial studies to understand the complex interactions between climate, air pollution (with main focus on O_3 and N deposition), and forests, at scales from single genes to the entire planet by making use of large-scale field data acquisition and long-term experiments utilizing Free-Air Controlled Exposure (FACE) systems to provide knowledge to managers, policymakers, and stakeholders (Sicard et al., 2016). For the Mediterranean region, there is also acknowledgement of the urgent need to implement common and coordinated research and experimental platforms along with wider and more representative environmental networks by groups of scientists both at the European (e.g. CAPERmed) and global scales (e.g. MEDECOS) with encouragement to participate more in large-scale initiatives such as the International Long Term Ecological Research (ILTER network) or the UNECE-CLRTAP International Cooperative Programme (ICP) with initiatives such as ICP-Forest, ICP-Vegetation and ICP-IM (Ochoa-Hueso et al., 2017). In relation to this, the networks to comply with EU regulation and the CLRTAP along experimental data collected in the framework of other European programs (LIFE, INTERREG, and H2020) distributed over Italy are already contributing with a high number of monitored parameters so that flux-based assessments are recommended as part of monitoring air pollution impacts on ecosystems in the revised EU National Emissions Ceilings Directive (NECD, 2016/2284/EU) (De Marco et al., 2019). The project MOTTLES "MOnitoring ozone injury for seTTing new critical LEvelS", is also a good example of using 17 long-term monitoring sites in France, Italy and Romania from main European networks involved in air-quality monitoring (MERA in France and ICP Forests in Italy and Romania) to assess the value of *AOT40* and *PODY* metrics in association with forest-health indicators such as radial growth, crown defoliation and visible leaf O_3 injury with this last indicator being better correlated with *PODY* and thus, being a good forest-health indicator of tree responses to O_3 (Paoletti et al., 2019).

3.2.2 US standards

The *W126* metric is used by the US Environmental Protection Agency (EPA) for assessing risk to vegetation from O_3 exposure. It is defined as the sigmoidal weighted sum of all hourly O_3 values observed during a specified daily and seasonal time window, where each

hourly O_3 value is given a weigh that increases from zero to one with increasing O_3 value. Its mathematical expression is given by:

$$W126 = \sum_{three-month\ period} (w_i\ x\ C_i)\Delta t \qquad (3)$$

C_i is the hourly mean O_3 concentration (in ppb) in a time interval, Δt, which is set to an hour for a period from 8:00 AM to 8:00 PM local time each day. The weight, w_i, is given by the following sigmoid function (US Federal Registry, 2015):

$$w_i = 1/[1 + M\ x \exp(-A\ x\ C_i/1000)] \qquad (4)$$

where M = 4403, A = 126, and where C_i is the hourly mean O_3 concentration at the specified daytime hours (in pbb). Moving 3-month sums are calculated from the monthly index values, and the highest of these 3-month sums per year is determined as the annual *W126* index. The annual *W126* index values are then averaged across each consecutive 3-year period to obtain the final *W126* values with units in parts per million-hours (ppm-hrs) (US Federal Registry, 2015). Analyses of data from air quality monitors showed that attainment of an 8-hour standard of 70 ppb (0.07 ppm) averaged over three years would also keep the averaged *W126* index below 17000 ppb-hrs. Thus, the US EPA established a secondary O_3 standard at the 70 ppb level to protect human welfare by improving protection for trees, plants, and ecosystems. This is the same as the primary standard for protection of human health. Primary standards provide public health protection, including protecting the health of "sensitive" populations such as asthmatics, children, and the elderly. Secondary standards provide public welfare protection, including protection against decreased visibility and damage to animals, crops, vegetation, and buildings (Lefohn et al., 2018; US Federal Registry, 2015). Table 3.3 offers an overview of standards and vegetation-based critical levels for O_3 in USA.

Table 3-3. Current exposure O_3 standards for vegetation in USA.

Source	Vegetation type	Accumulation period	Effect	CL_{ec} (ppb-hrs)
US National Ambient Air Quality standards for	Trees, plants and ecosystems *(NAAQS_Ecosystems, public welfare secondary standard).*	*W126*, highest consecutive three months	Any	17000 ppb-hrs, three-year average
	Crops	*W126*, highest consecutive three	To prevent median	15000 ppb-hrs,

vegetation (NAAQS)	*(NAAQS_Crops secondary standard.)*	months	crop loss from exceeding 5%	three-year average
	Tress, plants, and ecosystems *(NAAQS_Injury, public welfare secondary standard).*	*W126*, highest consecutive three months	To reduce foliar injury prevalence	10000 ppb-hrs, three-year average
	Trees *(NAAQS_Trees, public welfare secondary standard).*	*W126*, highest consecutive three months	To limit tree relative biomass loss to no greater than 2%	7000 ppb-hrs, three-year average
	Vegetation type	Accumulation period	Effect	CL (ppb)
	Tress, plants and ecosystems. Primary (public health protection) and Secondary (public welfare) standard.	The 4th highest 8-h average concentration (*MDA8*) beginning from 7:00 AM to 11:00 PM each day.	Any	70 ppb, three-year average

As in *AOT40*, *W126* is vegetation type/species-specific, higher O_3 levels have greater impact on vegetation, and the metrics are accumulated over specific time intervals and at particular times of the day to reflect the time-period when plants are most likely to absorb O_3 (Lefohn et al., 2018). *AOT40* and *W126* can be strongly correlated but *CLRTAP_CLs* appear to be more stringent than the US National Ambient Air Quality standards for vegetation critical levels (*NAAQS_CLs*) from correlation studies performed at the global scale for the tropospheric O_3 assessment report on vegetation (TOAR vegetation) with, for instance, the *CLRTAP_CL_AOT40* wheat-based for crops of 3000 ppb-hr corresponding to a *W126* of 2578 ppb-hrs (Mills et al., 2018). A similar observation has been provided by De Marco et al. (2010) who compared exceedance air quality standards in Italy and found that the higher protection (98.1%) of durum wheat sites was provided by the *CLRTAP_CL_AOT40* whereas the *NAAQS_CLs_W126* for the protection of O_3 sensitive species (7000 ppb-hrs) would protect a lower proportion of the sites (86.2%) when calculated over the April to June (A-J) durum wheat growing season.

3.2.3 Other metrics used at the global scale

Within the context of TOAR vegetation, several exposure metrics are proposed with the purpose to better assess present-day tropospheric ambient O_3 distribution and trends relevant to vegetation at a global scale. According to Lefohn et al. (2018), these are the following:

1. An exposure metric that focus on the mid-range of hourly average O_3 levels such as the daily 12-h (08:00–19:59h) average exposure metric (*M12*) (ppb). This exposure metric was also widely used in the past to characterize crop exposures and to establish crop-specific exposure–response relationships before it was realized that indices giving higher weight to the higher O_3 levels, such as *W126*, better fitted the yield loss observations for the experiments conducted in the US. The *M12* metric can be estimated for a 3-month period for wheat and rice, a 6-month period (or 7-month period where earlier starting growth cycles are required) for perennial crops (e.g. citrus or grape), or for a 12-month period for tropical or subtropical climate zones.
2. Exposure metrics that weight the higher O_3 levels and include mid-level values, like the *W126* and *AOT40*, which are estimated for various months and daily time periods. *AOT40* metrics are also estimated for night-time conditions (clear sky radiation <5 W m^{-2} or sun elevation angle < -5 degrees).
3. Exposure metrics that include O_3 concentrations such as seasonal (i.e., December–February, March–May, June–August, and September–November), percentiles (median, 5th, 25th, 75th, 95th, 98th, and 99th) of hourly average O_3. The units are ppb. Trends in each percentile by season can provide information on specific changes that occur within the O_3 distribution. These changes can influence the magnitude of the exposure and stomatal uptake metrics.

From a first assessment based on the use of *M12*, *AOT40* and *W126*, it was recommended to continue to develop policy-relevant indicators or thresholds in countries and regions where these are not yet available, besides increased O_3 monitoring at rural sites and the inclusion of meteorological data into the TOAR database. A more complete global assessment of O_3 impacts on vegetation should also be conducted in the future, using an expanded TOAR dataset, including flux-based indices, namely in Asia, Africa and South and Central America, where datasets are scarce (Mills et al., 2018).

3.3 OZONE EFFECTS ON THE GRAPEVINE

3.3.1 Historical development of present knowledge

Notwithstanding the economic relevance of vineyards in the Mediterranean regions and for the global economy, there are no specific standards for this kind of vegetation. This section reviews published observational and experimental studies performed since the late fifties that provide evidence on the phytotoxic effects of ambient O_3 on the grapevine, which can be used as a support for risk assessment studies and also to provide some guidance on further studies to move from scientific studies to policy-oriented standards.

According to the early research of Richards et al. (1959), oxidant or O_3 stipple was first reported on grapevines in San Bernardino Valley, Southern California, during the 1954 summer. Field observations performed during the following years also identified other affected areas near Los Angeles and San Francisco. The typical primary foliar lesions were described then as small, brown to black dot-like lesions varying in diameter from about 0.1 to 0.5 mm confined to group of cells in the upper leaf surface bounded by the smallest veins. The primary lesions can aggregate to larger lesions up to 2 mm in diameter, which are the ones that confer the typical stippled appearance of the leaves (Figure 3-1) whose size was usually small for most grapevine varieties present in the area but could be larger for a few of them. Field observations over 16 grapevine varieties revealed then that O_3 had an effect starting early in the growing season on young but fully expanded leaves and accumulating progressively throughout the foliage season. Secondary symptoms resulting from a cumulative effect resulted in leaf yellowing and premature senescence. A selection of 12 cuttings of uniform leaf and plant size for 10 varieties where six of the replicates for each of the varieties were placed in a filtered-air glasshouse, and the other six in a glasshouse receiving unfiltered-air, revealed different percentages of leaf surface affected by oxidant stipple depending on variety.

Figure 3-1. Photos on the different levels of O_3 stipple aggregation on grapevine leaves for a French American hybrid variety identified as 'Vidal blanc'. McFadden-Smith, Wendy Author's (OMAFRA). © Queen's Printer for Ontario, 2018.

Another experiment was performed by Thompson & Kats (1970) in a vineyard near Cucamonga, California, during two growing seasons in 1968 and 1969. 6 closed-top plastic greenhouses with charcoal-filtered air were compared with other 6 closed-top greenhouses with non-filtered air affected by photochemical smog which was known to contain peroxyacylnitrates (PAN), nitrogen dioxide (NO_2), and O_3 as the predominant pollutant. Each greenhouse contained four mature grapevines of the 'Zinfandel' variety. The experiment started in May 1968. After 14 weeks since the beginning of the treatment, the leaves of the grapevines of the charcoal-filtered treatment were much greener than those exposed to non-filtered air. A chlorophyll analysis revealed that the grapevines from the charcoal-filtered greenhouses had much higher chlorophyll concentrations. At harvest time, the fresh weight per berry, sugar content of juice, weight of pruning and yield of grapes per vine were also much higher in filtered ambient air conditions. Finally, in 1969, 103 comparable grapevines were randomly selected, and separated into two groups of 50 and 53 grapevines each. The group of 50 grapevines received three treatments throughout the growing season with N,N´-diphenyl-p-phenylenediamine (DPPD) increasing yield per vine by 20.3% on average at harvest season compared with the grapevines without DPPD treatment. It was thought then that DPPD could be a preventive antioxidant measure against photochemical smog.

Brewer & Ashcroft (1983) performed a four-year field investigation on the effects of ambient photochemical oxidants on yield of grapevines of the 'Thompson Seedless' variety in the central San Joaquin valley in California over the growing season (mid-April to mid-October) from 1979 to 1982. The experimental set-up consisted of eight large rectangular

open-top chambers divided into four charcoal-filtered air and four non-filtered air treatments. Each of the chambers contained three ten-year-old own-rooted irrigated grapevines. No differences were found in the first year of treatment showing the relevance of the previous season in terms of determining the grapevine crop potential. The second year was lost due to a severe mildew infection. Yield responses measured as total weight of the bunches through the rest of the seasons were 17% higher in the third treatment year, a high yield year, to over 28% in the fourth treatment, a low-yield year, than the respective yields of non-filtered chambers. Concerning number of bunches, the figures were 17% and 11% higher for the third and fourth seasons, respectively, indicating a higher effect of atmospheric pollution on bunch size than on bunch set. Other production parameters affected were less pruning (wood weight) and reduced fruit sugar content. The authors recognized the 'Thompson Seedless' grapevine variety as moderately vigorous but they had no reason to consider it more sensitive or more tolerant to photochemical oxidants than other table or wine grapevine varieties grown in the area. They estimated a mean negative impact of approximately 20% on yields on the crop as a whole for the east side of the San Joaquin valley.

A review by Weinstein (1984) on the effects of air pollution on grapevines highlights its classification as a deciduous perennial crop with capacity to maintain a high productivity rate over many decades as the most important characteristic in relation to its response to air pollution. The quantity and quality of fully expanded leaves, especially the basal leaves of the shoots, are crucial for the grapevine growth as they are the major source of sugar production. It must also be taken into account that the flower cluster primordia are developed during the year preceding cropping and therefore research cannot be confined to a single year. The pruning system and canopy management (e.g. trellising system) might be also important for experimental studies. Grapevines can have a considerable size and be quite vigorous and robust, making enclosures difficult and able to accommodate for one or two vines only. Other problems are the existence of 'chamber-effects' for long-term enclosures, and that the roots might spread over an area beyond the boundary of the enclosure which may result in differences in soil-water relationships inside and outside the chamber. Weinstein concluded its review stating that the research relating airborne phytotoxicants with grapevine yield and quality at the time was still inadequate and poorly understood. Chamber experiments could be useful to assess local effects but are

insufficient to build dose-response information that could be used in the assessment of risk of a crop that may be grown under other variables associated with dose. The observation of the extent of the foliar lesions had shown that there are varieties extremely susceptible whereas others had a great degree of tolerance, but there had not been studies relating the degree of foliage susceptibility with fruit yield. Moreover, little work had been done to understand how the effects of the 'oxidant complex' or 'photochemical smog' such as peroxyacylnitrates, aldehydes, ethylene etc., are associated with losses, either alone or in combination with O_3.

Using open-top chambers as described by the work of Brewer and Ashcroft (1983), Roper and Williams (1989) performed simultaneous measurements of net CO_2 assimilation rate (*A*), stomatal conductance (g_{sto}) and intercellular CO_2 partial pressure (c_i) on four year old grapevines, which were furrow-irrigated approximately every three-weeks at the University of California's Kearney Agricultural Center. The experiment started on May 1987 and measurements were taken on a representative day of the anthesis, *véraison* (berry softening), fruit growth and postharvest. The mean ambient O_3 concentration from May to September was 46 ppb. The differences found on *A* between the ambient air and the charcoal-filtered treatments ranged between decreases of 5% at anthesis and 13.7% at *véraison* with an average decrease value of 8.4 % being only significant at *véraison* which coincided with the highest O_3 daily means (52 ppb). It was uncertain whether this small reduction in *A* could be related with the reduction in yield previously reported by the work of Brewer and Ashcroft in 1983. They also found that the decrease of A throughout the growing season could not be related to O_3 exposure as it followed a normal senescence and nitrogen (N) remobilization pattern. Leaf fall could not be attributable to O_3 exposure either. Regarding carboxylation efficiency (A/c_i), although the differences found were not significant, they ranged between a 0% and 12% increase with an average value of a 9% greater leaf photosynthesis figure for the vines grown in the filtered chambers. No differences were found in shoot growth parameters, bunch set, bunch weight, crop yield or fruit sugar accumulation between the filtered and non-filtered chambers.

Roper and Williams (1989) also performed cuvette measurements taken on grapevine leaves under acute O_3 concentrations. Results revealed that stomatal conductance (g_{sto}) was significantly lower than controls after two hours of exposure to 200 ppb of O_3 with intercellular CO_2 partial pressure (c_i) showing a similar decreasing behaviour. Higher O_3

concentrations such as 600 ppb continued to reduce stomatal flux but c_i behaved in an intermediate manner between the control leaves and those exposed to 200 ppb during the first 3 hours to reach similar values to those of the controls during the last two hours of the experiment. No significant differences were found in CO_2 assimilation rate (*A*) between the control and the 200 ppb O_3 acute exposure treatments, but there was a significant reduction after 90 minutes when the leaves were exposed to 600 ppb. The authors indicated the potential existence of an O_3 air pollution threshold causing a significant reduction in *A* between 200 and 400 ppb. The dominant effect of O_3 pollution would be on stomatal conductance with the probable existence of an O_3 detoxifying mechanism, whose effectivity could depend on cultivar, where abscisic acid (ABA) would be produced as a response resulting in spatially heterogeneous stomatal closure and, ultimately, in grapevine leaf stipple.

The first reported of O_3 foliar stipple related to the grapevine in Europe corresponds to observations made in Tuscany, Italy, in summer 1983. O_3 maxima were estimated to be around 100-120 ppb then and cultivar Trebbiano was characterized as most sensitive followed by Sangiovese, Malvasia and Canaiolo (Lorenzini et al., 1984). Only in the summer of 1991 the first reported field experiment was performed in a vineyard located in Frankonia, Germany, with 17-year old Traminer cultivar grafted on SO4 rootstocks. Two different parcels were sprayed every 6-12 days with different antioxidants: for one of the parcels ethylenediurea (EDU) was used whereas for the other one Benomyl was applied. For untreated plants, the mean percentage of damaged foliage exceeded 25% from the beginning of August and was presumed to have a significant adverse effect on yield, and carbon allocation in shoots and grapes. Histological sections performed on leaves revealed a collapse of palisade cells at the microscopic level. EDU-treated plants displayed a percentage of leaf damage around 5% whereas no damage was found in Benomyl treated plants (Tiedemann and Herrmann, 1992).

Three years later, Soja et al. (2004) started a three-year open-top chamber experiment over *Vitis vinifera* cv. Welschriesling three-year old plants grafted on Kober 5BB rootstock under irrigated conditions 30 km south of Vienna, Eastern Austria. Four-treatments were compared: charcoal-filtered air, non-filtered air, non-filtered air +25 ppb of O_3 (O-25) and non-filtered air +50 ppb of O_3 (O-50). O_3 fumigation (8 hr d^{-1}, 5 days week) was performed from two weeks before anthesis (mid-May) until two weeks after harvest (mid-October). It

was found evidence of carry-over effects as expected in a perennial crop with non-structural-monosaccharides concentrations in grape juice (glucose and fructose) being more sensitive to O_3 exposure than plant yield. *POD* estimates were performed based on the multiplicative model described by Emberson et al. (2000b) and results were better correlated when a threshold (*Y*) of 6 nmol m^{-2} s^{-1} was used indicating some limitation for O_3 detoxification above those levels. A *POD6* critical level-II of 1.1 mmol m^{-2} was indicated to protect carbohydrate translocation to grapes and of 2.2 mmol m^{-2} for grape yield. For individual years, those critical levels increase to 2.3 $mmolm^{-2}$ and 3.5 $mmolm^{-2}$ respectively. However, the authors cautioned that the conclusions were based on minimally replicated experiments performed with one grapevine cultivar only at one site in Europe, grown under continental climate conditions , and it has also been pointed out that the *POD* uptake algorithm was not parameterised for local conditions (or evaluated against such parameterisation) with the exception of the maximum stomatal conductance of the studied grapevine cultivar (Mills and Emberson, 2003). As such, the *POD6* critical levels derived by Soja et al. (2004) were not included at the time in the Modelling and Mapping Manual of the CLRTAP and this continues to be the situation nowadays (CLRTAP, 2017c).

In an earlier publication, Soja et al. (1997) reported an exposure-based *AOT40* critical level for a 10% reduction of grape monosaccharides of 11.5 ppm-h which increased to 21 ppm-h during the first fumigation year. A single *AOT40* critical level for a 10% reduction in yield of 27 ppm-h with similar values among consecutive fumigation years was also given. At that time, it was also noticed that the grapevine plants experienced enhanced leaf senescence, leading to reduced photosynthetically active green leaf area, and that the senescence effect was also more pronounced in the second fumigation year as observed by the decrease of photochemical capacity (F_v/F_m). The same experiment used by Soja et al. (1997, 2004) also served the purpose to study the effects of increased O_3 exposure on the leaf cell wall structure, morphology and anatomy of the Welschriesling grapevine cultivar by using morphometry, and light, fluorescence and electron microscopy (Ljubeši and Britvec, 2006). At the macroscopical level, it was found that the non-filtered air +25 and +50 ppb O_3 treatments were associated to thicker leaves whereas, at the microscopical level, the thickening was related to an increase of the size of palisade and spongy mesophyll cells. In association to the non-filtered air +50 ppb of O_3 treatment, deposits of callose (a β-1, 3-linked glucose polymer) were found on the inner sides of the mesophyll cell walls causing

an overall increase of their thickness. As callose deposition separating injured cells from healthy ones had been described by Gravano et al. (2003) in *Ailanthus altissima,* and it was already known that there were chemical compounds (e.g. ascorbate, dehydroascorbate) and enzymes (e.g. peroxidases, glutathione-S-transferase) present in the aqueous matrix of these cell walls, it was concluded that thicker callose cell wall layers could act as a mechanical barrier against the spread of O_3 into the cell protoplasm besides providing a more complete decomposition of O_3. Small dense electron deposits near the mesophyll cell walls or large ones between the meshopyll cells were also considered signs of activated stress mechanisms.

Still based on the same experimental setup reported by Soja et al. (1997, 2004), Britvec et al. (2001) reported that under slightly elevated concentrations (e.g. mid-May to September *AOT40* of 2500 ppb-hr) a slight increase in number and size of plastoglobuly could be found in the chloroplats. This could be interpreted as a sign of changed or enhanced physiological activity leading to premature leaf ageing and accelerated senescence of leaves and, in agreement with the physiological measurements taken on the O_3-exposed leaves, also as an indication that the photochemical processes taking place in the thylakoid membrane were less sensible to O_3 compared to carboxylation taking place in the chloroplast stroma. As such, the thylakoid system was found still relatively well preserved under elevated O_3 O-25 concentrations (mid-May to September *AOT40* 13500 ppb-hr), but the O-50 leaves (mid-May to September *AOT40* 26900 ppb-hr) showed a disentegration of some chloroplasts and a reduction of chlorophyll a, chlorophyll a + b and chlorophyll a + b : carotenoids ratio. The decrease in chlrophyll a was indicative of progressive injury of the photosynthetic apparatus whereas the observed decrease in the chlrophyll a + b : carotenoids ratio pointed to a stimulation of light dissipitation mechanisms in the chloroplasts by O_3. Signs of O_3 stipple were found only in the above ambient O-25 and O-50 treatments. This work also served as a basis to a later field study along an expected ambient O_3 gradient due to complex orography and air mass circulation in the Rijeka Bay (Croatia) reported by Alebic-Juretic et al. (2017) where it was found that a May to July *AOT40* of 14030 ppb-hr could be related to changes in the concentrations of Chl a, Chl b and carotenoid contents due to possible damage by O_3 which could also speed up the natural ageing of the grapevine leaves.

Another field study was previously performed in Romania by Popescu et al. (2012) comparing the physiological response of grapevines located in an urban site vineyard near a power plant, which was also affected by a large traffic volume, to that of grapevines of another vineyard located in a rural site 12 km west not being subject to atmospheric pollution. The study area is characterized by a temperate continental climate with mild winters and dry summers and the same type of soils (preluvosoils). The plant material consisted of *V. vinifera* L., cv. *Merlot* organically grown (no pesticides applied) under irrigation so that no water stress could be induced in none of the sites. The study protocol included four visits per phenological stage (blooming, shoot growth, *véraison*, ripening) from June to September to take in-situ air pollution (sulfur dioxide - SO_2, NO_2 and O_3) and leave physiological measurements (net photosynthetic rate, transpiration rate, stomatal conductance). The urban site had constistently much higher values of pollutants than the rural site with June to September SO_2, NO_2 and O_3 mean concentrations of 30.6 µg/m^3, 25.0 µg/m^3 and 86.8 µg/m^3 respectively, whereas the corresponding rural site values were 11.5 µg/m^3, 10.7 µg/m^3, and 48.9 µg/m^3. For both sites, SO_2 and O_3 reached their maxima (36.8 µg/m^3 and 105.4 µg/m^3) during *véraison* (August) whereas NO_2 reached it (29.4 µg/m^3) during the ripening stage (September). It was found that the average physiological measurements for each of the phenological stages had much lower values in the vicinity of the power plants with reductions as much as 98.8% in photosynthetic rate at *véraison* stage, 61.5% in transpiration at rippening and 75.4% in stomatal conductance at shoot growth when compared to the non-polluted rural site. The relationship between the individual levels of SO_2 and O_3 and photosynthesis and stomatal conductance was found to be significantly negative whilst NO_2 had a greater impact on transpiration and stomatal conductance at the rural site. Foliar symtomps such as brown spots and necrosis appeared only at the urban site.

Also focusing on leaf physiological measurements, a fumigation experiment was performed from the end of April to the beginning of October in two experimental greenhouses in La Peira, Valencia, Spain. Two cultivars extensively grown in Tierra de Barros, Extremadura, Spain, were selected for the experiment: cv. Parda grafted on 110R CL7 standard rootstock and cv. Tempranillo grafted on 100R CL180 certified rootstock. One of the greenhouses was submitted to filtered air whereas the other greenhouse was submitted to an O_3 fumigation of 30 ppb over unfiltered ambient air. At the end of the experiment it was found that only

the Tempranillo cultivar had a significant decrease in *A* (22%) and g_{sto} (21%) along a significant increase in c_i (10%) under the O_3 enriched conditions (*AOT40* 51804 ppb-hr) when compared to the plants in the control treatment (*AOT40* 119 ppb-hr). As the Parda cultivar did not show any significant alteration in those measured parameters, it was concluded that the Tempranillo cultivar was less O_3 tolerant. No external signs of O_3 damage were reported in the leaves for the two varieties (Universidad de Extremadura, 2007).

Pellegrini et al. (2015) performed a fumigation experiment in the field-station of San Piero a Grado, Pisa, Italy, with two two-year old *V. vinifera* varieties extensively cultivated in central Italy: black-berried cv. Aleatico (ALE) and white-berried cv. Trebbiano giallo (TRE). The experiment was performed in a greenhouse fumigation facility in four Perspex boxes under controlled irrigation. Two of the boxes were ventilated with charcoal filtered air and the other two were fumigated from the end of May to the end of June 2012 (28 days) with O_3 concentrations simulating the daily typical O_3 profile in Tuscany, central Italy (80 ppb from 8:00-13:00h and 40 ppb from 13:00 to 18:00h). Both varieties showed leaf stipple at the end of the fumigation. Leaf anatomical and cell ultrastructure alterations indicative of oxidative processes associated with an apoplastic oxidative burst were found to be more pronounced in the ALE variety. It was also found that leaves with lower stomatal density, high values of leaf mass per area, high leaf thickness, and high constitutive photosynthetic capacity (e.g high values of maximum rate of Rubisco or carboxylation activity, V_{cmax}, and maximum rate of electron transport through the electron transport chain of chloroplasts, J_{max}), such as those of the TRE variety, would be associated with a higher degree of acclimation to an oxidative environment. In both varieties, lower A was associated with the slow-down of the Calvin cycle mainly due to the loss of carboxylation efficiency. O_3 also induced an alteration in CO_2 assimilation both at low and high light intensity in both varieties with a greater decrease in photosynthetic activity at light saturation conditions (A_{max}) in the ALE variety. Because of the reduction in the photosynthetic capacity, fluorescence signals (e.g. the F_v/F_m ratio) can be used to estimate the inhibition or damage in the process of electron transfer in photosystem II (PSII). A reversible decline of F_v/F_m was observed for both varieties, so it was associated to down-regulation rather than photodamage of PSII.

Photoinhibition can also be avoided by decreasing the absorption of light and/or consuming the excess excitation energy through non-photochemical mechanisms such as the activation of heat energy dissipation which can be associated with the de-epoxidation state (DEPS) of the xantophyll cycle pigments or the fraction of absorbed light (*%D*) that is thermally dissipated in the PSII antennae. In this sense, the work of Pellegrini et al. (2015) also discovered that the higher *%D* levels of the TRE cultivar could contribute to its lower sensitivity to oxidative stress. Under fumigation, both varieties underwent a decrease in total chlorophyll content, an increase of the chlorophyll a/b ratio and a reduction in β-carotene and α-tocopherol contents through the day, which were associated with a rearrangement of the pigment composition of the photosynthetic apparatus that could in turn also be associated with an increase in DEPS. However, this re-organisation of the photosynthetic apparatus did not preserve the PSII photochemistry in the ALE variety as there was a net α-tocopherol net loss which could induce lipid peroxidation and cell damage. The reduction of β-carotene, lutein and α-tocopherol could also be triggered by the oxidative cleavage of carotenoids associated to the production of ABA. However, the ABA-dependent regulation of the stomata and water losses could not prevent water deficit for the ALE variety either, and the high levels of ABA were monitored only in the early afternoon for this variety. In contrast, the O_3- treated leaves of the TRE variety had elevated levels of ABA during the light-period which could also stimulate the proline synthesis from glutamic acid to indirectly protect PSII, rise the water soluble contents of the leaves, and control CO_2 uptake and transpiration through stomatal conductance. Overall, it was found that the TRE variety was less sensitive to oxidative stress because its morphological functional traits and acclimatory response of its photosynthetic machinery.

Valletta et al. (2016) carried out another experiment over two *Vitis vinifera* cultivars, white grape Maturano and red grape San Giuseppe, which are also locally important autochthonous varieties in central Italy (Latium region). They compared control and fumigated plants (*AOT40* was about 850 ppb-h per day) response during 10 days for gas exchange and chlorophyll fluorescence parameters (JIP test) and during 10 days after the treatment for chlorogenic acid (CGA) concentrations among other biochemical compounds. They found that the Maturano cultivar was more sensitive to O_3 with early stomatal closure and decreasing of net photosynthesis after the first day of fumigation, whereas the San Giuseppe cultivar response on those two parameters was delayed until

the third day. Regarding the ratio between sub-stomatal and ambient CO_2 concentration (C_i/C_a), Maturano showed an increase after the second day, which was more pronounced from the fourth day on except for the last day of fumigation when no differences were observed with the control plants. San Giuseppe had an opposite behaviour maintaining slightly lower differences with the control plants, which indicated that mesophyll photosynthetic capacity was not altered by the high O_3 concentrations during the experiment, and that the gas exchange reduction observed in this cultivar is probably related to an O_3 avoidance mechanism such as O_3 induced stomatal closure. Whereas stomatal conductance and net photosynthesis were strongly coupled in San Giuseppe, there was a marked decoupling between these two physiological parameters in Maturano at the end of the experiment. The JIP test for the San Giuseppe cultivar also showed an increased photosystem I (PSI) activity after the third day of fumigation which could be related with an enhancement of the xanthophyll-cycle-controlled downregulation of PSII, the detoxification of reactive oxygen species (ROS) in the chloroplasts, and the supply of ATP, which also has a role in detoxification and repair processes. In contrast to the San Giuseppe variety, Maturano JIP results suggested the occurrence of structural damage of PSII reaction centres at the end of the fumigation. Finally, fumigation induced a decrease in chlorogenic acid (CGA) leaf content in both cultivars with a much earlier response in Maturano (after the first day of fumigation) than in San Giuseppe (only significant after the eight day of fumigation) with a recovery in both cultivars after eight days of the experiment end, especially in San Giuseppe. It is hypothesised that CGA is consumed as antioxidant or as precursor to other phenolic contents. At the end of the fumigation experiment, no difference was found on the extent of injury on affected leaves for the two varieties thus confirming visible O_3 symptoms cannot be considered a reliable indicator for biomass and productivity losses for these varieties.

An OTC experiment was performed by Geng et al. (2017) to submit one-year grapevines (cv. Cabernet Sauvignon) involving three levels of O_3 concentrations (50, 100 and 150 ppb) and light intensities (800, 1200, and 1600 µmol m^{-2} s^{-1}) in an experimental field located in a rural area of Shangdong Agriculture University, Tai'an, China. The grapevines were irrigated to avoid drought stress and fumigations lasted for 3-hr. 13 combinations among O_3 concentrations and light intensities were selected by using response surface methodology and related to a commonly fluorescence parameter, F_v/F_m, which is used for

plant stress detection affecting PSII. A decrease of F_v/F_m was found with increasing O_3 and light intensity. It was suggested that strong light induced a surplus light energy and leaded to ROS accumulation, aggravating photoinhibition and O_3 injury. For the new Chinese ambient O_3 pollution standard, 93.46 ppb, which is usually exceeded in most polluted areas in China, F_v/F_m reached a critical value for a light intensity of 1600 µmol m^{-2} s^{-1}. It was also reported that O_3 susceptible varieties can show visible O_3 injury symptoms in the field well below the critical O_3 standard (e.g maxima values between 47-40 ppb and mean values of 31-29 ppb) under long-term strong light exposures. (e.g. cvs FR 177-68, Beck memento and Frontenac). Another study combining light intensity and O_3 concentration for the same grapevine cultivar (Cabernet Sauvignon) performed in the same OTC facility in China reported reductions on stomatal conductance, net photosynthetic rate and PSI and PS II photosystems activities after 13-hr treatments with high O_3 concentrations (90 ppb) and light intensities ranging from low (10 µmol m^{-2} s^{-1}), to intermediate (800 µmol m^{-2} s^{-1}) and high (1600 µmol m^{-2} s^{-1}), and that the leaves could not recover from damage under the most severe treatment (Xing et al., 2018).

Recently, Decoteau et al. (2019) performed a five-year experiment exposing an O_3-susceptible French-American hybrid cultivar, Chambourcin, and an O_3-tolerant French-American hybrid cultivar, Vidal, to ambient air and charcoal-filtered air using OTC, in Pennsylvania, USA. The five years 12-hours per day (08:00-20:00h), from June to September, in the filtered treatment averaged 21 ppb of O_3, whereas concentration in the non-filtered treatment averaged 34 ppb. The O_3-susceptible cultivar Chambourcin had a mean of 5.28% leaf tissue injury for the five growing seasons when exposed to ambient O_3, though leaf tissue injury for this cultivar was only 0.48% for the same period under the charcoal-filtered treatment. In contrast, the O_3-tolerant Vidal cultivar averaged only 0.02% tissue injury for both treatments over the five seasons. Although there were significant variations on mean berry weight, juice pH, total acidity, and total sugars among the years for both cultivars, these could not be directly related to ambient O_3. These results can be compared to previously reported data from a one-season study with 12-hours per day mean of 18 ppb of O_3 in charcoal-filtered OTCs against 30 ppb in non-filtered OTCs. Under those conditions, the Chambourcin variety had 18% of their leaves injured whereas leaves injured in the clean-air treatment were less than 2%. Those figures for the O_3-tolerant Vidal variety were less than 6% and 1%, respectively. Regarding fruit yield and quality, it was

found that ambient O_3 decreased Vidal grapefruit size and increased juice total acidity (measured as titrable acidity, g/l tartaric acid) in both cultivars, whereas no effects were observed on juice pH or total sugar content (Booker et al., 2009).

Another OTC experiment performed in northern Italy and reported by Fumagalli et al. (2019) was focused on the effects of O_3 on yield and grape quality parameters over adult Merlot cultivar. The experiment consisted of two filtered OTC chambers (FOTC) with capacity to reduce ambient O_3 in 30%, and two unfiltered OTC chambers (UOTC) with each of the OTC chambers enclosing 4 grapevines. Other 8 grapevines were monitored externally in the field (E). The experiment took place from June to September 2011 and O_3 concentration was measured for the three treatments along with temperature and relative humidity allowing to estimate *AOT40* and *POD0* for the three cases (*AOT40* FOTC 2000, UOTC 6100, E 12300 ppb-hr; *POD0* FOTC 21.4, UOTC 32.0, E 38.1 mmol m^{-2}). Despite the experiment considered only one growing season, significant differences were noticed with higher O_3 concentrations decreasing bunch weight (31.2%) as well as affecting several other chemical parameters related with grape must and later wine quality which can also be beneficial for human health such as polyphenol content. Specifically, the grapevines under external higher O_3 concentration conditions had significantly lower contents of succrose (1.1%), total anthocyanins (8.5%), total polyphenols (14.8%), and total acidity (3.4%) but higher assimilable nitrogen (14.6%).

Finally, Wang et al. (2020) reported another OTC fumigation experiment that was performed along 12 weeks with two hours 75 ppb O_3 daily treatment, from 10:00 to 12:00, avoiding photosynthetic inhibition and heat stress, which was compared with a control treatment of 15-25 ppb O_3. The experiment covered the grapefruit hardening, the *véraison* and the ripening phenological stages and was performed in the vineyard of Shandong Agricultural University, China, in 2017. The 75 ppb O_3 treatment is close to the most pessimistic projections (80 ppb) on ambient O_3 concentrations by the end of the century (Fiscus et al., 2005). It was found that O_3 stress induced leaf damage (e.g. stipple and leaf ageing after the 4^{th} week of treatment), chlorophyll and photosynthesis reduction also resulting in reduced shoot growth and a bunch weight reduction (20.5%) compared with the control treatment. Moreover, carbon and nitrogen content in leaves were significantly reduced being transferred mostly to roots as a form of survival strategy. The deficiency in the nutrition of carbon and nitrogen in the leaves was also observed in the fruits and could

be related with a reduced content of reducing sugars (32.4%) and soluble solids (33.1%) in the grapes. It was also hypothesized that the reduced carbohydrates contents in the stressed plants could also have affected the flavonoid biosynthesis pathway also inducing the observed reduction of tannins (57.7%), total phenols (22.5%), flavonoids (33.7%) and flavanols (11.7%) and an increase of titrable acidity (9.2%) of the grapes under the fumigation treatment. The measurements of chlorophyll fluorescence parameters, such as maximum fluorescence (F_m) and maximum *P700* absorbance changes, indicated that PSII and PSI photosynthetic activity decreased under long term stress up to 57.1% and 31.7%, respectively, and that the leaf PSII and PSI energy distribution was altered increasing the degree of photoinhibition.

A summary of the main findings related to ambient O_3 effects on the grapevine concerning observational and experimental research performed since the late eighties as mentioned in this review can be found in Table 3-4.

Table 3-4. Main findings of experimental work concerning ambient O_3 effects on the grapevine.

Leaf damage at the macroscopic level
Plants experience enhanced leaf senescence, leading to reduced photosynthetically active green leaf area (Soja et al., 1997). High values of leaf area, thickness, mass per area along lower number of stomata per leaf surface unit can be correlated to a higher degree of tolerance (Pellegrini et al., 2015). Visible symptoms cannot be considered a reliable indicator for biomass and productivity losses (Valletta et al., 2016).
Leaf damage at the microscopic level
Leaf thickening after O_3 fumigation is related to an increase of the size of palisade and spongy mesophyll cells. Deposits of callose found on the inner sides of the mesophyll cell walls cause an overall increase of their thickness. The thicker callose cell wall layers can promote a more complete decomposition of O_3 acting as mechanical barrier and providing physiological protection by means of enzymes and antioxidant compounds (Ljubeši and Britvec, 2006).
Photosynthesis and carbon assimilation
O_3 reduces stomatal conductance, net CO_2 assimilation and carboxylation efficiency (Roper and Williams, 1989). It affects chlorophyll and carotenoids concentrations indicating stimulation of light dissipation mechanisms in the chloroplast or progressive injury of the photosynthesis apparatus leading to premature leaf ageing and accelerated senescence (Britvec et al., 2001). The degree of tolerance to O_3 stress can be related to slight genotypic differences in terms of constitutive photosynthetic capacity (e.g. high values of maximum rate of Rubisco or carboxylation activity, *Vcmax,* and maximum rate of electron transport through the electron transport chain of chloroplasts, *Jmax*) and the acclimatory response of photoprotective mechanisms (e.g. xantophyll cycle-dependent

energy dissipation, photorespiration and stomatal closure) (Pellegrini et al., 2015; Valletta et al., 2016).
Biomass allocation and plant growth
Carbon and nitrogen content in leaves can be significantly reduced being transferred mostly to roots as a form of survival strategy with an increase of the root:shoot ratio and an inhibition of the growth of the upland parts of the grapevine. The deficiency in the nutrition of carbon and nitrogen in the leaves can also be observed in the fruits (Wang et al., 2020).
Defence, repair and detoxification processes
The dominant effect of O_3 pollution would be on stomatal conductance with the probable existence of an O_3 detoxifying mechanism, whose effectivity could depend on cultivar, where abscisic acid (ABA) would be produced as a response resulting in stomatal closure (Roper and Williams, 1989). The re-organisation of the photosynthetic apparatus can also be related with oxidative cleavage of carotenoids leading to the production of ABA in order to control transpiration and diminish water losses and CO_2 uptake. High levels of ABA can also stimulate proline synthesis to indirectly project PSII and modulate water relations (Pellegrini et al., 2015). Stimulation of light dissipation mechanisms, such as alternative transport pathways in relation to PSI activity, detoxify photochemically produced ROS in the chloroplasts and supply additional ATP for plant response, repair processes and detoxification (Valletta et al., 2016).
Crop loss assessment studies: impact on yield and quality
Non-structural-monosaccharides concentrations in grape juice (glucose and fructose) can be more sensitive to O_3 exposure than plant yield (Soja et al., 2004, 1997). Ozone exposure can relate to a reduction in yield and grape quality parameters such as contents of sucrose (Fumagalli et al., 2019; Soja et al., 2004, 1997; Wang et al., 2020) and total polyphenols (Fumagalli et al., 2019; Wang et al., 2020).

3.3.2 Research gaps and prospects for future research

From the progressive understanding of the effects of O_3 on the grapevine since the late fifties, it is possible to associate O_3 exposure with visual effects on leaves such as necrosis, chlorosis, and early senescence under natural conditions in the field and controlled research experiments. The percentage of damage at the leaf level can vary considerably depending on grapevine variety. Although visual symptoms at the leaf level can be useful for detecting O_3 damage, it has not been possible to make use of them as reliable indicators for biomass and productivity losses. This has been also a common situation with trees and forests, especially under field conditions where interpretation becomes more doubtful due to complex interactions between O_3 and other environmental factors such as water or mineral availability of the soil (Jolivet et al., 2016). However, results from the LIFE MOTTLES project have recently indicated that visible foliar injury in light exposed sites was the best

forest-health indicator for O_3 under field conditions when compared with radial growth or crown defoliation (Paoletti et al., 2019). As such, detailed quantitative observation of visible foliar injury could also still be of use as possible grapevine-health indicator for O_3 if incorporated in an observational network comprising a range of cultivars and coexisting environmental conditions.

The use of ecophysiological measurements such as leaf photosynthetic CO_2 assimilation, stomatal conductance, plant water status and photosynthetic activity in combination with biochemical ones such ABA, proline and photosynthetic pigments contents have already proven to be effective means to assess grapevine response in relation to O_3 exposure in controlled experiments and field conditions. They have also provided insight about the existence of slight genotypic differences in terms of constitutive photosynthetic capacity and acclimatory response of photoprotective mechanisms from different cultivars. There is also an incipient proposal concerning the use of biochemical indicators in relation to antioxidant detoxification processes such as the work of Valletta et al. (2016) in relation to CGA. However, there is a much wider and complex network composed by signalling compounds (e.g. ethylene, salicylic acid, jasmonic acid), antioxidant metabolites (e.g. polyphenols) and enzymes (e.g. superoxide dismutases, peroxidases) besides changes in the global gene expression that can be related with O_3 plant detoxification capacity (Rai and Agrawal, 2012). Therefore, as it has been already pointed out by Jolivet et al. (2016) from a review of forestry cellular and molecular mechanisms impacted by O_3, further work is still required to identify a reliable detoxification parameter to be integrated in models for better risk assessment, as currently it is only considered in the form of empirically derived thresholds providing stronger relationship with plant productivity or quality loss. In this regard, detailed metabolomic studies are more advanced concerning grapevine response to water stress as it has been already possible to apply metabolite-based modelling to predict physiological stress, as shown by the work of Griesser et al. (2015), or quantity differences in stress response between grapevine cultivars, as illustrated by Hochberg et al. (2013), although it has been also acknowledged the need of further research to elucidate the genotype specific details of the physiological and molecular responses involved.

Precisely, proper consideration should be given to the need to increase the number of studies addressing the combined effects of O_3 with other concurrent climatic factors such

as drought or light intensity which could also act lowering or exceeding the detoxifying capacity of plants. In this sense, Geng et al. (2017) and Xing et al. (2018) have already provided results suggesting that strong light induces a surplus light energy leading to ROS accumulation which aggravates photoinhibition and O_3 injury in the grapevine for grapevine cv. Cabernet Sauvignon. The work of Biswas and Jiang (2011) has also demonstrated O_3 tolerance can be completely lost under combined drought and O_3 exposure for a drought-sensitive winter wheat species. These results clearly indicate the need to pay more attention to these type of interactions for better assessment of the impact of current and future climates on vegetation. Some thought could also be given to the suitability of using midday *gs* measurements as surrogates for integrated dial O_3 flux under water deficit (WD) conditions or where maximum O_3 concentrations are not observed during midday. Even though their use can be justified as sensitive indicators of plant growth and developmental responses to O_3 and WD, gs is subject to different regulatory processes at midday, where stomata are at quasi-steady state, than during periods of active opening or closing in early morning and evening. As such, an experimental study performed on an O_3-sensitive cultivar of Pima cotton (*Gossypium barbadense* L.; cv. S-6), showed that leaf pigmentation and shoot biomass under well-watered conditions were well predicted by midday *gs* measurements as they varied in response to O_3 and WD probably in relation to the dominance of dial gas exchange by larger values of gs and O_3 uptake at midday (Grantz et al., 2016). However, shoot parameters under WD, and root parameters under both well-watered (WW) and WD, were more related to gs in early morning, reflecting an earlier peak of gs under WD, and possible relationship between allocation to roots and responses to WD.

Concerning policy standards, full controlled experiments like those performed in adapted glass or greenhouses are well suited to derive cause-effect relationships to quantify the physiological and biochemical plant response to different ambient O_3 levels. However, it is difficult to extrapolate those results to field conditions. Field exposure systems, such as OTC, benefit from the possibility to control O_3 level and fumigation timing allowing plants to develop under conditions close to those found in the field. OTC have also provided most of the data currently in use to derive O_3 standards for vegetation protection in Europe. Nevertheless, data from OTC must be taken with caution as chamber effects can modify the plant response yielding frequently to over estimations (Bermejo Bermejo et al., 2009;

Fagnano et al., 2009). In fact, several OTC effects have been observed on grapevine leaves such as reduced CO_2 assimilation, stomatal conductance, carbohydrate concentration, palisade parenchyma thickness, leaf mass per unit area and lower values of red/far-red ratio transmitted, whereas water use efficiency, Soil Plant Analysis Development (SPAD) chlorophyll readings and osmotic potential at full turgor were found to be higher. Effects have been also identified concerning mineral nutrition concentrations such an increase in N and Mg and a reduction of K concentration in OTC leaves along reductions in yield and biomass indices (e.g. Ravaz index) (Moutinho-Pereira et al., 2010). Finally, field experiments under natural conditions provide results easier to extrapolate to the real field conditions, but there is no control of the different environmental variables involved and, therefore, it is difficult to isolate causes and interpret correctly the results (Bermejo Bermejo et al., 2009). In this context, chamber less Free Air Controlled Exposure (FACE) systems are advantageous. An example of a FACE system which could be used to impulse research on O_3 impacts on vegetation also allowing to investigate other stressors together with O_3 is the Free air O_3 eXposure system (FO_3x) located in Florence, Italy, which is one of the few O_3 FACEs currently available in the world, and the only one that is located in Mediterranean climate (Paoletti et al., 2017).

3.4 MODELLING O_3 PHYTOTOXIC RISK FOR THE GRAPEVINE

In order to generate O_3 critical level exceedance maps there is need to use data from atmospheric chemistry transport models or from monitoring networks. Atmospheric chemistry transport models can be classified according to their application scale as long-range transport (LRT) models, which can be applied to global or continental scales with a resolution of tens of kilometres, or higher resolution models applied to national or regional scales. When these models are supported by adequate atmospheric emission inventories they can serve the purpose to analyse past, present and future climate change and atmospheric pollution scenarios whereas data from monitoring networks are mostly used for model validation, model data assimilation or local studies (CLRTAP, 2014).

Among the long-range atmospheric chemical transport models, the photo-oxidant model of the European Monitoring and Evaluation Programme (EMEP) is aimed to simulate emissions, transport, transformation and removal of pollutants and is a key tool for European air pollution abatement strategy and legislation work. Concerning O_3, level I

standards can be derived from cumulative exposure metrics whereas a coupled deposition model, the deposition of O_3 for stomatal exchange model (DO3SE), allows for the derivation of level-II standards (Simpson et al., 2007). Following the formulations by Tuovinen et al. (2007), from a concentration of O_3, *c*, taken from the lowest vertical grid point of the EMEP model with height z_r of about 45 m, the total deposition flux can be estimated as follows:

$$F = \frac{c\,(z_r)}{R_a(z_0+d,z_r)+R_b+R_s} \qquad (5)$$

where $R_a\,(z_0+d,z_r)$ denotes the aerodynamic resistance between the heights z_0+d and z_r, z_0 is roughness length, d is zero-plane displacement, R_b is the canopy-scale quasi-laminar resistance and R_s is the bulk surface resistance including both a stomatal and a non-stomatal resistance to O_3 uptake or destruction by vegetation up-scaled from leaf to canopy. According to Emberson et al. (2000a) R_s can be calculated from the following expression:

$$R_s = \frac{1}{\frac{LAI}{R_{sto}}+\frac{SAI}{R_{ext}}+\frac{1}{R_{inc}+R_{gs}}} \qquad (6)$$

where, in turn, R_{sto} is the land-cover specific leaf/needle stomatal resistance to O_3 uptake through the stomata, R_{ext} is the resistance of the exterior plant parts, R_{inc} is the land-cover in-canopy resistance to transport of O_3 through the canopy to lower parts of the canopy and the soil, R_{gs} is the soil resistance to O_3 absorption or destruction at the ground by soil, litter, moss, *LAI* is leaf area index, and *SAI* is surface area index which is equal to *LAI* in the growing season and 1 when leaf material is not present. The non-stomatal resistance pathways to O_3 deposition, R_{gs}, R_{inc} and R_{ext} are derived from published data ensuring that estimated total land-cover surface resistances are broadly consistent with observations. The stomatal resistance is calculated from a multiplicative model which introduces sensitivity for plant species, phenology, climate and soils:

$$\frac{1}{R_{sto}} = g_{max} * g_{age} * \max\{g_{min}, (g_{light} * g_{temp} * g_{vpd} * g_{swp})\} \qquad (7)$$

where g_{max} is the maximum stomatal conductance on a projected leaf/needle area basis (mmol O_3 m^{-2} s^{-1}), and the rest of g_x factors range from 0-1 accounting for time of year or leaf age (g_{age}), leaf-temperature (g_{temp}), leaf-to-air vapour-pressure deficit (g_{vpd}), and soil-water potential (g_{swp}). The g_{min} factor ensures a minimum stomatal conductance consistent with observations. Further information on the parameterizations of each of the g_x factors

can be found in Emberson et al. (2000a). The given DO3SE formulation is suitable for large-scale deposition modelling (e.g. pan-European scale) where deposition is calculated independently for different land-cover classes weighted by their respective fractional coverage within a grid to estimate a net deposition rate. This approach has also been shown to perform relative well for several land-cover classes and plant species (Büker et al., 2007; Simpson et al., 2007; Tuovinen et al., 2004). The DO3SE-based Tuovinen et al. (2007) formulation also specifies that under the assumption of a constant O_3 deposition flux, the O_3 concentration at the canopy height, z_h, can be estimated as:

$$C(z_h) = [1 - \frac{R_a(z_h,z_r)}{R_a(z_0+d,z_r)+R_b+R_s}]c(z_r) \qquad (8)$$

From which a top-leaf stomatal flux can be estimated from:

$$F_{st} = g_{sto}c(z_h) \qquad (9)$$

Finally, *POD* can be estimated from equation 2. At this point it must be noted that the F_{st} values required for *POD* estimation represent maximum uptake by the upper-canopy sun-lit leaves and not net uptake for a whole canopy. Therefore, *POD* is often estimated by parallel procedures such as tiny fractions of artificial plant species of plant communities (e.g. wheat, potato, beech, birch, temperate perennial grasslands etc.) for each model grid square where an indication of O_3 phytotoxic risk is to be derived according to the CLRTAP *POD*-based standards introduced in Table 3-2. The parallel procedures also allow for refinement of species-dependent parameters (e.g. g_{max}, g_{min}, g_{age}) or physiological-based parametrizations (e.g. g_{light}, g_{temp}, g_{vpd}, g_{swp}), which are difficult to apply by large-scale modelling (Simpson et al., 2007; Tuovinen et al., 2007).

According to Emberson et al. (2005), the grapevine already received considerable attention since the early application of the DO3SE model at the beginning of the century along with other crops such as tomato, sunflower, maize or sugar beet. Therefore, the work here mainly consisted in a comprehensive literature search of the DO3SE stomatal flux (g_{sto}) parameters and g_{sto} relationships with environmental variables. For the grapevine case, the model was successfully validated against observed grapevine stomatal and O_3 flux data collected during the California Ozone Deposition Experiment (CODE) during July-August 1991, which was considered representative of Mediterranean conditions (Padro et al., 1994; Pederson et al., 1995). It was also thought that it would be possible to translate the

O_3 dose absorbed by the grapevine into effects on grapevine yield and quality by using the revised grapevine DO3SE g_{sto} parametrization and the fumigation dataset used by Soja et al. (2004). However, according to Mills et al. (2006), applying the DO3SE model to that grapevine fumigation dataset was finally considered unfeasible because the associated O_3 and meteorological data provided by the Soja et al. (2004) study were not recorded hourly or for conditions within the OTC, but they had been derived from mean monthly values instead, and as such, there wouldn't be a way to validate the DO3SE stomatal flux-response model either. Although there has been a continuous effort to update the grapevine DO3SE parameterizations for regional application by CLRTAP, as it has also been the case for other crops such as maize, sunflower and soybean, there has not been corresponding progress concerning the availability of enough experimental data so that flux-effect level II (or exposure-effect level I) relationships can be established. Currently, wheat, potato and tomato are the only crops where species-specific critical levels for yield or quality have been derived from comprehensive input for detailed risk assessment (CLRTAP, 2017a).

High-resolution level-I O_3 exposure and level-II O_3 stomatal uptake maps can also be computed by using high-resolution atmospheric chemical transport models, provided that the outputs are validated against available field measurements (CLRTAP, 2014). Whereas LRT models such as those of EMEP have been often used to provide average concentration and deposition rates for larger grid squares (e.g. 10 x 10 km^2 to 50 x 50 km^2) at a continental or country by country basis, they can also be run in nested mode to higher resolutions (e.g. 1 x 1 km^2) nowadays. High resolution modelling is better suited for more detailed regional analyses taking advantage of using more detailed meteorological, elevation and land-cover datasets. Both approaches can be used for the assessment of emission abatement scenarios as high-resolution models can also be associated with different emission inventories. Some examples of high-resolution regional atmospheric modelling systems (RAMS), coupled with DO3SE deposition, applied to estimate O_3 uptake by vegetation are provided by Watanabe et al. (2016), who used ADMER-PRO, a RAMS able to calculate meteorological fields and transport of chemical substances simultaneously, in a two-domain nested approach with a 5 x 5 km^2 inner domain to assess phytotoxic risk of deciduous forests in the Kanto region of Japan, and that of De Marco et al. (2016), where the CHIMERE RAMS was forced by the Weather Research and Forecasting (WRF) model to produce hourly O_3 data, in another two-nested domain approach to derive a 6 x 6 km^2 inner

domain to assess soil water content (*SWC*) effects on the estimation of stomatal fluxes of temperate and Mediterranean tree species in France, Slovenia and northern Italy.

Figure 3-2 displays a high-resolution 0.1° x 0.1° *POD1_AIM*_map over the April to September season for deciduous forests (*POD1_AIM_DF*) over the Mediterranean basin as derived from EMEP/MSC-W modelled air concentrations simulated by the Norwegian Meteorological Institute (Met Norway) for the year 2018 (*EMEP Status Report*, 2019).

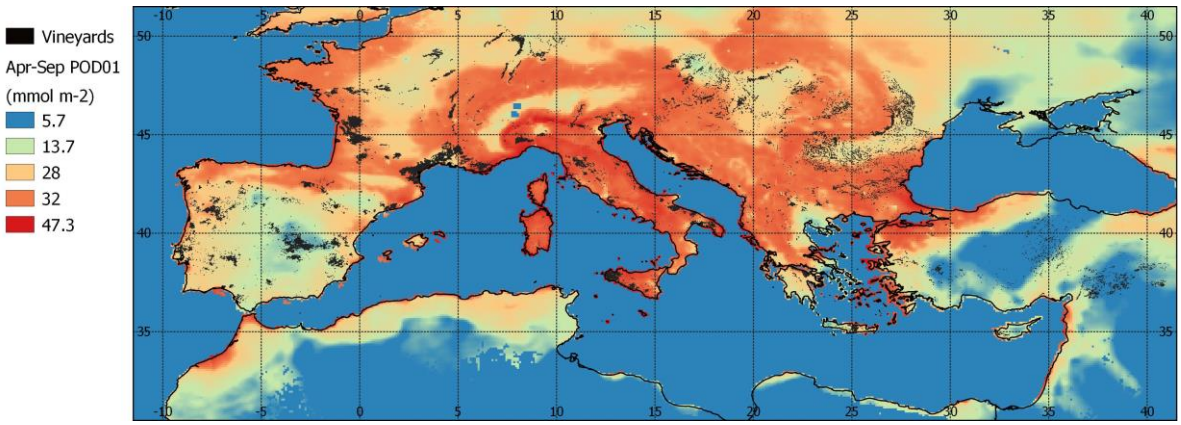

Figure 3-2. 0.1° x 0.1° crop *PO13IAM* Deciduous Forest map produced for the year 2018 based on EMEP/MSC-W model data provided by the Norwegian Meteorological Institute and downloaded from the EMEP MSC-W modelled air concentrations and depositions data web site ([dataset] Norwegian Meteorological Institute, 2019).

It can be observed that extensive areas of the Mediterranean basin exceed the CLRTAP flux-based critical level for Mediterranean deciduous trees (13.7 mmol m^{-2}), and that many grape growing areas, with the same or very similar April to September growing season could be affected too. A reduction on yield and quality have been reported for cv. Welschriesling with a Jun-Sep POD0 exceeding 12.5 mmol m^{-2} (Soja et al., 2003) and for cv. Merlot, which is considered a global variety as it is extensively cultivated through the World, for a *Jun-Sep POD0* exceeding 32 mmol m^{-2} (Fumagalli et al., 2019). Although *Apr-Sep POD1_AIM_DF* cannot be taken as an equivalent parameter to a grapevine-based Jun-Sep POD0 parameter, it could be expected some degree of correlation based on the deciduous leaf character, the overlap in growing season length, and the low value of the *Y* detoxifying thresholds used (1 or 0), besides the fact that all these flux-based parameters still neglect soil induced water limitation stress.

Figure 3-3 shows a map produced for the *Apr-Sep AOT40* parameter for forests (*AOT40_Forest*) derived from the same source (EMEP/MSC-W).

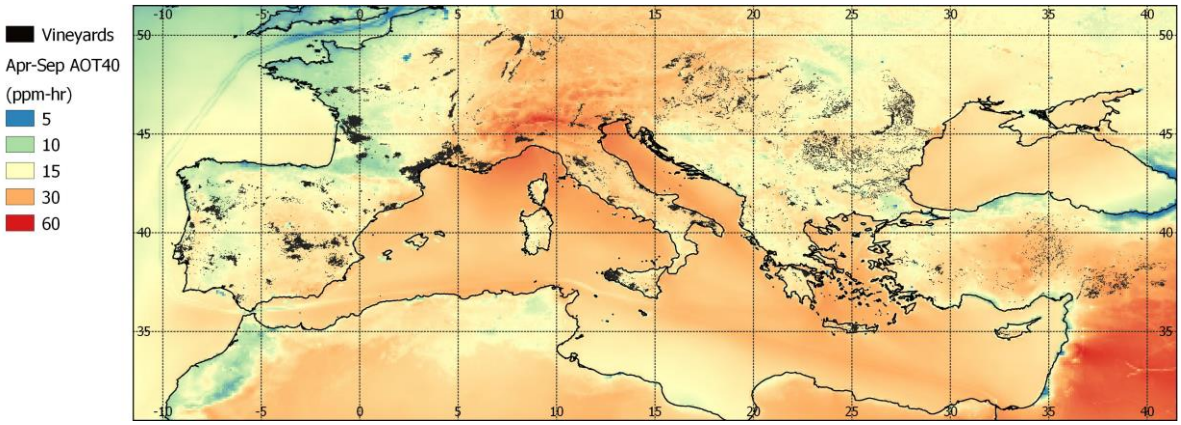

Figure 3-3. 0.1° x 0.1° EU *AOT40* Forest map produced for the year 2018 based on EMEP/MSC-W model data provided by the Norwegian Meteorological Institute and downloaded from the EMEP MSC-W modelled air concentrations and depositions data web site ([dataset] Norwegian Meteorological Institute, 2019).

As expected, it can be observed that the flux pattern is very different to that displayed using the exposure map. Once again, many grapevine growing areas exceed *AOT40* values that have been associated with effects on yield and quality for cultivars such as Welschriesling with a yearly *Jun-Sep AOT40* exposure of 27 ppm-h corresponding to a 10% reduction of yield and 21 ppm-h (11.5 ppm-h for a second year) for a 10% reduction of monosaccharides (glucose and fructose) (Soja et al., 1997), or the global Merlot cultivar with a yearly *Jun-Sep AOT40* exposure of 6.1 ppm-h being associated to a 31.2% reduction of bunch yield and several effects on quality (e.g. 14.8% reduction of total polyphenols) (Fumagalli et al., 2019). Another cultivar grown globally, Tempranillo, has also been reported to significantly alter leaf gas exchange parameters (A, g_s, c_i) in association to a 51.8 ppm-hr *May-Sep AOT40* level (Universidad de Extremadura, 2007). Caution must be taken to interpret the *AOT40* parameter in relation to grapevine yield and quality beyond a mere indicative of potential risk as it does not relate directly with the dose of O_3 entering with the plant as already explained in section 3-2. The grapevine-based *POD* critical levels mentioned should not be used for any other purpose either as they are based on only one OTC experiment per cultivar under different environmental conditions.

Although the DO3SE model currently constitutes the backbone of the CLRTAP methodology for O_3 phytotoxic risk assessment in Europe (De Marco et al., 2016), there are also other alternative and well-established methods to estimate g_{sto} O_3 entrance into the plant. For instance, a semi-mechanistic photosynthesis-based approach which relates g_{sto} with net photosynthetic rate and prevailing climatic conditions has also been applied for grapevine

and wheat in comparison with the DO3SE model (Büker et al., 2007). Results indicated a similar performance in predicting g_{sto} for time-steps of various lengths (from minute to seasonal) with the DO3SE multiplicative model performing marginally better when capturing the observational variation in the field validation datasets than the photosynthesis-based algorithm, which also required more detailed meteorological input data (e.g. ambient CO_2, dew-point temperature) and plant-physiological parameters (e.g. V_{cmax}, J_{max}) that are often not available (Büker et al., 2007). Another approach is given by the work of Rydsaa *et al.* (2016), who applied another widely and versatile dry deposition scheme used for global and regional studies, the Wesely dry deposition scheme as included in the WRF-Chem modelling system with the purpose to validate stomatal uptake estimates derived from a high resolution 3 x 3 km^2 domain against field measurements of three vegetation types in a Mediterranean environment (i.e. barley, holm oak forest and maquis) in Italy. Results showed that improvements were required to avoid overestimation systematic biases concerning assumed minima stomatal conductance, and stomatal conductance dependencies on optima temperature ranges, available *SWC* and *VPD*.

3.5 DISCUSSION

There has been a considerable development on policy oriented standard proposals from those based on exposure-based critical levels (level I approach), in the late 1990s, to those based on the actual dose or flux entering the plant through the stomata as a function of ambient O_3 and several other environmental variables (level II approach), in the early 2010s. Although these later standards have a stronger biological basis, they have not been adopted yet by any European directive concerning atmospheric pollution abatement policies and vegetation protection despite the fact that it is already known that risk assessments based on level I or level II approaches have not comparable results. For instance, some success has been reported on atmospheric emissions abatement policies yielding to a levelling off or a reduction on ambient O_3 exposure in the Northern Hemisphere based on recent tropospheric O_3 changes (Oltmans et al., 2013) or mid-century projections for Europe (Klingberg et al., 2014). In the most positive scenarios, ambient O_3 could already fall below the critical levels used for vegetation in the EU directive 2008/50/EC. However, for the phytotoxically more relevant stomatal flux, critical levels are still exceeded under those scenarios. Moreover, climate change could cancel the benefits

of emission reductions due to changes in chemical reactions, local meteorology, long-range transport, sensitiveness of the vegetation growing period lengths or adoption of cultural practices such as irrigation. In this sense, flux-based assessments were recently recommended to evaluate air pollution impacts on ecosystems in the scope of the revision of the EU National Emissions Ceilings Directive (NECD, 2016/2284/EU). Currently, according to the CLRTAP: "*AOT40*-based critical levels are suitable for estimating the risk of damage where no climatic data or suitable flux models are not available, and/or areas where no climatic or water restrictions to stomatal O_3 flux are expected, and economic losses should not be estimated using this method" (CLRTAP, 2017b).

There has also been substantial advancement on understanding the effects of O_3 on physiological and biochemical processes, including effects on yield and quality of the grapevine, through observational and experimental studies mostly performed by mean of adapted greenhouses or OTCs. In these sense, ambient O_3 exposure cause-effect relationships for yield and sugar content based on *AOT40* were derived by Soja et al. (1997, 2003 and 2004). Based on the level-I *AOT40* cause-effect relationship for grapevine yield estimated in those studies coupled with the EMEP photooxidant model, grapevine yield losses across Europe in 1990 were estimated to be 6% of the total crop damages, with an approximate value of 258 million 1990 £ (661 M € as of 2020), and France, Italy and Spain concentrating the greatest detriments (Holland et al., 2002). However, these estimates have a great level of uncertainty as they were based on only one Austrian grapevine variety classified as moderately sensitive to O_3 according to its own *AOT40* response function (Mills et al., 2007) under irrigation in continental climate conditions, which are not representative of the more extensive European Mediterranean grapevine growing areas. Furthermore, Soja's et al. experiments (1997, 2003 and 2004) lacked hourly O_3 and meteorological records for conditions within the OTC and results were estimated from mean monthly data. Therefore, it is not possible to accurately derive O_3 flux level-II standards for the grapevine based on these experiments as the data to assess stomatal conductance and O_3 concentrations are not available (Mills et al., 2006). In this regard, several more greenhouse or OTC O_3 fumigation experiments have been carried out on the grapevine since the works of Soja et al. in 1997 and 2004 (e.g. Pellegrini et al. 2015, Valleta et al. 2016, Geng et al. 2017, Decotteau et al., 2016, Fumagalli et al., 2019 and Wang et al., 2019). These experiments have been very useful to confirm effects on yield and quality on globally

cultivated cultivars, such as Cabernet Sauvignon and Merlot, or to better understand the different acclimatization capacity of different varieties in terms of the existence of functional traits, genetic variability, response of photosynthetic machinery, production of solutes (e.g. proline) mediated by hormones (e.g. ABA), and antioxidant molecules (e.g. CGA). However, they had different research focuses (e.g. seasonal versus shorter term O_3 fumigation) and there has not been any further publishing of any more exposure or stomatal uptake-effect relationship according to the CLRTAP protocols, and it has not been yet possible to derive a species-specific critical level for the grapevine as there is not yet a coherent and shared input for detailed risk assessment.

With the development of computer and web technology, there is greater access to meteorological and atmospheric pollution data and modelling systems that couple meteorological and atmospheric chemistry allowing risk assessment studies at global, regional and local scales. Nowadays, models can provide results at high spatial and temporal resolution (e.g. 1 km and hourly) for present times or in the context of climate change (Miranda et al., 2020). For a crop such as a grapevine, continuous agronomical, physiological and biochemical research allows to refine and update stomatal flux parametrization by different approaches (e.g. EMEP approach, effect on photosynthesis). Yet all this development continues to be impaired by the lack of ambient O_3 level I and level II cause-effect relationships for the grapevine, and risk assessment remains uncertain, mainly at the regional scale, concerning the different tolerances of different varieties and the effect of different cultural practices (e.g. irrigation, pruning systems, canopy management, age factor etc.). Some field studies have been performed at the local scale by applying antioxidants on canopies or at the regional one by observing leaf or chlorophyll damage. These methods have their own uncertainties such as the concentration of antioxidant to use. Besides, there can be O_3 damage without clear leaf symptoms, different tolerances according to variety, and there is no control of other environmental variables such as soil type or altitude. Therefore, the specific effects of O_3 on the crop are more difficult to interpret and extrapolation of results remains elusive.

There is great awareness on the potential impacts of climate change and the need of mitigation measures within the wine industry, but most of the work is focusing on atmospheric physical variables, bioclimatic and climate change indices (e.g. Blanco-Ward et al., 2019; Fraga et al., 2016; Mira de Orduña, 2010; van Leeuwen and Darriet, 2016).

Taking advantage of this awareness, some of the future studies concerning the potential impact of climate change and suitable mitigation measures could also consider ambient O_3 and its effects on commonly affected physiological mechanisms or biochemical pathways by using suitably adapted greenhouses, OTC or field studies. The availability of modern free air-controlled exposure systems (FACE), which allow to expose crops to different O_3 concentrations without the need of any chamber or adapted greenhouse, should also be considered to stimulate further research on O_3 impacts on vegetation and derive stomatal flux dose-response functions.

As in the case of forests, awareness of needs concerning integrated common and coordinated research on atmospheric chemical composition and climate change potential effects on a major global crop such as the grapevine could continue to be promoted at the European level by groups of scientists such as CAPERmed at the European level, and by MEDECOS at the global scale, with encouragement to participate more in large-scale initiatives such as the UNECE-CLRTAP International Cooperative Programme (ICP) on effects of air pollution on natural vegetation and crops (ICP-Vegetation) and on Integrated Monitoring of Air Pollution Effects on Ecosystems (ICP-IM). Data collected in the framework of other European programs (LIFE, INTERREG, and H2020) could also be considered. As vineyards also have immense ecological, cultural and economic relevance in the European Mediterranean basin, besides being the major fruit crop at the global scale in terms of acreage and economic value, it would also seem reasonable to propose the existence of a network of vineyards across Mediterranean countries to assess the relation of O_3 based metrics (e.g. *AOT40*, *PODY*) with grapevine health indicators derived from visual symptoms (leaf stipple, leaf yellowing and premature senescence), leaf gas exchange parameters (A, g_{sto}, c_i), leaf fluorometry-based plant stress parameters (F_v/F_m), phenology, biomass (e.g. pruning), yield (e.g. bunch weight) and grape quality (e.g. reducing sugars, titrable acidity, soluble solids, total phenols).

Publishing under common agreed standards and data sharing is also a key issue in terms of assessment of potential impacts of ambient O_3 and climate change on the grapevine. As an example, a 2010-2014 "summer" *AOT40* global map as derived from 3098 non-urban sites from the TOAR database is illustrated in figure 3-4. Following the TOAR procedure, the "summer" period corresponds to April-September for the Northern Hemisphere (NH), and October-March for the Southern Hemisphere (SH). These 6-month time intervals are

expected to capture the main growing season for long-living vegetation, perennial crops such as the grapevine, and trees in most areas of the world (Mills et al., 2018).

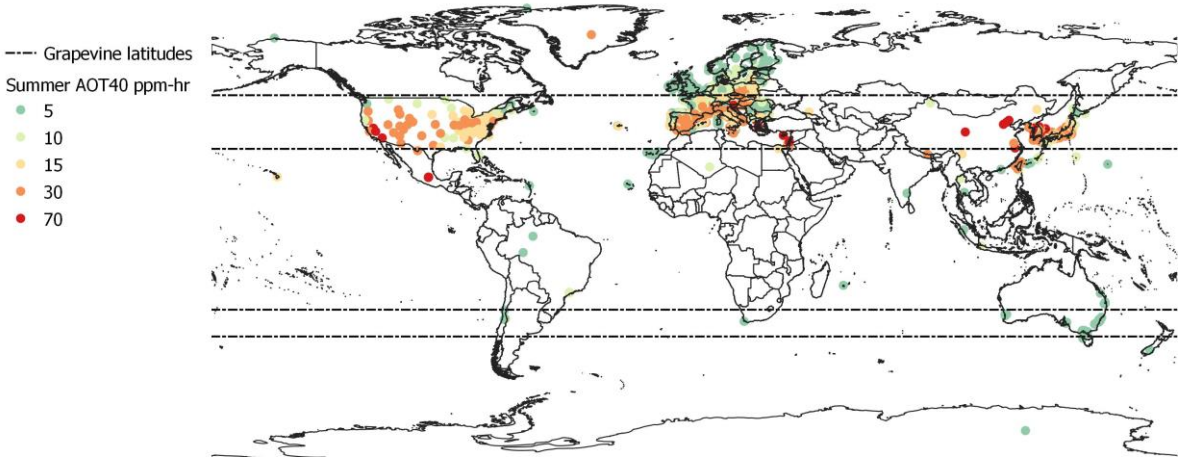

Figure 3-4. 2010-2014 "summer" *AOT40* World map derived from 3098 non-urban sites from the TOAR-Surface O_3 Database ([dataset] Schultz et al., 2017).

Through warm and cool periods of the past, most areas suitable for wine production have been traditionally located within relatively narrow latitudinal bands between 30° and 50° N and 30° and 40° S. These latitudinal bands also correspond approximately to the 12° to 22°C grapevine growing season isotherms (April-October in the northern hemisphere, October-April in the southern one) and are likely to move south and north in relation to climate change (Antivilo et al., 2017; Schultz and Jones, 2010). Between those narrow latitudinal bands there are areas of Mediterranean, maritime and moderate continental climates characterized by wet winters and hot summers, relatively mild winters and dry cool summers, and cool winters and warm summers with relatively uniform annual precipitation respectively (Jackson, 2008). It can be observed that the "summer" *AOT40* exposure is frequently well above the CLRTAP exposure-based critical level for trees (5 ppm) between those latitudes in the northern hemisphere whereas it is below in the few stations available for the southern hemisphere. It can also be observed that the *AOT40* critical levels already commented in section 3-4 as potential risk indicators for global cultivars such as Merlot (*June-September AOT40* exposure of 6.1 ppm-hr being associated with reductions of 31.2% for bunch yield and 14.8% for total polyphenols) or Tempranillo (*May-September AOT40* exposure of 51.8 ppb-hr associated with significant alteration of gas exchange parameters) are also likely to be exceeded at the global scale between those parallels with the exception of the southern hemisphere.

From a 2010-2014 "summer" mean ambient O_3 map also derived from the TOAR database (figure 3-5), we can observe most of the sites exceed the 30 ppb and 40 ppb levels between 30 – 50 ° N. Under such ambient O_3 exposure conditions, significant effects on gas exchange parameters have also been reported for the global varieties Tempranillo (Universidad de Extremadura, 2007) and Merlot (Popescu et al., 2012) with visible foliar symptoms such as stipple present under high summer light intensities in other varieties (e.g. Beck memento, Frontenac) (Geng et al., 2017). Mean ambient concentrations between 50 and 60 ppb correspond to the most polluted areas where another global grapevine variety, Cabernet Sauvignon, has also been reported to be affected in crop yield (bunch weight reduction, 20.5%) and quality (reducing sugars reduction 32.4%, soluble solids reduction 33.1%, tannings 57.7%, total phenols 22.5%) (Wang et al., 2020) benefiting from protective canopies when summer light intensity is above 1.600 µmol m^{-2} s^{-1} (Geng et al., 2017). The reduction on yield estimated for heavily polluted areas in east China coincides with the mean negative impact of approximately 20% on yields of the Thompson Seedless variety in the San Joaquin valley of California, back in the early eighties (Brewer and Ashcroft, 1983) and which constitutes an area where O_3 exposure continues to be high. These estimates can only be taken as mere indications about the possible range of potential effects on yield and quality over global grapevine cultivars under a extensively spread "summer" *AOT40* level greater than 30 ppm-hr (Mediterranean basin) or "summer" mean O_3 levels greater than 60 ppm-hr (east China or San Joaquim valley, California) as no limitations due to climate or water restrictions to stomatal O_3 flux have been considered and there have not been common protocols to derive the reported effects.

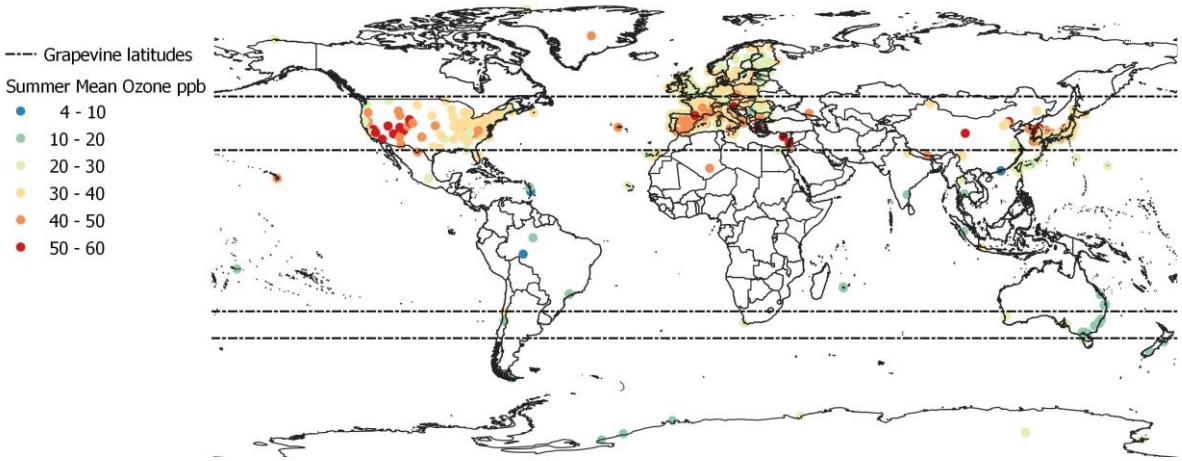

Figure 3-5. 2010-2014 Apr-Sep ambient O_3 mean concentration world map derived from 3098 non-urban sites from the TOAR-Surface O_3 Database ([dataset] Schultz et al., 2017).

Table 3-5 summarizes the discussion based on the current-state-of-the-art following a SWOT approach on assessing the risk of tropospheric O_3 phytotoxic effect on a Mediterranean crop such as the grapevine.

Table 3-5. SWOT concerning the state-of-the-art on tropospheric O_3 risk assessment on the grapevine.

Strengths	1. There has been much development concerning modelling of level-I and level-II standards. 2. There is progress on the physiological and molecular effects of ambient O_3 on the grapevine including photosynthetic activity, defence mechanisms, and genotypic/functional traits variability.
Weaknesses	1. Except for wheat, potato and tomato, there are not level-I exposure-effect nor level-II stomatal uptake-effect relationships derived from comprehensive input data that could be applied for a detailed risk assessment. 2. The applicability of the level-I approach is questioned in Mediterranean environments. 3. Regional assessments would need to consider different grapevine varietal tolerances as there is evidence of a range of sensitivities for this crop.
Opportunities	1. There is opportunity to perform valuable experimental O_3 fumigation studies by using facilities, such as free air-controlled exposure experiments, overcoming the OTC limitations for perennial crops such as the grapevine. 2. Other fumigation or photoprotective methods are also valuable considering grapevine varietal variability. 3. There is opportunity to perform valuable experimental and modelling work in association to related and pertinent traits such as drought tolerance. 4. As the defence mechanisms concerning environmental variables (e.g. solar radiation, drought, CO_2 levels, and pest incidence) interact through common physiological mechanisms and biochemical pathways, combined studies should be promoted concerning grape adaptation to climate change. 5. There is opportunity to advance high-resolution (e.g. over topographically complex terrains) O_3 exposure and O_3 deposition modelling systems. 6. There is opportunity to advance on incorporating the effect of drought on O_3 deposition modelling. 7. There is opportunity to propose a network of vineyards across Mediterranean countries to assess the relation of

	O_3-based metrics (e.g. *AOT40*, *PODY*) with grapevine health indicators. 8. There is opportunity to benefit from publishing under common agreed standards and protocols and to develop public access databases (e.g. TOAR vegetation).
Threats	1. Recent studies are showing some effect of emission policies on reducing vegetation O_3 exposure. However, fluxes could still harm crops, such as the grapevine, as exposure continues to be much higher than preindustrial times. In addition to the extensive requirements needed to perform reliable experimental studies for a perennial crop such as the grapevine, there is a threat for this type of studies to count with not enough support compared to other ones (e.g. drought tolerance studies). However, cross-tolerance studies are crucial to predict agricultural yield under natural changing climate conditions.

3.6 CONCLUSION

Focusing on the advances made since the beginning of this century, there is increased knowledge on the O_3 phytotoxic effects on the grapevine at the cellular, structural and anatomical leaf level, and leaf gas exchange parameters which can be accentuated depending on variety. It has also been verified that there is a diverse capacity for biochemical response and adaptation of the photosynthetic machinery and hormonal and antioxidant response depending on the specific cultivar too. It would be of interest to continue research on the combined effect of drought, high temperatures, light intensity, pests or other atmospheric compounds (e.g. CO_2, NO_2, SO_2, PAN).

To date, there is still only one series of works (Soja et al. 1997, 2003, 2004) where exposure or flux based ambient O_3 critical levels were derived for the grapevine with grape quality being more sensitive than yield. However, these critical levels have not been accepted by CLRTAP for detailed impact assessment as they are based only on a variety grown in European continental conditions (e.g. Austria) and only g_{sto} max was parameterized to estimate POD. Since the late 2010s, there have been studies focusing on global varieties such as Cabernet Sauvignon and Merlot which are second and fourth according to total cultivated extension in the World (341000 and 266000 ha respectively) (OIV, 2017), but there have not been further advances to derive ambient O_3 critical levels for yield and quality for these varieties.

There is already a FACE facility in the European Mediterranean environment, which avoids depending on greenhouses or OTCs for experimentation on ambient O_3 effects on crops such as the grapevine in combination with other stressors. There is still very little experience concerning monitoring of grapevine health indicators in the field and the few isolated studies cannot be extrapolated to other regions. Similarly to what has been recently started to be done with trees (e.g. De Marco et al. 2019; Paoletti et al. 2019), it would be useful to perform research on a series of health indicators specifically selected for the grapevine which, for instance, could relate foliar damage (e.g. stipple, browning, premature leaf ageing), plant stress (e.g. F_v/F_m), leaf nutritional and biochemical status, yield and quality with ambient O_3 along a network of selected vineyards also monitored for the effects of climate change.

According to the state-of-the-art, exposure and flux-based grid maps available from EMEP for Europe, and global exposure data from the TOAR database, there is risk for O_3 phytotoxic effects on a major fruit crop such as the grapevine, not only across extensive Mediterranean areas in the northern hemisphere, but also under moderate continental climate conditions across Europe (e.g. Germany and Austria) or maritime climates in East Asia (e.g. China, Japan, South Korea). Taking into consideration the recently available studies performed on global varieties, such as Cabernet Sauvignon and Merlot, effects could be in the order of 20-31% for yield reduction, and of 15-23% for quality compounds such as total polyphenols. Recent levelling off or decrease of exposure levels such as those recently reported in the Western Mediterranean basin could decrease risk, but phenological advancement due to increased temperature associated to climate change, and interaction between O_3 and other climatic variables (e.g. drought or light intensity) could also offset the benefit. It is necessary to enforce common protocols so that more detailed assessments can be performed both at the global and regional scales.

Photo credits.

McFadden-Smith, Wendy Author's (Ontario Ministry of Agriculture, Food and Rural Affairs). © Queen's Printer for Ontario, 2018. Photos on the different levels of O_3 stipple aggregation on grapevine leaves for a French American hybrid variety identified as *Vidal blanc*.

4 VALIDATION OF METEOROLOGICAL AND GROUND-LEVEL OZONE WRF-CHIMERE SIMULATIONS IN A MOUNTAINOUS GRAPEVINE GROWING AREA FOR PHYTOTOXIC RISK ASSESSMENT

This chapter was published as:

Blanco-Ward, D., A, R., Viceto, C., Ribeiro, A.C., Feliciano, M., Paoletti, E., Miranda, A.I., 2021. Validation of meteorological and ground-level ozone WRF-CHIMERE simulations in a mountainous grapevine growing area for phytotoxic risk assessment. Atmos. Environ. 259, 118507. https://doi.org/10.1016/j.atmosenv.2021.118507

I mainly contributed with the postprocessing of the WRF simulations, performed and postprocessed the CHIMERE simulations, and analysed the field campaign data. I was also responsible for the writing of the paper.

Abstract

Ozone is the most damaging phytotoxic air pollutant to crop yield quantity and quality. This study presents the validation of a simulation with the WRF-CHIMERE modelling system in order to assess the risk of phytotoxicity by tropospheric ozone for an important and characteristic Mediterranean crop, i.e. the grapevine. The study region was the Douro wine region in Portugal, which is characterized by a rugged relief and a Mediterranean climate. The simulation covered a reference grapevine growing season in the Northern Hemisphere (from April to September 2017), during which a particular measuring campaign was also carried out. The validation of the meteorological simulations on a daily and hourly time resolution was performed based on data from three weather stations, namely on temperature, global solar radiation, relative humidity, wind speed and direction values. The ozone phytotoxicity was assessed with data from two measuring stations. A specific grapevine growth parameter based on monitored phenological observations was introduced for ozone stomatal uptake assessment. Concerning meteorology, validation statistics were acceptable and within the range of what has been found in other regional climate modelling simulations. Ground-level ozone-based values were calculated for a better assessment of the phytotoxic risk, in particular cumulative standards for vegetation protection. Stomatal flux estimates were within the range of those measured for the local cultivars in the field campaign when there was not severe water stress limitation. Both field and statistically adjusted model values indicate that considerable areas in the Demarcated Douro Region of Portugal can exceed the critical exposure values for vegetation according

to current European legislation standards. Moreover, measured and simulated results indicate an ozone impact on grapevine yield and quality in the target region because the exposure- and flux-based indices exceed the criteria based on current open-top-chamber experimental knowledge.

4.1 INTRODUCTION

Ozone (O_3) stands out as the tropospheric pollutant with greatest phytotoxic effect on crops, pastures and forests (Ainsworth et al., 2012; Booker et al., 2009; Li et al., 2017). Yield losses have been estimated to range between 5 to 20% for important crops, such as wheat, rice and legumes, and they can reach greater figures depending on the sensitivities of the different cultivars (Avnery et al., 2011b; Feng et al., 2019; van Dingenen et al., 2009). It is expected that background levels of tropospheric O_3 will continue to increase globally in relation to the increasing industrialization of developing countries and intercontinental transport. However, the effects of emission reduction policies, such as the reduction of maximum O_3 peak levels or levelling off or even declines of long-term trends have also been observed in Europe, North America and Japan (Oltmans et al., 2013; Paoletti et al., 2014; Sicard et al., 2013; The Royal Society, 2008). Concerning O_3 metrics of relevance for vegetation, the highest 2010-2014 O_3 levels were found in the mid-latitudes of the Northern Hemisphere including southern United States of America, the Mediterranean basin, northern India, north, north-west and east China, the Republic of Korea, and Japan (Mills et al., 2018). Moreover, the Mediterranean area is susceptible to a greater exposure to environmental O_3 with a higher incidence of warm summers and heat waves (Jacob and Winner, 2009; Katragkou et al., 2011; Meleux et al., 2007). Considering projected surface O_3 concentrations simulated by six global atmospheric chemistry transport models on the basis of a representative concentration scenario (RCP8.5), Sicard et al. (2017) found that many areas of the Northern Hemisphere (e.g. North America, Greenland, Europe, southern Asia, north-eastern China) would undergo an increase of O_3 levels and risk of O_3 injury for vegetation in association with an increase in methane emissions, global warming and weakened nitric oxide titration. These results are in line with those found under RCP8.5 by Fortems-Cheiney et al. (2017) for Europe.

The grapevine is the crop where the phytotoxic effects of O_3 were first noticed (Richards et al., 1959). Although it is not a food security crop, such as wheat, rice, soybean, maize or potato, it has immense cultural, economic and ecological importance within the Mediterranean basin, besides being the fruit crop with the largest acreage and highest economic value globally (Ponti et al., 2018). Since the early observations from the fifties, there is nowadays a greater knowledge and awareness of the effects of O_3 on grapevine and its defence mechanisms (Blanco-Ward et al., 2021a; Pellegrini et al., 2015; Valletta et al., 2016), but there are wide gaps that prevent to relate the exposure or stomatal uptake of O_3 with grapevine yield and quality (CLRTAP, 2017a; Mills *et al*., 2006).

There is already a good number of studies in relation with climate change as a potential threat to wine production and typicity (e.g. Blanco-Ward et al., 2019; Fraga et al., 2016; Mira de Orduña, 2010; van Leeuwen and Darriet, 2016), but there is still a lack of studies addressing the potential effects of changes in the meteorological fields, drought or carbon dioxide atmospheric enrichment in relation to surface O_3 for this crop. An example where the potential phytotoxic effect of O_3 in the context of climate change has been considered is the work of Miranda et al. (2020) in the Demarcated Douro Region (DDR) of Portugal suggesting that the tropospheric O_3 levels in the future would influence the quality and productivity of wine in the region. However, further refinement is needed in order to not rely solely on O_3 exposure, but also on the stomatal O_3 uptake by the grapevine in the study area.

A modelling approach can be very useful when assessing the risks of climate change on crops, but it is necessary to validate simulations with data from meteorological and air quality station measuring networks, as well as data of the physiological behaviour of the crops. The purpose of this paper is to evaluate high resolution (1 km x 1 km) meteorological and ground-level O_3 simulations aimed at performing a crop risk assessment for grapevine, based on current O_3 standards for vegetation protection, including the phytotoxic O_3 dose (POD) i.e. the accumulated stomatal O_3 uptake over the growing season (CLRTAP, 2017a). To accomplish this objective, the following research questions are addressed. Can a chemical transport modelling (CTM) system successfully replicate the meteorological and ground level ozone patterns in a complex terrain under Mediterranean climate conditions such as those present in the Douro wine region in Portugal? To which extend the range of simulated stomatal fluxes adequately represents those of the grapevine cultivars present

in the study area to estimate POD? Can current ground-level O_3 be related to any potential risk for a renowned wine producing region such as the Douro river valley in Portugal?

4.2 STUDY AREA

The Portuguese Douro Demarcated Region (DDR) crosses the two banks of the Douro River from the border with Spain until halfway through its course. The Douro valley stretches along 90 km in the west-east direction and along 50 km in the north-south direction (Figure 4-1). The westernmost region is located 70 km away from the Atlantic Ocean. The landscape is characterized by mountainous terrain, rising above the Douro river and its tributaries, with moderate to steep slopes and different expositions. The average elevation in the region is 443 m, but varies from about 40 m to a maximum of more than 1400 m. The Region covers about 250 thousand hectares with vineyard areas representing 43480 hectares, 17.4 % of the total area. It is divided into three sub-regions: Baixo Corgo with the smaller area (45000 ha), Cima Corgo, with intermediate extension (95000 ha), and Douro Superior with the greater extension (110000 ha). The vineyard area for these subregions is 13368, 20270 and 9842 ha, respectively (IVDP, 2017a).

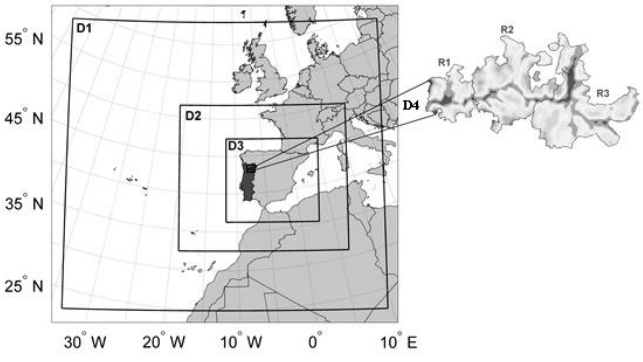

a)

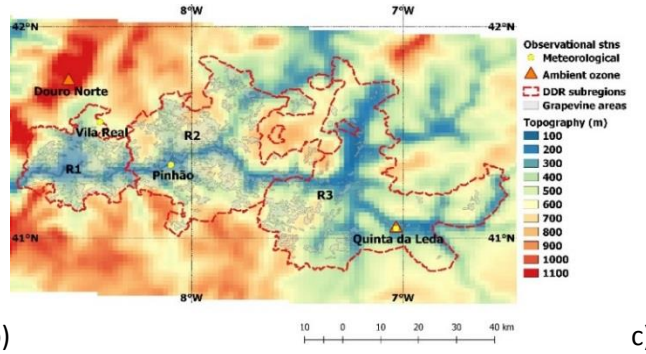

b)

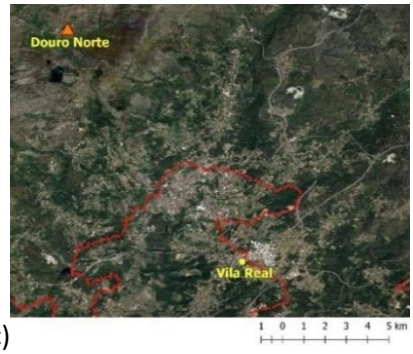

c)

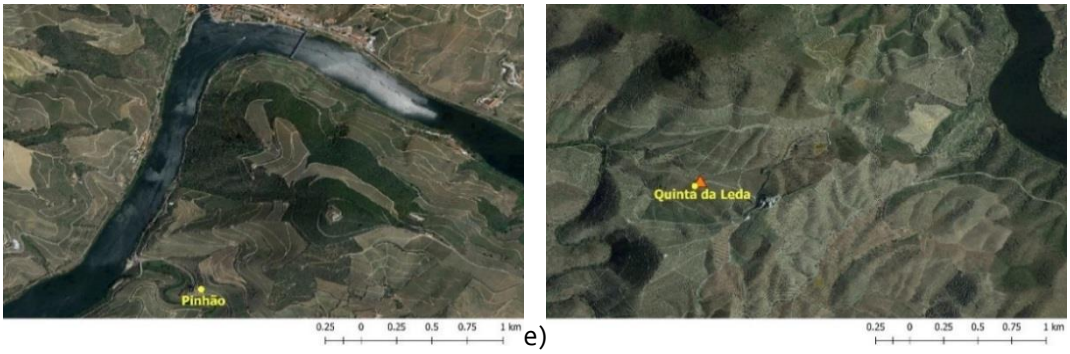

d) e)

Figure 4-1. a) Nested modelling domains and location of the Douro Demarcated Region (DDR) in northern Portugal. b) Subregions "Baixo Corgo" (R1), "Cima Corgo" (R2) and "Douro Superior" (R3), along vineyard areas and observational sites. c, d, e) Detail of observational sites.

The DDR presents a warm temperate climate (Köppen Csb), with average annual temperatures, for the period 1980-2009, of 15.4°C, mean minimum daily temperature (*Tmin*) in the coldest month of 2.7°C and average of the maximum daily temperature (*Tmax*) in the hottest month of 32.1°C. The mean rainfall of the driest month (July) is only 11.2 mm, but highly variable rainfall events are concentrated in the winter months. The region is protected from the humid and cold winds of the Atlantic Ocean by two mountain ranges, Marão and Montemuro, which are located on its western border. The temperature increases and precipitation decreases from west to east. The westernmost sub-region of the Douro Valley (Baixo Corgo) is closer to the Atlantic Ocean and therefore more affected by the moist sea winds. The easternmost sub-regions are further away from the Atlantic Ocean, thus having a more continental climate influence. Low precipitation values, together with high temperatures and high radiation exposure, give rise to intense water and thermal stresses, particularly in the Cima Corgo and Douro Superior subregions (Jones and Alves, 2012).

4.3 DATA SOURCES AND CALCULATIONS

Modelled and measured meteorological and O_3 values were compared and analyzed using selected statistical quality indicators for a field campaign period from April to September 2017. Moreover, O_3 standards for vegetation were calculated and assessed.

4.3.1 Field campaign data

The meteorological data were obtained from two meteorological stations (Pinhão and Vila Real) from the Portuguese Institute for the Sea and the Atmosphere (IPMA) and one

meteorological station (Quinta da Leda) from a wine company in Portugal, Sogrape Vinhos. The Pinhão (130 m) and Quinta da Leda (228 m) are located in the Douro valley under Mediterranean climate conditions whereas Vila Real (561 m) represents plateau conditions where there is a stronger sub-Atlantic oceanic influence (Ribeiro, 2000). Two observational sites for ambient O_3 were also available: the Douro Norte station (1086 m) belonging to the Portuguese Environmental Agency and the Quinta da Leda station (228 m), which was made operative specifically in the scope of the DOUROZONE project, and from April to September 2017. The location of the meteorological and O_3 monitoring stations can be observed in Figure 4-1 (b, c, d, e). The April to September growing season length is commonly taken as a valid reference grapevine growing season in the Northern Hemisphere (Tonietto and Carbonneau, 2004) and is used concerning O_3 risk assessment for perennial crops and deciduous trees (Mills et al., 2018).

Along the same period, in Quinta da Leda, the phenological development of two grapevine cultivars characteristic of the DDR, 'Touriga Franca' and 'Touriga Nacional', was monitored once per week according to the Biologische Bundesanstalt, Bundessortenamt und CHemische Industrie (BBCH) phenological scale. Six representative plants per cultivar were chosen. For each of the two cultivars, it was considered that certain phenological stage had been reached when at least two of the six plants manifested it in a dominant way whereas the remaining ones had also started to display it. Table 4-1 shows the dates of the main phenological stages considered for those cultivars at Quinta da Leda in 2017. No major differences were found in the phenological development of the two cultivars although there was more variation in the first phenological stages.

Table 4-1. Dates of main phenological stages for two characteristic grapevine cultivars of the DDR as observed at Quinta da Leda through the 2017 field campaign.

BBCH Phenological stage	**Date**	**cv. Touriga Nacional**	**cv. Touriga Franca**
Bud burst	29/03/17	3 (9D), 3 (9I)	4 (9D), 2 (11D)
Beginning of flowering	03/05/17	1 (61D), 3 (60D), 2 (60I)	1 (61D), 1 (60D), 4 (60I)
Beginning of ripening	05/07/17	6 (81D)	6 (81D)
Berries ripe for harvest	23/08/17	6 (89D)	6 (89D)

Beginning of leaf-fall	27/09/17	6 (93D)	6 (93D)

Note: the phenological summary for each of the cultivars is expressed as the number of plants that have reached a given BBCH phenological stage. BBCH code 9 stands for bud burst, 11 for first leaf unfolded, 60 first flower hoods detached from the receptacle, 61 10% of flower hoods fallen, 81 beginning of ripening: berries begin to develop variety-specific colour, 89 berries ripe for harvest, 93 beginning of leaf-fall. For this specific monitoring, letters D and I are used to indicate a dominant or incipient stage manifestation. For instance, 3(D9), 3(I9) corresponds with 3 grapevine plants reaching bud burst (BBCH code 9) as a dominant stage and other 3 grapevine plants which start to manifest that phenological stage.

4.3.2 Model simulations

The Weather Research and Forecasting (WRF) model is a mesoscale numerical weather prediction system, which can be used in a wide range of applications across scales from tens to thousands of kilometres. A detailed description of the model is provided by Skamarock et al. (2008), and further information on parameterizations, specifically suited for the Iberian Peninsula, is in Marta-Almeida et al. (2016). The WRF model was used initially as a dynamical downscaling tool to obtain regional meteorological information from the ERA-Interim reanalysis dataset. The WRF high-resolution climate simulations were implemented for four nested domains with increasing horizontal resolution, namely 81 (D1), 27 (D2), 9 (D3), and 1 km (D4) (Figure 4-1a). The WRF modelled period analysed for meteorological validation purposes consisted of hourly results from April 1st to September 30th.

The chemical and atmospheric transport model CHIMERE (Menut et al., 2013) was used to estimate ground-level O_3 exposure while the dose of O_3 entering the plant was calculated based on the dry deposition of O_3 for stomatal exchange (DO3SE) model of the European Monitoring and Evaluation Programme for long-range transmission of air pollutants (EMEP) (Emberson et al., 2000a), updated according to the last parametrizations available for grapevine (CLRTAP, 2017c; Emberson et al., 2005). WRF simulations results were used as meteorological inputs for CHIMERE together with anthropogenic pollutants emission data from the emission database of EMEP, which were pre-processed for the four domain configurations. Biogenic emissions were computed using the global Model of Emissions of Gases and Aerosols from Nature (MEGAN). Land use types needed by CHIMERE to calculate biogenic emissions, as well as other processes such as deposition, were derived from the U.S. Geological Survey (USGS) 1 km resolution land cover database. The CHIMERE chemical

mechanism is based on the MELCHIOR scheme (Mailler et al., 2016). Hourly O_3 simulated values were obtained for the field campaign period - April 1st to September 30th.

4.3.3 Selected variables and O_3 standards

High ambient O_3 concentrations do not always correspond to high stomatal O_3 fluxes as stomatal closure is induced by low solar radiation and high vapour pressure deficit. Wind also affects laminar resistance to ozone flux into plant leaves. Therefore, the following variables selected for the evaluation of the meteorological simulated values from April to September 2017, were considered: daily maximum temperature (*Tmax*), hourly mean temperature (*Tmean*), daily maximum global solar radiation (*Radmax*), hourly mean global solar radiation (*Rad*), daily minimum relative humidity (*RHmin*), hourly mean relative humidity (*RH*), hourly mean wind speed (*Ws*) and daily mean wind direction (*Wdmean*).

Concerning ground-level O_3 risk assessment exposure-based standards for vegetation, *AOT40* corresponds to the sum of the daylight (8:00 – 20:00 according to the European Union Directive 2008/50/EC, and daytime hours with > 50 Wm^{-2} according to the Convention on Long-range Transboundary Air Pollution, CLRTAP) hourly O_3 concentrations greater than 40 ppb accumulated at the top of the canopy during the growing season and is calculated by equation 1:

$$AOT40 = \sum_{accumulation\ period} (0; C_c - 40)\Delta t \qquad (1)$$

where C_c represents the O_3 concentration value.

According to the European Union (EU) legislation (Directive 2008/50/EC), the May to July time window can be used to evaluate the negative effects of ozone (e.g. yield reduction, growth reduction, visible injury) on any kind of vegetation whereas, according to CLRTAP (CLRTAP, 2017a), the *AOT40* index can also be used with longer time-windows, such as 6 months (e.g. April to September) corresponding to the growing season of perennial-dominated (semi-)natural vegetation or forest deciduous trees, so that it can be related with growth reduction effects for those vegetation types. The *AOT40* indices are commonly associated with exposure-based critical levels (CLe_c) above which adverse effects on sensitive vegetation may occur according to present knowledge (CLRTAP, 2017a). The EU *May-July AOT40* has a CLe_c value of 9 ppm-h as 5-year (or 3-yr) average and 3 ppm-h as long-target value, which also coincides with the CLRTAP Cle_c value for agricultural crops

when applied during a 3-month growing season in a year. However, the CLRTAP Cle_c value associated to a 6 month time window and growth reduction effects for perennial-dominated (semi)natural vegetation and trees is 5 ppm-h in a year (Paoletti and Manning, 2007). For grapevine, the only *AOT40* Cle_c published values so far are those related with the experimental work of Soja et al. (1997) which are based on a Welschriesling cultivar exposed to different levels of O_3 in open-top-chambers under a continental climate in eastern Austria. This experimental work acknowledged the relevance of a memory effect for a perennial crop such as grapevine, and a Cle_c of 27 ppm-h for a 10% reduction of grape yield was established, without no variation in a second exposure year, whereas the values associated with a 10% reduction in grape monosaccharide yield were 21 ppm-h in the first exposure year and 11.5 ppm-h in the second experimental year.

The cumulative exposure (level-I) approach has been extensively criticized, because it does not reflect the actual dose or flux of O_3 entering the plant (Emberson et al., 2000b; Massman, 2004; Mauzerall and Wang, 2001; Musselman et al., 2006; Paoletti and Manning, 2007). To overcome these limitations, a flux-based or level-II approach was developed under the CLRTAP convention (Mills et al., 2011b). This approach has a stronger biological basis since it considers a Phytotoxic Ozone Dose (*PODY*) by considering the O_3 stomatal uptake, which can be understood as the amount of O_3 molecules that penetrate the leaf tissue through the stomata as a function of ambient O_3 concentration and several other critical environmental parameters such as temperature, water vapour pressure, light, soil water potential and plant growth (phenological) stage (Emberson et al., 2000b). *PODY* is defined as (CLRTAP, 2017a):

$$PODY = \sum_{accumulation\ period} (0; Fst - Y)\Delta t \qquad (2)$$

Where *Fst* is the instantaneous flux of O_3 through the stomatal openings per unit projected leaf area (PLA). It refers specifically to the sunlit leaves at the top of the canopy. It is regarded here as the hourly mean flux of O_3 into the stomata. *Y* is the threshold stomatal flux per PLA. Both parameters have units of nmol $O_3 m^{-2} s^{-1}$. Critical levels based on stomatal flux (Cle_f) are then cumulative stomatal fluxes above which adverse effects may occur according to present knowledge (CLRTAP, 2017a). In a later work, Soja et al. (2004) also published Cle_f values for grapevine associated with a *POD6* index (stomatal O_3 flux above 6 nmol O_3 $m^{-2} s^{-1}$). A Cle_f of 3.5 mmol m^{-2} for a 10% reduction of grape yield was established

for the first experimental year and 2.2 mmol m^{-2} for the second year whereas the values associated with a 10% reduction in grape monosaccharide yield were 2.3 mmol m^{-2} in the first year of the experiment and 1.1 mmol m^{-2} in the second year.

Both *AOT40* and *POD* based approaches were used to assess our model results and measurements. The ground-level O_3 variables and vegetation risk assessment standards selected for evaluation of the simulations were the following: daily O_3 max (*O_3 max*), hourly O_3 mean (*O_3 mean*), EU legislation-based *May to July AOT40* (*May-Jul AOT40*), CLRTAP-based *April to September AOT40* (*Apr-Sep AOT40*), *June to September AOT40* as proposed by Soja et al. (1997, 2004) for the grapevine (*Jun-Sep S AOT40*), CLRTAP-based *April to September POD* (*Apr-Sep POD*), *June to September POD* as proposed by Soja et al. (1997, 2004) for the grapevine (*Jun-Sep POD*), CLRTAP-based *April to September POD6* (*Apr-Sep POD6*), and *June to September POD6* as proposed by Soja et al. (1997, 2004) for the grapevine (*June-Sep POD6*).

4.3.4 Assessment of modelling performance

Considering several studies (Borrego et al., 2008; Emery et al., 2017; Marta-Almeida et al., 2016; Politi et al., 2017; Soares et al., 2012; Willmott et al., 2012; Zittis et al., 2014) related to assess photochemical and meteorological model performance, the following methods and statistics were selected:

Daily scale

1. Time series plots of field data versus 1 km WRF-CHIMERE results.
2. Comparison of the probability distributions of the observed and modelled variables including a statistical test, the Kolmogorov-Smirnov (KS) test.
3. Evaluation metrics, such as the bias (BIAS), the ratio of the standard deviation between modelled and observed variables (SD Ratio), the mean absolute error (MAE), the mean absolute percent error (MAPE), the root mean square error (RMSE), the Pearson's correlation coefficient (CORR), and the modified index of agreement (MIA). For wind direction, MIA was replaced by the standard deviation of the errors (STDE), as it can be taken as an indicator of correct simulations physics if it is low, even when there is high BIAS or RMSE (Carvalho et al., 2012).

Hourly scale

1. Taylor diagrams, which also include correlations between observed and modelled variables, similarity in variable distributions (standard deviation comparisons) and root mean square error (RMSE).

Regional weather and chemical transport models can exhibit systematic simulation biases. When that is the case, the simulations could be post-processed in order to obtain more reliable estimates of the local weather or ambient air pollutants. Among the diversity of methods available, a non-parametric quantile-quantile (QQ) transformation was selected due to its relative simplicity and good skill to reduce bias in modelled fields, such as precipitation, as suggested by Gudmundsson et al. (2012). The QQ transformation was only applied to the WRF-CHIMERE final results related to O_3 phytotoxic risk assessment, ambient O_3 and O_3 stomatal flux.

For the comparison between modelled and measured values, a cell bilinear interpolation filter was applied to the WRF-CHIMERE neighbouring cells to the location of the field observational stations. Next, the results of comparing the meteorological and air quality simulated and measured values are presented.

4.4 RESULTS AND DISCUSSION

This section focuses first on results related with temperature, global solar radiation, relative humidity, and wind as principal meteorological drivers related to plant O_3 exposure and phytotoxic O_3 dose. Results related with daily *O_3 max*, hourly *O_3 mean* profiles, and seasonal standards for vegetation protection are described afterwards. The relevance of simulation bias, field campaign data for model parametrization and validation, and variability and significance of results also in relation to climate extremes is discussed.

4.4.1 Meteorological variables

Tables 4-2 to 4-5 present the obtained validation statistics for temperature, global solar radiation, relative humidity and wind speed and direction, respectively. These statistics are based on modelled WRF results versus observed values at Vila Real (R1), Pinhão (R2) and Quinta da Leda (R3), during the 2017 Apr-Sep grapevine growing season. Further information, namely maps, time series, density plots and Taylor diagrams can be assessed in the Supplementary Material.

Table 4-2. Validation statistics for daily *Tmax* and hourly *Tmean* (April-September 2017 period).

Daily *Tmax* (°C)	**Field value**	**BIAS**	**SD Ratio**	**MAE**	**MAPE (%)**	**RMSE**	**CORR**	**MIA**
Vila Real	26.0 (μ) 5.4 (σ)	-1.5	0.98	2.0	8.0	2.5	0.93	0.78
Pinhão	30.7 (μ) 5.4 (σ)	-2.7	0.99	2.9	9.7	3.4	0.92	0.68
Quinta da Leda	31.5 (μ) 5.7 (σ)	-3.1	0.97	3.3	10.5	3.7	0.93	0.66
Hourly *Tmean* (°C)	**Field value**	**BIAS**	**SD Ratio**	**MAE**	**MAPE (%)**	**RMSE**	**CORR**	**MIA**
Vila Real	19.1 (μ) 6.3 (σ)	-0.7	0.97	2.1	11.6	2.5	0.92	0.80
Pinhão	22.4 (μ) 7.0 (σ)	-1.6	0.95	3.0	14.3	3.2	0.89	0.73
Quinta da Leda	23.1 (μ) 7.4 (σ)	-1.8	0.93	2.2	10.1	2.0	0.96	0.81

The measured daily *Tmax* mean and standard deviation increased from the most northwestern location (Vila Real) to the most southeastern one (Quinta da Leda). The average bias of the WRF simulations increased from the northwest to the southeast too. The linear correlation was very strong (CORR > 0.90) in all cases. The SD ratios also indicated a similar spread of the observed and modelled data.

The hourly *Tmean* evaluation metrics were similar to those of the daily *Tmax* data, although there was a lower bias and a better model agreement reflected by higher MIA in all cases and the worst WRF performance was at the Pinhão location as revealed by its higher MAE and RMSE error (Table 4-2).

The higher *Tmean* error statistics estimated for the Pinhão were most likely associated with the greater difficulty to model the Mediterranean conditions present at the lower altitudes and deep and narrow valley locations (Figure 4-1d), in contrast with those present in the sub-plateau Vila Real location (Figure 4-1c) or more open Mediterranean locations towards the east such as Quinta da Leda (Figure 4-1e). Those conditions were more pronounced for daily *Tmax* with the model indicating worse accuracy and precision for both Pinhão and Quinta da Leda than for the sub-plateau Vila Real location under a more sub-Atlantic climate influence. This was also in connection with the greater difference between the station elevation and the value used by the model as derived from the digital elevation

model (DEM), respectively 130 and 225 m for Pinhão, 228 and 278 m for Quinta da Leda, and 561 and 568 m for Vila Real.

Overall, the results indicate a good agreement concerning patterns at the seasonal, daily and hourly scale for temperature, with probability distributions and error statistics within the range of those reported by other studies about the validation of WRF simulations in the Iberian Peninsula (Marta-Almeida et al., 2016; Soares et al., 2012) and other Mediterranean areas such as Greece (Politi et al., 2017). For instance, according to Soares *et al.* (2012) the validation statistics for a 5 km horizontal resolution WRF simulation for northeastern Portugal presented the following range for daily *Tmax*: CORR ≥ 0.90, BIAS -3.3 – 0.5 °C, RMSE 2.5 – 4.6 °C. This range of values is very similar to those found in Table 4-2 for daily *Tmax*.

Table 4-3. Validation statistics for daily *Radmax* and hourly *Rad* (April-September 2017 period).

Daily *Radmax* (kJ m^{-2})	**Field value**	**BIAS**	**SD Ratio**	**MAE**	**MAPE (%)**	**RMSE**	**CORR**	**MIA**
Vila Real	3159(μ) 478(σ)	110	0.66	227	9.3	409	0.57	0.65
Pinhão	3227(μ) 440(σ)	29	0.71	217	8.2	365	0.57	0.63
Quinta da Leda	3410(μ) 452(σ)	-132	0.68	332	10.5	402	0.55	0.44
Hourly Rad (kJ m^{-2})	**Field value**	**BIAS**	**SD Ratio**	**MAE**	**MAPE (%)**	**RMSE**	**CORR**	**MIA**
Vila Real	993(μ) 1210(σ)	44	1.03	159	-	368	0.96	0.93
Pinhão	981(μ) 1225(σ)	59	1.02	277	-	470	0.93	0.87
Quinta da Leda	1081(μ)1301(σ)	-39	0.96	272	-	456	0.94	0.88

In Table 4-3 it can also be observed that the performance of the WRF model improved in relation with hourly mean *Rad* with much greater MIA and CORR values in comparison with the daily *Radmax* case. Quinta da Leda showed again the higher hourly mean value but the differences among stations concerning average *Rad* values were smaller than for *Radmax*. All in all, the model performed slightly better for the higher sub-plateau location, with correlation and precision improving considerably at the hourly scale at all locations. The magnitude of the errors and correlation statistics shown for hourly *Rad* in Table 4-3 were very close or within the range of other validation studies performed with WRF solar radiation simulations in the Iberian peninsula (López et al., 2020; Perdigão et al., 2017) and France (Boulard et al., 2016). For instance, according to López et al. (2020), the validation statistics for a 1 km horizontal resolution WRF simulation for central continental Portugal presented the following ranges for daily *Radmax* radiation and hourly *Rad*: BIAS -72 - 324

kJ m^{-2}, MAE 108 -378 kJ m^{-2}, RMSE 180 – 558 kJ m^{-2} (*Radmax*) and BIAS 3.6 - 144 kJ m-2, MAE 144 - 216 kJ m^{-2}, RMSE 216 – 396 kJ m^{-2} (*Rad*).

The relative humidity validation statistics included in Table 4-4 show that linear correlation was strong for daily *RHmin* in all three locations, but BIAS, MAE, RMSE and MIA indicated a better performance of the simulations for the Vila Real location.

Table 4-4. Validation statistics for daily *RHmin* and hourly *RHmean* (April-September 2017 period).

Daily RH*min* (%)	**Field value**	**BIAS**	**SD Ratio**	**MAE**	**MAPE (%)**	**RMSE**	**CORR**	**MIA**
Vila Real	37.3 (μ) 12.6 (σ)	-2.5	1.01	6.7	18.4	8.8	0.78	0.69
Pinhão	22.3 (μ) 9.5 (σ)	6.9	1.10	8.1	44.6	9.8	0.76	0.53
Quinta da Leda	22.7 (μ) 8.9 (σ)	3.2	1.01	5.6	28.7	7.1	0.75	0.61
Hourly RH*mean* (%)	**Field value**	**BIAS**	**SD Ratio**	**MAE**	**MAPE (%)**	**RMSE**	**CORR**	**MIA**
Vila Real	59.9 (μ) 20.3(σ)	-3.3	0.95	9.5	16.5	12.4	0.82	0.72
Pinhão	46.3 (μ) 19.7 (σ)	6.0	0.97	10.2	28.1	12.4	0.84	0.70
Quinta da Leda	45.7 (μ) 19.3 (σ)	3.1	0.99	7.8	19.8	9.9	0.88	0.76

The hourly mean *RH* values also followed and inverse relationship with hourly *Tmean* with decreasing values from the NW to the SE (Table 4-4). There was also better performance of the WRF model in all cases if compared with daily *RHmin* with slightly higher correlation and MIA statistics. However, the WRF model performance was now better at Quinta da Leda as observed by its higher MIA and lower MAE and RMSE errors. The validation statistics were within or close to the range of other WRF mesoescale simulation studies (Boulard et al., 2016; Kryza et al., 2017; López et al., 2020; Pan and Li, 2011). For instance, the error range for a one year 5 km horizontal resolution WRF simulation after comparison with data from 7 meteorological stations in the Heihe river basin (continental China) reported by Pan and Li (2011) for hourly *RH* was the following: CORR 0.55-0.75, BIAS -7.3 - 13.3%, RMSE 16.5 – 23.6%).

The validation statistics for wind speed and wind direction can be found in Table 4-5.

Table 4-5. Validation statistics for hourly *Ws* and daily *Wdmean* (April-September 2017 period).

Hourly *Ws* (m/s)	**Field value**	**BIAS**	**SD Ratio**	**MAE**	**MAPE (%)**	**RMSE**	**CORR**	**MIA**
Vila Real	1.8 (μ) 1.3 (σ)	1.1	1.36	1.3	-	1.7	0.65	0.50
Pinhão	1.9 (μ) 1.1 (σ)	0.8	1.78	1.3	-	1.8	0.63	0.48
Quinta da Leda	1.4 (μ)	1.4	1.50	1.6	-	2.1	0.59	0.41

	1.3 (σ)							
Daily *Wdmean* (°)	**Field value**	**BIAS**	**SD Ratio**	**MAE**	**MAPE (%)**	**RMSE**	**CORR**	**STDE**
Vila Real	284 (μ) 46 (σ)	24.7	1.17	34.9	12.3	50.9	0.72	44.5
Pinhão	336 (μ) 37 (σ)	-9.6	1.73	94.4	28.1	103.4	-0.39	102.9
Quinta da Leda	279 (μ) 58 (σ)	10.2	0.88	38.9	13.9	54.0	0.24	53.1

Hourly *Ws* correlation values varied from 0.59 (Quinta da Leda) to 0.65 (Vila Real), and the accuracy values provided by MIA were low. The daily *Wdmean* clockwise bias for Vila Real was 24.7° and 10.2° for Quinta da Leda with respective STDE 44.5 and 53.1 (Table 4-5). The greatest divergence was found for the Pinhão location where the simulated wind direction was 269° compared to the 336° observed one. The results for the Pinhão location probably were related to the more sheltered location of the monitoring station along the Douro's river canyon which is not fully captured by the WRF model. In fact, we have already pointed out that the Pinhão station had the greatest difference between measured ground altitude and the altitude used by the WRF-CHIMERE modeling system (130 m and 225 m, respectively). The worse model performances concerning precision and accuracy were also found for the Pinhão location for hourly *Tmean*, hourly *Rad*, daily *RHmin* and hourly *RH*, although the differences in these cases were rather slight when compared with the other locations.

Overall, the WRF wind simulation for the 2017 Apr-Sep grapevine growing season in the DDR can be associated to the predominance of westerly-north-westerly flows, which result from the deflection of the northerly winds of the Atlantic coast, by the orientation of the valley and by the Iberian thermal low favoured by most of the synoptic weather situations in areas such as the Douro river basin (Lorente-Plazas et al., 2015). Except for daily *Wdmean* at the Pinhão location, the error statistics estimated for wind velocity and wind direction at the daily and hourly scale were very close or within the range found by other WRF mesoscale validation studies where the greater inaccuracies were also associated with mismatches between the model and the actual terrain elevation and the inability to reproduce the lower atmosphere conditions of complex terrains (Jiménez et al., 2013; Pan et al., 2018; Pan and Li, 2011; Zhang et al., 2013). For instance, the work by Pan and Li (2011) concerning one year 5 km horizontal resolution WRF simulation in the Heihe river basin (continental China) presented the following error statistics for hourly *Ws*: BIAS from

-0.6 to 1.8 m/s, RMSE from 1.3 to 3.6 m/s. As for daily *Wdmean*, Carvalho et al., (2012) reported the following statistics at hourly level from a 3.6 km horizontal resolution WRF simulation performed during January in a mountainous area of central Portugal: BIAS from -3.8° to -9.7°, RMSE 37.3° to 52.0°, and STDE from 37.2° to 51.1°.

In summary, excepting for the meteorological variables associated to wind, it has been observed that model performance tended to be more precise and accurate when hourly values are analyzed than when considering daily maxima data. Differences among locations were slight, apart from *Radmax* and *RHmin* where there was a drop in model performance (MIA < 0.6) for one of the sites (Quinta da Leda for *Radmax* and Pinhão for *RHmin*). Validation statistics were acceptable and within the range of what has been found in other RCM simulations with the lower values associated to the moderate correlations estimated for *Radmax* (between 0.55 and 0.57). Model accuracy performance was lower (MIA < 0.6) for all observational sites for wind speed and there was only a strong correlation value for wind direction in one of the locations (Vila Real).

4.4.2 Ground-level O_3

Table 4-6 and Figure 4-2 show the validation statistics and graphs, respectively, associated with ground-level O_3 values at Douro Norte and Quinta da Leda air quality stations. The measured values for daily O_3 maxima and hourly O_3 means were similar in the two sites. The correlation values were moderate for daily O_3 maxima and strong for hourly O_3 at Quinta da Leda, whereas they were strong for daily O_3 maxima and hourly values at Douro Norte. The BIAS, RMSE, MAE and MAPE errors were lower for the Quinta da Leda site and the SD ratios indicated a lower spread of the simulated values for both locations. The lower spread of the simulated values was also observable in the time series plots (Figure 4-2a), where the simulated values failed to capture the maxima and minima values, and in the density plots (Figure 4-2b), where the KS test indicated significant differences between the distribution of observed and simulated data ($p < 0.01$). The Taylor diagrams (Figure 4-2c) for the hourly O_3 mean values indicated a similar WRF-CHIMERE model performance for the two sites at the hourly scale. Monteiro et al. (2012) in a previous simulation of a high O_3 episode in the Douro Norte site presented higher error statistics and similar correlation values. However, as the MIA values were low for all cases, a QQ statistical transformation

of the WRF-CHIMERE O_3 simulated values was applied in order to be able to use them for vegetation risk assessment.

Table 4-6. Validation statistics for daily *O_3 max* and hourly *O_3 mean* (April-September 2017 period).

Daily *O_3 max* (ppb)	**Field value**	**BIAS**	**SD Ratio**	**MAE**	**MAPE (%)**	**RMSE**	**CORR**	**MIA**
Douro Norte	50 (μ) 15 (σ)	5	0.57	10	21.3	12	0.68	0.46
Quinta da Leda	55 (μ) 11 (σ)	1	0.55	7	12.7	9	0.55	0.46
Hourly *O_3 mean* (ppb)	Field value	BIAS	SD Ratio	MAE	MAPE (%)	RMSE	CORR	MIA
Douro Norte	38 (μ) 12 (σ)	12	0.59	13	42.0	14	0.69	0.39
Quinta da Leda	41 (μ) 12 (σ)	7	0.70	9	27.3	11	0.70	0.51

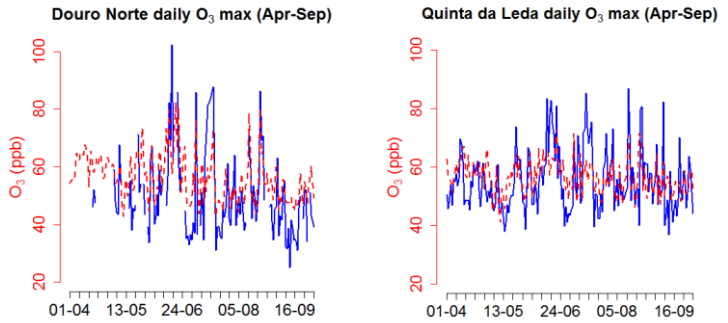

a)

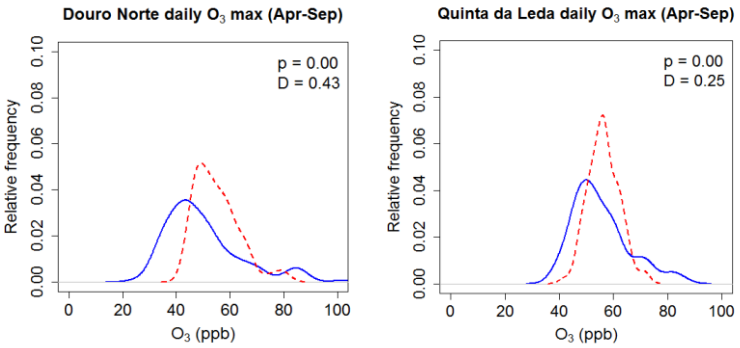

b)

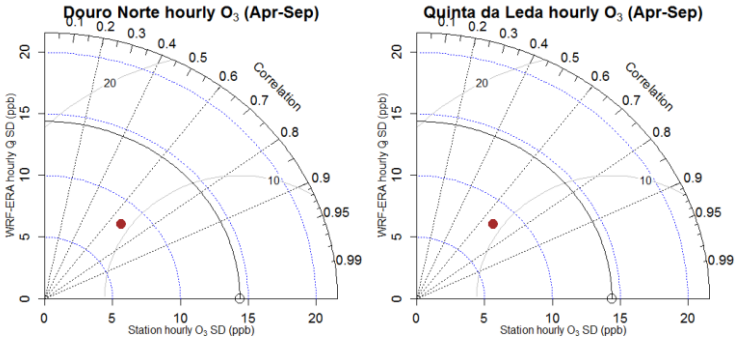

c)

Figure 4-2. a) Time series, b) density plots, and c) Taylor diagrams for ground-level O_3.

Table 4-7 presents the validation statistics after the QQ transformation and Figure 4-3 illustrates the results of the QQ transformation, in terms of monthly and hourly boxplots, where the spread of the simulated values is closer to that of the observed ones.

Table 4-7. Validation statistics for QQ transformed daily O3 maxima (*O3 max*) and hourly O3 means (*O3 mean*).

Daily O_3 *max* (ppb)	**Field value**	**BIAS**	**SD Ratio**	**MAE**	**MAPE (%)**	**RMSE**	**CORR**	**MIA**
Douro Norte	50 (μ) 15 (σ)	-5	1.03	9	17.2	13	0.66	0.61
Quinta da Leda	55 (μ) 11 (σ)	-1	1.01	8	14.0	10	0.54	0.54
Hourly O_3 *mean* (ppb)	**Field value**	**BIAS**	**SD Ratio**	**MAE**	**MAPE (%)**	**RMSE**	**CORR**	**MIA**
Douro Norte	38 (μ) 12 (σ)	0	0.98	7	20.5	9	0.68	0.61
Quinta da Leda	41 (μ) 12 (σ)	0	1.01	7	18.7	9	0.70	0.63

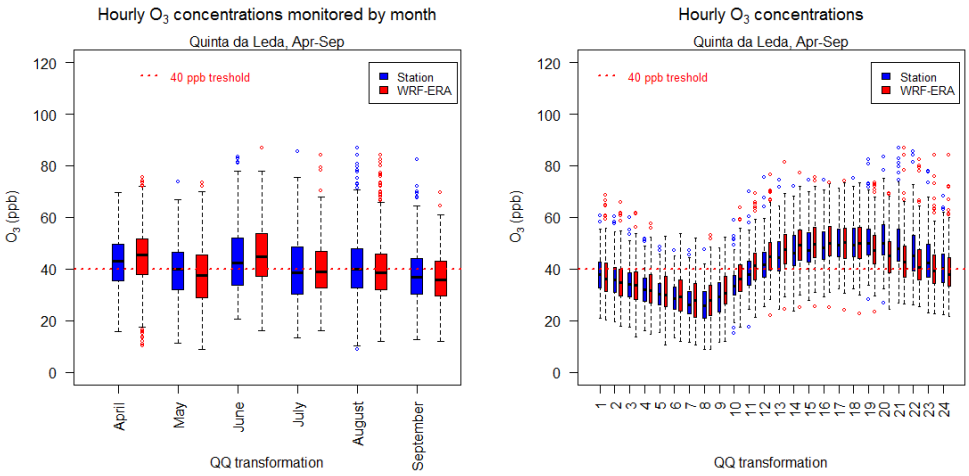

a)

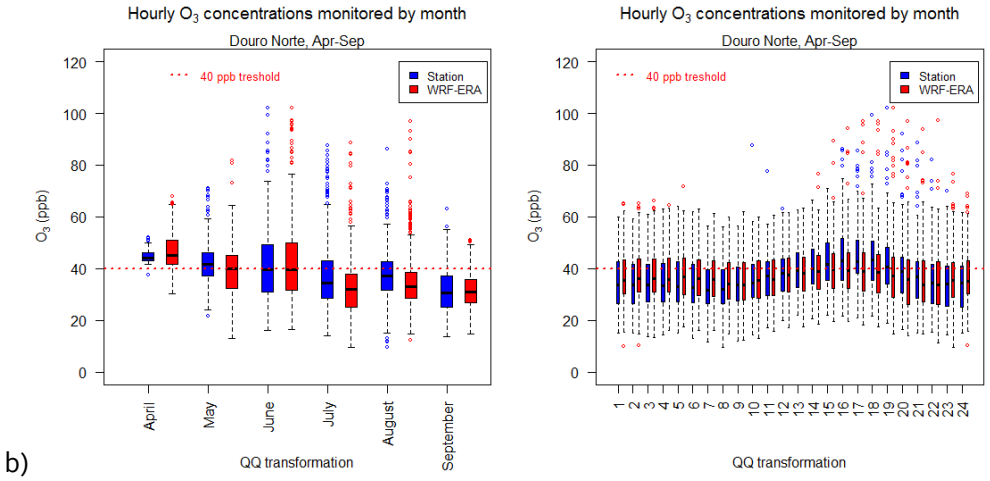

b)

Figure 4-3. a) Monthly, and b) hourly boxplot O_3 profiles at Quinta da Leda and Douro Norte.

The QQ transformation corrected the BIAS and lowered the spread of the hourly *O_3 mean* simulated data yielding a better model performance as also observed in the lower error MAE and RMSE statistics and higher MIA. Daily *O_3 max* simulated values also approximated better the range of the observed values with a higher MIA although the effects on error statistics such as BIAS, MAE and RMSE were negligible. CORR was not affected by the QQ transformation.

Previous studies for an elevated site such as the Douro Norte (Carvalho et al., 2010; Sousa et al., 2011) also highlighted a drop in values from July to September, which was captured by the simulations (before and after the QQ transformation). As it happened with the Douro Norte site, the seasonal and hourly time patterns were also well captured by the simulations for Quinta da Leda. Although there were no previous measurements for the Quinta da Leda site, which displayed a more marked hourly variation, Pires et al. (2012) mentioned this type of hourly behavior as typical of lower elevation rural stations in northern Portugal.

Concerning *AOT40* indices estimated at Quinta da Leda (Table 4-8), the measured EU *May-Jun AOT40* value (8 ppm.h) exceeded the long-target value of 3 ppm.h and was close to what has been set as the general standard to protect vegetation (9 ppm.h) by Directives 2002/03/EC and 2008/50/EC. Higher mean values (11 ppm.h) were frequently observed at the Douro Norte monitoring station in the past (Agência Portuguesa do Ambiente, 2011, 2009) between 2005 and 2010. Thus, probably the standard set to protect vegetation

would also be exceeded at Quinta da Leda for longer exposure years. The measured day light-based *Apr-Sep AOT40* (13.8 ppm.h) exceeded the Cle_c (5 ppm.h) for a 5% biomass reduction in perennial-dominated (semi)natural vegetation and trees. The field *Jun-Sep AOT40* reached 9.5 ppm.h but is below the specific yearly Cle_c values for a 10% reduction in yield and quality (27 ppm.h and 21 ppm.h, respectively) as set by Soja et al. (1997) for the Welschriesling grapevine cultivar. WRF-CHIMERE simulated values were higher (16.2 ppm.h) than measurements and they could indicate risk of exceeding the Cle_c for a 10% reduction in monosaccharide yield over two consecutive years (11.5 ppm.h), if there was not ground control, and no fit to observational data, as the QQ transformation was not be applied.

Table 4-8. O_3 exposure indices estimated at Quinta da Leda.

EU *May-Jun AOT40* (ppm.h)			*Jun-Sep AOT40* (ppm.h)			CLRTAP *Apr-Sep AOT40* (ppm.h)		
Field	WRF-CHIMERE	QQ Trans	Field	WRF-CHIMERE	QQ Trans	Field	WRF-CHIMERE	QQ Trans
8.1	12.3	8.5	9.5	16.2	10.6	13.8	24.5	16.6

Figure 4-4 presents maps of QQ transformed *AOT* exposure simulated values. The daily mean maxima Apr-Sep O_3 values show that larger values were associated to higher elevations in the Marão and Montemuro mountain ranges towards the northwest of the DDR and spread through the Douro valley across the DDR (Figure 4-4b). Daily mean Apr-Sep O_3, EU's *May-Jun AOT40* and CLRTAP *Apr-Sep AOT40* (Figure 4-4a, c and d) had similar spatial patterns with higher O_3 concentrations associated mostly with higher elevations (Figure 4-4f) inside and outside the DDR and particularly affecting a transitional area between the Cima Corgo and the Douro Superior subregions within the DDR. The *AOT40* estimated according the procedure of Soja's (Figure 4-4e) indicates that besides the previously commented areas, most of the Douro Superior subregion, with a warmer and drier climate, can be affected by high O_3 levels between June and September (Jun-Sep).

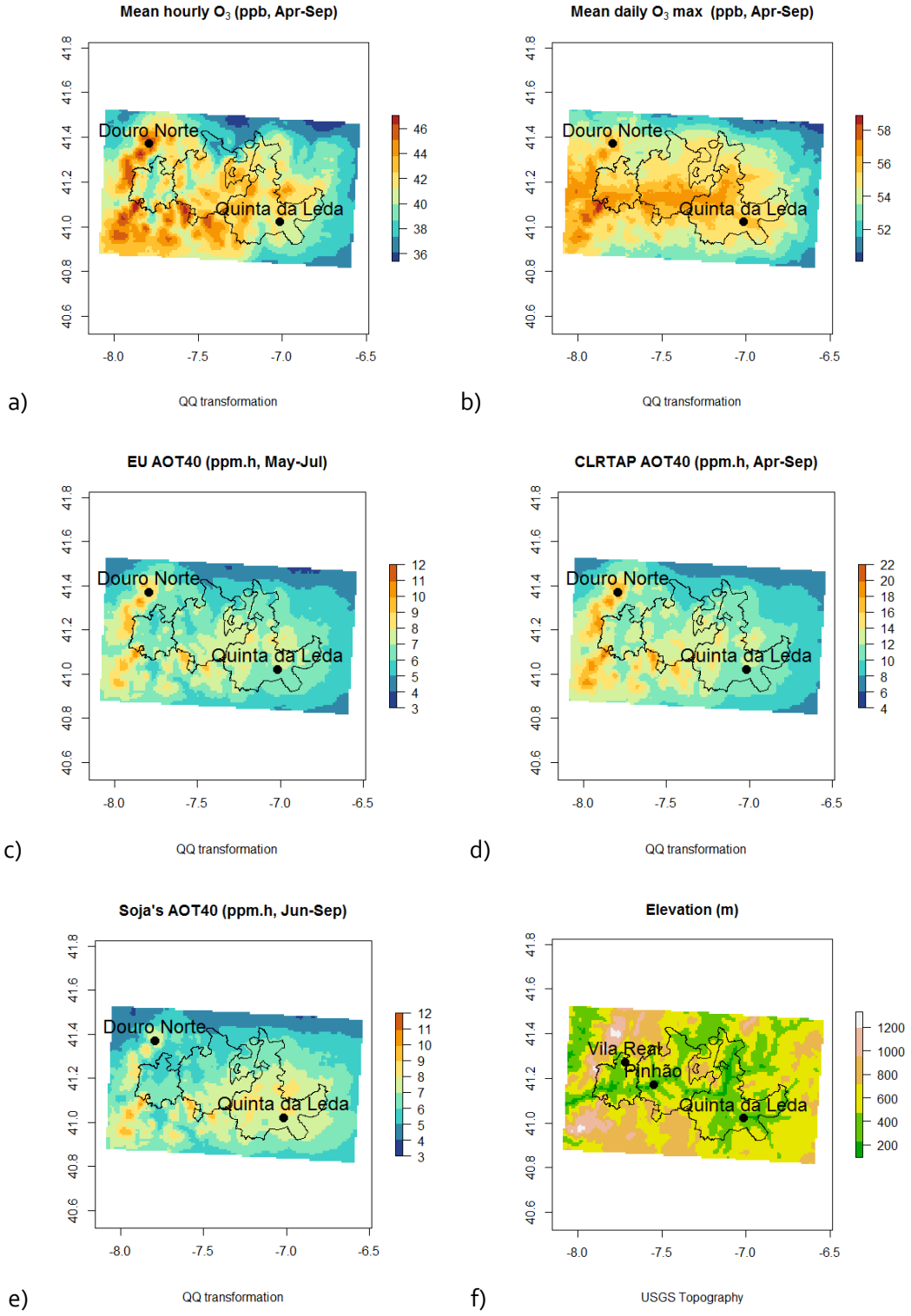

Figure 4-4. Maps of a) mean hourly O_3, b) mean daily O_3 max, c) EU's directive May-Jul *AOT40*, d) CLRTAP *Apr-Sep AOT40*, e) Soja's *Jun-Sep AOT40*, and f) elevation, as obtained from the WRF-CHIMERE transformed simulations and associated elevation database.

4.4.3 O_3 uptake by stomata

Table 4-9 and Figure 4-5 present the O_3 dose values expressed as *POD* and *POD6*, based on measurements and simulations.

Table 4-9. Observational and WRF-CHIMERE-based POD and POD6.

April to September POD (mmol m^{-2})			*April to September POD6* (mmol m^{-2})		
Field	WRF-CHIMERE	QQ Trans	Field	WFR-CHIMERE	QQ Trans
28.3	34.1	28.2	1.2	2.4	1.2
June to September POD (mmol m^{-2})			*June to September POD6* (mmol m^{-2})		
Field	WRF-CHIMERE	QQ Trans	Field	WFR-CHIMERE	QQ Trans
17.8	23.3	19.6	0.4	1.8	1.0

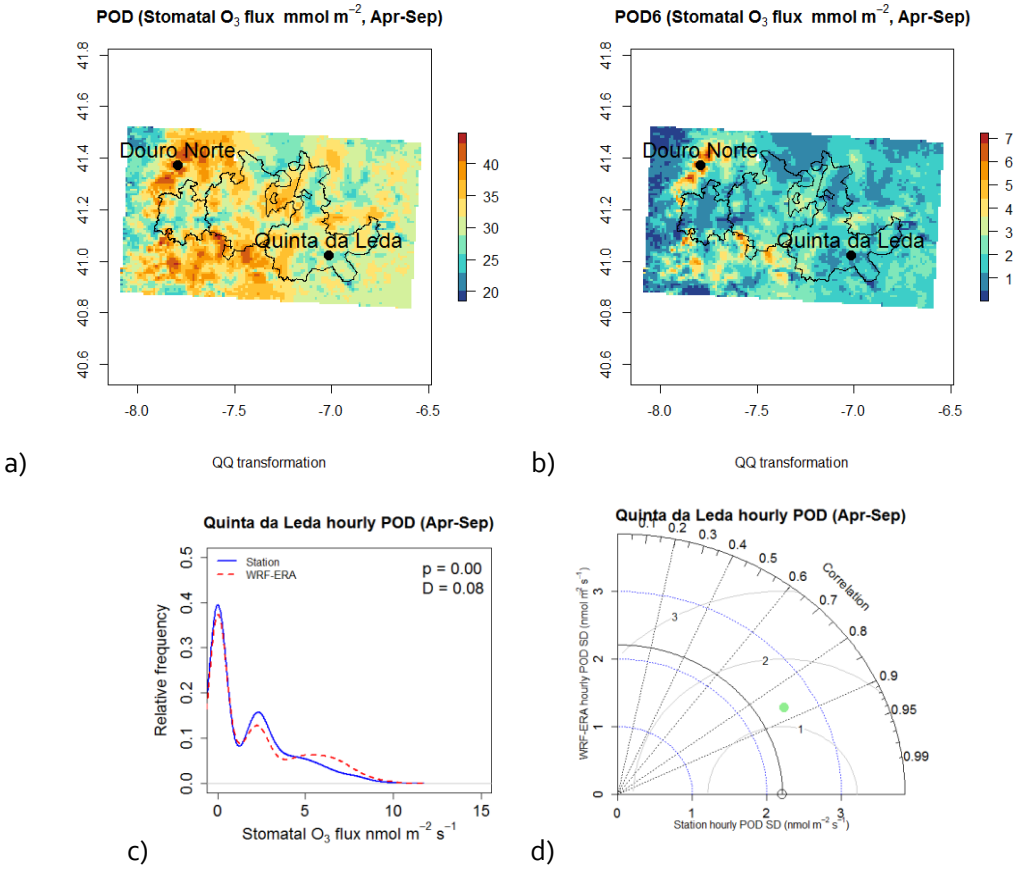

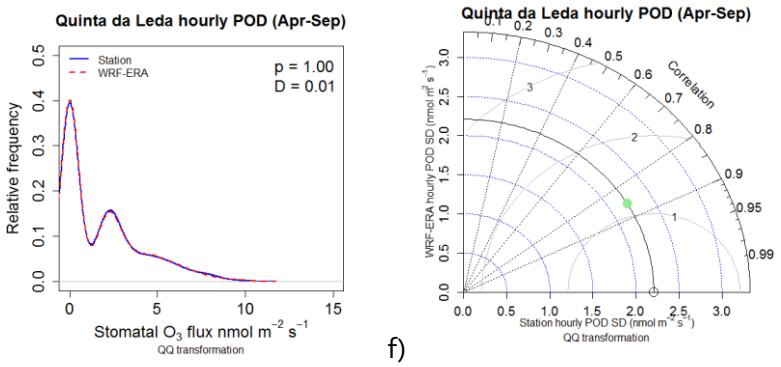

e) f)

Figure 4-5. a,b) QQ transformed Apr-Sep (AS) *POD* and *POD6* maps for the DDR, c,d) Density and Taylor plots for Apr-Sep first *POD* estimates and for e,f) QQ transformed *POD* at Quinta de Leda.

The observational based stomatal flux and the WRF-CHIMERE based stomatal flux presented a similar temporal pattern at Quinta da Leda with a 17% and 50% positive difference for *Apr-Sep POD* and *Apr-Sep POD6*, respectively, when these are estimated from WRF-CHIMERE without any statistical transformation (Table 4-9). A field-observational exceedance of the grapevine Cl_{ef} for 10% reduction in monosaccharide concentrations over consecutive years (1.1 mmol m^{-2}), as derived from Soja et al. (2004), was observed at Quinta da Leda with a *POD6* of 1.2 mmol m^{-2}. If we were to rely on the POD6 derived from the WRF-CHIMERE simulations (2.4 mmol m^{-2}) as calculated here without any other adjustment, the grapevine Cl_{ef} value for 10% reduction in monosaccharide concentrations would also be reached for the non-consecutive case (2.3 mmol m^{-2}) besides that for yield over consecutive years (2.2 mmol m^{-2}). The modelled values of grapevine stomatal flux were in the range 100-250 mmol H_2O m^{-2} s^{-1} (Barreales et al., 2018; Ribeiro et al., 2018) also corresponding to those of autochthonous grapevine cultivars present in the study area (e.g. 'Touriga Franca' and 'Touriga Nacional) when there is not severe water stress condition.

The associated QQ transformed *POD* and *POD6* maps (Figure 4-5a and 4-5b) were also related with elevation showing a higher biological control where warmer and drier areas have lower stomatal fluxes. The *Apr-Sep POD6* adjusted map (Figure 4-5b) showed that considerable extensions of the DDR can exceed critical values for grapevine yield and quality, especially in the central and eastern part of the DDR. These results clearly manifested the relevance of performing suitable modelling validation and parametrization in order to increase the accuracy of ambient O_3 risk assessments for agriculture, especially for the grapevine case where there is still much uncertainty and lack of experimental work.

A significant difference was found between the field-based and the WRF-CHIMERE based *POD* data distribution (KS test $p < 0.05$) (Figure 4-5c) along uneven SDs ratios (Figure 4-5d) which were corrected after QQ transformation (Figure 4-5e, f).

4.4.4 O_3 phytotoxic risk per phenological stage

Phenological observations are also important to appropriately assess risk. Figure 4-6 displays O_3 exposure per grapevine phenological stage (a), the age parameter that was specifically introduced into the used DO3SE deposition model (b), and variation of vegetation protection standards according to length of selected growing season (c,d).

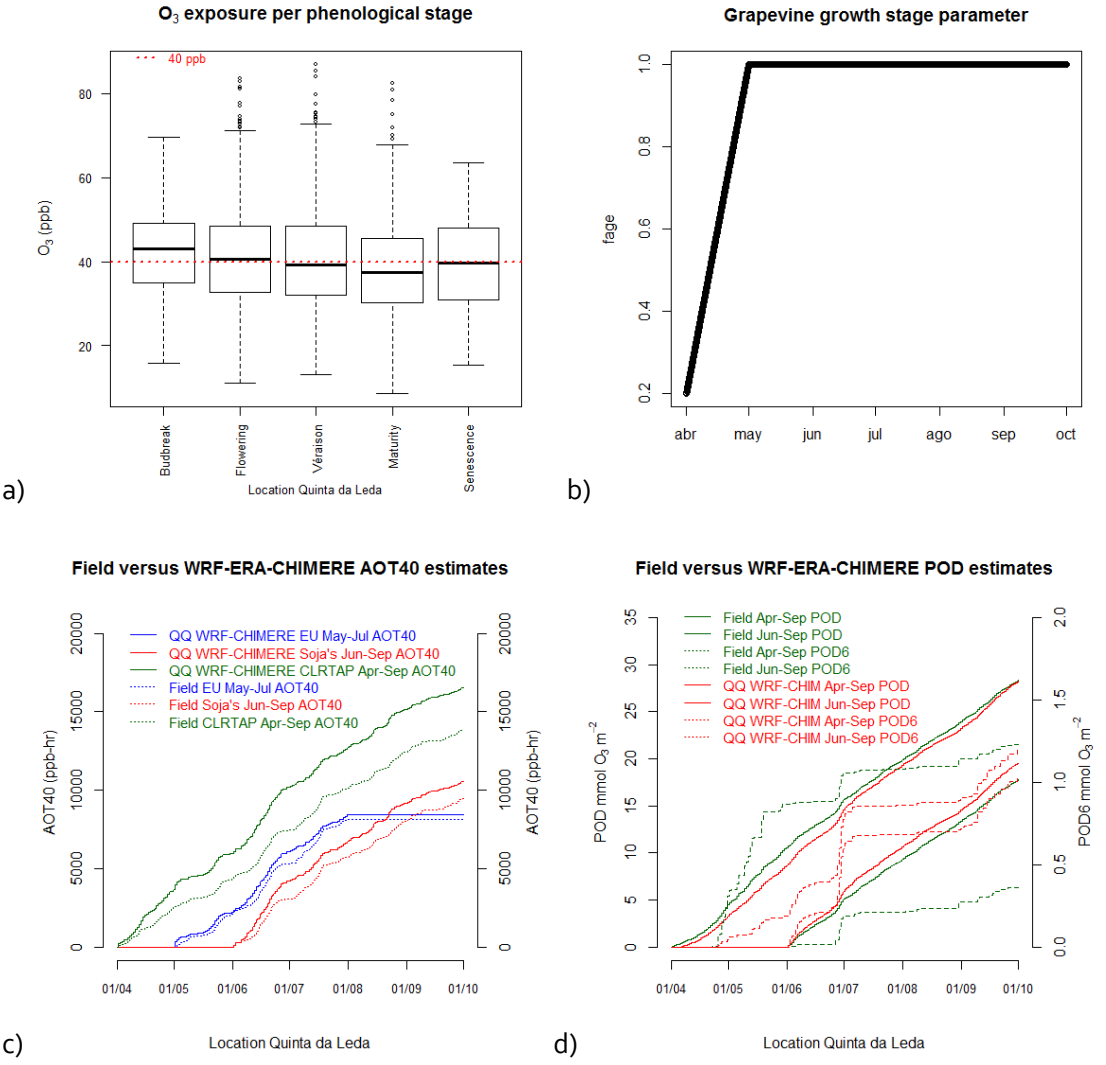

Figure 4-6. a) Possible critical periods according to phenological phase, b) plant growth parameter derived from phenological observations, and variation of c) exposure and d) dose-based vegetation protection standards according to length of selected growing season.

It can be observed that in Quinta da Leda the O_3 40-ppb threshold was exceeded for all growth stages (Figure 4-6a) reaching high values in rather sensitive stages, such as flowering, which in a perennial crop such as the grapevine, influences the development of the next growing season also affecting yield and quality. In fact, climate extremes in relation to early heatwaves in spring and accumulated hydric stress through the rest of the growing season in 2017 were reported to have had an effect in the DDR on grapevine vegetative growth and yield (i.e. reduction in berry weight), although the sugar and phenolic compound levels were considered good (ADVID, 2017). The availability of phenological observations for the 2017 campaign also allowed to define a specific growth stage parameter (Figure 4-6b) to modify stomatal conductance better representing when grapevine leaves are fully developed besides timing of sensitive stages (i.e. flowering) in relation to O_3 exposure in the DDR.

The estimation of both exposure (Figure 4-6c) and stomatal uptake standards (Figure 4-6d) for assessment of O_3 phytotoxic risk on grapevine yield and quality was still subjected to a great range of variation depending on the length of the cumulative period selected to estimate those standards. It can be observed that even when the QQ transformed WRF-CHIMERE simulation-based AOT40 values were closer to measurement-based values, there was still a tendency to overestimate them, especially through the longer Apr-Sep observational period. However, adjusted modelling results were very good for both *Apr-Sep* and *June-Sep POD* and for *Apr-Sep POD6*, although there is still a great amount of overestimation for *June-Sep POD6*.

4.5 DISCUSSION

Even though the magnitude and the different signs of the errors in RCM can at times compensate and be within an acceptable range for purposes such as water balance computation (e.g. Boulard et al., 2016), it has been found in this work that these errors can have an effect on ambient O_3 simulations inducing a relevant bias, which, in turn, can yield to an overestimation of cumulative standards for vegetation protection if no statistical transformation is used to match them with observational values. Another but not less relevant issue that relates with simulation bias has to do with the representativeness of emission inventories and their disaggregation methods. In this context, statistical

transformations are a suitable postprocessing tool to reproduce more reliable estimates at local level.

Concerning *POD* estimation, it is also advisable to check that stomatal conductance values are in range with values measured in the field. This was possible for this study as they were also measured across the DDR during the field campaign, in particular along the *véraison* and maturity stages. Further work still needs to be done to better accommodate the model to the more severe water stress conditions that can be associated to non or controlled irrigated conditions, especially in the drier Cima Corgo and Douro Superior subregions. This could be done by effectively introducing a soil water balance parameter into the DO3SE model. There has not been a specific parametrization concerning the local varieties grown in the area either, excepting the plant growth (phenological) stage parameter. Despite those limitations, simulated values of stomatal conductance were representative of the less water stressed conditions in the DDR. Therefore, probably the Cima Corgo and Douro Superior subregions present larger areas that could exceed *POD* standards, as stomatal closure could exert a greater control to O_3 entering the grapevine under the more severe water stress conditions of these regions. However, it must also be kept in mind that there is little knowledge on possible interaction of O_3 with other concurrent environmental factors such as severe summer water deficit, heat waves, or strong light conditions which could also affect plant defense mechanisms.

4.6 CONCLUSIONS

The results of this work stress the relevance of performing modelling validation in order to increase the accuracy of high-resolution ambient O_3 risk assessments for agriculture, especially for a case such as grapevine, where there is still much uncertainty due to the lack of experimental work. This is particularly important due to the grapevine production immense value for social, economic and environmental sustainability in Mediterranean areas and beyond. Both field and statistically adjusted model values indicate that considerable areas in the Demarcated Douro Region of Portugal exceed the critical exposure values for vegetation according to current European legislation standards, and for grapevine yield and quality criteria based on current OTC experimental knowledge. The simulations already included a plant growth stage parameter taking into account grapevine phenological observations in the study area, but further work is still required to better

represent the more water stressed conditions in the study area, as a soil water limiting factor has not yet been effectively included into the DO3SE model. These results also indicate the need for rethinking air-quality standards under the potential impacts of climate change and extreme climate events when assessing the ozone risk for strategic crops in Mediterranean areas, such as the grapevine.

5 IMPROVEMENT OF LOCAL OZONE PHYTOTOXICITY MODELLING FOR AUTOCHTHONOUS GRAPE CULTIVARS

This chapter was submitted to Atmospheric Environment on 02/04/2022 as:

Blanco-Ward, D., Ribeiro A.C., Feliciano, M., Barreales D., Paoletti, E., Miranda, A.I. Improvement of local ozone phytotoxicity modelling for autochthonous grape cultivars. Journal of Atmospheric Environment.

I mainly contributed with performing and postprocessing the CHIMERE and DO3SE simulations and analysed the field campaign data. I was also responsible for the writing of the paper.

Abstract

The grapevine is a key crop for Mediterranean environments and is both sensitive to climate warming and air pollutants, of which ozone is the most damaging to crop yield and quality. Ambient ozone effects on the grapevine have been noticed since the late fifties but risk assessments are still impaired by the lack of information concerning differences in cultivar sensitivity, and adaptation capacity to environmental factors including drought conditions. This study develops a specific parametrization for autochthonous grape cultivars within a leaf-level stomatal flux model, the DO3SE model, coupled with a meteorological and atmospheric chemical transport modelling system, the WRF-CHIMERE, by using a renowned wine producing area, the Douro wine region of Portugal, as case study. The DO3SE model parametrization introduced in this study included phenology, photosynthetic active radiation, air temperature, air vapour pressure deficit, and leaf water potential as a proxy of soil water content. The modelling experiments, which included simulations with the current (default) Convention on Long-Range Transboundary Air Pollution DO3SE parametrization and with the proposed parametrization, covered a reference grapevine growing season (from April to September 2017), during which a measuring campaign was carried out. Simulation results show that the proposed parametrization succeeded to replicate the observed grapevine leaf-level stomatal flux gradient in the region. Both field and modified DO3SE model values indicate that considerable areas in the Douro wine region of Portugal can exceed critical phytotoxic ozone dose (*POD*) values, although with a lower and different spatial extent when compared to the default DO3SE parametrization for the grapevine. However, under

irrigated conditions, the *POD* values increase, and the values are close to those obtained with the default parametrization. Overall, the research results indicate that air quality management, in particular the reduction of ozone levels in the ambient air, must also be considered to define sustainable grape and wine production strategies in the context of climate and wine production management change.

5.1 INTRODUCTION

Surface ozone (O_3) is considered to be by far the most phytotoxic air pollutant worldwide at present (Krupa et al., 2000; Sicard et al., 2017; The Royal Society, 2008). Surface O_3 has its main entrance through plant stomata causing foliar and tissue injury, impairing photosynthesis, and reducing growth, yield and quality on many agronomic and horticultural crops (Booker et al., 2009; Cho et al., 2011; Hayes et al., 2007). It is produced by a series of chemical reactions involving primary pollutants such as nitrogen oxides (NOx), carbon monoxide (CO) and volatile organic compounds (VOC) and is favoured by high light intensity and temperature conditions, such as those found in summer days (Marshall et al., 1997; Monks et al., 2015; The Royal Society, 2008). It is expected that background levels of surface O_3 will continue to increase globally in relation to the increasing industrialization of developing countries and intercontinental transport, despite the fact that emission reduction polices have caused a reduction of O_3 peak levels, levelling off or even declining long-term trends in Europe, North America and Japan (Oltmans et al., 2013; Paoletti et al., 2014; Sicard et al., 2013). Hence, it has been estimated that by 2050 global staple crop production of wheat, rice, maize and soybean could be reduced in more than 10% by global warming alone, but those losses could even reach 40% for sensitive crops in the more polluted areas (Burney and Ramanathan, 2014; Tai et al., 2014).

Perennial crops can also show a high vulnerability to ambient ozone. Based on historical records, Hong *et al.* (2020) estimated a reduction of yield from 2% (strawberries) to 22% (table grapes) and economic losses of approximately US $ 1 billion per year in areas with high ambient O_3 levels in California, indicating a large opportunity to improve crop yields through pollution mitigation. The grapevine is the crop where the phytotoxic effects of ambient O_3 were first noticed (Richards et al., 1959). Although it is not a food security crop, such as wheat, rice, soybean, maize or potato, it has immense cultural, economic and

ecological importance for Mediterranean areas, besides being the fruit crop with the largest acreage and highest economic value globally (Ponti et al., 2018). Wide regions of the world between latitudes 30˚ and 50°N where the grapevine has been traditionally cultivated are exposed to ambient O_3 levels that can affect both yield and quality with potential yield (i.e. grape fresh weight) reductions in the range of 20-31% and reductions in quality (i.e. polyphenols) in the range 15-23% (Blanco-Ward et al., 2021a).

Risk assessment studies concerning ambient O_3 for a crop such as the grapevine face however important limitations. A first issue is that the cumulative exposure (level-I) approach has been extensively criticized, because it does not reflect the actual dose or flux of O_3 entering the plant (Massman, 2004; Mauzerall and Wang, 2001; Musselman et al., 2006; Paoletti and Manning, 2007). To overcome these limitations, a flux-based, or level-II approach, was developed under the Convention on Long-range Transboundary Air Pollution (CLRTAP) (Mills et al., 2011b). This approach has a stronger biological basis since it considers a Phytotoxic Ozone Dose (*POD*) by taking into account the O_3 stomatal uptake, which can be understood as the amount of O_3 molecules that penetrate the leaf tissue through the stomata as a function of ambient O_3 concentration and several other critical environmental parameters, such as temperature, water vapour pressure, light, soil water potential and plant growth (phenological) stage (Emberson et al., 2000a, 2000b). Most commonly, the parametrization of those functions is performed by a semiempirical Jarvis type process model, the DO3SE model, as described and currently used by the CLRTAP (CLRTAP, 2017a). Even though the DO3SE model can be used to give broad estimates at the continental European scale (e.g. Anav et al., 2016), it does not account for the existing varietal and niche adaptation at the regional scale for a crop such as the grapevine. Furthermore, even though the standard CLRTAP DO3SE model also considers the inclusion of a leaf water or soil water potential factor, these are not frequently incorporated due to the lack of such measured data or reliable soil moisture models at the global scale (Anav et al., 2018; De Marco et al., 2016). Thus, although the use of stomatal flux process type models in combination with regional or downscaled results from climate or atmospheric chemical transport models is already reachable for phytotoxic O_3 risk assessment for the grapevine at the continental (CLRTAP, 2017b) or even at regional scale (Blanco-Ward et al., 2021b), there is still a lack of research concerning the specific parametrization for autochthonous cultivars also including the role of the water balance in the soil. The

inclusion of a soil related factor is a key issue for Mediterranean crops such as the grapevine where there is also the need to define irrigation policies on a sustainable basis to maintain yield and quality in the context of climate change (Bernardo et al., 2018; Fraga et al., 2018).

The main purpose of this work is to develop a phytotoxic ozone risk assessment including specific parametrization for autochthonous grapevine cultivars and the soil water component, and to assess to what extent the results differ from those produced without refining the methodology. For this purpose, the leaf-level stomatal flux model, the DO3SE model, was coupled with a meteorological and atmospheric chemical transport modelling system, the WRF-CHIMERE, to simulate ozone phytotoxicity of grapevines from the Demarcated Douro Region using data from a specific field campaign. The simulation and the measuring campaign covered a reference grapevine growing season.

5.2 STUDY AREA

The Portuguese Douro Demarcated Region (DDR) is the oldest wine region in Portugal and is famous for its Port wine (Fraga et al., 2017). It integrates areas of both banks of the Douro River from the border with Spain until halfway of its course. The Douro valley stretches along 90 km in the west-east direction and along 50 km in the north-south direction (Figure 5-1).

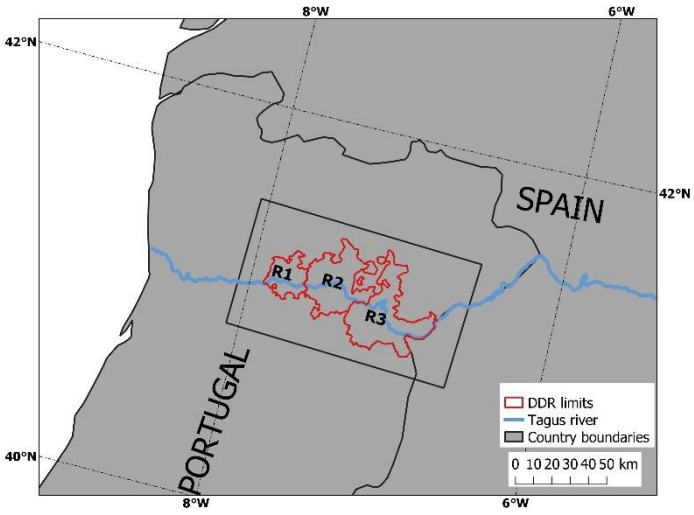

Figure 5-1. The Douro Demarcated Region (DDR) with Subregions “Baixo Corgo” (R1), “Cima Corgo” (R2) and “Douro Superior” (R3).

The westernmost region is located 70 km away from the Atlantic Ocean. The landscape is characterized by mountainous terrain, rising above the Douro river and its tributaries, with moderate to steep slopes and different expositions. The average elevation in the region is 443 m, but varies from about 40 m to a maximum of more than 1400 m. The Region covers about 250 thousand hectares with vineyard areas representing 43,480 ha, 17.4 % of the total area. It is divided into three sub-regions: Baixo Corgo with the smaller area (45,000 ha), Cima Corgo, with intermediate extension (95,000 ha), and Douro Superior with the greatest extension (110,000 ha). The vineyard area for these subregions is 13368, 20270 and 9842 ha, respectively (IVDP, 2017a). According to the last published reports, the wine produced in the DDR represents more than one fifth of all wine produced in Portugal (IVV, 2018, 2017). The *Touriga Nacional*, *Touriga Franca* and *Tinta Roriz* (*Tempranillo*) grapevine cultivars are the most common varieties in the DDR, but many other regional varieties are also present in the region (Corte-Real, 2014; Santos et al., 2013).

The DDR presents a warm Mediterranean climate with hot summers (Köppen Csa) (Andrade et al., 2021; Climaco et al., 2012). The region is protected from the humid and cold winds of the Atlantic Ocean by two mountain ranges, Marão and Montemuro, which are located on its western border. The temperature increases and precipitation decreases from west to east. The westernmost sub-region of the Douro Valley (Baixo Corgo) is closer to the Atlantic Ocean and therefore more affected by the moist sea winds. The easternmost sub-regions are further away from the Atlantic Ocean, thus having a more continental climate (Corte-Real, 2014; Corte-Real et al., 2016). Low precipitation values, together with high temperatures and high radiation exposure, give rise to intense water and thermal stresses, particularly in the Cima Corgo and Douro Superior subregions (Jones and Alves, 2012). Particularly, the 2017 April to September grape growing season, when the field campaign was developed, was categorized as extremely hot and dry in comparison with 1971-2000 climatological observations (ADVID, 2017).

5.3 METHODOLOGY

Based on data from a field campaign, local parameterizations were included in the model setup and were evaluated by comparing modelling results with measured data for grapevine phenological development, stomatal conductance and estimated *POD*. This

section describes the field campaign, the modelling system and the *POD* standards to assess O_3 phytotoxic risk for the grapevine in the study area.

5.3.1 Field campaign

Data for ozone phytotoxic risk assessment were gathered at three main sites (Figure 5-2), named Quinta A (Baixo Corgo), Quinta B (Cima Corgo) and Quinta C (Douro Superior), during the grapevine growing season from April to September 2017. The April to September growing season length is commonly taken as a valid reference grapevine growing season in the Northern Hemisphere (Tonietto and Carbonneau, 2004) and is also used concerning O_3 risk assessment for perennial crops and deciduous trees (Mills et al., 2018).

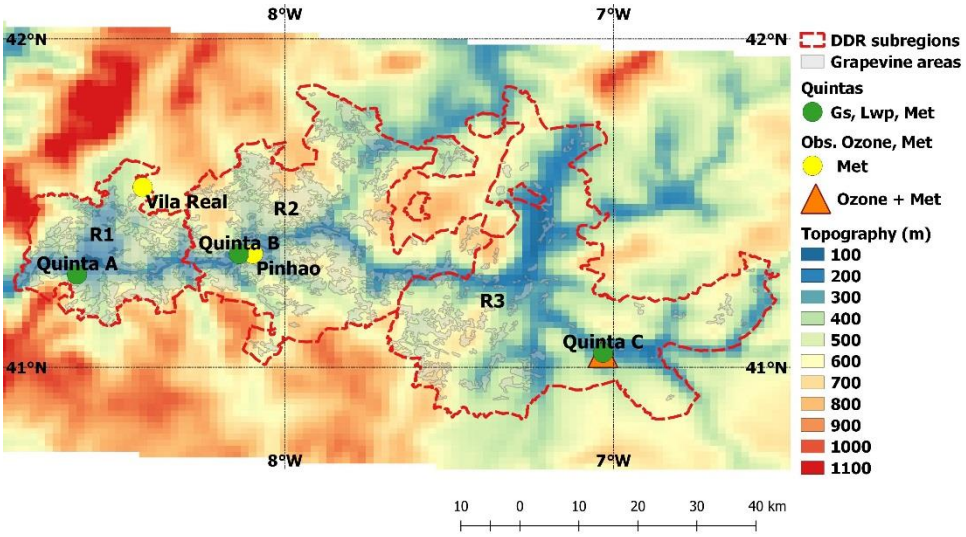

a)

b)

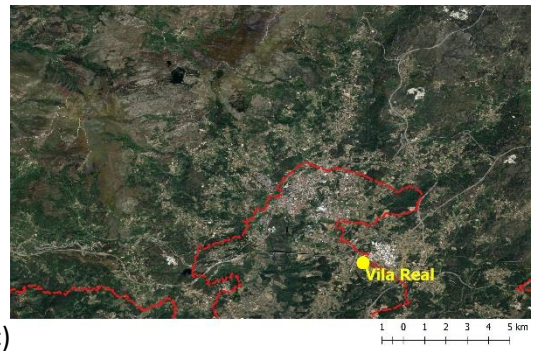

c)

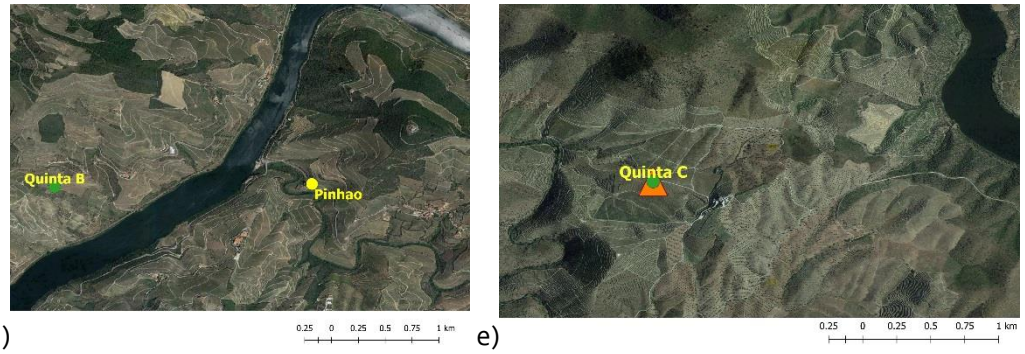

d) e)

Figure 5-2. a) Subregions "Baixo Corgo" (R1), "Cima Corgo" (R2) and "Douro Superior" (R3), along vineyard areas and observational sites. b, c, d, e) Details on field measurement locations of ambient ozone, meteorology and grapevine physiology.

Furthermore, meteorological data were obtained from two meteorological stations (Pinhão and Vila Real) from the Portuguese Institute for the Sea and the Atmosphere, and three meteorological stations located at the selected places (Quinta B and Quinta C) or nearby (Cambres from the Association for the Development of Viticulture in the Douro Region, ADVID, which is located close to Quinta A) (Figure 2). Cambres (136 m), Quinta B (174 m), Pinhão (130 m) and Quinta C (228 m) are located in the Douro valley under Mediterranean climate conditions, whereas Vila Real (561 m) represents plateau conditions where there is a stronger sub-Atlantic oceanic influence (Ribeiro, 2000).

5.3.2 Grapevine phenological and physiological data

The phenological development of two grapevine cultivars characteristic of the DDR, *Touriga Franca* (TF) and *Touriga Nacional* (TN), was monitored once per week across Quinta A, Quinta B and Quinta C according to the *Biologische Bundesanstalt, Bundessortenamt und CHemische Industrie* (BBCH) phenological scale. Six representative plants per cultivar were chosen for Quinta A and Quinta C and three for Quinta B.

Physiological measurements, namely predawn leaf water potential (Ψd) and stomatal conductance (*gs*), were also measured at the three sites on two dates, July 6th and August 1st, 2017, which were representative of the onset of the ripening and ripening phenological stages, respectively. Predawn leaf water potential was monitored using a Scholander pressure chamber (Model 1000, PMS Instrument Company, Albany, USA) and measurements were performed in four fully expanded leaves per variety and location (16 per treatment). Stomatal conductance was measured using a portable infrared analyzer (IRGA-LCA-4, Analytical Development Co., Hoddesdon, England). Measurements were

performed in eight fully expanded leaves per variety and location at 11- and 15-hours solar time. For Quinta C, measurements on plants subjected to deficit irrigation equivalent to the 25% daily reference evapotranspiration (ET_0) of the site were also performed.

5.3.3 Meteorological and ambient ozone observations

Daily data on temperature, relative humidity, incoming solar radiation and wind speed from Vila Real, Pinhão and Quinta C meteorological stations were used to estimate reference ET_0 according to the FAO Penman-Monteith method (Allen et al., 1998), whereas the temperature records from Cambres, Quinta B and Quinta C were used to derive grapevine phenological thermal requirements. Moreover, an observational site for ambient O_3 was also available at Quinta C (Figure 2), which was made operative for this study, from April to September 2017.

5.4 MODELLING

5.4.1 Modelling system

The chemical transport model CHIMERE (Menut et al., 2013) was used to estimate ground-level O_3 exposure while the dose of O_3 entering the plant was calculated based on the dry deposition of O_3 for stomatal exchange (DO3SE) model of the European Monitoring and Evaluation Programme for long-range transmission of air pollutants (EMEP) (Emberson et al., 2000a), updated according to the last parametrizations available for grapevine (CLRTAP, 2017c; Emberson et al., 2005). CHIMERE simulations were implemented for four nested domains with increasing horizontal resolution, namely 81 (D1), 27 (D2), 9 (D3), and 1 km (D4) (Figure 5-3).

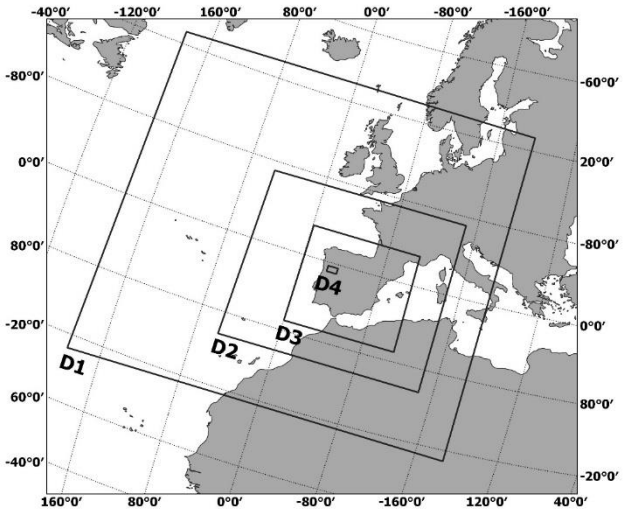

Figure 5-3. Nested modelling domains implement for the WRF-CHIMERE simulations.

Anthropogenic atmospheric emission data from the emission database of EMEP were pre-processed for the simulation domains, as well as biogenic emissions, which were computed using the global Model of Emissions of Gases and Aerosols from Nature (MEGAN). Land use types needed by CHIMERE to calculate biogenic emissions, as well as other processes such as deposition, were derived from the U.S. Geological Survey (USGS) 1 km resolution land cover database. The CHIMERE chemical mechanism is based on the MELCHIOR scheme (Mailler et al., 2016). Hourly ozone results were simulated for the period between April 1st to September 30th, 2017, using as meteorological inputs values calculated by the Weather Research and Forecasting (WRF) model, which is a mesoscale numerical weather prediction system. Ozone and meteorological simulations were successfully validated against measured data as described by Blanco-Ward et al. (2021b).

5.4.2 DO3SE parametrization for a representative grapevine cultivar in the DDR

The DO3SE model was parametrized both for a generic grapevine and for the *Touriga Nacional* (TN) as a representative Portuguese grapevine cultivar present in the DDR. This model makes use of a semi-empirical multiplicative function and includes the modifying influence on leaf-level stomatal conductance of the phenological stage (*fphen*) and four environmental variables: photosynthetic active radiation (*flight*), temperature (*ftemp*), vapour pressure deficit (*fvpd*) and plant available water (*fpaw*), which can be related to soil water potential (*fswp*) or leaf water potential (*flwp*), as is the case in this study (CLRTAP, 2017a):

$$gs = gmax * fphen * flight * \max\{fmin, (ftemp * fvpd * flwp)\} \quad (1)$$

fmin is the relative minimum stomatal conductance that occurs during daylight hours. The parameters fphen, flight, ftemp, fvpd, flwp and fmin range between 0 and 1, as a proportion of the species specific maximum stomatal conductance (gmax), expressed as mmol O_3 m^{-2} PLA s^{-1}, where the projected leaf area, PLA, is the total area of sunlit leaves. A top-leaf stomatal flux (*Fst*) can then be estimated from (CLRTAP, 2017a):

$$Fst = gs * [O_3] * \frac{r_c}{r_b + r_c} \quad (2)$$

where *Fst* has units of nmol m^{-2} s^{-1} and represents the instantaneous flux of O_3 through the stomatal pores per unit of projected leaf area. It refers specifically to the sunlit leaves at the top of the canopy and is regarded as the hourly mean flux of O_3 into the stomata. $[O_3]$ is ambient ozone at the canopy top, r_c is bulk leaf surface resistance (s/m), and r_b denotes bulk quasi-laminar resistance (s/m).

The generic grapevine DO3SE parametrization (CLRTAP DO3SE parametrization) for *flight*, *ftemp*, *fvpd* was implemented according to the last published data for this crop (CLRTAP, 2017c) and does not take into account *fpaw* through the growing season (*fpaw* = 1). The required data to configure the DO3SE model with parameters *flight*, *ftemp*, *fvpd* and *flwp* for Touriga Nacional (TN DO3SE parametrization) through boundary non-linear regression analysis were obtained from a three-year study performed on a representative vineyard in the DDR as compiled by Moutinho-Pereira et al. (2001) and Moutinho-Pereira (2000). The age component or phenological factor, *fphen*, was adjusted for the two cases, CLRTAP and TN, by phenological modelling as explained in the next section.

5.4.2.1 Inclusion of daily phenological factor into DO3SE

The age component was derived from the relationship between the development rate of the grapevine and temperature as a sum of heat degrees or growing degree days (GDD, °C units), which were estimated as a daily temperature summation above a temperature base required for a given crop to complete a specific phenological stage:

$$\Theta = \int (T - Tb)dt \quad (1)$$

where Θ (°C days) represents the thermal duration of a specific phenological stage, *T* is the daily average temperature, *Tb* is a threshold above which there is plant development within that phenological stage and *dt* represents a daily temporal scale. A specific phenological

scheme partitioning the annual development cycle of the grapevine into three major phases (*b* – budburst-early leaf development to flowering, *f* – flowering to grape colour onset, and *g* – grape colour-ripening onset to maturity) was therefore proposed for Touriga Nacional (TN) and also Touriga Franca (TF) cultivars, as both are early varieties at the budburst and flowering stages and middle-season ones at the maturity stage and therefore have similar thermal requirements (Lopes et al., 2008). This phenological model was used to define the required GDD to reach budburst, flowering, grape colour onset and maturity. This work makes use of the specific varietal GDD requirements as observed at the Portuguese National Ampelographic Collection (Lopes et al., 2008) for maturity and later observations made available specifically for the Douro Valley region (Alves et al., 2013).

5.4.2.2 Inclusion of hourly leaf water potential factor into DO3SE

Under sustained drought conditions, such as those found in 2017 in the DDR, it is possible to find a strong association between accumulated daily reference evapotranspiration (ET_0) and predawn leaf water potential in grapevines (Gaudin et al., 2017). This relationship was tested both with the observed data collected in the field campaign for the three vineyards across the DDR under non-irrigated (NI) conditions and also for 25% ET_0 deficit-irrigated (DI) conditions at Quinta C, and supplementary leaf water potential data reported for the Cima Corgo subregion through the same summer field campaign season by ADVID (2017) (Figure 5-4a). From the same bibliographic sources used to derive the DO3SE parametrization for the Touriga Nacional grapevine cultivar (i.e. Moutinho-Pereira et al., 2001 and Moutinho-Pereira 2000), it was also possible to derive a relationship between predawn leaf water potential and midday leaf water potential (Figure 5-4b). Subsequently, a circadian function was fitted to simulate the hourly evolution of the grapevine leaf water potential factor under both non-irrigated and *25%* ET_0 deficit-irrigated conditions by setting predawn and midday leaf water potential to happen at 3AM and 3PM, respectively, as in Carbonneau et al. (2004) (Figure 5-4c and d). Finally, a simple zoning of the grapevine leaf water potential as surrogate of a drought factor across the DDR was made according to the seasonal evolution observed at the different vineyards and literature sources that also indicated frequent insufficient rainfall and earlier offset of summer drought from the more eastern side of the Cima Corgo subregion and all of the Douro Superior subregion (Jackson, 2008; Jones, 2013; Jones and Alves, 2012) (Figure 5-4e,f).

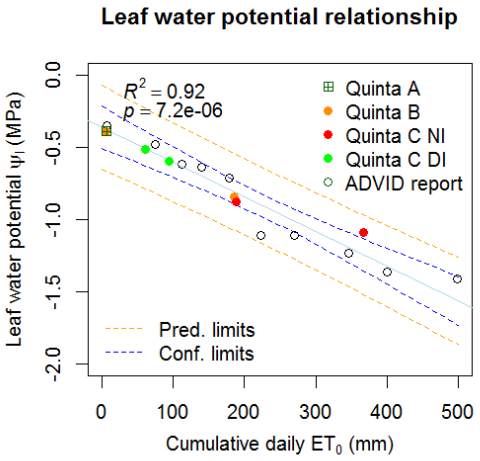

a)

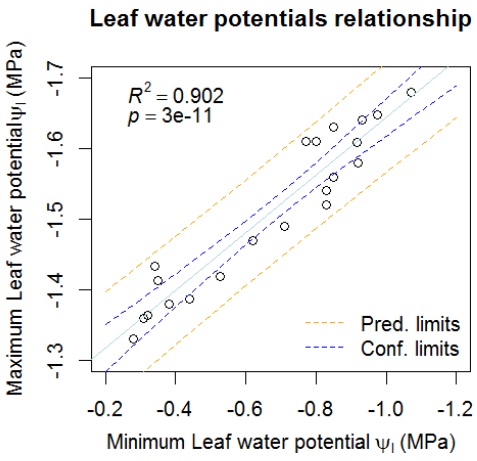

b)

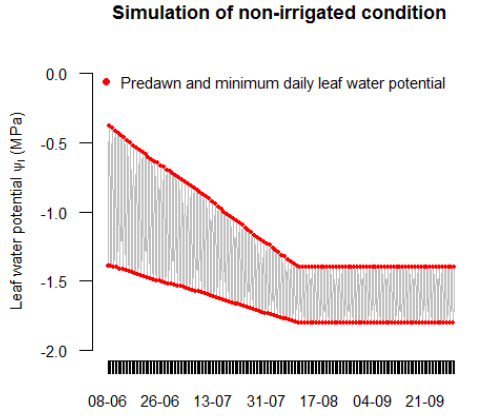

c) Quinta C, Summer 2017

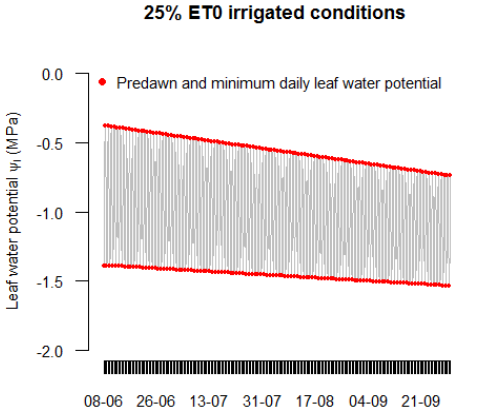

d) Quinta C, Summer 2017

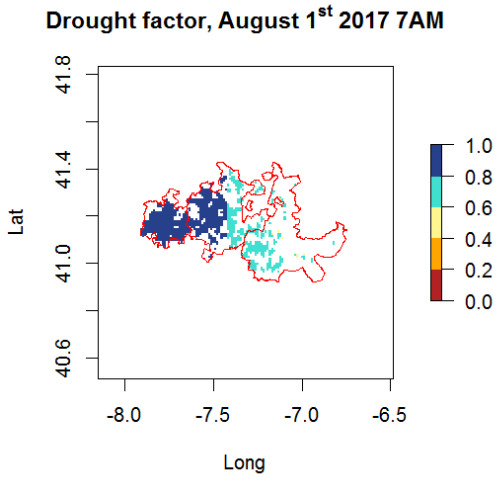

e)

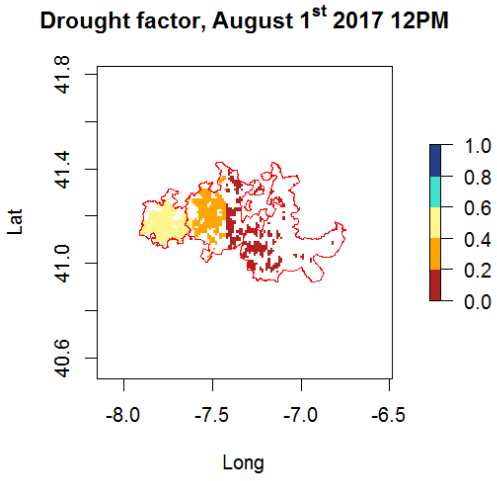

f)

Figure 5-4. a) Relationship between cumulative daily ET_0 and grapevine leaf water potential; b) Relationship between predawn and midday leaf water potential; c) Simulated hourly evolution of leaf water potential at Quinta C for unirrigated conditions during the 2017 summer drought season; d) Simulated hourly evolution of leaf water potential at Quinta C for 25% ET_0 deficit-irrigated conditions through the 2017 drought season; e) and f) Examples of hourly drought DDR factor maps derived for August 1st, 2017 at 7AM and 12 PM respectively.

5.4.3 O3 Phytotoxic Ozone Dose (*POD*) standards

The ground-level vegetation risk assessment standards selected for the evaluation of the simulated results were: CLRTAP-based April to September *POD0* (*Apr-Sep POD0*); June to September *POD0* (*Jun-Sep POD0*) as proposed by Soja et al. (2003) and Fumagalli et al. (2019) for the grapevine; CLRTAP-based April to September *POD6* (*Apr-Sep POD6*); June to September *POD6* (*June-Sep POD6*) as proposed by (Soja et al., 2004) for the grapevine. PODY is defined as (CLRTAP, 2017a):

$$PODY = \sum_{accumulation\ period} max(0; Fst - Y)\Delta t \quad (3)$$

where *Fst* is the instantaneous flux of O_3 through the stomatal openings per unit projected leaf area (PLA) and Δt is the time scale in seconds. It refers specifically to the sunlit leaves at the top of the canopy. It is regarded here as the hourly mean flux of O_3 into the stomata. Y is the threshold stomatal flux per PLA and it can be related to plant defence, repair and detoxification processes (De Marco et al., 2016; Soja et al., 2004). Both parameters have units of nmol O_3 $m^{-2}s^{-1}$. Critical levels based on stomatal flux (*Clef*) are then cumulative stomatal fluxes above which adverse effects may occur according to present knowledge (CLRTAP, 2017a).

5.5 RESULTS

Results presented and analysed here are organized based on the needed information for the local parametrization, the calculation, and the validation of the stomatal conductance values, namely the phenological stage and the grapevine physiology (i.e. predawn leaf water potential and stomatal conductance to water vapour). Comparison between values estimated by the CLRTAP DO3SE model and the local TN DO3SE model are also presented.

5.5.1 Grapevine phenology

Grapevine phenology was estimated using field measured data and meteorological WRF results. Table 5-1 illustrates the dates of the main phenological phases observed in the field and derived from the phenological thermal modelling applied to the WRF simulations for the three vineyard sites (Quintas). A more detailed description on how the dates for the main phenological stages were derived from the field observations can be found in the supplementary materials (Table C-1).

Table 5-1. Comparison between phenological dates (day of year, *DOY*) observed at the three field sites and simulated by coupling WRF daily temperatures with phenological modelling.

	Quinta A		**Quinta B**		**Quinta C**	
	Field	Simulations	Field	Simulations	Field	Simulations
Budburst	81	82	81	88	88	95
Flowering	123	135	123	136	123	140
Grape colour onset	186	194	186	193	186	193
Maturity	235	232	235	230	235	229

It can be observed that the phenological thermal model is quite accurate concerning the bud burst at Quinta A with only one day of delay, but that this model delay increases to 7 days at Quinta B and Quinta C. The phenological model flowering date delays between 12-13 at Quinta A and Quinta B and up to 17 days at Quinta C. There is a decrease in model delay in relation to the onset of grape colour oscillating between 7 days at Quinta B and Quinta C and 8 days at Quinta A. The opposite happens with maturity, where the dates derived from the phenological simulations are ahead 3 days at Quinta A, 5 days at Quinta B and 6 days at Quinta C.

Figure 5-5 (a,b,c) illustrates the dates of main phenological stages as derived from the thermal models applied to the WRF simulations for both Touriga Nacional and Touriga Franca for the main areas cultivated with grapevine within the DDR. As expected, earlier dates are related to sheltered sites provided by the Douro river course and its tributaries and the more thermic locations toward the west in the Douro Superior subregion. Figure5-5 (d) shows the age factor for the three vineyards as derived from the phenological thermal model where it can also be observed that Quinta C has a later budburst date, as reported in the field.

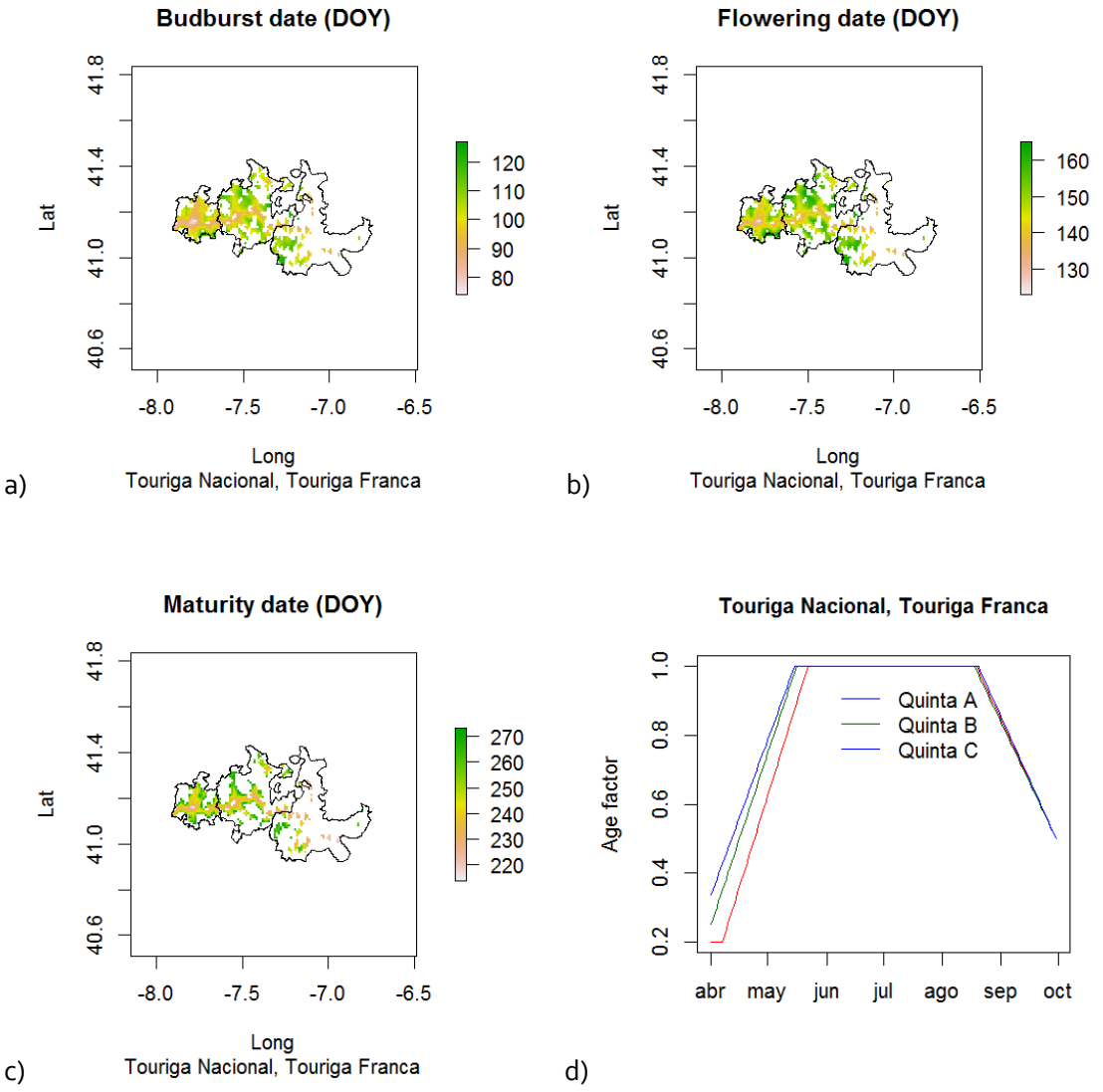

Figure 5-5. Spatial phenological maps as derived from the phenological model applied to the WRF simulations for budburst date (a), flowering date (b), and maturity (c) in two cultivars, where the units given are day of year (*DOY*), along with the respective phenological factors for the three vineyard sites (A, B and C) as derived from those maps (d).

The delays of the phenological dates for bud break, flowering and grape colour onset can be related with the negative bias present on the WRF temperature simulations which were in the range of -1.8 °C for hourly mean temperature and -3.1 ˚C for daily maximum temperature at Quinta C and within the range of other studies concerning validation of WRF simulations in the Iberian Peninsula (Blanco-Ward et al., 2021b). Errors in the range of up to 8 days for budbreak, 6 days for flowering, 12 days for grape colour onset have been

reported for grapevine using the type of phenological model used in this work (Moncur et al., 1989; Zapata et al., 2017). The change in the error from delay to advancement of the date compared to the field observations in the maturation stage can be related to an inhibition of the physiological development of the grapevine due to high temperatures (i.e. T > 35 °C), light and water deficit (Bernardo et al., 2018). Such conditions were reached during the summer of 2017 in the Douro region (ADVID, 2017).

5.5.2 Grapevine physiology

The statistical analysis of physiological measurements taken in the field are summarized in Figure 5-6. It can be observed that predawn leaf water potential (Ψd) and stomatal conductance to water vapour (gs_{H2O}) follow a similar pattern with an increase of the summer stress conditions from Quinta A within the Baixo Corgo subregion or under deficit-irrigated conditions to the higher ones at Quinta C within the Douro Superior subregion. Under sustained drought conditions, grapevine leaf water potentials become more negative through the summer whereas there is also a reduction on leaf stomatal conductance.

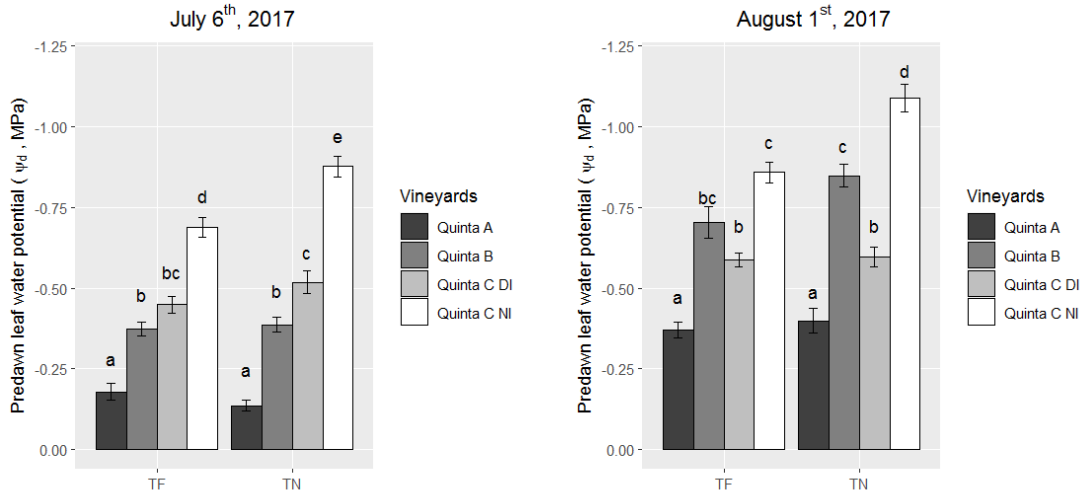

a) b)

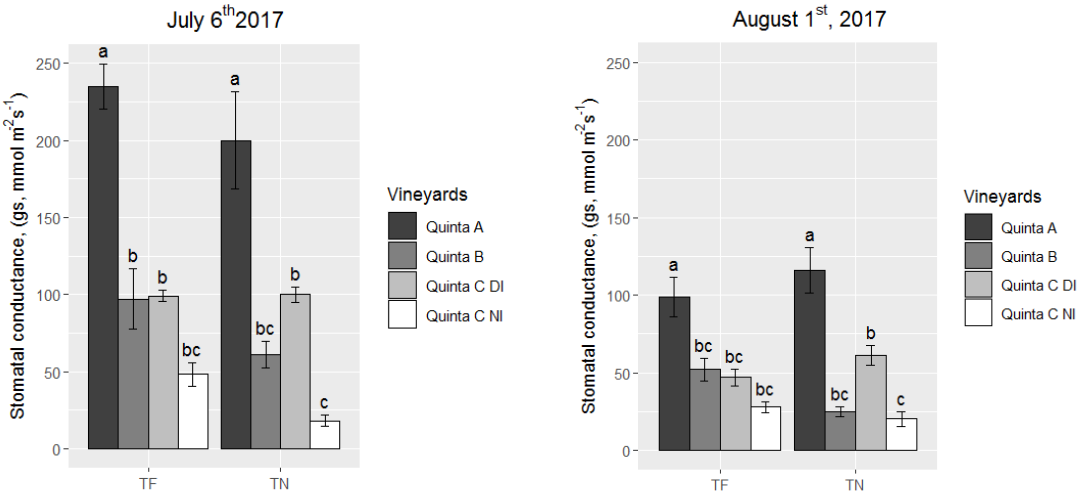

Figure 5-6. Statistical analysis summary of a) leaf water potential on July 6th, 2017, b) leaf water potential August 1st, 2017, c) stomatal conductance to water vapour (gs_{H2O}) on July 6th, 2017 and (d) stomatal conductance to water vapour (gs_{H2O}) on August 1st, 2017. Different letters indicate significant differences between treatments ($p<0.05$) for each day of measurement.

According to commonly used Ψd threshold values such as those proposed by Carbonneau et al. (2004) and Deloire et al. (2005) and the mean predawn leaf water potential values observed at the three vineyards, there was no sign of water deficit in the grapevines sampled at Quinta A on July 7th (Ψd > -0.2 MPa), a mild to moderate water deficit was present in the grapevines sampled at Quinta B (-0.2 MPa < Ψd < -0.4 MPa), whereas the water deficit reached moderate to severe conditions (-0.4 MPa < Ψd < -0.6 MPa) under 25% ETP_0 deficit-irrigated conditions and severe to high water deficit (Ψd < - 0.6 MPa) under unirrigated conditions at Quinta C. As the dry and hot 2017 summer progressed, the grapevines sampled at Quinta A reached a mild to moderate water deficit condition while those sampled at Quinta B and Quinta C displayed a severe to high water deficit where vegetative growth was reduced or inhibited except for those plants under deficit-irrigated conditions, which continued within the moderate to severe Ψd range of values.

Consistent with the works of Cifre et al. (2005), Flexas and Medrano (2002) and Medrano et al. (2002), it is also possible to relate gs_{H2O} to the degree of water stress and its effects on photosynthesis limitations. As it happened with Ψd, the measured July 7th gs_{H2O} values indicate that: there is mild or no water stress at Quinta A (150 mmol H_2O m^{-2} s^{-1}< gs_{H2O} < 500 mmol H_2O m^{-2} s^{-1}) where gs_{H2O} would probably be the only limitation to photosynthesis;

there is mild to moderate water stress (50 mmol H_2O m^{-2} s^{-1}< gs_{H2O} < 150 mmol H_2O m^{-2} s^{-1}) at Quinta B and under deficit-irrigated conditions at Quinta C where stomatal limitations would then still be dominant and photosynthesis could be rapidly reversed upon re-watering although non-stomatal limitations (reduced photochemistry and carboxylation efficiency and, eventually, photoinhibition) could also develop; and there is severe water stress at Quinta C under non- irrigated conditions (gs_{H2O} < 50 mmol H_2O m^{-2} s^{-1}) where non-stomatal limitations to photosynthesis would prevail and photosynthesis would not recover after irrigation if the drought is prolonged. By August 1st, mild to moderate water stress is already present at the monitored grapevines at Quinta A, where those located at Quinta B are close to (TF) or present (TN) severe water stress which is definitely present at Quinta C under non-irrigated conditions for both cultivars. Under 25% ET_0 deficit-irrigated conditions at Quinta C, the Touriga Franca cultivar mean gs_{H2O} is under the 50 mmol H_2O m^{-2} s^{-1} severe water stress threshold while Touriga Nacional is slightly above it.

The observed Ψd and gs_{H2O} have a good degree of coincidence in highlighting the existence of severe water stress condition which could inhibit photosynthesis and vegetative growth for the grapevines sampled at Quinta C under non-irrigated conditions from about June 6th, with that condition intensifying and also spreading to unirrigated grapevines at Quinta B from about August 1st. This coincidence was expected due to the strong correlation existing between these parameters (Williams and Araujo, 2002) which for both varieties reached the same Pearson correlation coefficient (0.88, p-value = 0.004). As it was hypothesized before, the photosynthetic and vegetative inhibition of the grapevines due to water stress, extreme temperatures and strong light conditions could contribute to the advancement of the phenological thermal model in comparison to the observed maturity dates. In fact, the advancement increases from three days of advancement, to five at Quinta B and six at Quinta C (without no distinction there between non-irrigated or deficit-irrigated conditions). A similar spatial and temporal pattern for Ψd and gs_{H2O} was already observed in the DDR by Moutinho-Pereira et al. (2004).

5.5.3 DO3SE parametrization

The specific parameters and resulting functions used for the generic grapevine and for the *Touriga Nacional* DO3SE grapevine parametrizations can be found in Table 5-2 and Figure5-7.

Table 5-2. DO3SE parameters and functions for a generic grapevine (as available in CLRTAP 2017) and the Touriga Nacional (TN) cultivar, as parameterized from data compiled in the DDR by Moutinho-Pereira et al. (2001) and Moutinho-Pereira (2000). The age component, fphen, was adjusted for the two cases, CLRTAP and TN, by means of the field phenological observations and phenological modelling as explained in section 5.4.2.1.

Parameter	Unit	*Vitis vinifera*	*Touriga Nacional*	Function
g_{max}	mmol O_3 m^{-2} PLA s^{-1}	229	250	
f_{min}	fraction	0.01	0.05	
light	unitless	0.0076	0.0046	flight= 1 – exp(light**PFD*) where *PFD* is the photosynthetic photon flux density
T_{min}	˚C	9	9	*Tmin*, *Tmax* > T ; *ftemp* = *fmin* *Tmin* < *T* < *Tmax ;* *ftemp* = max{*fmin*, [(*T*-*Tmin*)/(*Topt*-*Tmin*)]*[(*Tmax*- *T*)/(*Tmax* – *Topt*)]^{bt}} bt = (*Tmax* – *Topt*)/(*Topt* – *Tmin*)
Topt	˚C	30	30.3	
Tmax	˚C	43	44.5	
VPDmax	kPa	1.6	1.4	*fvpd* = min{1, max{*fmin*,((1-*fmin*)*(*VPDmin*-*VPD*)/(*VPDmin* – *VPDmax*))+fmin}}
VPDmin	kPa	6.2	7.4	
LWP α	unitless	----	-1.36	*flwp* = 1 / (1 + exp(α – *lwp*)/ β)
LWP β	unitless	----	0.14	
fphen_a *fphen_1_FD*	Unitless ˚C days	0.2 523	0.2 523	
fphen_b *fphen_2_FD*	Unitless ˚C days	1 360	1 360	
fphen_d *fphen_3_FD*	Unitless ˚C days	1 1573	1 1573	
fphen_e *fphen_4_FD*	Unitless Days	0.5 273	0.5 273	

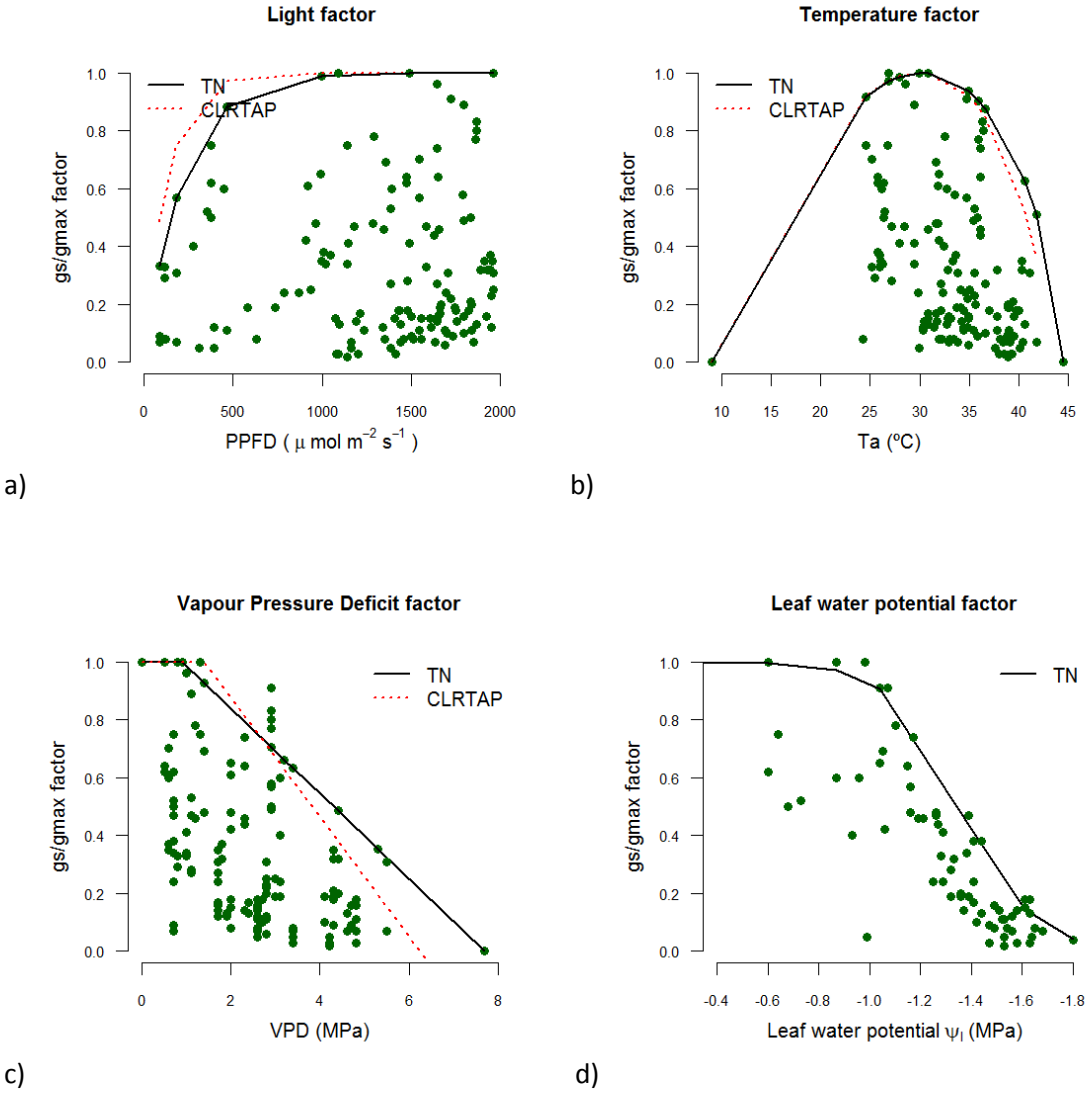

Figure 5-7. DO3SE parametrizations used in the last revised CLRTAP DO3SE model for *Vitis vinifera* L. and obtained for Touriga Nacional (TN) in the DDR: a) light factor, b) temperature factor, c) vapour pressure deficit factor, and d) leaf water potential factor.

It can be observed that g_{max}, T_{max}, and VPD_{min} parameters are greater for the TN parametrization compared to the CLRTAP one whereas the light factor and VPD_{max} are lower. The TN parametrization reflects a greater adaptation to maintain a higher stomatal conductance at higher temperatures and lower VPDs although it also tends to decrease activity at higher VPDs and lower light flux densities than the more general CLRTAP grapevine parametrization. T_{min} was set to 9°C, in common with the CLRTAP parametrization, as the available stomatal conductance measurements taken both from the field campaign and from bibliographic sources would not cover the colder periods of

the growing period being a value close to the commonly accepted 10°C base temperature for grapevine development activity (Corte-Real et al., 2015). The phenological growth component is the same for CLRTAP and TN parametrizations and is based on the thermal requirements and phenological observations derived from the April-September field campaign. The CLRTAP parametrization lacks the factor related with leaf water potential component as this factor is associated to specific observations made for the *Touriga Nacional* grapevine cultivar in the Douro Demarcated Region (DDR).

Furthermore, Figure 5-8 illustrates the daily profile of gs_{H20} and controlling factors at Quinta C for both the WRF CLRTAP and TN DO3SE parametrizations. The gs_{H20} values remain quite stable, increasing along the daylight hours and decreasing in the afternoon, in the CLRTAP DO3SE with the temperature factor exerting the greatest control on July 6th, whereas the vapour pressure factor does so on August 1st.

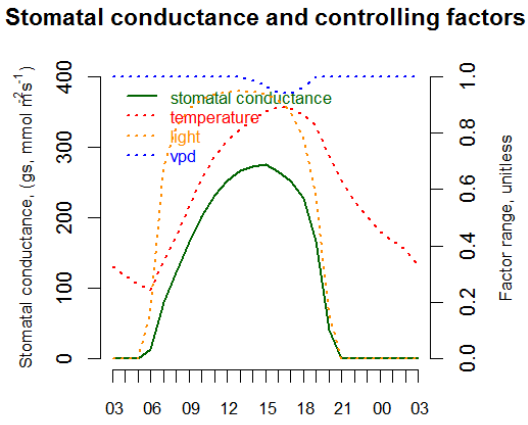

a) Quinta C, CLRTAP July 6th, 2017

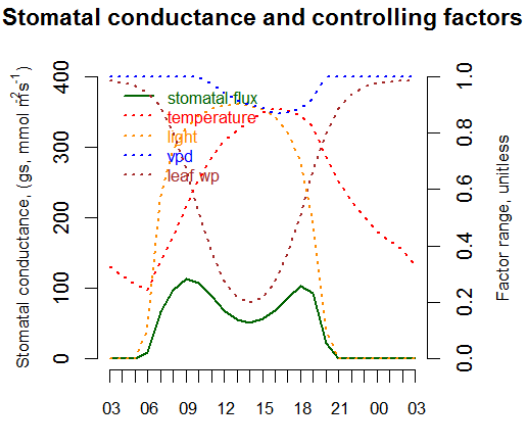

b) Quinta C, Touriga Nacional July 6th, 2017

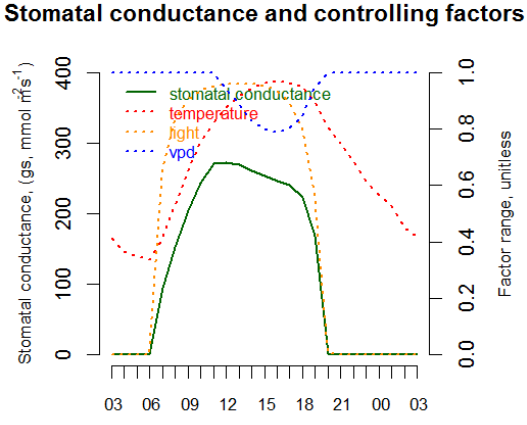

c) Quinta C, CLRTAP August 1st, 2017

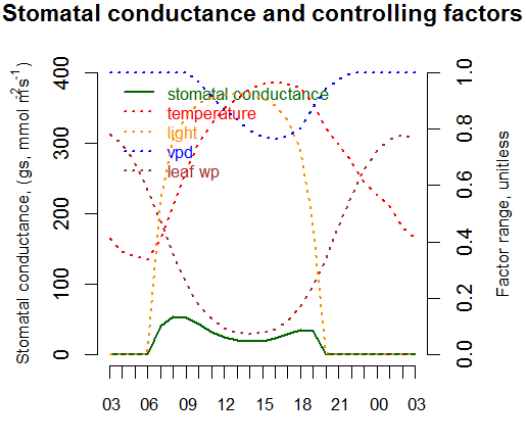

d) Quinta C, Touriga Nacional August 1st, 2017

Figure 5-8. Daily profile of stomatal conductance and environmental control factors on July 6th (grape colour onset phenological stage) and August 1st, 2017 (maturity). Quinta C.

For both the temperature and the vapour pressure factor, the TN DO3SE parametrization shows a similar hourly pattern to the CLRTAP DO3SE, but the leaf water potential factor, which is not included in the CLRTAP DO3SE parametrization, exerts a much greater control over gs_{H20}, which increases through the summer. Figures C-2 and C-3 (in supplementary material) show the same type of results for the other two vineyard sites.

5.5.4 DO3SE stomatal conductance validation

The stomatal conductance to water vapour, gs_{H20}, as derived from the TN DO3SE parametrization both through the use of meteorological station (MET) or WRF-simulated meteorological data is closer to the values and ranges measured in the field than the respective results estimated by the CLRTAP parametrization (Figure 5-9). No significant difference was found between WRF and MET fed DO3SE simulations.

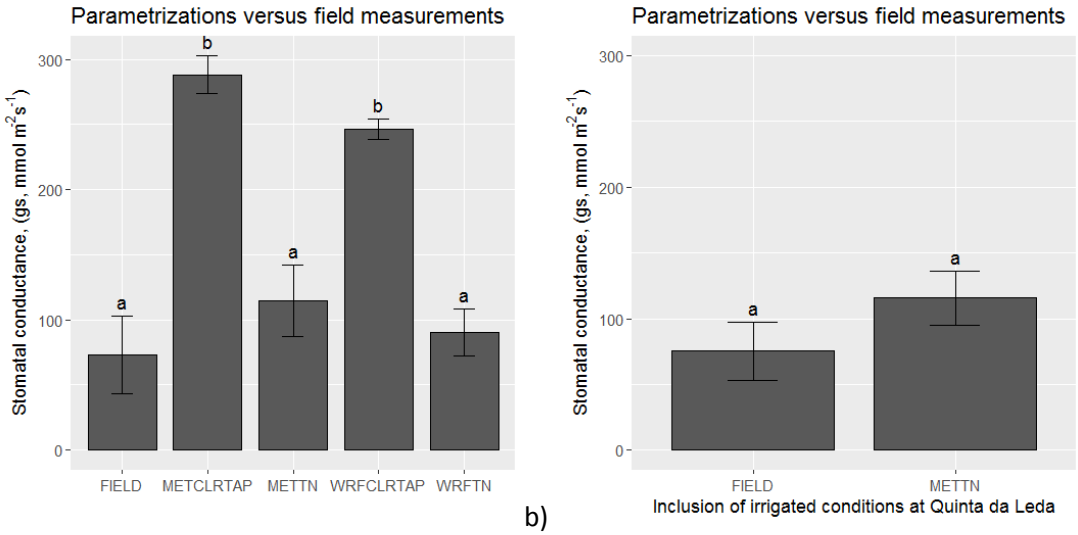

a) b)

Figure 5-9. a) Statistical summary of mean group comparisons among 11AM-15PM solar time gs_{H20} values collected in the field through the three vineyard sites and those derived from CLRTAP and TN DO3SE-based parametrizations feed by on site meteorological observations (MET) and WRF simulations (WRF). b) Mean group comparisons in the field and derived from TN DO3SE-based parametrizations feed by on site meteorological observations (MET) at Quinta C under 25% ET_0 deficit-irrigated conditions.

5.5.5 DO3SE *POD*

For the eastern most vineyard, Quinta C (Douro Superior), where an observational site for ambient O_3 was also available from April to September 2017, the TN DO3SE

parametrization yielded lower April to September and June to September *POD0* values than the ones derived from the CLRTAP DO3SE model (Table 3). This was expected as stomatal conductance values had lower values during the dry season in the TN DO3SE parametrization, as it has been seen previously. However, the results for 25% ET_0 deficit-irrigated conditions were close to the CLRTAP parametrization. When a 6 nmol m^{-2} s^{-1} detoxification threshold was introduced, as in Soja et al. (2004), the TN parametrization gave much lower values than the CLRTAP ones, and no difference was observed between the deficit-irrigated and non-irrigated conditions for the TN case.

Table 5-3. *POD0* and *POD6* field-based estimates from CLRTAP and TN DO3SE parametrizations. Values in bold indicate ozone phytotoxic risk according to the Jun-Sep POD0 standards set by Soja et al. (2003, 2004).

April to September POD0 (mmol m^{-2})			*April to September POD6* (mmol m^{-2})		
MET-CLRTAP	MET-TN	MET-TN-25% ET_0	MET-CLRTAP	MET-TN	MET-TN-25% ET_0
28.3	16.8	23.4	1.2	0.1	0.1
WRF-CLRTAP	WRF-TN		WRF-CLRTAP	WRF-TN	
28.6	13.5		0.9	0.2	
June to September POD0 (mmol m^{-2})			*June to September POD6* (mmol m^{-2})		
MET-CLRTAP	MET-TN	MET-TN-25% ET_0	MET-CLRTAP	MET-TN	MET-TN-25% ET0
17.8	7.8	**14.3**	0.4	0.1	0.1
WRF-CLRTAP	WRF-TN		WRF-CLRTAP	WRF-TN	
22.9	8.5		0.8	0.1	

The maps derived from the WRF-CHIMERE simulations involving the CLRTAP and TN DO3SE parametrizations for the grapevine cultivated areas in the DDR can be found in Figure 5-10.

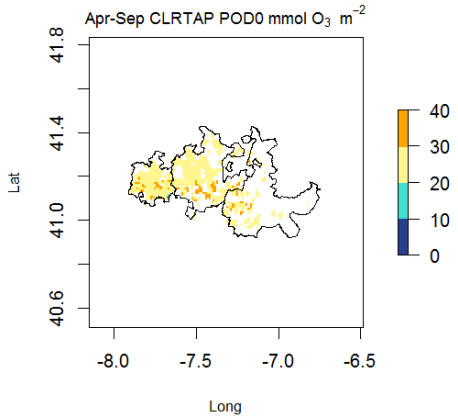

a)

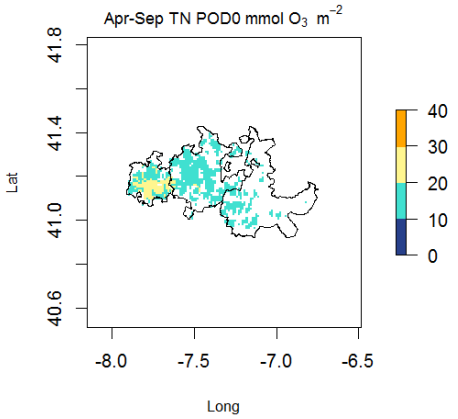

b)

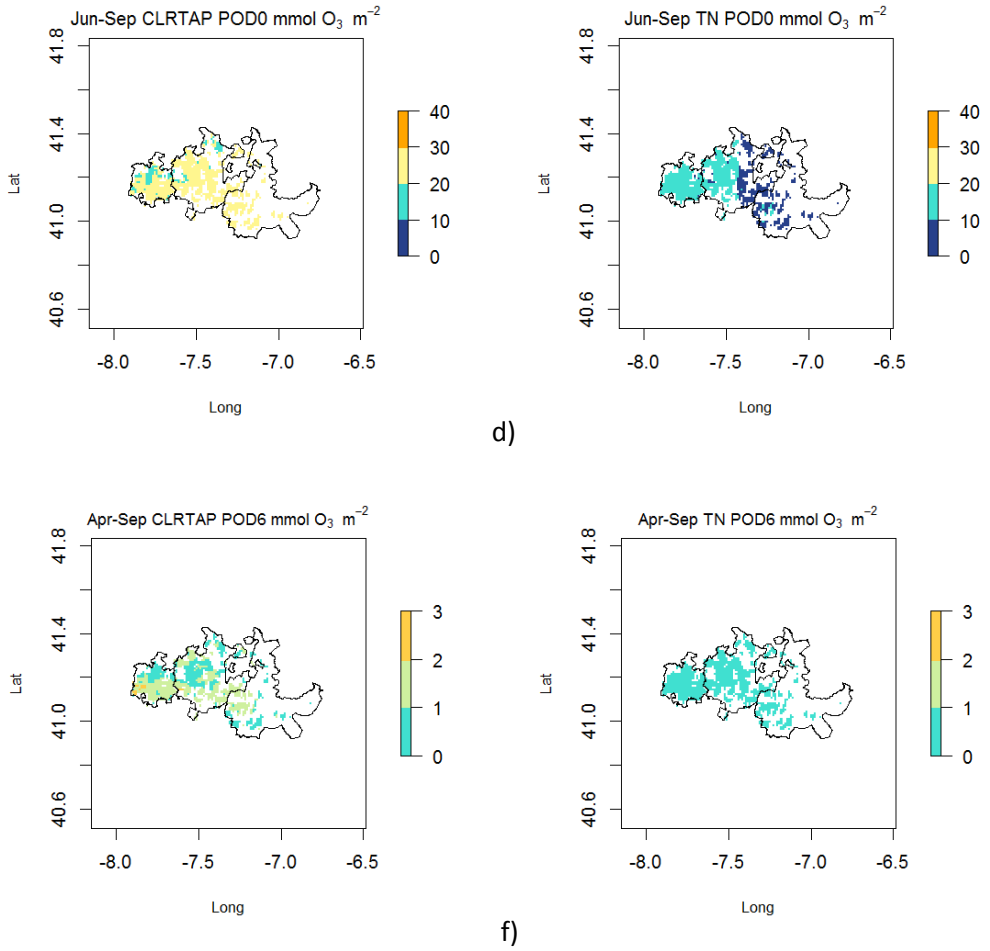

Figure 5-10. *Apr-Sep* and *June-Sep POD0* and *POD6* maps for non-irrigated cases, for CLRTAP and TN DO3SE parametrizations.

Whereas the CLRTAP DO3SE parametrization shows values above 20 and 30 nmol m^{-2} along all the DDR for the *POD0 April to September* standard, the higher values derived from the TN DO3SE model do not exceed 30 nmol m^{-2} and those exceeding 20 nmol m^{-2} are mainly located in the western Baixo Corgo subregion with some minor areas in the Cima Corgo subregion. For the *June to September POD* standard, values between 20-30 nmol m^{-2} can be found across all the DDR for the CLRTAP DO3SE parametrization but they are not above 20 nmol m^{-2} for the TN DO3SE model, which shows the higher values located almost exclusively in the Baixo and Cima Corgo subregions. Finally, the *POD6* standard shows values between 1 and 2 nmol m^{-2} across all the DDR for the CLRTAP DO3SE parametrization but are below 1 nmol m^{-2} for the TN DO3SE one.

5.6 DISCUSSION

Leaf water potential measurements are regularly used by the wine industry to monitor grapevine water stress and can be empirically related with meteorological variables, such as reference evapotranspiration, through the dry summers common in rain-fed Mediterranean environments (Bernardo et al., 2018; Gaudin et al., 2017). Thus, leaf water potential can be a very valuable proxy to include the soil drought factor into the DO3SE parametrization and it has also been already used in other POD assessment research studies including Mediterranean environments as in Alonso et al. (2008), and Büker et al. (2012). The TN DO3SE model results did not present significant differences with the gs_{H2O} observed ones in the field through the summer season, while the DO3SE CLRTAP model overestimated these observations. This is mainly due to inclusion of the leaf water potential factor as a proxy of soil drought in the DO3SE TN parametrization. The same type of observation has been made with forest species in Mediterranean environments (De Marco et al., 2016).

Although the greater proportion in the difference in the estimation of the standard *POD* values is related to the inclusion of the leaf water potential factor since early June, a cultivar effect can also be appreciated from before, as it can be observed in Figure 5-11.

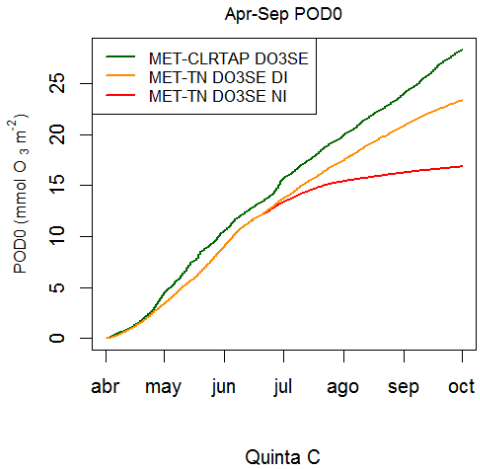

Figure 5-11. *April to September POD0* cumulative increase for the CLRTAP DO3SE and the TN-DO3SE parametrizations at Quinta C (Douro Superior).

To perform a *POD*-based risk assessment at the regional or local scale, it is also necessary to consider the adaptation to the niche of the cultivars present in the study area. In this

case, Touriga Franca, which was also present in the DDR, had slightly higher values of Ψd and gs_{H2O} under the more severe non-irrigated water stress conditions, but the interpretation of the possible effects in terms of the inhibition of growth and photosynthesis according to the keys commonly used for irrigation management, has been practically the same for the two grapevine varieties, as it has been previously explained.

Phenology is also important in terms of which interval of the vegetative cycle is selected to estimate *POD*. In this regard, Touriga Franca and Touriga Nacional have also been classified in the same interval corresponding to cultivars of early budburst and intermediate maturity range (i.e. within 2068 ˚C – 2190 ˚C day to achieve the maturity stage in comparison to other early or late to mature cultivars) in an extensive field study involving 16 years of phenological observations among 34 grapevine cultivars in an experimental site at Lisbon (Lopes et al., 2008).

As can also be seen in Figure 5-11, a too short phenological window from developed stages well after flowering from June or with low physiological activity along summers with high temperatures, strong light and dry conditions, characteristic in Mediterranean environments, could underestimate the risk. In the present study, the relevance of *POD* flux from early stages makes more advisable to use wider Apr-Sep intervals similarly to what has been made to assess *POD* risk for forest species also in Mediterranean environments. On the other hand, it is also known that the flowering stage is very sensitive for the grapevine and with effects that determine the subsequent phases or the harvests of future years, so it is also convenient to carry out studies that include more than one growing season (Guilpart et al., 2014; Soja et al., 1997).

Although the present work was limited to a single year of observation, there is some indication for the TN DO3SE adapted model for the DDR that both *Apr-Sep* and *Jun-Sep POD* could exceed Cle_f associated with grapevine yield and quality as it ranges between 10 and 20 mmol O_3 PLA m^{-2} for many areas, specially towards the west in the Baixo Corgo and Cima Corgo subregions. It has also been shown for Quinta C in the eastern Douro Superior subregion of the DDR, which is often severely affected by summer drought, that moderate irrigation (25% ET_o) can increase the value of *POD* substantially, and therefore also increase the risk of O_3 phytotoxic damage for this area. However, the information to assess if there is ozone phytotoxic risk for the grapevine in the study area in relation to grape yield and

quality based on *POD* standards is currently limited by the fact that there are only two open top chamber (OTC) O_3 fumigation experiments that were performed in continental Austria and northern Italy for two varieties which are not currently grown in the DDR. For the *Jun-Sep POD0* standard, Soja et al. (2003) referred that a 10% reduction in yield is expected if the uptake exceeds 12.5 mmol m^{-2} for two consecutive years; they also noticed that sugar yield was more sensitive than yield with a *Clef* of 12.0 mmol m^{-2} although these results were limited to a three-year OTC experiment over *Vitis vinifera* cv. Welschriesling three-year old plants grafted on Kober 5BB rootstock under irrigated conditions 30 km south of Vienna, Eastern Austria. In a later work based on the same fumigation experiment, Soja et al. (2004) also published *Clef* values for grapevine associated with the *Jun-Sep POD6* index (stomatal O_3 flux above a *Y* threshold of 6 nmol O_3 $m^{-2}s^{-1}$). A *Jun-Sep POD6 Clef* of 3.5 mmol m^{-2} for a 10% reduction of grape yield was established for the first experimental year and 2.2 mmol m^{-2} for the second year, whereas the values associated with a 10% reduction in grape monosaccharide yield were 2.3 mmol m^{-2} in the first year of the experiment and 1.1 mmol m^{-2} in the second year. In addition to the work of Soja et al. (2003, 2004), a *Jun-Sep POD0* exceeding 32 mmol m^{-2} was reported by Fumagalli et al. (2019) to have an effect on yield and polyphenols for cv. Merlot, which is considered a global variety as it is extensively cultivated through the world (OIV, 2017).

The use of *PODY* thresholds has to be done carefully, because the variability of the *POD* standards calculated by the different DO3SE formulations is greater as the thresholds increase. The variability in the estimation of *POD* with thresholds with respect to variations in the formulation of the DO3SE model has also been observed by De Marco et al. (2016) and currently low threshold standards such as *POD1* and *POD2* are being considered for forest species in Mediterranean environments.

With all of the above, the value given by the default grapevine CLRTAP DO3SE based parametrization can be considered a worst-case scenario where there is no limitation of the water available in the soil, while the refined TN DO3SE based model would be better adjusted to the local conditions for the studied varieties, Touriga Nacional and Touriga Franca. Although detailed parametrization of the DO3SE model for the local DDR grapevine cultivars was only possible for the Touriga Nacional (TN) case, the field campaign measurements indicated that the Touriga Franca (TF) cultivar stomatal fluxes fluctuate within the same range of values in response to drought. As both varieties share similar

thermal requirements for phenological stage development and present similar response in parameters such as leaf water potential and stomatal conductance, it could also be expected a similar rate of *POD* accumulation through the growing season. Both varieties are commonly grown (Corte-Real, 2014; Santos et al., 2013) and appreciated due to its good niche adaptation and high oenological potential in the DDR.

Finally, climate change forecasts for the DDR indicate a reduction in cold periods and precipitation, in addition to an increase in temperatures, and heat waves with the consequent advance in the phenology of the grapevine and the accentuation of its water stress within this century. Traditionally, irrigation has not been allowed in the Douro region in order to maintain the typicity of the wines, but these conditions could favour a change so that the use of precision irrigation strategies becomes more extensive in order to maintain profitability especially in the innermost regions of the DDR, such as the Douro Superior subregion. The results of this study indicate that the use of precision irrigation could increase the phytotoxic risk of ozone for the vineyard.

5.7 CONCLUSIONS

The results of this research illustrate the relevance of including a specific parametrization for autochthonous grapevine varieties, with leaf water content as a proxy of the soil water balance, to perform an O_3 phytotoxic risk assessment. Adapting the methodology for a renowned wine producing area, the Demarcated Douro Region of Portugal, not only has a relevant effect on the POD, but it also modifies substantially the spatial patterns of the *POD* maps produced for phytotoxic risk assessment. Both the field measurements and the TN DO3SE *POD* model estimates indicate that considerable areas in the Demarcated Douro Region can still exceed critical dose values for the grapevine, although with a lower extent when compared to the default CLRTAP DO3SE which does not include any soil water component for the grapevine. 25% ET_0 deficit-irrigated conditions increase the fine-tuned TN DO3SE POD values close to the default grapevine CLRTAP DO3SE results. Thus, notwithstanding the information available to derive dose-response functions can only be approximated by limited OTC research performed with other varieties and agro-climatological niches, a higher ozone risk of yield and quality loss is expected for deficit-irrigated conditions. Overall, the research results indicate that air quality management, in particular the reduction of ozone levels in the ambient air, must also be considered to

define sustainable grape and wine production strategies in the context of climate and wine production management change.

6 CONCLUSIONS AND FUTURE DEVELOPMENTS

The main objective of this Thesis was to develop and evaluate a modelling system able to comprehensively simulate exposure and ozone uptake for grapevines under Mediterranean conditions besides contributing to the current state of the art on the influence of climate in viticulture and wine production in the context of climate change. The study aimed to advance knowledge on which key factors, model formulations and parameterizations should be considered in order to successfully assess potential climate and phytotoxic O_3 risk under Mediterranean conditions.

In summary, by means of this research, it has been possible to relate the WRF-ERA recent-past climate simulations with vintage yield and quality in the DDR. The mid-term and long term WRF-MPI climate scenarios revealed shifts to warmer and drier conditions not remaining within the ranges for quality and production. At the global level, wide regions of the world, mainly between latitudes 30° and 50° N, where the grapevine has been traditionally cultivated, are exposed to O_3 concentrations that can affect both the yield and quality of the grape. Concerning exposure to ozone (*AOT40*), the 2017 WRF-CHIMERE simulations indicated that considerable areas of the Douro Demarcated Region of Portugal can exceed the critical exposure values for vegetation and the grapevine according to European legislation standards and current OTC research. This is also the case concerning phytotoxic ozone dose (*POD*), which could increase under irrigated conditions. However, it is still necessary to adopt common experimental and monitoring protocols to establish grapevine specific O_3 relationships, as there is not yet a coherent and shared database for detailed risk assessment for this crop.

The answer to each of the formulated research questions formulated as part of the objectives of this Thesis is presented in Section 6.1, whereas the limitations found in this work and its possible future developments are discussed in Section 6.2.

6.1 MAIN FINDINGS

Can coupled Global Climate Model-Regional Climate Model (GCM-RCM) simulations be related to grapevine yield and quality in order to assess potential risks in the context of climate change?

To capture the effects of climate change in grapevine's yield and quality in mountainous areas it is crucial to dynamically downscale GCM to RCM and to come down to higher spatial resolutions through nested simulations and using selected climate indices. Despite the limitations of the 9 km × 9 km WRF-ERA simulations to reproduce the viticulture climate of an area of complex topography such as the DDR, it is still possible to select a representative cell or group of cells, for which the difference between the average modelled and observed characteristics is not relevant (e.g. the eastern subregion), to relate the 1986–2005 recent-past climate to vintage yield and Port wine vintage rating records in the area. Correlations found by using a thermal phenological model are often higher than those using conventional calendar-based monthly phenological divisions. Therefore, the phenological modelling also provided insight to understand the interactions between surface atmospheric conditions and vintage yield and quality in the DDR.

Moreover, for the potential risks in the context of climate change, the WRF-MPI very-high 1 km × 1 km resolution simulations show an important increase in summer days (*SU25*) and very hot days (*SU35*) and an important reduction in frost days (*FD0*). These variations in climate extreme indices could relate to a higher incidence of heatwaves and fewer chilling units during dormancy and could pose a threat to maintenance of vintage quality. The simulations also illustrate an important advancement in phenology and shortening of the budburst to *véraison* period which could also expose the berries to warmer atmospheric conditions.

Concerning bioclimatic parameters and indices, there is an increase in *GST*, and a concurrent decrease in *GSP*, with the greatest changes taking place in the second half of the 21st century. The future WRF-MPI climate scenarios show a decrease in the diversity of *WI* regions towards warm or very warm areas associated with the intensive production of wines of intermediate quality, especially by the end of the century. *HI* also exhibits a potential change from temperate or temperate-warm conditions to warm or very warm conditions. In the recent past, *CI* was associated mainly with very cool night conditions which are commonly related to the production of quality wines, but from the mid-term future scenario there is also a marked shift to temperate night conditions, reaching even warm night conditions for several areas at the end of the century. Finally, *DI* indicates that there is a considerable increase in water stress, which is already considered high under the present climate.

Can the current European Monitoring and Evaluation Programme (EMEP) dry deposition model under CLRTAP adequately represent ozone uptake by local grapevine varieties in a Mediterranean area such as the DDR?

The stomatal conductance to water vapour, gs_{H20}, as derived from the Touriga Nacional (TN) DO3SE parametrization both through the use of meteorological station (MET) or WRF-simulated meteorological data is closer to the values and ranges measured in the field than the respective results estimated by the CLRTAP parametrization. No significant difference was found between WRF and MET fed DO3SE simulations. The results of this research illustrate the relevance of including a specific parametrization for autochthonous grapevine varieties, with leaf water content as a proxy of the soil water balance, to perform an O_3 phytotoxic risk assessment. Adapting the methodology for a renowned wine producing area, the Demarcated Douro Region of Portugal, not only has a relevant effect on the *POD* estimates, but it also modifies substantially the spatial patterns of the *POD* maps produced for phytotoxic risk assessment.

What are the most important variables affecting ozone uptake by grapevine in the DDR and how could they be taken into account by the modelling system?

Different variables were tested and included through the multiplicative DO3SE modelling system, such as phenology, photosynthetic active radiation, air temperature, air vapour pressure deficit, and leaf water potential as a proxy of soil water content. All these variables are relevant to assess phytotoxic risk. Phenological observations are helpful to accurately describe the growing season. Photosynthetic active radiation and air temperature play more of a role at the initial and final stages of the growing season. Atmospheric and soil water deficits became the greatest environmental factors during late spring and the summer season. Including information regarding the soil water balance is of utmost importance in Mediterranean environments and this could be done through the use of a proxy like the leaf water content.

From the specific parameters and resulting functions used for the generic grapevine CLRTAP and for the Touriga Nacional (TN) DO3SE grapevine parametrizations, it could be observed that *gmax*, *Tmax*, and *VPDmin* parameters were greater for the TN parametrization compared to the CLRTAP one whereas the light factor and *VPDmax* were lower. The TN parametrization reflected a greater adaptation to maintain a higher stomatal

conductance at higher temperatures and lower VPDs although it also tends to decrease activity at higher VPDs and lower light flux densities than the more general CLRTAP grapevine parametrization. The phenological growth component was made the same for CLRTAP and TN parametrizations and was based on the thermal requirements and phenological observations derived from the April-September 2017 field campaign. The CLRTAP parametrization did not include the factor related with leaf water potential component as this factor is associated to specific observations made for the Touriga Nacional grapevine cultivar in the Douro Demarcated Region.

From the simulated daily profile of gs_{H20} and controlling factors at Quinta C (Douro superior DDR subregion) for both the WRF CLRTAP and TN DO3SE parametrizations, it could be observed that the gs_{H20} values remained quite stable, increasing along the daylight hours and decreasing in the afternoon, in the CLRTAP DO3SE with the temperature factor exerting the greatest control on July 6th, whereas the vapour pressure factor does so on August 1st. For both the temperature and the vapour pressure factor, the TN DO3SE parametrization shows a similar hourly pattern to the CLRTAP DO3SE, but the leaf water potential factor, which is not included in the CLRTAP DO3SE parametrization, exerts a much greater control over gs_{H20}, which increases through the summer. The same type of results was obtained from the other two vineyard sites (Quinta A located in Baixo Corgo and Quinta B located in Baixo Corgo). A stronger control on stomatal conductance from the leaf water potential factor was also observed at the eastern, drier sites.

Finally, it was also observed that 25% ET_0 deficit-irrigated conditions increased the fine-tuned TN DO3SE POD values close to the default grapevine CLRTAP DO3SE results. Thus, notwithstanding the information available to derive dose-response functions can only be approximated by limited OTC research performed with other varieties and agro-climatological niches, a higher ozone risk of yield and quality loss is expected for deficit-irrigated conditions.

What is the actual picture concerning ozone phytotoxic risk indicators once the dry deposition model is refined and fitted to local observational data?

Current ground-level O_3 can already pose a potential threat for a wine producing area such as the Douro region in Portugal. Moreover, ambient O_3 can affect grapevine yield and quality across wide regions of the Northern Hemisphere too. As such, ground level O_3 and

O_3 extremes should also be considered along heatwaves and drought as compromising factors for the grapevine.

Concerning exposure to ambient O_3 in the Douro Demarcated Region, it can be observed that in Quinta C (Douro superior subregion) the O_3 40-ppb threshold was exceeded for all growth stages reaching high values in rather sensitive stages, such as flowering, which in a perennial crop such as the grapevine, influences the development of the next growing season also affecting yield and quality.

Concerning *AOT40* indices estimated at the same location, the measured EU *May-Jun AOT40* value (8 ppm.h) exceeded the long-target value of 3 ppm.h and was close to what has been set as the general standard to protect vegetation (9 ppm.h) by Directives 2002/03/EC and 2008/50/EC. The measured day light-based *Apr-Sep AOT40* (13.8 ppm.h) exceeded the *Clec* (5 ppm.h) for a 5% biomass reduction in perennial-dominated (semi)natural vegetation and trees. The field *Jun-Sep AOT40* reached 9.5 ppm.h but is below the specific yearly *Clec* values for a 10% reduction in yield and quality (27 ppm.h and 21 ppm.h, respectively) as set by Soja et al. (1997) for the Welschriesling grapevine cultivar.

As for the WRF-CHIMERE modelling simulations, the daily mean maxima *Apr-Sep* O_3 map values showed that larger values were associated to higher elevations in the Marão and Montemuro mountain ranges towards the northwest of the DDR and spread through the Douro valley across the DDR. The daily mean *Apr-Sep* O_3, EU's *May-Jun AOT40* and CLRTAP *Apr-Sep AOT40* maps had similar spatial patterns with higher O_3 concentrations associated mostly with higher elevations inside and outside the DDR and particularly affecting a transitional area between the Cima Corgo and the Douro Superior subregions within the DDR. The *AOT40* map estimated according to the procedure of Soja's indicated that besides the previously commented areas, most of the Douro Superior subregion, with a warmer and drier climate, can be affected by high O_3 levels between June and September.

In relation to the dose-based standards, both field and WRF-CHIMERE adjusted TN DO3SE *POD* model estimates indicated that considerable areas in the Demarcated Douro Region can exceed critical dose values for the grapevine, although with a lower extent when compared to the default CLRTAP DO3SE parametrization which does not include any soil water component for the grapevine.

The estimation of both exposure and stomatal uptake standards for assessment of O_3 phytotoxic risk on grapevine yield and quality was still subjected to a great range of variation depending on the length of the cumulative period selected to estimate them.

What evidence can be derived from this work to support strategies aimed to preserve high-quality wine production sustainably in the context of climate change?

Concerning O_3 phytotoxic risk assessment for the DDR, the research results indicated that air quality management, in particular the reduction of ozone levels in the ambient air, must also be considered to define sustainable grape and wine production strategies in the context of climate and wine production management change. The reduction of O_3 precursor's emissions (e.g. NOx and VOCs) is already contemplated by the EU National Emissions Ceiling Directive (NECD, 2016/2284/EU). Concerning ambient O_3, the European Air Quality directive (2008/50/EC) sets *AOT40* as the standard to monitor and protect vegetation. More recently, the CLRTAP has given more emphasis to the use of species-specific stomatal flux-based standards such as *POD*. The *POD* values given by the default grapevine CLRTAP DO3SE based parametrization can be considered a worst-case scenario where there is no or less limitation of the water available in the soil, while the refined TN DO3SE based model ones would be better adjusted to the local conditions for the studied varieties, Touriga Nacional and Touriga Franca.

Concerning climate change impact assessment several actions can be proposed to preserve as much as possible the DDR wine typicity in a compromise to balance as much as possible economic, environmental and social costs. Short-term adaptations to increased temperatures and water deficits include the selection of suitable rootstocks, and late-ripening clones or varieties. Adapted training systems, and canopy management can be applied to reduce water consumption, delay phenology or limit solar exposure too. Soil management can also be considered to increase the soil water holding capacity (*SWHC*). When there is need of irrigation, precise strategies such as deficit irrigation should be considered. It is also possible to relocate the vineyards in the long term to cooler sites such as higher elevations or areas with lower solar exposures or closer to the sea. These relocations should also be carefully planned in order to maintain as much as possible freshwater resources and natural habitats.

6.2 FUTURE DEVELOPMENTS

The conclusions derived from Chapter 3 (Assessment of tropospheric ozone phytotoxic effects on the grapevine (*Vitis vinifera* L.): a review) and the experience gained from the field campaign and modelling aspects associated to this Thesis offer a good opportunity to reflect on the present limitations and opportunities to advance research. Focusing on the advances made since the beginning of this century, there is increased knowledge on the O_3 phytotoxic effects on the grapevine at the cellular, structural and anatomical leaf level, and leaf gas exchange parameters which can be accentuated depending on variety. It has also been verified that there is a diverse capacity for biochemical response and adaptation of the photosynthetic machinery and hormonal and antioxidant response depending on the specific cultivar too. It would be of interest to continue research on the combined effect of drought, high temperatures, light intensity, pests or other atmospheric compounds (e.g. CO_2, NO_2, SO_2, PAN).

To date, there is still only one series of works (Soja et al. 1997, 2003, 2004) where exposure or flux based ambient O_3 critical levels were derived for the grapevine with grape quality being more sensitive than yield. However, these critical levels have not been accepted by CLRTAP for detailed impact assessment as they are based only on a variety grown in European continental conditions (e.g. Austria) and only g_{sto} *max* was parameterized to estimate *POD*. Since the late 2010s, there have been studies focusing on global varieties such as Cabernet Sauvignon and Merlot which are second and fourth according to total cultivated extension in the World (341000 and 266000 ha respectively) (OIV, 2017), but there have not been further advances to derive ambient O_3 critical levels for yield and quality for these varieties. As such, there is opportunity to benefit from publishing under common agreed standards and protocols and to develop public access databases (e.g. TOAR vegetation).

There is also opportunity to perform valuable experimental O_3 fumigation studies by using facilities, such as free air-controlled exposure experiments (FACE) overcoming the OTC limitations for perennial crops such as the grapevine. Other fumigation or photoprotective methods are also valuable considering grapevine varietal variability. As the defence mechanisms concerning environmental variables (e.g. solar radiation, drought, CO_2 levels, and pest incidence) interact through common physiological mechanisms and biochemical

pathways, cross-tolerance studies should be promoted concerning grape adaptation to climate change.

There is still very little experience concerning monitoring of grapevine health indicators in the field and the few isolated studies cannot be extrapolated to other regions. Similarly to what has been recently started to be done with trees (e.g. De Marco et al. 2019; Paoletti et al. 2019), it would be useful to perform research on a series of health indicators specifically selected for the grapevine which, for instance, could relate foliar damage (e.g. stipple, browning, premature leaf ageing), plant stress (e.g. F_v/F_m), leaf nutritional and biochemical status, yield and quality with ambient O_3 along a network of selected vineyards also monitored for the effects of climate change. It is necessary to enforce common protocols so that more detailed assessments can be performed both at the global and regional scales. Regional assessments would need to consider different grapevine varietal tolerances as there is evidence of a range of sensitivities to O_3 for this crop.

Focusing more on the modelling component of this Thesis, it is clear that good progress has been made on the capacity to simulated high-resolution meteorology, O_3 exposure and O_3 deposition over topographically complex terrains. A key issue for advancement is the availability of observations in the field concerning meteorology, grapevine physiology and ambient O_3. For the DDR study area, it has been possible to have access to data from meteorological stations maintained by the IPMA and by interested parties related to the wine industry (i.e. SOGRAPE, ADVID). In that sense, the heightened awareness of the potential effects of climate change and the development of precision agriculture by the wine industry and intermediate parties also contributes fundamentally to the possibilities of expanding and refining research. However, the availability of ambient O_3 measurements has been much more limited, with only one air quality measurement station maintained by the Portuguese Environmental Agency located at high elevation (1086 m) and, thus, not being really representative of vineyard areas in the study area, and another made available specifically for the DOUROZONE research project which was located in a vineyard with the permission of one of the collaborating associates (i. e. SOGRAPE). The lack of simultaneous collection of ozone exposure data in vineyard areas for research purposes could be partially addressed in future studies through cross-tolerance studies and a network of selected vineyards also monitored for the effects of climate change, as has already been mentioned.

Another pending aspect to be developed is the projection of *POD* standards to future scenarios through modelling. Although the scope of this work regarding the modelling of ozone exposure and phytotoxic dose does not exceed the scope of a field campaign, light has been shed on the need to contemplate longer estimation times than those used up to now in the derivation of exposure-effect relationships of ozone for the vineyard (e.g. *Jun-Sep POD* in the experimental works of Soja et al. 1997, 2003, 2004 and Fumagalli et al. 2019) or standards proposed as part of community directives (i.e. *May-Jun AOT40*). Taking into account the phenological advance of the vineyard with the early increase in temperatures and the cumulative effect of the phytotoxicity of ozone through the growing season, it seems more convenient to use standards such as those proposed by the CLRTAP for perennial-dominated (semi)–natural vegetation and trees cases (i.e. 6 months by default, Apr-Sep NH) or to account at least for a five-month period from May (NH).

Despite the limitations, it has been possible to discern different situations that are already relevant today and that will continue to be a concern in the future, such as all those derived from the increase in water stress. It has been clearly observed a difference between adopting a POD standard that considers the availability of water for the grapevine (i.e. the *POD-TN* specific parametrization) versus another that usually does not consider it due to lack of data (i.e. *POD-CLRTAP*). In face of the greater water stress forecasted for the medium- and long-term climate scenarios, the possible effect of the use of irrigation in order to maintain the viability of vineyards would be particularly relevant. This would also allow adding greater modelling precision to the biological response of the crop which is an aspect also to be considered along the accurate specification of future scenarios, both in terms of climate and emissions.

References

[dataset] Norwegian Meteorological Institute, 2019. Depositions of sulphur (S) and nitrogen (N), and air concentrations of ozone (O3) and particulate matter (PM) as calculated with the EMEP MSC-W model as reported in the annual EMEP status reports. https://emep.int/mscw/mscw_moddata.html.

[dataset] Schultz, M.G., Schröder, S., Lyapina, O., Cooper, O.R., Galbally, I., Petropavlovskikh, I., von Schneidemesser, E., Tanimoto, H., Elshorbany, Y., Naja, M., Seguel, R.J., Dauert, U., Eckhardt, P., Feigenspan, S., Fiebig, M., Hjellbrekke, A.-G., Hong, Y.-D., Kjeld, P.C., Koide, H., Lear, G., Tarasick, D., Ueno, M., Wallasch, M., Baumgardner, D., Chuang, M.-T., Gillett, R., Lee, M., Molloy, S., Moolla, R., Wang, T., Sharps, K., Adame, J.A., Ancellet, G., Apadula, F., Artaxo, P., Barlasina, M.E., Bogucka, M., Bonasoni, P., Chang, L., Colomb, A., Cuevas-Agulló, E., Cupeiro, M., Degorska, A., Ding, A., Fröhlich, M., Frolova, M., Gadhavi, H., Gheusi, F., Gilge, S., Gonzalez, M.Y., Gros, V., Hamad, S.H., Helmig, D., Henriques, D., Hermansen, O., Holla, R., Hueber, J., Im, U., Jaffe, D.A., Komala, N., Kubistin, D., Lam, K.-S., Laurila, T., Lee, H., Levy, I., Mazzoleni, C., Mazzoleni, L.R., McClure-Begley, A., Mohamad, M., Murovec, M., Navarro-Comas, M., Nicodim, F., Parrish, D., Read, K.A., Reid, N., Ries, L., Saxena, P., Schwab, J.J., Scorgie, Y., Senik, I., Simmonds, P., Sinha, V., Skorokhod, A.I., Spain, G., Spangl, W., Spoor, R., Springston, S.R., Steer, K., Steinbacher, M., Suharguniyawan, E., Torre, P., Trickl, T., Weili, L., Weller, R., Xu, X., Xue, L., Zhiqiang, M., 2017. Tropospheric Ozone Assessment Report, links to Global surface ozone datasets. Suppl. to Schultz, MG al. Tropospheric Ozone Assess. Rep. Database Metrics Data Glob. Surf. Ozone Obs. Elem. - Sci. Anthr. 558, 26 pp, https//doi.org/10.1525/elementa.244. https://doi.org/10.1594/PANGAEA.876108

Agência Portuguesa do Ambiente, 2011. Avaliação dos Níveis de Ozono no Ar Ambiente em Portugal. Amadora.

Agência Portuguesa do Ambiente, 2009. Avaliação dos Níveis de Ozono no Ar Ambiente em Portugal. Amadora.

Ainsworth, E., Yendrek, C.R., Sitch, S., Collins, W.J., Emberson, L.D., 2012. The effects of tropospheric ozone on net primary productivity and implications for climate change. Annu. Rev. Plant Biol. 63, 637–61. https://doi.org/10.1146/annurev-arplant-042110-103829

Alebic-Juretic, A., Bokan-Vucelic, I., Mifka, B., Zatezalo, M., Zubak, V., 2017. Impact of Ozone Gradient on Grapevine Leaves, in: Proceedings of the 19th EGU General Assembly, Vienna, Austria, 23–28 April 2017; p. 5660.

Allen, R.G., Pereira, L.S., Raes, D., Smith, M., 1998. Crop evapotranspiration (guidelines for computing crop water requirements)., FAO and drainage paper 56. Rome.

Alonso, R., Elvira, S., Sanz, M.J., Gerosa, G., Emberson, L.D., Bermejo, V., Gimeno, B.S., 2008. Sensitivity analysis of a parameterization of the stomatal component of the DO3SE model for Quercus ilex to estimate ozone fluxes. Environ. Model. Softw. 155, 473–480. https://doi.org/10.1016/j.envpol.2008.01.032

Alves, F., Edlmann, M., Costa, J., Costa, P., Macedo, P., Leal Da Costa, P., Symington, C., 2013. Heat requirements and lenght of phenological stages. Effects of rootstock on red grape varieties at Douro region., in: 18th International Symposium GIESCO, Porto, Portugal, 7-11, July 2013.

Anav, A., De Marco, A., Proietti, C., Alessandri, A., Dell'Aquila, A., Cionni, I., Friedlingstein, P., Khvorostyanov, D., Menut, L., Paoletti, E., Sicard, P., Sitch, S., Vitale, M., 2016. Comparing concentration-based (AOT40) and stomatal uptake (PODY) metrics for ozone risk assessment to European forests. Glob. Chang. Biol. 22, 1608–1627. https://doi.org/10.1111/gcb.13138

Anav, A., Proietti, C., Paoletti, E., Menut, L., Carnicelli, S., De, M., 2018. Sensitivity of stomatal conductance to soil moisture: Implications for tropospheric ozone. Atmos. Chem. Phys. 18, 5747–5763. https://doi.org/10.5194/acp-18-5747-2018

Anderson, J.D., Jones, G. V., Tait, A., Hall, A., Trought, M.C.T., 2012. Analysis of viticulture region climate structure and suitability in New Zealand. J. Int. des Sci. la Vigne du Vin 46, 149–165.

Andrade, C., Fonseca, A., Santos, J.A., 2021. Are land use options in viticulture and oliviculture in agreement with bioclimatic shifts in portugal? Land 10, 869. https://doi.org/10.3390/land10080869

Andrews, T., Gregory, J.M., Webb, M.J., Taylor, K.E., 2012. Forcing, feedbacks and climate sensitivity in CMIP5 coupled atmosphere-ocean climate models. Geophys. Res. Lett. 39, 1–7. https://doi.org/10.1029/2012GL051607

Antivilo, F.G., Paz, R.C., Keller, M., Borgo, R., Tognetti, J., Juñent, F.R., 2017. Macro- and microclimate conditions may alter grapevine deacclimation: variation in thermal amplitude in two contrasting wine regions from North and South America. Int. J. Biometeorol. 61, 2033–2045. https://doi.org/10.1007/s00484-017-1400-7

Associação para o Desenvolvemento da Viticultura Duriense (ADVID), 2017. Boletím 14-17. Ano Vitícola 2017. Balanço final. Vila Real.

Avnery, S., Mauzerall, D.L., Liu, J., Horowitz, L.W., 2011a. Global crop yield reductions due to surface ozone exposure: 1. Year 2000 crop production losses and economic damage. Atmos. Environ. 45, 2284–2296. https://doi.org/10.1016/j.atmosenv.2010.11.045

Avnery, S., Mauzerall, D.L., Liu, J., Horowitz, L.W., 2011b. Global crop yield reductions due to surface ozone exposure: 2. Year 2030 potential crop production losses and economic damage under two scenarios of O3 pollution. Atmos. Environ. 45, 2297–2309. https://doi.org/10.1016/j.atmosenv.2011.01.002

Barreales, D., Verdial, J., Feliciano, M., Castro, J., Rodrigues, M., Blanco-ward, D., Ribeiro, A.C., 2018. Effect of deficit irrigation in the cultivars Touriga Nacional and Touriga Franca (Vitis vinifera L .), in: XIIth International Terroir Congress, Zaragoza, Spain. 18th-22nd of June 2018.

Bassin, S., Volk, M., Fuhrer, J., 2007. Factors affecting the ozone sensitivity of temperate European grasslands: An overview. Environ. Pollut. 146, 678–691.

https://doi.org/10.1016/j.envpol.2006.06.010

Bermejo Bermejo, V., Alonso del Amo, R., Elvira Cozar, S., Rábago Juan-Aracil, I., García Vivanco, M., 2009. El ozono troposférico y sus efectos en la vegetación. Ministerio de Medio Ambiente, y Medio Rural y Marino (MARM) y el Centro de Investigaciones, Energéticas Medioambientales y Tecnológicas (CIEMAT), Madrid.

Bernardo, S., Dinis, L.-T., Machado, N., Moutinho-Pereira, J., 2018. Grapevine abiotic stress assessment and search for sustainable adaptation strategies in Mediterranean-like climates. A review. Agron. Sustain. Dev. 38:66. https://doi.org/10.1007/s13593-018-0544-0

Biswas, D.K., Jiang, G.M., 2011. Differential drought-induced modulation of ozone tolerance in winter wheat species 62, 4153–4162. https://doi.org/10.1093/jxb/err104

Blanco-Ward, D., Queijeiro, J.M.G., Jones, G. V, 2007. Spatial climate variability and viticulture in the Mino River Valley of Spain. Vitis 46, 63–70.

Blanco-Ward, D., Ribeiro, A., Paoletti, E., Miranda, A.I., 2021a. Assessment of tropospheric ozone phytotoxic effects on the grapevine (Vitis vinifera L.): a review. Atmos. Environ. 244, 117924. https://doi.org/https://doi.org/10.1016/j.atmosenv.2020.117924

Blanco-Ward, D., Rocha, A., Viceto, C., Ribeiro, A.C., Feliciano, M., Paoletti, E., Miranda, A.I., 2021b. Validation of meteorological and ground-level ozone WRF-CHIMERE simulations in a mountainous grapevine growing area for phytotoxic risk assessment. Atmos. Environ. 259, 118507. https://doi.org/10.1016/j.atmosenv.2021.118507

Blanco-Ward, D., Monteiro, A., Lopes, M., Borrego, C., Silveira, C., Viceto, C., Rocha, A., Ribeiro, A., Andrade, J., Feliciano, M., Castro, J., Barreales, D., Neto, J., Carlos, C., Peixoto, C., Miranda, A., 2019. Climate change impact on a wine-producing region using a dynamical downscaling approach: Climate parameters, bioclimatic indices and extreme indices. Int. J. Climatol. 39, 5741–5760. https://doi.org/10.1002/joc.6185

Bonhomme, R., 2000. Bases and limits to using “degree.day” units. Eur. J. Agron. 13, 1–10.

Booker, F., Muntifering, R., McGrath, M., Burkey, K., Decoteau, D., Fiscus, E., Manning, W., Krupa, S., Chappelka, A., Grantz, D., 2009. The Ozone Component of Global Change: Potential Effects on Agricultural and Horticultural Plant Yield, Product Quality and Interactions with Invasive Species. J. Integr. Plant Biol. 51, 337–351. https://doi.org/10.1111/j.1744-7909.2008.00805.x

Borrego, C., Monteiro, A., Ferreira, J., Miranda, A.I., Costa, A.M., Carvalho, A.C., Lopes, M., 2008. Procedures for estimation of modelling uncertainty in air quality assessment. Environ. Int. 34, 613–620. https://doi.org/10.1016/j.envint.2007.12.005

Boulard, D., Castel, T., Camberlin, P., Sergent, A.-S., Bréda, N., Vincent, B., Rossi, A., Pohl, B., 2016. Capability of a regional climate model to simulate climate variables requested for water balance computation: a case study over northeastern France. Clim. Dyn. 46, 2689–2716. https://doi.org/10.1007/s00382-015-2724-9

Brewer, R.F., Ashcroft, R., 1983. The effects of ambient air pollution on Thompson seedless grapes. Parlier.

Britvec, M., Reichenauer, T., Soja, G., Ljubesic, N., Elu, M., Pecina, M., 2001. Ultrastructure changes in grapevine chloroplasts caused by increased tropospheric ozone concentrations. Biol. 56, 417–424.

Büker, P., Emberson, L.D., Ashmore, M.R., Cambridge, H.M., Jacobs, C.M.J., Massman, W.J., Müller, J., Nikolov, N., Novak, K., Oksanen, E., Schaub, M., de la Torre, D., 2007. Comparison of different stomatal conductance algorithms for ozone flux modelling. Environ. Pollut. 146, 726–735. https://doi.org/10.1016/j.envpol.2006.04.007

Büker, P., Morrissey, T., Briolat, A., Falk, R., Simpson, D., Tuovinen, J.P., Alonso, R., Barth, S., Baumgarten, M., Grulke, N., Karlsson, P.E., King, J., Lagergren, F., Matyssek, R., Nunn, A., Ogaya, R., Pẽuelas, J., Rhea, L., Schaub, M., Uddling, J., Werner, W., Emberson, L.D., 2012. DO3SE modelling of soil moisture to determine ozone flux to forest trees. Atmos. Chem. Phys. 12, 5537–5562. https://doi.org/10.5194/acp-12-5537-2012

Burney, J., Ramanathan, V., 2014. Recent climate and air pollution impacts on Indian agriculture. Proc. Natl. Acad. Sci. U. S. A. 111, 16319–16324. https://doi.org/10.1073/pnas.1317275111

Caetano, M., Nunes, V., Nunes, A., 2009. Corine Land Cover 2006 for Continental Portugal, Relatorio técnico, Instituto Geográfico Portugués.

Carbonneau, A., Deloire, A., Costanza, P., 2004. Leaf water potential: meaning of different modalities of measurements. J. Int. des Sci. la Vigne du Vin 38, 15–19. https://doi.org/10.20870/oeno-one.2004.38.1.928

Carbonneau, A., Riou, C., Guyon, D., Riom, J., Schneider, C., 1992. Agrometeorologie de la vigne en France. Luxembourg.

Carvalho, A., Monteiro, A., Ribeiro, I., Tchepel, O., Miranda, A.I., Borrego, C., Saavedra, S., Souto, J.A., Casares, J.J., 2010. High ozone levels in the northeast of Portugal: Analysis and characterization. Atmos. Environ. 44, 1020–1031. https://doi.org/10.1016/j.atmosenv.2009.12.020

Carvalho, D., Rocha, A., Gómez-Gesteira, M., Santos, C., 2012. A sensitivity study of the WRF model in wind simulation for an area of high wind energy. Environ. Model. Softw. 33, 23–34. https://doi.org/10.1016/j.envsoft.2012.01.019

Cho, K., Tiwari, S., Agrawal, S.B., Torres, N.L., Agrawal, M., Sarkar, A., Shibato, J., Agrawal, G.K., Kubo, A., Rakwal, R., 2011. Tropospheric ozone and plants: Absorption, responses, and consequences. Rev. Environ. Contam. Toxicol. 212, 61–111. https://doi.org/10.1007/978-1-4419-8453-1_3

Cieslik, S., 2009. Ozone fluxes over various plant ecosystems in Italy: A review. Environ. Pollut. 157, 1487–1496. https://doi.org/10.1016/j.envpol.2008.09.050

Cifre, J., Bota, J., Escalona, J.M., Medrano, H., Flexas, J., 2005. Physiological tools for irrigation scheduling in grapevine (Vitis vinifera L.): An open gate to improve water-

use efficiency? Agric. Ecosyst. Environ. 106, 159–170. https://doi.org/10.1016/j.agee.2004.10.005

Climaco, P., Ricardo-da-Silva, J., Laureano, O., Tonietto, J., 2012. O clima vitícola das principais regiões produtoras de uvas para vinho de Portugal., in: Tonietto, J; Sotés Ruiz, V.; Gómez-Migues, V. (Ed.), Clima, Zonificación, y Tipicidad Del Vino En Regiones Vitivinícolas Iberoamericanas. Programa Iberoamericano de Ciencia y Tecnología para el Desarrollo (CYTED), Madrid, pp. 315–357.

CLRTAP, 2017a. Mapping Critical Levels for Vegetation, Chapter III, Manual on Methodologies and Criteria for Modelling and Mapping Critical Loads and Levels and Air Pollution Effects, Risks and Trends. Bangor.

CLRTAP, 2017b. Supplement of Chapter III (Mapping critical levels for vegetation), Manual on Methodologies and Criteria for Modelling and Mapping Critical Loads and Levels and Air Pollution Effects, Risks and Trends. Bangor.

CLRTAP, 2017c. Developing areas of research of relevance to chapter III (Mapping critical levels for vegetation) of the modelling and mapping manual of the LRTAP convention. Scientific background document B. Bangor.

CLRTAP, 2014. Guidance on mapping concentrations levels and deposition levels, Chapter II, in: Manual on Methodologies and Criteria for Modelling and Mapping Critical Loads and Levels and Air Pollution Effects, Risks and Trends. Bangor, pp. 1–33.

Corte-Real, A., 2014. Analyzing the influence of the Douro valley weather on the quality and yield of vintage Port. PhD. dissertation. University of Porto.

Corte-Real, A., Borges, J., Cabral, J.S., Jones, G. V., 2015. Partitioning the grapevine growing season in the Douro Valley of Portugal: accumulated heat better than calendar dates. Int. J. Biometeorol. 59, 1045–1059. https://doi.org/10.1007/s00484-014-0918-1

Corte-Real, A., Borges, J., S. Cabral, J., V. Jones, G., 2016. A climatology of Vintage Port quality. Int. J. Climatol. https://doi.org/10.1002/joc.4953

Cristofanelli, P., Bonasoni, P., 2009. Background ozone in the southern Europe and Mediterranean area: Influence of the transport processes. Environ. Pollut. 157, 1399–1406. https://doi.org/10.1016/j.envpol.2008.09.017

Dairies, R.H., Brennan, E., Leone, I.A., 1982. Air pollution, plant response and productivity, in: Miloslav Rechcigl (Ed.), Handbook of Agricultural Productivity. CRC Press, Boca Raton, pp. 375–399. https://doi.org/https://doi.org/10.1201/9781351072878

De Andrés, J.M., Borge, R., De La Paz, D., Lumbreras, J., Rodríguez, E., 2012. Implementation of a module for risk of ozone impacts assessment to vegetation in the Integrated Assessment Modelling system for the Iberian Peninsula. Evaluation for wheat and Holm oak. Environ. Pollut. 165, 25–37. https://doi.org/10.1016/j.envpol.2012.01.048

De Marco, A., Proietti, C., Anav, A., Ciancarella, L., D'Elia, I., Fares, S., Fornasier, M.F., Fusaro, L., Gualtieri, M., Manes, F., Marchetto, A., Mircea, M., Paoletti, E., Piersanti,

A., Rogora, M., Salvati, L., Salvatori, E., Screpanti, A., Vialetto, G., Vitale, M., Leonardi, C., 2019. Impacts of air pollution on human and ecosystem health, and implications for the National Emission Ceilings Directive: Insights from Italy. Environ. Int. 125, 320–333. https://doi.org/10.1016/j.envint.2019.01.064

De Marco, A., Screpanti, A., Paoletti, E., 2010. Geostatistics as a validation tool for setting ozone standards for durum wheat. Environ. Pollut. 158, 536–542. https://doi.org/10.1016/j.envpol.2009.08.006

De Marco, A., Sicard, P., Fares, S., Tuovinen, J.-P., Anav, A., Paoletti, E., 2016. Assessing the role of soil water limitation in determining the Phytotoxic Ozone Dose (PODY) thresholds. Atmos. Environ. 147, 88–97. https://doi.org/10.1016/j.atmosenv.2016.09.066

Decoteau, D.R., Marini, R.P., Davis, D.D., 2019. Influence of Ambient Ozone on Grape Cultivars ' Chambourcin ' and ' Vidal ' in. J. Plant Sci. Res. 6, 1–5.

Dee, D.P., Uppala, S.M., Simmons, A.J., Berrisford, P., Poli, P., Kobayashi, S., Andrae, U., Balmaseda, M.A., Balsamo, G., Bauer, P., Bechtold, P., M Beljaars, A.C., van de Berg, L., Bidlot, J., Bormann, N., Delsol, C., Dragani, R., Fuentes, M., Geer, A.J., Haimberger, L., Healy, S.B., Hersbach, H., olm, E. V, Isaksen, L., Kållberg, P., Köhler, M., Matricardi, M., McNally, A.P., Monge-Sanz, B.M., Morcrette, J., Park, B., Peubey, C., de Rosnay, P., Tavolato, C., Thépaut, J., Vitart, F., Acm, B., de Berg, van L., J-j, M., B-k, P., Rosnay, de P., 2011. The ERA-Interim reanalysis: configuration and performance of the data assimilation system. Q. J. R. Meteorol. Soc. Q. J. R. Meteorol. Soc 137, 553–597. https://doi.org/10.1002/qj.828

Deloire, A., Vaudour, E., Carey, V., Bonnardot, V., van Leeuwen, C., 2005. Grapevine responses to terroir: A global approach. J. Int. des Sci. la Vigne du Vin 39, 149–162. https://doi.org/10.20870/oeno-one.2005.39.4.888

Emberson, L., Büker, P., Ashmore, M., Mills, G., Jackson, L., Agrawal, M., Cinderby, S., Engardt, M., Jamir, C., Kobayashi, K., Oanh, N., Quadir, Q., Wahid, A., 2009. A comparison of North American and Asian exposure–response data for ozone effects on crop yields. Atmos. Environ. 43, 1945–1953. https://doi.org/10.1016/j.atmosenv.2009.01.005

Emberson, L.D., Ashmore, M.R., Cambridge, H.M., Simpson, D., Tuovinen, J.-P., 2000a. Modelling stomatal ozone flux across Europe. Environ. Pollut. 109, 403–413. https://doi.org/10.1016/S0269-7491(00)00043-9

Emberson, L.D., Massman, W.J., Büker, P., Soja, G., van De Sand, I., Mills, G., Jacobss, C., 2005. The development, evaluation and application of O3 flux and flux-response models for additional agricultural crops, in: Wieser, G., M.T. (Ed.), Proceedings on the Workshop "Critical Levels of Ozone: Further Applying and Developing the Flux-Based Concept." Obergurgl, pp. 220–225.

Emberson, L.D., Simpson, D., Tuovinen, J.-P., Ashmore, M.R., Cambridge, H.M., 2000b. Towards a model of ozone deposition and stomatal uptake over Europe. Norwegian Meteorological Institute, Oslo.

EMEP Status Report 1/2019, 2019. Transboundary particulate matter, photo-oxidants, acidifying and eutrophying components. Oslo.

Emery, C., Liu, Z., Russell, A.G., Odman, M.T., Yarwood, G., Kumar, N., 2017. Recommendations on statistics and benchmarks to assess photochemical model performance. J. Air Waste Manag. Assoc. 67, 582–598. https://doi.org/10.1080/10962247.2016.1265027

EPA, 1996. Environmental effects of ozone and related photochemical oxidants, Chapter V, in: Air Quality Criteria for Ozone and Related Photochemical Oxidants. Washington, pp. 5.1-5.349.

Fagnano, M., Maggio, A., Fumagalli, I., 2009. Crops' responses to ozone in Mediterranean environments. Environ. Pollut. 157, 1438–1444. https://doi.org/10.1016/j.envpol.2008.09.001

Falloon, P., Betts, R., 2009. Climate impacts on European agriculture and water management in the context of adaptation and mitigation—The importance of an integrated approach. Sci. Total Environ. 408, 5667–5687. https://doi.org/10.1016/j.scitotenv.2009.05.002

Feng, Z., De Marco, A., Anav, A., Gualtieri, M., Sicard, P., Tian, H., Fornasier, F., Tao, F., Guo, A., Paoletti, E., 2019. Economic losses due to ozone impacts on human health, forest productivity and crop yield across China. Environ. Int. 131, 104966. https://doi.org/10.1016/j.envint.2019.104966

Feng, Z., Xu, Y., Kobayashi, K., Dai, L., Zhang, T., Agathokleous, E., Calatayud, V., Paoletti, E., Mukherjee, A., Agrawal, M., Park, R.J., Oak, Y.J., Yue, X., 2022. Ozone pollution threatens the production of major staple crops in East Asia. Nat. Food 3, 47–56. https://doi.org/10.1038/s43016-021-00422-6

Ferretti, M., Fagnano, M., Amoriello, T., Badiani, M., Ballarin-Denti, A., Buffoni, A., Bussotti, F., Castagna, A., Cieslik, S., Costantini, A., De Marco, A., Gerosa, G., Lorenzini, G., Manes, F., Merola, G., Nali, C., Paoletti, E., Petriccione, B., Racalbuto, S., Rana, G., Ranieri, A., Tagliaferri, A., Vialetto, G., Vitale, M., 2007. Measuring, modelling and testing ozone exposure, flux and effects on vegetation in southern European conditions—What does not work? A review from Italy. Environ. Pollut. 146, 648–658. https://doi.org/10.1016/j.envpol.2006.05.012

Fiore, A.M., Dentener, F.J., Wild, O., Cuvelier, C., Schultz, M.G., Hess, P., Textor, C., Schulz, M., Doherty, R.M., Horowitz, L.W., MacKenzie, I.A., Sanderson, M.G., Shindell, D.T., Stevenson, D.S., Szopa, S., van Dingenen, R., Zeng, G., Atherton, C., Bergmann, D., Bey, I., Carmichael, G., Collins, W.J., Duncan, B.N., Faluvegi, G., Folberth, G., Gauss, M., Gong, S., Hauglustaine, D., Holloway, T., Isaksen, I.S.A., Jacob, D.J., Jonson, J.E., Kaminski, J.W., Keating, T.J., Lupu, A., Marmer, E., Montanaro, V., Park, R.J., Pitari, G., Pringle, K.J., Pyle, J.A., Schroeder, S., Vivanco, M.G., Wind, P., Wojcik, G., Wu, S., Zuber, A., 2009. Multimodel estimates of intercontinental source-receptor relationships for ozone pollution. J. Geophys. Res. 114, D04301. https://doi.org/10.1029/2008JD010816

Fiscus, E.L., Booker, F.L., Burkey, K.O., 2005. Crop responses to ozone: Uptake, modes of action, carbon assimilation and partitioning. Plant, Cell Environ. 28, 997–1011. https://doi.org/10.1111/j.1365-3040.2005.01349.x

Flexas, J., Medrano, H., 2002. Drought-inhibition of photosynthesis in C3 plants: Stomatal and non-stomatal limitations revisited. Ann. Bot. 89, 183–189. https://doi.org/10.1093/aob/mcf027

Fortems-Cheiney, A., Foret, G., Siour, G., Vautard, R., Szopa, S., Dufour, G., Colette, A., Lacressonniere, G., Beekmann, M., 2017. A 3 °C global RCP8.5 emission trajectory cancels benefits of European emission reductions on air quality. Nat. Commun. 8, 89. https://doi.org/10.1038/s41467-017-00075-9

Fraga, H., García de Cortázar Atauri, I., Malheiro, A.C., Moutinho-Pereira, J., Santos, J.A., 2017. Viticulture in Portugal: A review of recent trends and climate change projections. OENO One 51, 61. https://doi.org/10.20870/oeno-one.2016.0.0.1621

Fraga, H., García de Cortázar Atauri, I., Malheiro, A.C., Santos, J.A., 2016. Modelling climate change impacts on viticultural yield, phenology and stress conditions in Europe. Glob. Chang. Biol. 22, 3774–3788. https://doi.org/10.1111/gcb.13382

Fraga, H., García de Cortázar Atauri, I., Santos, J.A., 2018. Viticultural irrigation demands under climate change scenarios in Portugal. Agric. Water Manag. 196. https://doi.org/10.1016/j.agwat.2017.10.023

Fraga, H., Malheiro, A.C., Moutinho-Pereira, J., Jones, G. V., Alves, F., Pinto, J.G., Santos, J.A., 2014. Very high resolution bioclimatic zoning of Portuguese wine regions: present and future scenarios. Reg. Environ. Chang. 14, 295–306. https://doi.org/10.1007/s10113-013-0490-y

Fraga, H., Pinto, J.G., Santos, J.A., 2019. Climate change projections for chilling and heat forcing conditions in European vineyards and olive orchards: a multi-model assessment. Clim. Change 152, 179–193. https://doi.org/10.1007/s10584-018-2337-5

Fraga, H., Santos, J.A., 2017. Daily prediction of seasonal grapevine production in the Douro wine region based on favourable meteorological conditions. Aust. J. Grape Wine Res. Apr, 1–9. https://doi.org/10.1111/ajgw.12278

Fumagalli, I., Cieslik, S., De Marco, A., Proietti, C., Paoletti, E., 2019. Grapevine and Ozone: Uptake and Effects. Climate 7, 140. https://doi.org/10.3390/cli7120140

Fumagalli, I., Gimeno, B.S., Velissariou, D., De Temmerman, L., Mills, G., 2001. Evidence of ozone-induced adverse effects on crops in the Mediterranean region. Atmos. Environ. 35, 2583–2587. https://doi.org/10.1016/S1352-2310(00)00468-4

Gaudin, R., Roux, S., Tisseyre, B., 2017. Linking the transpirable soil water content of a vineyard to predawn leaf water potential measurements. Agric. Water Manag. 182, 13–23. https://doi.org/10.1016/j.agwat.2016.12.006

Geng, Q., Xing, H., Sun, Y., Hao, G., Zhai, H., Du, Y., 2017. Analysis of the interaction effects of light and O3 on fluorescence properties of 'Cabernet Sauvignon' grapes

based on response surface methodology. Sci. Hortic. (Amsterdam). 225, 599–606. https://doi.org/10.1016/J.SCIENTA.2017.07.030

Gerosa, G., Anfodillo, T., 2003. Modelling stomatal uptake of ozone: data requirements and applicability to the CONECOFOR PMPs in Italy. Ann. Ist. Sper. Selv. 30, 85–98.

Gerosa, G., Vitale, M., Finco, A., Manes, F., Denti, A.B., Cieslik, S., 2005. Ozone uptake by an evergreen Mediterranean Forest (Quercus ilex) in Italy. Part I: Micrometeorological flux measurements and flux partitioning. Atmos. Environ. 39, 3255–3266. https://doi.org/10.1016/j.atmosenv.2005.01.056

Giorgetta, M.A., Jungclaus, J.H., Reick, C.H., Legutke, S., Bader, J., Böttinger, M., Brovkin, V., Crueger, T., Esch, M., Fieg, K., Glushak, K., Gayler, V., Haak, H., Hollweg, H.-D., Ilyina, T., Kinne, S., Kornblueh, L., Matei, D., Mauritsen, T., Mikolajewicz, U., Mueller, W., Notz, D., Pithan, F., Raddatz, T., Rast, S., Redler, R., Roeckner, E., Schmidt, H., Schnur, R., Segschneider, J., Six, K.D., Stockhause, M., Timmreck, C., Wegner, J., Widmann, H., Wieners, K.-H., Claussen, M., Marotzke, J., Stevens, B., 2013. Climate and carbon cycle changes from 1850 to 2100 in MPI-ESM simulations for the coupled model intercomparison project phase 5. J. Adv. Model. Earth Syst. 5, 572–597. https://doi.org/10.1002/jame.20038

González-Fernández, I., Calvo, E., Gerosa, G., Bermejo, V., Marzuoli, R., Calatayud, V., Alonso, R., 2014. Setting ozone critical levels for protecting horticultural Mediterranean crops: Case study of tomato. Environ. Pollut. 185, 178–187. https://doi.org/10.1016/j.envpol.2013.10.033

Grantz, D.A., Paudel, R., Vu, H., Shrestha, A., Grulke, N., 2016. Diel trends in stomatal response to ozone and water deficit: a unique relationship of midday values to growth and allometry in Pima cotton? 18, 37–46. https://doi.org/10.1111/plb.12355

Gravano, E., Giulietti, V., Desotgiu, R., Bussotti, F., Grossoni, P., Gerosa, G., Tani, C., 2003. Foliar response of an Ailanthus altissima clone in two sites with different levels of ozone-pollution. Environ. Pollut. 121, 137–146. https://doi.org/10.1016/S0269-7491(02)00180-X

Griesser, M., Weingart, G., Schoedl-Hummel, K., Neumann, N., Becker, M., Varmuza, K., Liebner, F., Schuhmacher, R., Forneck, A., 2015. Severe drought stress is affecting selected primary metabolites, polyphenols, and volatile metabolites in grapevine leaves (Vitis vinifera cv. Pinot noir). Plant Physiol. Biochem. 88, 17–26. https://doi.org/10.1016/j.plaphy.2015.01.004

Gudmundsson, L., Bremnes, J.B., Haugen, J.E., Engen-Skaugen, T., 2012. Technical Note: Downscaling RCM precipitation to the station scale using statistical transformations - a comparison of methods. Hydrol. Earth Syst. Sci. 16, 3383–3390. https://doi.org/10.5194/hess-16-3383-2012

Guerreiro, C.B.B., Foltescu, V., de Leeuw, F., 2014. Air quality status and trends in Europe. Atmos. Environ. 98, 376–384. https://doi.org/10.1016/j.atmosenv.2014.09.017

Guilpart, N., Metay, A., Gary, C., 2014. Grapevine bud fertility and number of berries per bunch are determined by water and nitrogen stress around flowering in the previous

year. Eur. J. Agron. 54, 9–20. https://doi.org/10.1016/j.eja.2013.11.002

Hannah, L., Roehrdanz, P.R., Ikegami, M., Shepard, A. V, Shaw, M.R., Tabor, G., Zhi, L., Marquet, P.A., Hijmans, R.J., 2013. Climate change, wine, and conservation. Proc. Natl. Acad. Sci. U. S. A. 110, 6907–6912. https://doi.org/10.1073/pnas.1210127110

Hargreaves, G.H., Asce, F., Allen, R.G., 2003. History and Evaluation of Hargreaves Evapotranspiration Equation. J. Irrig. Drain Eng. 129, 53–63. https://doi.org/10.1061/ASCE0733-94372003129:153

Hayes, F., Mills, G., Harmens, H., Norris, D., 2007. Evidence of Widespread Ozone Damage to Vegetation in Europe (1990-2006). Programme Coordination Centre for the ICP Vegetation. Bangor.

Haylock, M.R., Hofstra, N., Klein Tank, A.M.G., Klok, E.J., Jones, P.D., New, M., 2008. A European daily high-resolution gridded data set of surface temperature and precipitation for 1950–2006. J. Geophys. Res 113, D20119. https://doi.org/10.1029/2008JD010201

Hidalgo, L., 1980. Caracterización macrofísica del ecosistema medio-planta en los viñedos españoles. Comun. INIA. Ser. Prod. Veg. 29, 5-255,.

Hochberg, U., Degu, A., Toubiana, D., Gendler, T., Nikoloski, Z., Rachmilevitch, S., Fait, A., 2013. Metabolite profiling and network analysis reveal coordinated changes in grapevine water stress response. BMC Plant Biol. 13:184. https://doi.org/10.1186/1471-2229-13-184

Holland, M., Mills, G., Hayes, F., Buse, A., Emberson, L., Cambridge, H., Cinderby, S., Terry, A., Ashmore, M., 2002. Economic Assessment of Crop Yield Losses from Ozone Exposure. Gwynedd.

Hong, C., Mueller, N.D., Burney, J.A., Zhang, Y., AghaKouchak, A., Moore, F.C., Qin, Y., Tong, D., Davis, S.J., 2020. Impacts of ozone and climate change on yields of perennial crops in California. Nat. Food 1, 166–172. https://doi.org/10.1038/s43016-020-0043-8

Huglin, P., 1986. Biologie et Ecologie de la Vigne. Lausanne.

IPCC (International Panel on Climate Change), 2014. Chapter 4 Terrestrial and Inland Water Systems., in: Field, C.B., V.R. Barros, D.J. Dokken, K.J. Mach, M.D. Mastrandrea, T.E. Bilir, M. Chatterjee, K.L. Ebi, Y.O. Estrada, R.C. Genova, B. Girma, E.S. Kissel, A.N. Levy, S. MacCracken, P.R. Mastrandrea, and White, L.L. (Eds.) Climate Change 2014: Impacts, Ada. Cambridge, United Kingdom and New York, NY: Cambridge University Press, pp. 271–359.

IPCC (International Panel on Climate Change), 2013. Climate Change 2013: the Physical Science Basis. Summary for Polycymakers., in: In: Stocker,T.F., D. Qin, G.-K. Plattner, M. Tignor, S.K. Allen, J. Boschung, A. Nauels, Y. Xia, V. Bex and P.M. Midgley (Eds.) Climate Change 2013: The Physical Science Basis. Contribution of Working Group I to the Fifth Assessment Report of the Intergov. Cambridge, United Kingdom and New York, NY: Cambridge University Press, pp. 3–29.

IPPC (International Panel on climate Change), 2013. Climate Change 2013. The Physical Science Basis. Contribution of Working Group I to the Fifth Assessment Report of the Intergovernmental Panel on Climate Change . Cambridge University Press, Cambridge, United Kingdom and New York, NY, USA.

IVDP (Instituto dos Vinhos do Douro e Porto), 2017a. Areas dedicated to grapevine cultivation. Statistics for the year 2016. [WWW Document]. URL https://www.ivdp.pt (accessed 4.18.17).

IVDP (Instituto dos Vinhos do Douro e Porto), 2017b. Wine production. Statistics for the 2016 year [WWW Document]. URL https//www.ivdp.pt (accessed 4.18.17).

IVV, 2018. Vinhos e Aguardentes de Portugal 2018 Anuário, Vinhos E Aguardentes Em Portugal. Ministério da Agricultura, do Desenvolvimento Rural e das Pescas: Instituto da Vinha e do Vinho, Lisboa.

IVV, 2017. Vinhos e Aguardentes de Portugal 2017 Anuário. Ministério da Agricultura, do Desenvolvimento Rural e das Pescas: Instituto da Vinha e do Vinho, Lisboa.

Jackson, R.S., 2008. Wine science: principles and applications., Third edit. ed. Elsevier, San Diego.

Jacob, D.J., Winner, D.A., 2009. Effect of climate change on air quality. Atmos. Environ. 43, 51–63. https://doi.org/10.1016/j.atmosenv.2008.09.051

Jiménez, P.A., Dudhia, J., González-Rouco, J.F., Montávez, J.P., García-Bustamante, E., Navarro, J., Vilà-Guerau De Arellano, J., Muñoz-Roldán, A., 2013. An evaluation of WRF's ability to reproduce the surface wind over complex terrain based on typical circulation patterns. J. Geophys. Res. Atmos. 118, 7651–7669. https://doi.org/10.1002/jgrd.50585

Jolivet, Y., Bagard, M., Cabané, M., Vaultier, M., Gandin, A., Afif, D., Dizengremel, P., Thiec, D. Le, 2016. Deciphering the ozone-induced changes in cellular processes : a prerequisite for ozone risk assessment at the tree and forest levels. Ann. For. Sci. 923–943. https://doi.org/10.1007/s13595-016-0580-3

Jones, G., 2013. Uma Avaliação do Clima para a Região Demarcada do Douro : Uma análise das condições climáticas do passado , presente e futuro para a produção de vinho. Peso da Régua.

Jones, G. V., Alves, F., 2012. Impact of climate change on wine production: a global overview and regional assessment in the Douro Valley of Portugal. Int. J. Glob. Warm. 4, 383–406.

Jones, G. V., Andrew, D.A., Hall, A., Myers, J.W., 2010. Spatial Analysis of Climate in Winegrape Growing Regions in the Western United States. Am. J. Enol. Vitic. 61, 313–326.

Jones, G. V., White, M.A., Cooper, O.R., Storchmann, K., 2005. Climate change and global wine quality. Clim. Change 73, 319–343. https://doi.org/10.1007/s10584-005-4704-2

Karlsson, P.E., Uddling, J., Braun, S., Broadmeadow, M., Elvira, S., Gimeno, B.S., Le Thiec, D., Oksanen, E., Vandermeiren, K., Wilkinson, M. & Emberson, L., 2003. New critical

levels for ozone impact on trees based on AOT40 and leaf cumulated uptake of ozone., in: Karlsson, P.E., Selldén, G. & Pleijel, H. (Eds.), Establishing Ozone Critical Levels II. IVL, Publikationsservice, Gothenburg, pp. 236–250.

Katragkou, E., Zanis, P., Kioutsioukis, I., Tegoulias, I., Melas, D., Krüger, B.C., Coppola, E., 2011. Future climate change impacts on summer surface ozone from regional climate-air quality simulations over Europe. J. Geophys. Res. Atmos. 116, 1–14. https://doi.org/10.1029/2011JD015899

Klingberg, J., Engardt, M., Karlsson, P.E., Langner, J., Pleijel, H., 2014. Declining ozone exposure of European vegetation under climate change and reduced precursor emissions. Biogeosciences 11, 5269–5283. https://doi.org/10.5194/bg-11-5269-2014

Krupa, S., Mcgrath, M.T., Andersen, C.P., Booker, F.L., Burkey, K.O., Chappelka, A.H., Chevone, B.I., Pell, E.J., Zilinskas, B.A., 2000. Ambient Ozone and Plant Health. Plant Dis. 85, 4–12.

Kryza, M., Wałaszek, K., Ojrzyńska, H., Szymanowski, M., Werner, M., Dore, A.J., 2017. High-Resolution Dynamical Downscaling of ERA-Interim Using the WRF Regional Climate Model for the Area of Poland. Part 1: Model Configuration and Statistical Evaluation for the 1981–2010 Period. Pure Appl. Geophys. 174, 511–526. https://doi.org/10.1007/s00024-016-1272-5

Lacressonnière, G., Peuch, V.H., Vautard, R., Arteta, J., Déqué, M., Joly, M., Josse, B., Marécal, V., Saint-Martin, D., 2014. European air quality in the 2030s and 2050s: Impacts of global and regional emission trends and of climate change. Atmos. Environ. 92, 348–358. https://doi.org/10.1016/j.atmosenv.2014.04.033

Lefohn, A.S., Malley, C.S., Smith, L., Wells, B., Hazucha, M., Simon, H., Naik, V., Mills, G., Schultz, M.G., Paoletti, E., De Marco, A., Xu, X., Zhang, L., Wang, T., Neufeld, H.S., Musselman, R.C., Tarasick, D., Brauer, M., Feng, Z., Tang, H., Kobayashi, K., Sicard, P., Solberg, S., Gerosa, G., 2018. Tropospheric ozone assessment report: Global ozone metrics for climate change, human health, and crop/ecosystem research. Elem Sci Anth 6; 28. https://doi.org/10.1525/elementa.279

Li, P., Feng, Z., Catalayud, V., Yuan, X., Xu, Y., Paoletti, E., 2017. A meta-analysis on growth, physiological, and biochemical responses of woody species to ground-level ozone highlights the role of plant functional types. Plant. Cell Environ. 40, 2369–2380. https://doi.org/10.1111/pce.13043

Ljubeši, N., Britvec, M., 2006. Tropospheric ozone-induced structural changes in leaf mesophyll cell walls in grapevine plants. Biol. Bratislava, Sect. Bot. 61, 85–90. https://doi.org/10.2478/s11756-006-0012-1

Lopes, J., Eiras-Dias, J.E., Abreu, F., Clímaco, P., Cunha, J.P., Silvestre, J., 2008. Exigências térmicas, duração e precocidade de estados fenológicos de castas da colecção ampelográfica nacional. Cieência Tèc. Vitiv. 23, 61–71.

López, J., Troncoso, F., Granada, E., Eguía, P., 2020. Comparison between Geostatistical Interpolation and Numerical Weather Model Predictions for Meteorological Conditions Mapping. Infrastructures 5: 15.

https://doi.org/10.3390/infrastructures5020015

Lorente-Plazas, R., Montávez, J.P., Jimenez, P.A., Jerez, S., Gómez-Navarro, J.J., García-Valero, J.A., Jimenez-Guerrero, P., 2015. Characterization of surface winds over the Iberian Peninsula. Int. J. Climatol. 35, 1007–1026. https://doi.org/10.1002/joc.4034

Lorenzini, G., Triolo, E., Materazzi, A., 1984. Evidence of visible injury to crop species by ozone in Italy. Riv. di Ortoflorofruttic. Ital. 68, 81–84.

Lorenzo, M.N., Taboada, J.J., Lorenzo, J.F., Ramos, A.M., 2012. Influence of climate on grape production and wine quality in the Rías Baixas, north-western Spain. Reg. Environ. Chang. https://doi.org/10.1007/s10113-012-0387-1

Mailler, Sylvain, Menut, L., Khvorostyanov, D., Valari, M., Couvidat, F., Siour, G., Turquety, S., Briant, R., Tuccella, P., Bessagnet, B., Colette, A., Létinois, L., Meleux, F., Mailler, S, 2016. CHIMERE-2016: From urban to hemispheric chemistry-transport modeling. Geosci. Model Dev 10, 2397–2423. https://doi.org/10.5194/gmd-2016-196

Malheiro, A., Santos, J., Fraga, H., Pinto, J., 2010. Climate change scenarios applied to viticultural zoning in Europe. Clim. Res. 43, 163–177. https://doi.org/10.3354/cr00918

Marshall, F., Ashmore, M., Hinchcliffe, F., 1997. Gatekeeper Series No. 73 A hidden threat to food production: Air pollution and agriculture in the developing world. International Institute for Environment and Development. London.

Marta-Almeida, M., Teixeira, J., Carvalho, M.J., Melo-Gonçalves, P., Rocha, A.M., 2016. High resolution WRF climatic simulations for the Iberian Peninsula: Model validation. Phys. Chem. Earth 94, 94–105. https://doi.org/10.1016/j.pce.2016.03.010

Massman, W.J., 2004. Toward an ozone standard to protect vegetation based on effective dose: A review of deposition resistances and a possible metric. Atmos. Environ. 38, 2323–2337. https://doi.org/10.1016/j.atmosenv.2003.09.079

Matyssek, R., Innes, J.L., 1999. Ozone - a Risk Factor for Trees and Forests in Europe? Water. Air. Soil Pollut. 116, 199–226. https://doi.org/10.1023/A:1005267214560

Mauzerall, D.L., Wang, X., 2001. Protecting agricultural crops from the effects of tropospheric ozone exposure. Annu. Rev. Energy Env. 26, 237–268.

Mcmaster, G.S., Wilhelm, W.W., 1997. Growing degree-days: one equation, two interpretations. Agric. For. Meteorol. 87, 291–300.

Medrano, H., Escalona, J.M., Bota, J., Gulías, J., Flexas, J., 2002. Regulation of photosynthesis of C3 plants in response to progressive drought: Stomatal conductance as a reference parameter. Ann. Bot. 89, 895–905. https://doi.org/10.1093/aob/mcf079

Meleux, F., Solmon, F., Giorgi, F., 2007. Increase in summer European ozone amounts due to climate change. Atmos. Environ. 41, 7577–7587. https://doi.org/10.1016/j.atmosenv.2007.05.048

Menut, L., Bessagnet, B., Khvorostyanov, D., Beekmann, M., Blond, N., Colette, A., Coll, I.,

Curci, G., Foret, G., Hodzic, A., Mailler, S., Meleux, F., Monge, J.-L., Pison, I., Siour, G., Turquety, S., Valari, M., Vautard, R., Vivanco, M.G., 2013. CHIMERE 2013: a model for regional atmospheric composition modelling. Geosci. Model Dev. 6, 981–1028. https://doi.org/10.5194/gmd-6-981-2013

Millan, M., Mantilla, E., Salvador, R., Carratal, A.N., José Sanz, M., Alonso, L., Gangoiti, G., Navazo, M., 2000. Ozone Cycles in the Western Mediterranean Basin: Interpretation of Monitoring Data in Complex Coastal Terrain. J. Appl. Meteorol. 39, 487–508.

Mills G., Harmens H., Hayes F., Jones L., Williams P., Emberson L., Cinderby S., Terry A., Ashmore M., Holland M., G.E. and P.S., 2006. The UNECE International Cooperative Programme on Vegetation Final Report.

Mills, G., Buse, A., Gimeno, B., Bermejo, V., Holland, M., Emberson, L., Pleijel, H., 2007. A synthesis of AOT40-based response functions and critical levels of ozone for agricultural and horticultural crops. Atmos. Environ. 41, 2630–2643. https://doi.org/10.1016/j.atmosenv.2006.11.016

Mills, G., Emberson, L., 2003. Report from the working group on agricultural crops. (No. B 1523 A), Establishing Ozone Critical Levels II. Gothenburg.

Mills, G., Hayes, F., Simpson, D., Emberson, L., Norris, D., Harmens, H., Büker, P., 2011a. Evidence of widespread effects of ozone on crops and (semi-)natural vegetation in Europe (1990-2006) in relation to AOT40- and flux-based risk maps. Glob. Chang. Biol. 17, 592–613. https://doi.org/10.1111/j.1365-2486.2010.02217.x

Mills, G., Pleijel, H., Braun, S., Büker, P., Bermejo, V., Calvo, E., Danielsson, H., Emberson, L., Fernández, I.G., Grünhage, L., Harmens, H., Hayes, F., Karlsson, P.-E., Simpson, D., 2011b. New stomatal flux-based critical levels for ozone effects on vegetation. Atmos. Environ. 45, 5064–5068. https://doi.org/10.1016/j.atmosenv.2011.06.009

Mills, G., Pleijel, H., Malley, C.S., Sinha, B., Cooper, O.R., Schultz, M.G., Neufeld, H.S., Simpson, D., Sharps, K., Feng, Z., Gerosa, G., Harmens, H., Kobayashi, K., Saxena, P., Paoletti, E., Sinha, V., Xu, X., 2018. Tropospheric Ozone Assessment Report: Present-day tropospheric ozone distribution and trends relevant to vegetation. Elem Sci Anth 6: 47. https://doi.org/10.1525/elementa.273

Mira de Orduña, R., 2010. Climate change associated effects on grape and wine quality and production. Food Res. Int. 43, 1844–1855. https://doi.org/10.1016/j.foodres.2010.05.001

Miranda, A.I., Ascenso, A., Gama, C., Blanco-Ward, D., Monteiro, A., Silveira, C., Viceto, C., Rocha, A., Lopes, D., Lopes, M., Borrego, C., 2020. Ozone Risk for Douro Vineyards in Present and Future Climates, in: Mensink, C., Gong, W., Hakami, A. (Eds.), Air Pollution Modeling and Its Application XXVI. ITM 2018. Proceedings in Complexity. Springer, Cham, pp. 439–444. https://doi.org/10.1007/978-3-030-22055-6_70

Moncur, M.V., Rattigan, K., Mackenzie, D.H., Mc. Intyre, G.N., 1989. Base temperatures for budbreak and leaf appearance of grapevines. Am.J.Enol.Vitic. 40, 21–26.

Monks, P.S., Archibald, A.T., Colette, A., Cooper, O., Coyle, M., Derwent, R., Fowler, D., Granier, C., Law, K.S., Mills, G.E., Stevenson, D.S., Tarasova, O., Thouret, V., Von

Schneidemesser, E., Sommariva, R., Wild, O., Williams, M.L., 2015. Tropospheric ozone and its precursors from the urban to the global scale from air quality to short-lived climate forcer. Atmos. Chem. Phys 15, 8889–8973. https://doi.org/10.5194/acp-15-8889-2015

Monteiro, A., Strunk, A., Carvalho, A., Tchepel, O., Miranda, A.I., Borrego, C., Saavedra, S., Rodríguez, A., Souto, J., Casares, J., Friese, E., Elbern, H., 2012. Investigating a high ozone episode in a rural mountain site. Environ. Pollut. 162, 176–189. https://doi.org/10.1016/j.envpol.2011.11.008

Moriondo, M., Jones, G. V, Bois, B., Dibari, C., Ferrise, R., Trombi, G., Bindi, M., Ferrise, : R, 2013. Projected shifts of wine regions in response to climate change. Clim. Change 119, 825–839. https://doi.org/10.1007/s10584-013-0739-y

Moss, R., Babiker, M., Brinkman, S., Calvo, E., Carter, T., Edmonds, J., Elgizouli, I., Emori, S., Erda, L., Hibbard, K., Jones, R., Kainuma, M., Kelleher, J., Lamarque, J.F., Manning, M., Matthews, B., Meehl, J., Meyer, L., Mitchell, J., Nakicenovic, N., O'Neill, B., Pichs, R., Riahi, K., Rose, S., Runci, P., Stouffer, R., Vuuren, D. van, Weyant, J., Wilbanks, T., Ypersele, J.P. van, Zurek, M., 2008. Towards New Scenarios for Analysis of Emissions, Climate Change, Impacts, and Response Strategies. Intergovernmental Panel on Climate Change (IPPC). Geneva.

Moutinho-Pereira, J., Magalhâes, N., Torres-Pereira, J.M., 2001. Comportamento fisiológico e vitícola da cv . Touriga Nacional numa parcela de vinha " ao alto " na Região Demarcada Do Douro. Ciéncia Téc. Vitiv 16(2), 49-63 16, 49–63.

Moutinho-Pereira, J.M., 2000. Caracterização fisiológica e agronómica de diferentes estratégias culturais para minimizar o stress estival em Vitis vinifera L. na regiâo demarcada do Douro. PhD. dissertation. Universidade de Trás-Os-Montes e Alto Douro, Vila Real.

Moutinho-Pereira, J.M., Bacelar, E.A., Gonçalves, B., Ferreira, H.F., Coutinho, J.F., Correia, C.M., 2010. Effects of Open-Top Chambers on physiological and yield attributes of field grown grapevines. Acta Physiol. Plant. 32, 395–403. https://doi.org/10.1007/s11738-009-0417-x

Moutinho-Pereira, J.M., Correia, C.M., Gonçalves, B.M., Bacelar, E.A., Torres-Pereira, J.M., 2004. Leaf gas exchange and water relations of grapevines grown in three different conditions. Photosynthetica 42, 81–86. https://doi.org/10.1023/B:PHOT.0000040573.09614.1d

Musselman, R.C., Lefohn, A.S., Massman, W.J., Heath, R.L., 2006. A critical review and analysis of the use of exposure-and flux-based ozone indices for predicting vegetation effects. Atmos. Environ. 40, 1869–1888. https://doi.org/10.1016/j.atmosenv.2005.10.064

Nali, C., Paoletti, E., Marabottini, R., Della Rocca, G., Lorenzini, G., Paolacci, A.R., Ciaffi, M., Badiani, M., 2004. Ecophysiological and biochemical strategies of response to ozone in Mediterranean evergreen broadleaf species. Atmos. Environ. 38, 2247–2257. https://doi.org/10.1016/j.atmosenv.2003.11.043

Nussbaum, S., Remund, J., Rihm, B., Mieglitz, K., Gurtz, J., Fuhrer, J., 2003. High-resolution spatial analysis of stomatal ozone uptake in arable crops and pastures. Environ. Int. 29, 385–392. https://doi.org/10.1016/S0160-4120(02)00174-5

Ochoa-Hueso, R., Munzi, S., Alonso, R., Arróniz-Crespo, M., Avila, A., Bermejo, V., Bobbink, R., Branquinho, C., Concostrina-Zubiri, L., Cruz, C., Cruz de Carvalho, R., De Marco, A., Dias, T., Elustondo, D., Elvira, S., Estébanez, B., Fusaro, L., Gerosa, G., Izquieta-Rojano, S., Lo Cascio, M., Marzuoli, R., Matos, P., Mereu, S., Merino, J., Morillas, L., Nunes, A., Paoletti, E., Paoli, L., Pinho, P., Rogers, I.B., Santos, A., Sicard, P., Stevens, C.J., Theobald, M.R., 2017. Ecological impacts of atmospheric pollution and interactions with climate change in terrestrial ecosystems of the Mediterranean Basin: Current research and future directions. Environ. Pollut. 227, 194–206. https://doi.org/10.1016/J.ENVPOL.2017.04.062

OIV (International Organisation of Vine and Wine), 2017. Distribution of the world's grapevine varieties, Focus OIV 2017. Paris.

Oltmans, S.J., Lefohn, A.S., Shadwick, D., Harris, J.M., Scheel, H.E., Galbally, I., Tarasick, D.W., Johnson, B.J., Brunke, E.G., Claude, H., Zeng, G., Nichol, S., Schmidlin, F., Davies, J., Cuevas, E., Redondas, A., Naoe, H., Nakano, T., Kawasato, T., 2013. Recent tropospheric ozone changes - A pattern dominated by slow or no growth. Atmos. Environ. 67, 331–351. https://doi.org/10.1016/j.atmosenv.2012.10.057

Padro, J., Massman, W.J., Den Hartog, G., Neumann, H.H., 1994. Dry deposition velocity of O3 over a vineyard obtained from models and observations: The 1991 California ozone deposition experiment. Water. Air. Soil Pollut. 75, 307–323. https://doi.org/10.1007/BF00482943

Pan, L., Liu, Y., Knievel, J., Delle Monache, L., Roux, G., 2018. Evaluations of WRF Sensitivities in Surface Simulations with an Ensemble Prediction System. Atmosphere (Basel). 9, 106. https://doi.org/10.3390/atmos9030106

Pan, X., Li, X., 2011. Validation of WRF model on simulating forcing data for Heihe River Basin. Sci. Cold Arid Reg. 3, 344–357. https://doi.org/10.3724/SP.J.1226.2011.00344

Paoletti, E., 2006. Impact of ozone on Mediterranean forests: A review. Environ. Pollut. 144, 463–474. https://doi.org/10.1016/j.envpol.2005.12.051

Paoletti, E., Alivernini, A., Anav, A., Badea, O., Carrari, E., Chivulescu, S., Conte, A., Ciriani, M.L., Dalstein-Richier, L., De Marco, A., Fares, S., Fasano, G., Giovannelli, A., Lazzara, M., Leca, S., Materassi, A., Moretti, V., Pitar, D., Popa, I., Sabatini, F., Salvati, L., Sicard, P., Sorgi, T., Hoshika, Y., 2019. Toward stomatal–flux based forest protection against ozone: The MOTTLES approach. Sci. Total Environ. 691, 516–527. https://doi.org/10.1016/j.scitotenv.2019.06.525

Paoletti, E., De Marco, A., Beddows, D.C.S., Harrison, R.M., Manning, W.J., 2014. Ozone levels in European and USA cities are increasing more than at rural sites, while peak values are decreasing. Environ. Pollut. 192, 295–299. https://doi.org/10.1016/j.envpol.2014.04.040

Paoletti, E., Manning, W.J., 2007. Toward a biologically significant and usable standard for

ozone that will also protect plants. Environ. Pollut. 150, 85–95. https://doi.org/10.1016/j.envpol.2007.06.037

Paoletti, E., Materassi, A., Fasano, G., Hoshika, Y., Carriero, G., Silaghi, D., Badea, O., 2017. A new-generation 3D ozone FACE (Free Air Controlled Exposure). Sci. Total Environ. 575, 1407–1414. https://doi.org/10.1016/j.scitotenv.2016.09.217

Pederson, J.R., Massman, W.J., Mahrt, L., Delany, A., Oncley, S., Hartog, G.D., Neumann, H.H., Mickle, R.E., Shaw, R.H., Paw U, K.T., Grantz, D.A., MacPherson, J.I., Desjardins, R., Schuepp, P.H., Pearson, R., Arcado, T.E., 1995. California ozone deposition experiment: Methods, results, and opportunities. Atmos. Environ. 29, 3115–3132. https://doi.org/10.1016/1352-2310(95)00136-M

Pellegrini, E., Campanella, A., Paolocci, M., Trivellini, A., Gennai, C., Muganu, M., Nali, C., Lorenzini, G., 2015. Functional leaf traits and diurnal dynamics of photosynthetic parameters predict the behavior of grapevine varieties towards ozone. PLoS One 10. https://doi.org/10.1371/journal.pone.0135056

Perdigão, J., Salgado, R., Magarreiro, C., Soares, P.M.M., João Costa, M., Dasari, H.P., 2017. An Iberian climatology of solar radiation obtained from WRF regional climate simulations for 1950-2010 period. Atmos. Res. 151–162. https://doi.org/10.1016/j.atmosres.2017.08.016

Pfleeger, T.G., Plocher, M., Bichel, P., 2010. Response of pioneer plant communities to elevated ozone exposure. Agric. Ecosyst. Environ. 138, 116–126. https://doi.org/10.1016/j.agee.2010.04.009

Pires, J.C.M.C.M., Alvim-Ferraz, M.C.M.C.M., Martins, F.G.G., 2012. Surface ozone behaviour at rural sites in Portugal. Atmos. Res. 104, 164–171. https://doi.org/10.1016/j.atmosres.2011.10.001

Pleijel, H., 2000. Ground-level ozone a problem largely ignored in southern Europe. Swedish NGO Secretariat on Acid Rain. Göteborg.

Politi, N., Nastos, P.T., Sfetsos, A., Vlachogiannis, D., Dalezios, N.R., Gounaris, N., Cardoso, M.R., Soares, M.M.P., 2017. Comparison and Validation of WRF Model Physics Parameterizations Over the Domain of Greece, in: Perspectives on Atmospheric Sciences. Springer, Cham, pp. 55–61. https://doi.org/10.1007/978-3-319-35095-0_8

Pons, A., Allamy, L., Schüttler, A., Rauhut, D., Thibon, C., Darriet, P., Ollat, N., 2017. What is the expected impact of climate change on wine aroma compounds and their precursors in grape? J. Int. des Sci. la Vigne du Vin 51, 141–146. https://doi.org/10.20870/oeno-one.2016.0.0.1868

Ponti, L., Gutierrez, A.P., Boggia, A., Neteler, M., 2018. Analysis of grape production in the face of climate change. Climate 6, 1–15. https://doi.org/10.3390/cli6020020

Popescu, S.M., Popa, A., Gavrilescu, E., Gruia, M., 2012. The effects of air pollution on the main physiological processes of the grapevine grown in the vicinity of a power plant. Carpathian J. Earth Environ. Sci. 7, 61–70.

Rai, R., Agrawal, M., 2012. Impact of tropospheric ozone on crop plants. Proc. Natl. Acad.

Sci. India Sect. B - Biol. Sci. 82, 241–257. https://doi.org/10.1007/s40011-012-0032-2

Riahi, K., Rao, S., Krey, V., Cho, C., Chirkov, V., Fischer, G., Kindermann, G., Nakicenovic, N., Rafaj, P., 2011. RCP 8.5—A scenario of comparatively high greenhouse gas emissions. Clim. Change 109, 33–57. https://doi.org/10.1007/s10584-011-0149-y

Ribeiro, A.C., Barreales, D., Andrade, J., Rodrigues, M.A., Blanco-ward, D., Monteiro, A., Lopes, M., Borrego, C., Silveira, C., Viceto, C., Feliciano, M., Castro, J., Miranda, A., 2018. Physiological response of the grapevine cultivars Touriga Nacional and Touriga Franca to increasing summer stress conditions in the Douro, in: XIIth International Terroir Congress, Zaragoza, Spain, 18th-22nd of June 2018.

Ribeiro, J.A., 2000. Caracterização genérica da região vinhateira do Alto Douro. Douro - Estud. Doc. V (10), 11–29.

Richards, B.L., Middleton, J.T., Hewitt, W.B., 1959. Ozone Stipple of Grape Leaf. Calif. Agric. 4–11.

Richards, B.L., Taylor, O.C., 1965. Significance of Atmospheric Ozone as a Phytotoxicant. J. Air Pollut. Control Assoc. 15, 191–193. https://doi.org/10.1080/00022470.1965.10468360

Riou, C., 1994. Le determinisme climatique de la maturation du raisin : application au zonage de la teneur en sucre dans la Communaute europeenne. Institut National de la Recherche Agronomique. Bordeaux.

Roper, T.R., Williams, L.E., 1989. Effects of Ambient and Acute Partial Pressures of Ozone on Leaf Net CO2 Assimilation of Field-Grown Vitis vinifera L. Plant Physiol 91, 1501–1506.

Rydsaa, J.H., Stordal, F., Gerosa, G., Finco, A., Hodnebrog, 2016. Evaluating stomatal ozone fluxes in WRF-Chem: Comparing ozone uptake in Mediterranean ecosystems. Atmos. Environ. 143, 237–248. https://doi.org/10.1016/j.atmosenv.2016.08.057

Sacchelli, S., Carrari, E., Paoletti, E., Anav, A., Hoshika, Y., Sicard, P., Screpanti, A., Chirici, G., Cocozza, C., De Marco, A., 2021. Economic impacts of ambient ozone pollution on wood production in Italy. Sci. Rep. 11, 1–9. https://doi.org/10.1038/s41598-020-80516-6

Santillán, D., Iglesias, A., La Jeunesse, I., Garrote, L., Sotes, V., 2019. Vineyards in transition: A global assessment of the adaptation needs of grape producing regions under climate change. Sci. Total Environ. 657, 839–852. https://doi.org/10.1016/j.scitotenv.2018.12.079

Santos, J.A., Costa, R., Fraga, H., 2018. New insights into thermal growing conditions of Portuguese grapevine varieties under changing climates. Theor. Appl. Climatol. https://doi.org/10.1007/s00704-018-2443-3

Santos, J.A., Grätsch, S.D., Karremann, M.K., Jones, G. V., Pinto, J.G., 2013. Ensemble projections for wine production in the Douro Valley of Portugal. Clim. Change 117, 211–225. https://doi.org/10.1007/s10584-012-0538-x

Santos, J.A., Malheiro, A.C., Karremann, M.K., Pinto, J.G., 2011. Statistical modelling of

grapevine yield in the Port Wine region under present and future climate conditions. Int J Biometeorol 55, 119–131. https://doi.org/10.1007/s00484-010-0318-0

Schultz, H.R., Jones, G. V., 2010. Climate induced historic and future changes in viticulture. J. Wine Res. 21, 137–145. https://doi.org/10.1080/09571264.2010.530098

Seinfeld, J., Pandis, S., 1998. Atmospheric chemistry and physics: from air pollution to climate change, 1st ed. John Wiley and Sons, New York.

Sicard, P., Anav, A., De Marco, A., Paoletti, E., 2017. Projected global ground-level ozone impacts on vegetation under different emission and climate scenarios. Atmos. Chem. Phys. 17, 12177–12196. https://doi.org/10.5194/acp-17-12177-2017

Sicard, P., Augustaitis, A., Belyazid, S., Calfapietra, C., de Marco, A., Fenn, M., Bytnerowicz, A., Grulke, N., He, S., Matyssek, R., Serengil, Y., Wieser, G., Paoletti, E., 2016. Global topics and novel approaches in the study of air pollution, climate change and forest ecosystems. Environ. Pollut. 213, 977–987. https://doi.org/10.1016/J.ENVPOL.2016.01.075

Sicard, P., De Marco, A., Carrari, E., Dalstein-Richier, L., Hoshika, Y., Badea, O., Pitar, D., Fares, S., Conte, A., Popa, I., Paoletti, E., 2020. Epidemiological derivation of flux-based critical levels for visible ozone injury in European forests. J. For. Res. https://doi.org/10.1007/s11676-020-01191-x

Sicard, P., De Marco, A., Troussier, F., Renou, C., Vas, N., Paoletti, E., 2013. Decrease in surface ozone concentrations at Mediterranean remote sites and increase in the cities. Atmos. Environ. 79, 705–715. https://doi.org/10.1016/j.atmosenv.2013.07.042

Sillmann, J., Kharin, V. V., Zhang, X., Zwiers, F.W., Bronaugh, D., 2013a. Climate extremes indices in the CMIP5 multimodel ensemble: Part 1. Model evaluation in the present climate. J. Geophys. Res. Atmos. 118, 1716–1733. https://doi.org/10.1002/jgrd.50203

Sillmann, J., Kharin, V. V., Zwiers, F.W., Zhang, X., Bronaugh, D., 2013b. Climate extremes indices in the CMIP5 multimodel ensemble: Part 2. Future climate projections. J. Geophys. Res. Atmos. 118, 2473–2493. https://doi.org/10.1002/jgrd.50188

Simpson, D., Ashmore, M.R., Emberson, L., Tuovinen, J.-P., 2007. A comparison of two different approaches for mapping potential ozone damage to vegetation. A model study. Environ. Pollut. 146, 715–725. https://doi.org/10.1016/j.envpol.2006.04.013

Skamarock, W.C., Klemp, J.B., Dudhi, J., Gill, D.O., Barker, D.M., Duda, M.G., Huang, X.-Y., Wang, W., Powers, J.G., 2008. A Description of the Advanced Research WRF Version 3, National Center for Atmospheric Research (NACR) Technical Note. Boulder, Colorado. https://doi.org/10.5065/D6DZ069T

Skarby, L., Ro-Poulsen, H., Wellburn, F.A.M., Sheppard, L.J., 1998. Impacts of ozone on forests: a European perspective. New Phytol. 139, 109–122. https://doi.org/10.1046/j.1469-8137.1998.00184.x

Soares, P.M.M., Cardoso, R.M., Pedro, Miranda, M.A., De Medeiros, J., Belo-Pereira, M., Espirito-Santo, F., 2012. WRF high resolution dynamical downscaling of ERA-Interim for Portugal. Clim. Dyn. 39, 2497–2522. https://doi.org/10.1007/s00382-012-1315-2

Soja, G., Eid, M., Gangl, H., Redl, H., 1997. Ozone Sensitivity of Grapevine (Vitis vinifera L.): Evidence for a Memory Effect in a Perennial Crop Plant? Phyton (B. Aires). 37, 265–270.

Soja, G., Reichenauer, T., Eid, M., Schaber, R., Gangl, H., 2003. Long-term Ozone Exposure and Ozone Uptake of Grapevines in Open-Top Chambers, in: Karlsson, P.E., Selldén, G., Pleijel, H. (Eds.), In Establishing Ozone Critical Levels II. IVL Swedish Environmental Research Institute, Gothenburg, pp. 104–109.

Soja, G., Reichenauer, T.G., Eid, M., Soja, A.-M., Schaber, R., Gangl, H., 2004. Long-term ozone exposure and ozone uptake of grapevines in open-top chambers. Atmos. Environ. 38, 2313–2321. https://doi.org/10.1016/j.atmosenv.2003.12.038

Sousa, S.I.V.I. V, Alvim-Ferraz, M.C.M.C.M., Martins, F.G.G., 2011. Identification and origin of nocturnal ozone maxima at urban and rural areas of Northern Portugal – Influence of horizontal transport. Atmos. Environ. 45, 942–956. https://doi.org/10.1016/j.atmosenv.2010.11.008

Tai, A.P.K., Martin, M.V., Heald, C.L., 2014. Threat to future global food security from climate change and ozone air pollution. Nat. Clim. Chang. 4, 817–821. https://doi.org/10.1038/nclimate2317

Teixeira, A., Eiras-Dias, J., Castellarin, S.D., Gerós, H., 2013. Berry phenolics of grapevine under challenging environments. Int. J. Mol. Sci. 14, 18711–18739. https://doi.org/10.3390/ijms140918711

The Royal Society, 2008. Ground-level ozone in the 21st century: future trends, impacts and policy implications. Science policy report. 15/08. London.

Thompson, C.R., Kats, G., 1970. Antioxidants reduce grape yield reductions from photochemical smog. Calif. Agric. 12–13.

Tiedemann, V., Herrmann, J. V, 1992. First record of grapevine oxidant stipple in Germany and effects of field treatments with Ethylenediurea (EDU) and Benomyl on the disease. J. Plant Dis. Prot. 99, 533–541.

Tonietto, J., Carbonneau, A., 2004. A multicriteria climatic classification system for grape-growing regions worldwide. Agric. For. Meteorol. 124, 81–97. https://doi.org/10.1016/j.agrformet.2003.06.001

Tuovinen, J.-P., Ashmore, M.., Emberson, L.., Simpson, D., 2004. Testing and improving the EMEP ozone deposition module. Atmos. Environ. 38, 2373–2385. https://doi.org/10.1016/j.atmosenv.2004.01.026

Tuovinen, J.P., Simpson, D., Emberson, L., Ashmore, M., Gerosa, G., 2007. Robustness of modelled ozone exposures and doses. Environ. Pollut. 146, 578–586. https://doi.org/10.1016/j.envpol.2006.03.011

Universidad de Extremadura, 2007. Diagnóstico y vigilancia del impacto por vía

atmosférica de un complejo refinero en Extremadura, Servicio de publicaciones de la Universidad de Extremadura.

US Federal Registry, 2015. National Ambient Air Quality Standards for Ozone, 40 CFR Part 50, 51, 52, 53 and 58.

Valletta, A., Salvatori, E., Rita Santamaria, A., Nicoletti, M., Toniolo, C., Caboni, E., Bernardini, A., Pasqua, G., Manes, F., 2016. Ecophysiological and phytochemical response to ozone of wine grape cultivars of Vitis vinifera L. Nat. Prod. Res. 30, 2514–2522. https://doi.org/10.1080/14786419.2015.1118631

van der Linden, P., Mitchell, J.F.B., 2009. ENSEMBLES: Climate Change and its Impacts: Summary of research and results from the ENSEMBLES project. Met Office Hadley Centre. Exeter.

van Dingenen, R., Dentener, F.J., Raes, F., Krol, M.C., Emberson, L., Cofala, J., 2009. The global impact of ozone on agricultural crop yields under current and future air quality legislation. Atmos. Environ. 43, 604–618. https://doi.org/10.1016/j.atmosenv.2008.10.033

van Leeuwen, C., Darriet, P., 2016. The Impact of Climate Change on Viticulture and Wine Quality. J. Wine Econ. 11, 150–167. https://doi.org/10.1017/jwe.2015.21

van Leeuwen, C., Schultz, H.R., Garcia de Cortazar-Atauri, I., Duchene, E., Ollat, N., Pieri, P., Bois, B., Goutouly, J.-P., Quenol, H., Touzard, J.-M., Malheiro, A.C., Bavaresco, L., Delrot, S., 2013. Why climate change will not dramatically decrease viticultural suitability in main wine-producing areas by 2050. Proc. Natl. Acad. Sci. 110, E3051–E3052. https://doi.org/10.1073/pnas.1307927110

Viceto, C., Marta-Almeida, M., Rocha, A., 2017. Future climate change of stability indices for the Iberian Peninsula. Int. J. Climatol. https://doi.org/10.1002/joc.5094

Volk, M., Bungener, P., Contat, F., Montani, M., Fuhrer, J., 2006. Grassland yield declined by a quarter in 5 years of free-air ozone fumigation. Glob. Chang. Biol. 12, 74–83. https://doi.org/10.1111/j.1365-2486.2005.01083.x

Wang, H., Xing, H., Wang, Y.-F., Zhai, H., Mei-Ling, T., Du, Y.-P., 2020. Ozone risk assessment of grapevine 'Cabernet Sauvignon' using open-top chambers. Sci. Hortic. (Amsterdam). 260, 108874. https://doi.org/10.1016/J.SCIENTA.2019.108874

Watanabe, T., Izumi, T., Matsuyama, H., 2016. Accumulated phytotoxic ozone dose estimation for deciduous forest in Kanto, Japan in summer. Atmos. Environ. 129, 176–185. https://doi.org/10.1016/j.atmosenv.2016.01.016

Weinstein, L., 1984. Effects of air pollution on grapevines. Vitis 23, 274–303.

Williams, L.E., Araujo, F.J., 2002. Correlations among predawn leaf, midday leaf, and midday stem water potential and their correlations with other measures of soil and plant water status in Vitis vinifera. J. Am. Soc. Hortic. Sci. 127, 448–454. https://doi.org/10.21273/jashs.127.3.448

Willmott, C.J., Robeson, S.M., Matsuura, K., 2012. A refined index of model performance. Int. J. Climatol. 32, 2088–2094. https://doi.org/10.1002/joc.2419

Winkler, A., Cook, J., Kliiewer, W., Lider, L., 1974. General viticulture, 4th ed. University of California Press, Berkeley.

Xing, H., Hao, G., Bian, F., Chen, Z., Hui, W., Zhai, H., Yongjiang, S., Du, Y., 2018. The Response of Light System Activity in Grapevine Leaves During Ozone Stress and Recovery Periods. Acta Hortic. Sin. 45, 2321–2330. https://doi.org/10.16420/J.ISSN.0513-353X.2018-0220

Zapata, D., Salazar-Gutierrez, M., Bernardo, C., Keller, M., Hoogenboom, G., 2017. Predicting Key Phenological Stages for 17 Grapevine Cultivars (Vitis vinefera L.). Am. J. Enol. Vitic. 68, 60–72.

Zhang, H., Pu, Z., Zhang, X., 2013. Examination of Errors in Near-Surface Temperature and Wind from WRF Numerical Simulations in Regions of Complex Terrain. Weather Forecast. 28, 893–914. https://doi.org/10.1175/WAF-D-12-00109.1

Zittis, G., Hadjinicolaou, P., Lelieveld, J., 2014. Comparison of WRF Model Physics Parameterizations over the MENA-CORDEX Domain. Am. J. Clim. Chang. 03, 490–511. https://doi.org/10.4236/ajcc.2014.35042

APPENDICES.

A. SUPPLEMENTARY MATERIAL OF CHAPTER 2.

Table A-1. Classes of viticultural climate for the grapevine mean growing-season temperature, the Winkler index, the Huglin index, the cool night index and the dryness index.

Variable	Classes	Class limits
Mean growing season temperature (*GST*) April-October Jones (2013)	Too cold	≤ 13 °C
	Cold	13 – 15 °C
	Intermediate	15 – 17 °C
	Temperate	17 – 19 °C
	Warm	19 – 21 °C
	Very warm	21 - 24 °C
	Too warm	> 24 °C
Winkler index (*WI*) April-October as refined and used by Anderson et al. (2012) and Jones et al. (2010) based on Winkler et al. (1974)	Too Cool	< 850 GDD
	Region Ia	850 – 1111 GDD
	Region Ib	1111 - 1389 GDD
	Region II	1389 - 1667 GDD
	Region III	1667 - 1944 GDD
	Region IV	1944 - 2222 GDD
	Region V	2222 - 2700 GDD
	Too warm	> 2700 GDD
Huglin or Heliothermal index (*HI*) April - September Tonietto and Carbonneau (2004)	Very cool (HI-3)	<= 1500
	Cool (HI-2)	1500 - 1800
	Temperate (HI-1)	1800 - 2100
	Temperate warm (HI+1)	2100 - 2400
	Warm (HI+2)	2400 - 3000
	Very warm (HI+3)	> 3000
Dryness index (*DI*) April - September Tonietto and Carbonneau (2004)	Very dry (DI+2)	<= -100 mm
	Moderately dry (DI+1)	-100 - 50 mm
	Sub-humid (DI-1)	50 – 150 mm
	Humid (DI-2)	> 150 mm
Cool night index (*CI*) April - September Tonietto and Carbonneau (2004)	Very cool nights (CI+2)	<= 12 °C
	Cool nights (CI+1)	12 - 14 °C
	Temperate nights (CI-1)	14 - 18 °C
	Warm nights (CI-2)	> 18 °C

Table A-2. List of abbreviations used in this work.

b subscript: budburst to flowering phenological stage.
CDD: maximum number of continuous dry days (P < 1 mm) per year.
CI: cool night index (°C).
CSDI: cool spell duration index or total number of days being part of cool spells longer than 6 consecutive days in duration. A day is considered to belong to a cold spell if *Tmin* is less than the calendar-day *Tmin* 10th percentile centred on a 5-day window for the base period studied.
CSDI-3d: cold spell index accounting for the total number of days per year with at least 3 continuous days with *Tmin* < 0 °C.
CSDI-6d: cold spell index accounting for the total number of days per year with at least 6 continuous days with *Tmin* < 0 °C.
CWD: maximum number of continuous wet days (*P* ≥ 1 mm) per year.
DDR: Douro Demarcated Region.
DI: dryness index (mm).
DTR: daily temperature range or annual mean difference between *Tmax* and *Tmin* (°C).
ERA-Interim: European Reanalysis-Interim forcing.
f subscript: flowering to *véraison* phenological stage.
FD0: the number of frost days per year where *Tmin* < 0 °C.
GDD: growing degree days (°C units).
GSP: growing-season total precipitation (mm).
GST: growing-season mean temperature (°C).
HI: Huglin index (unitless).
MCC: multicriteria climatic classification.
MPI-EMS-LR: Max Plank Institute Earth System low-resolution model forcing.
P: daily total precipitation (mm).
R10: number of days with heavy precipitation per year (*P* > 10 mm).
R20: number of days with very heavy precipitation per year (*P* > 20 mm).
SU25: number of summer days per year.
SU35: number of very hot days per year.
SU35-f: yearly *SU35* from flowering to *véraison* (days).
Tave: daily mean temperature as (*Tmax* + *Tmin*)/2 (°C).
Tmax: daily maximum temperature (°C).
Tmax Apr-May: mean of daily maximum temperatures from April to May (°C).
Tmax-f: mean of daily maximum temperatures from the flowering to *véraison* phenological stage (°C).
Tmin: daily minimum temperature (°C).
TR20: the number of tropical nights per year where *Tmin* > 20 °C.
v subscript: *véraison* to maturity phenological stage.
WI: Winkler index (GDD or growing degree days, °C units).

WRF: Weather and Research Forecasting model.
WSDI: warm spell index accounting for the total number of days being part of warm spells longer than 6 consecutive days in duration. A day is considered to belong to a warm spell if *Tmax* is greater than the calendar-day *Tmax* 90th percentile centred on a 5-day window for the base period studied.
WSDI-3d: warm spell index accounting for the total number of days per year with at least 3 continuous days with *Tmax* > 35 °C.
WSDI-6d: warm spell index accounting for the total number of days per year with at least 6 continuous days with *Tmax* > 35 °C.

Table A-3. Sources of vintage ratings for Port vintages.

Source	Acronym	Rating
Berry Bros & Rudd	BBR	1–10
Decanter	DC	1–5
Michael Broadbent	MB	0–5
Sotheby's Wine Encyclopaedia	SWE	0–100
Vintages	VT	0–10
Wine Advocate	WA	50–100
Wine Enthusiast	WE	50–100
Wine Spectator	WS	50–100
Instituto dos Vinhos do Douro e do Porto	IVDP	0–1

Vintage rating charts along with their acronyms and rating intervals. The higher the value of the rating, the better the quality of the specific vintage wine quality evaluated.

Table A-4. Original vintage scores for the 1986-2005 recent-past climate scenario.

	Vintage chart								
Vintage	BBR	DC	IVDP	MB	SWE	VT	WA	WE	WS
86			0					84	
87		3	1	3		8		85	88
88			0					83	
89			1	3				86	
90			0	3				85	
91	7	4	1	4	95	9	90	92	93
92	8	4	1	4	85	9	95	93	94
93			0						
94	9	5	1	4	95	10	92	96	99
95		1	0	3	88	9		91	92
96		2	0	3				85	
97	8	4	1	4	90	10	89	93	96
98	6	3	0	3	80			87	
99			0	3	75			86	
00	9	5	1	5	95	10	92	90	97
01		4	0	3	86	8		84	
02		2	0	3	70			84	
03	8	4	1	5	94	10	90	96	98
04		4	0	4	88	9		90	
05		5	0	5	80	8		91	

Source: Corte-Real et al. (2016).

Table A-5. Simulated years ordered to greater GST (˚C).

ERA-hist		MPI-hist		MPI-med		MPI-long	
1987	17.9173	**2000**	**17.3588**	**2049**	**19.2282**	2098	21.6467
1990	17.5283	2004	16.5871	2059	19.1899	**2097**	**21.4504**
2003	17.4042	2002	16.4841	2064	19.1270	2094	21.3265
1995	17.3476	1995	16.3585	2063	18.9828	2092	21.2289
2005	17.2309	1991	16.3525	2065	18.8678	2085	20.9843
1989	17.2534	1999	16.2426	2061	18.6705	2096	20.8667
1997	17.1556	1986	16.1949	2056	18.4121	2100	20.7140
1991	16.9594	1987	16.1727	2058	18.2730	2088	20.6201
1999	16.8471	2005	15.9104	2060	18.2130	2091	19.9178
2004	16.7073	1997	15.5396	2048	18.1918	2086	19.8982
1998	16.6938	1988	15.1940	2053	18.1073	2093	19.7387
1992	16.5305	1998	15.1886	2055	18.0965	2090	19.7270
2001	16.3799	2003	15.0170	2057	17.9884	2089	19.7069
1996	16.2069	1989	14.9735	2047	17.4543	2081	19.7497
2000	16.1376	1990	14.9541	2054	17.4189	2082	19.7160
2002	15.9784	2001	14.9061	2051	17.2460	2087	19.4782
1993	15.8506	1993	14.8413	2062	17.1187	2084	19.4377
1988	15.7892	1992	14.8234	2046	16.7172	2095	19.3590
1986	15.7571	1996	14.5915	2050	16.3491	2099	19.0744
1994	15.7082	1994	13.9901	2052	16.1175	2083	18.0506
$\bar{x}$	16.6692		15.5840		17.9885		20.1346

B. SUPPLEMENTARY MATERIAL OF CHAPTER 4.

This supplement focuses on results related with temperature, global solar radiation, relative humidity, and wind as principal meteorological drivers related to plant O_3 exposure and phytotoxic O_3 dose.

a. Temperature

Figure B-1 depicts temperature maps based on simulated data, as well as validation results from the comparison between measured and modelled values.

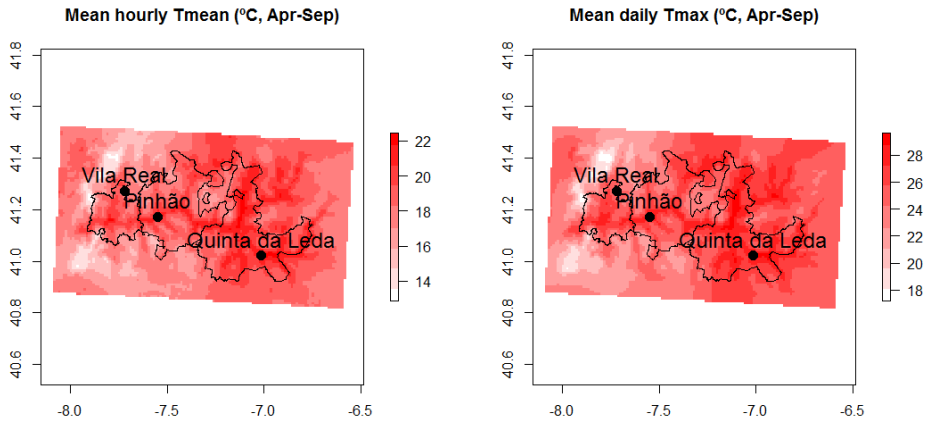

a)

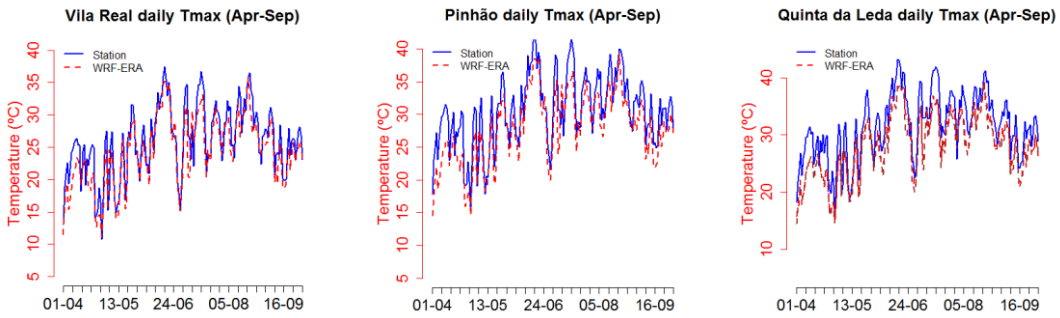

b)

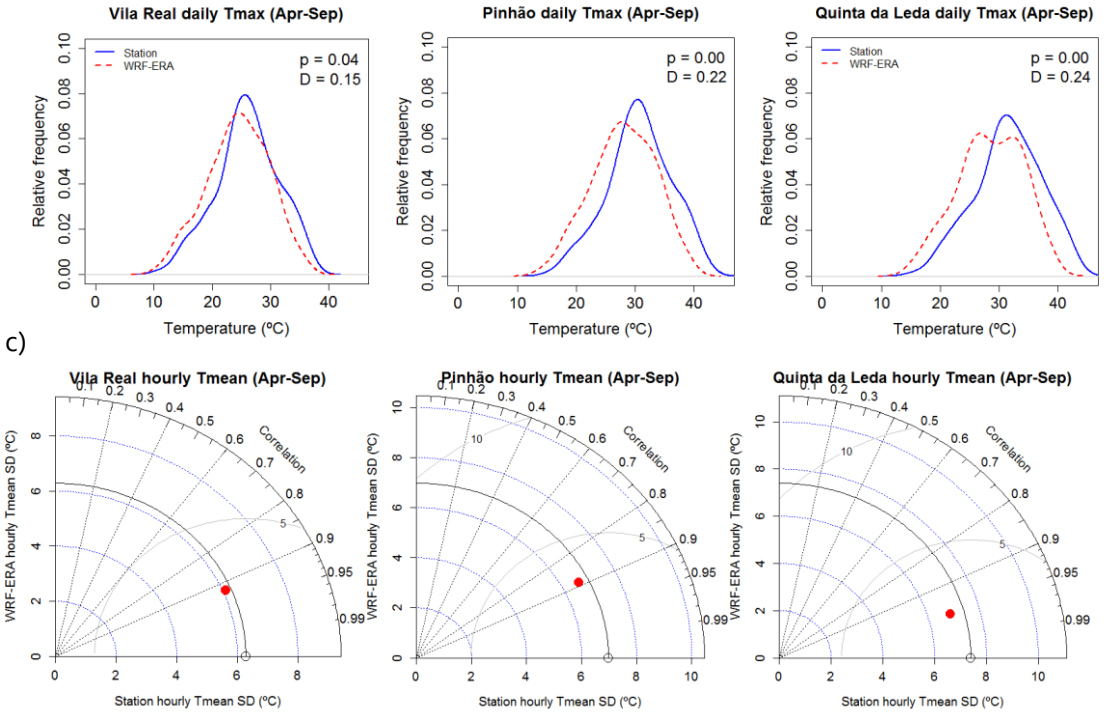

Figure B-1. a) Maps, b) time series, c) density plots and d) Taylor diagrams for temperature.

An initial inspection of the modelled April to September (Apr-Sep) temperature maps in Figure B-1a confirms the expected pattern for the DDR, with warmer values associated with lower altitudes and greater distance from the sea both for hourly mean temperature and mean daily maximum temperature. The WRF simulations were successful in replicating the temporal evolution of daily *Tmax* (Figure B-1b). The standard deviation (SD) ratios indicate an increase from the most northwestern location (Vila Real) to the most southeastern one (Quinta da Leda), with a similar spread of the observed and modelled data, as observed in the density plots (Figure B-1c). However, the KS tests indicate that the shape of the distributions was not the same for the Pinhão and Quinta da Leda locations at the 99% confidence level and that the same happened for Vila Real at the 95% confidence level.

b. Global solar radiation

Figure B-2a shows the pattern of mean hourly *Rad* and mean daily *Radmax* as derived from the WRF April-September 2017 simulations. There are areas where both elevation and slope orientation play a role in the global solar radiation regime with lower elevations at the bottom of the valleys and northern slope orientations receiving less radiation. The further west areas receive much less solar global radiation, which can be related to the Marão and Montemuro mountain ranges.

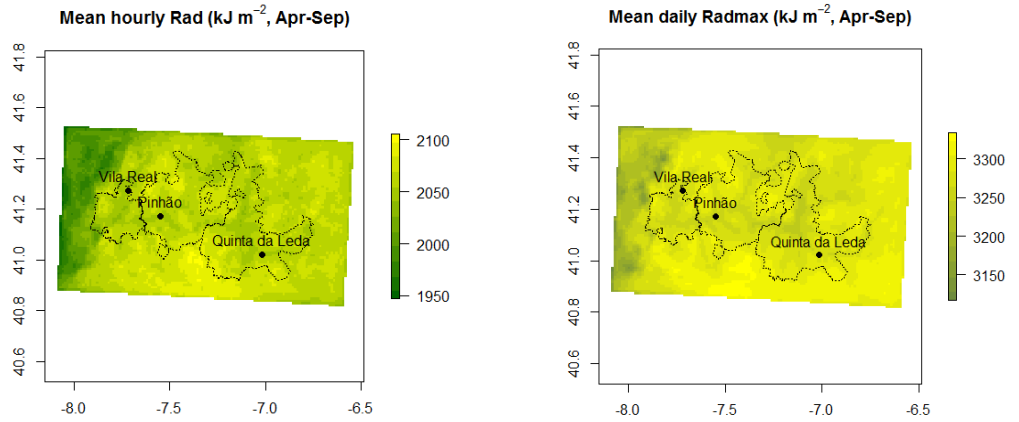
Mean hourly Rad (kJ m^{-2}, Apr-Sep)
Mean daily Radmax (kJ m^{-2}, Apr-Sep)
Vila Real
Pinhão
Quinta da Leda
WRF-ERA
WRF-ERA

a)

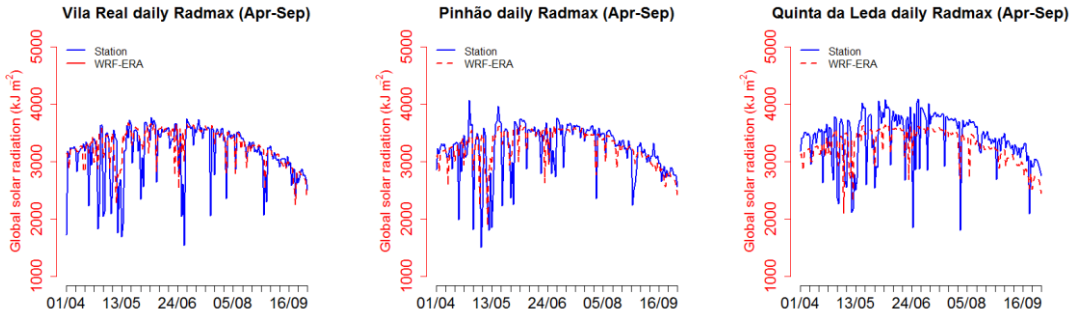
Vila Real daily Radmax (Apr-Sep)
Pinhão daily Radmax (Apr-Sep)
Quinta da Leda daily Radmax (Apr-Sep)
Station
WRF-ERA
Global solar radiation (kJ m^{-2})
01/04
13/05
24/06
05/08
16/09

b)

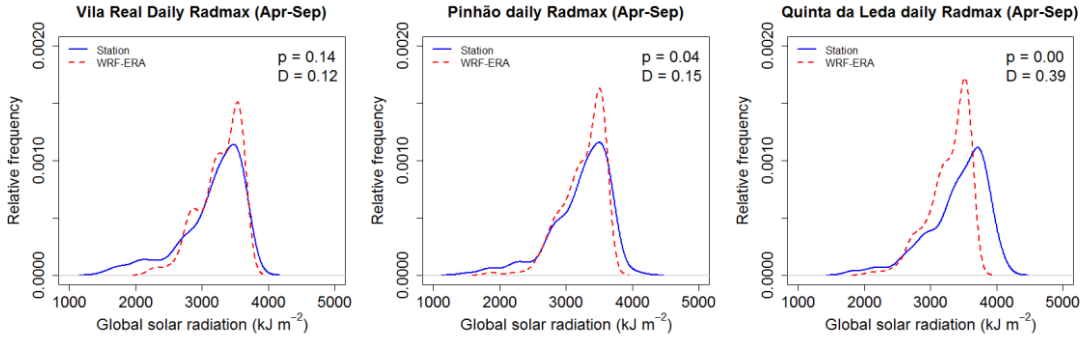
Vila Real Daily Radmax (Apr-Sep)
Pinhão daily Radmax (Apr-Sep)
Quinta da Leda daily Radmax (Apr-Sep)
Station
WRF-ERA
p = 0.14
D = 0.12
p = 0.04
D = 0.15
p = 0.00
D = 0.39
Relative frequency
Global solar radiation (kJ m^{-2})

c)

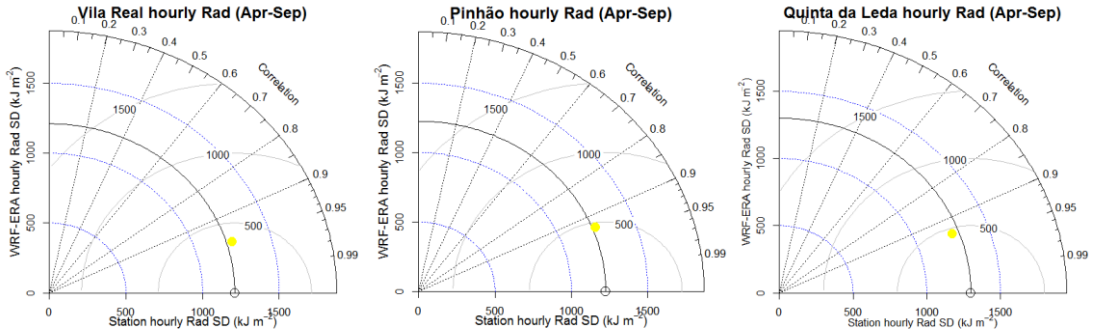

d)

Figure B-2. a) Maps, b) time series, c) density plots and d) Taylor diagrams for global solar radiation.

There was a better match between measured and modelled daily *Radmax* for Vila Real and Pinhão than for Quinta da Leda. Quinta da Leda was also distinctive for displaying a clear negative bias which was clearly observable in the respective time series plot (Figure B-2b). It can also be noted that the measured *Radmax* displayed the same NW-SE increasing trend as observed for daily *Tmax*, and hourly *Tmean*. Modelled *Radmax* data probability distributions also showed a better match for Vila Real and Pinhão than for Quinta da Leda (Figure B-2c).

c. Relative humidity

Figure B-3a presents the spatial pattern of the modelled mean hourly *RH* and mean daily *RHmin*. The mapped values of relative humidity estimated by WRF decreased towards the east and with lower elevations in the DDR. As expected, mean hourly *RH* and daily *RHmin* values followed an inverse pattern to what was found for hourly *Tmean* and daily *Tmax*, with similar values in Quinta da Leda and Pinhão, at the southeastern corner and central part of the DDR, and higher values for Vila Real in its northwestern side (Figure B-3b). A better performance of the simulations was found for the Vila Real location, where the equality of the distribution between observed and modelled data hypothesis was accepted by the KS test (Figure B-3c).

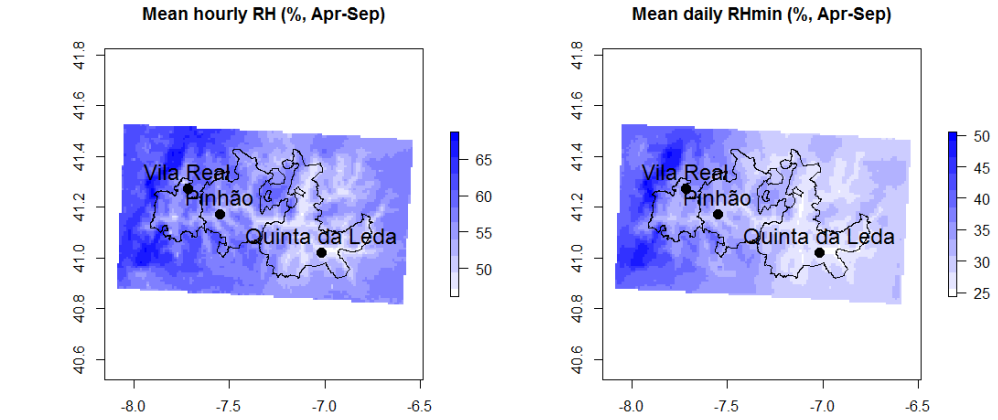
Mean hourly RH (%, Apr-Sep)
Mean daily RHmin (%, Apr-Sep)
Vila Real
Pinhão
Quinta da Leda
WRF-ERA
WRF-ERA

a)

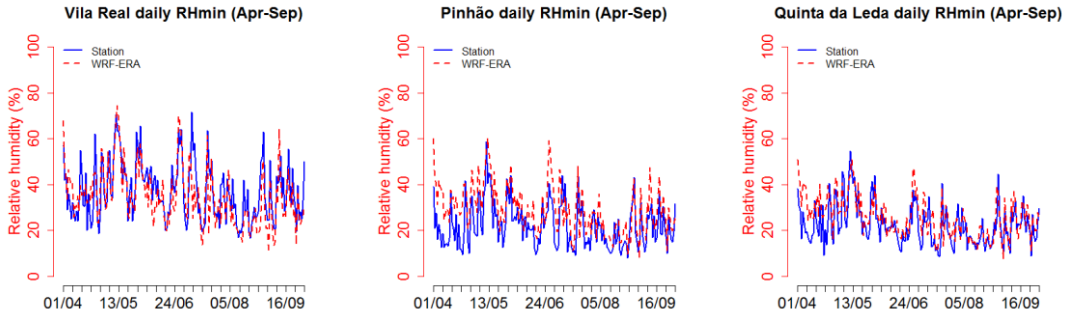
Vila Real daily RHmin (Apr-Sep)
Pinhão daily RHmin (Apr-Sep)
Quinta da Leda daily RHmin (Apr-Sep)
Station
WRF-ERA
Relative humidity (%)
01/04
13/05
24/06
05/08
16/09

b) c)

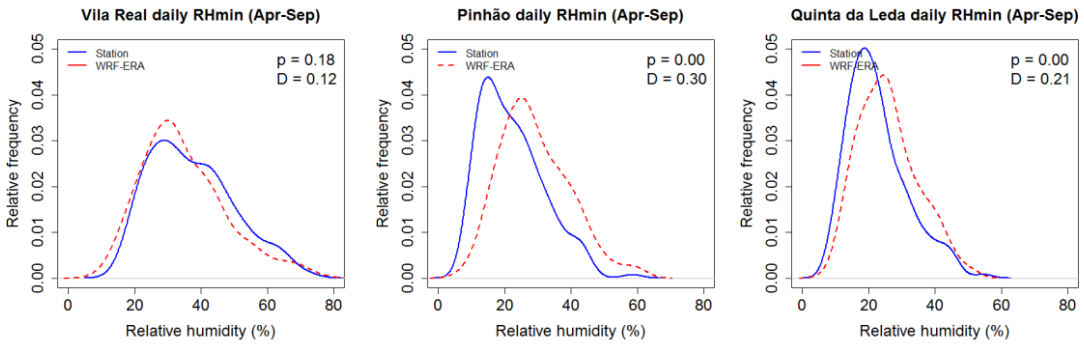
Vila Real daily RHmin (Apr-Sep)
Pinhão daily RHmin (Apr-Sep)
Quinta da Leda daily RHmin (Apr-Sep)
Station
WRF-ERA
p = 0.18
D = 0.12
p = 0.00
D = 0.30
p = 0.00
D = 0.21
Relative frequency
Relative humidity (%)

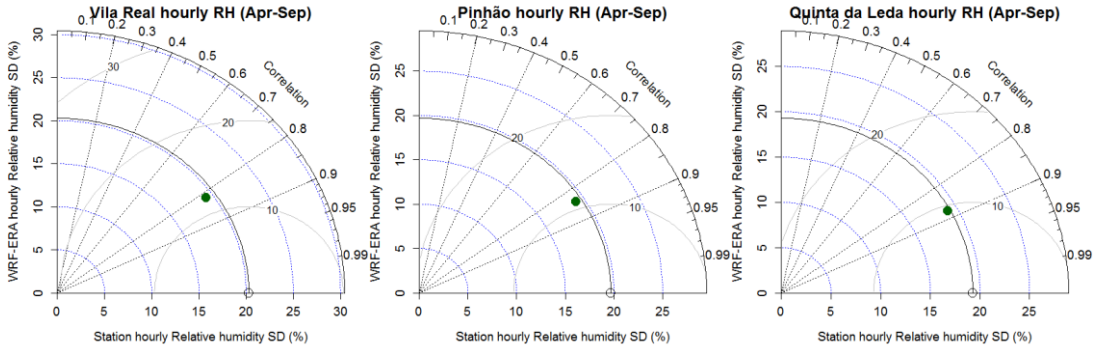

d)

Figure B-3. a) Maps, b) time series, c) density plots and d) Taylor diagrams for relative humidity.

d. Wind speed and direction.

The mean 2017 Apr-Sep hourly *Ws* and predominant daily *Wd* maps for the DDR derived from the WRF simulations can be found in Figure B-4a. According to these simulations, higher *Ws* in the study area was associated with higher elevation, and predominant *Wd* corresponded to winds coming from the NW with some minor occurrence from winds coming from the NE.

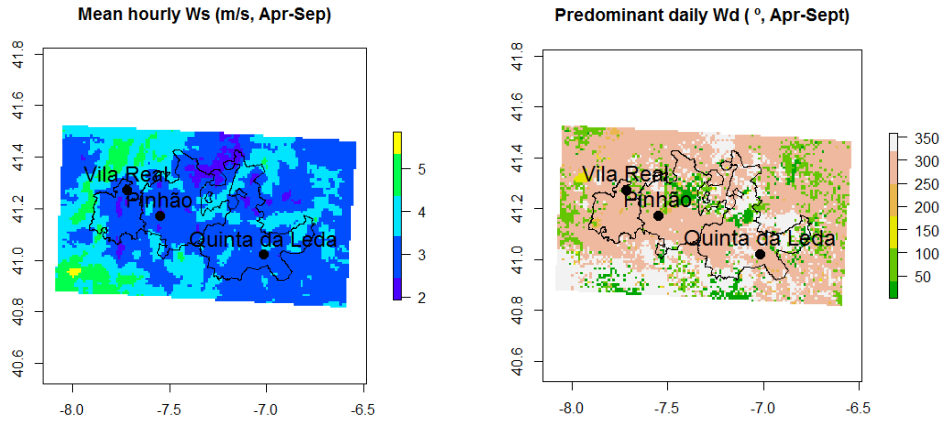

a)

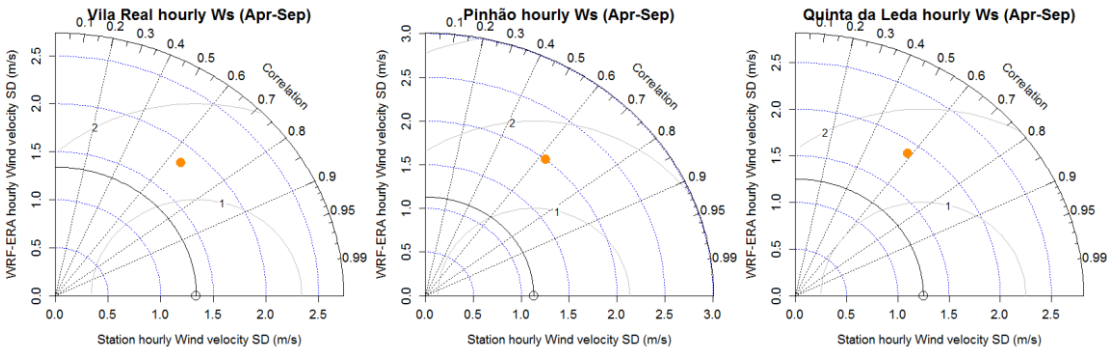

b)

c)

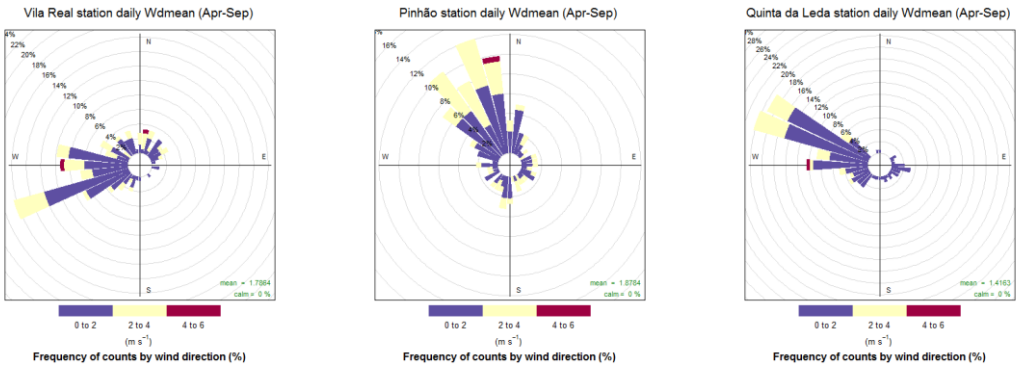

d)

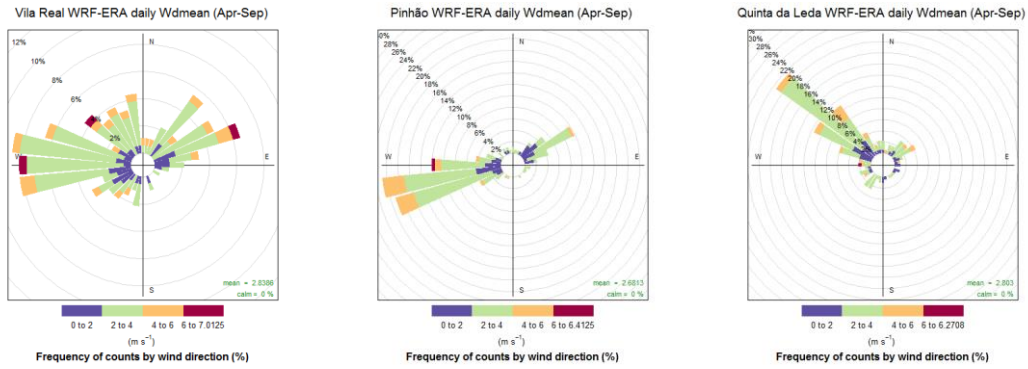

Figure B-4. a) Maps of mean hourly Ws and predominant daily Wd, b) hourly Ws Taylor diagrams, c) field-based daily Wdmean wind roses, and d) simulation-based Wdmean wind roses.

Overall, the Taylor diagrams for hourly *Ws* were similar for the three locations (Figure B-4b). The observed daily mean Apr-Sep wind direction (*Wdmean*) indicated NW-W winds at the three locations (Vila Real 284°, Pinhão 336° and Quinta da Leda 279°) (Figure B-4c). A great divergence in the simulated *Wd*mean rose diagrams (Figure B-4d) was observed at Pinhão indicating a lower physical meaning for simulated *Wdmean* for this location.

C. SUPPLEMENTARY MATERIAL OF CHAPTER 5.

a. Methodology

- ***Field campaign***

Table C-1. Field phenological dates.

Phenological stage	Quinta A (Baixo Corgo)	Quinta B (Cima Corgo)	Quinta C (Douro Superior)
Budburst/early leaf dev. 22-3 (Quintas A and B) 29-3 (Quinta C)	TF: 6 (14D, 15I) TN: 6 (12D, 13I)	TF: 2 (12D, 13I), 1 (11D, 12I) TN: 2 (9D, 11I) 1 (11D, 12I)	TF: 2 (9D, 9I), 2(11D, 9I), 1(11D,1I), 1(11D,12I) TN: 3(7D,9I) 1 (9D,9I) 2 (9D,12I)
Flowering (3-5)	TF: 2 (61D, 62I), 2 (61D, 63I), 1 (62D, 64I), 1 (63D, 64I) TN: 4 (61D, 63I), 2 (60D, 61I)	TF: 1 (60D, 61I), 2 (62D, 63I) TN: 3 (62D, 61I)	TF: 4 (57D, 60I) 1 (60D, 60I) 1 (61D, 63I) TN: 2 (57D, 60I), 1 (60D, 61I), 2 (55D,60I) 1 (57D, 61D)
Grape colour onset (5-7)	TF-TN: 6 (81D, 83I)	TF-TN: 3 (81D, 83I)	TF-TN: 6 (81D, 83I)
Maturity (23-8)	TF-TN: 6 (89D, 89I)	TF-TN: 3 (89D, 89I)	TF-TN: 6 (89D, 89I)
Early senescence (13-9)	TF-TN: 6 (91 D, 91I)	TF-TN: 3 (91 D, 91I)	TF-TN: 6 (91 D, 91I)
Leaf discolouration/fall (27-9)	TF: 6 (93D, 93I) TN: 6 (92D, 93I)	TF-TN: 3 (93 D, 93I)	TF-TN: 6 (93 D, 93I)

The phenological summary for each of the cultivars is expressed as the number of plants that have reached a given BBCH phenological stage for Touriga Franca (TF) and Touriga Nacional (TN) Portuguese grapevine cultivars. BBCH code 7 stands for beginning of budburst, 9 green shoot tips clearly visible, 11-15 one to five leaves unfolded and spread away from shoot, 55 inflorescences swelling, 57 inflorescences fully developed, 60 first flower hoods detached from the receptacle, 61-63 10% to 30% of flower hoods fallen, 81 beginning of ripening, 83 berries developing colour, 89 berries ripe for harvest, 91 end of wood maturation, 92 beginning of leaf discolouration, and 93 beginning of leaf-fall. For this specific monitoring, letters D and I are used to indicate a dominant or incipient stage manifestation. For instance, 3 (7D, 9I) corresponds with 3 grapevine plants reaching the beginning of bud burst (BBCH code 7) as a dominant stage which also start to manifest the green shoot tips clearly visible stage (BBCH code 9)

b. Results

This supplement focuses on results related with reference potential evapotranspiration (ET_0), the specific parameters and functions used for the DO3SE CLRTAP and Touriga Nacional (TN) parametrizations, and the respective evolution of the stomatal control factors for Quinta A (Baixo Corgo DDR subregion) and Quinta B (Cima Corgo DDR subregion).

- ***Reference Potential Evapotranspiration***

Penman-Monteith reference potential evapotranspiration (ET_0) (Allen et al., 1998) was estimated from field meteorological observations and WRF simulations at the daily scale for Vila Real (Baixo Corgo), Pinhão (Cima Corgo) and Quinta C (Douro Superior) from April to September 2017. Figure 5-12S illustrates the time series plots, the probability distributions along a statistical, the Kolmogorov-Smirnov (KS) test, and the scatter plots for the estimated ET_0 based on the field meteorological observations and the WRF-simulations for the three sites. The time series of the field and WRF-based ET_0 values follow similar temporal series, the KS test indicates equal distributions at the 95% confidence level for Pinhão and Quinta C and at the 99% confidence level for Vila Real, and the scatter plots indicates a strong linear relationship between the field meteorological-based estimations and the WRF-simulation-based ones for all cases. In table C-2, evaluation metrics, such as the bias (BIAS), the mean absolute error (MAE), the mean absolute percent error (MAPE), the root mean square error (RMSE), the Pearson's correlation coefficient (CORR), and the ratio of the standard deviation between modelled and observed variables (SD Ratio) also indicate strong correlation, small differences and similar data spread between daily ET_0 estimated from meteorological observations and ET_0 estimated from WRF simulations. The WRF-based ET_0 values have a small positive bias with respect to the meteorological station-based ET_0 values.

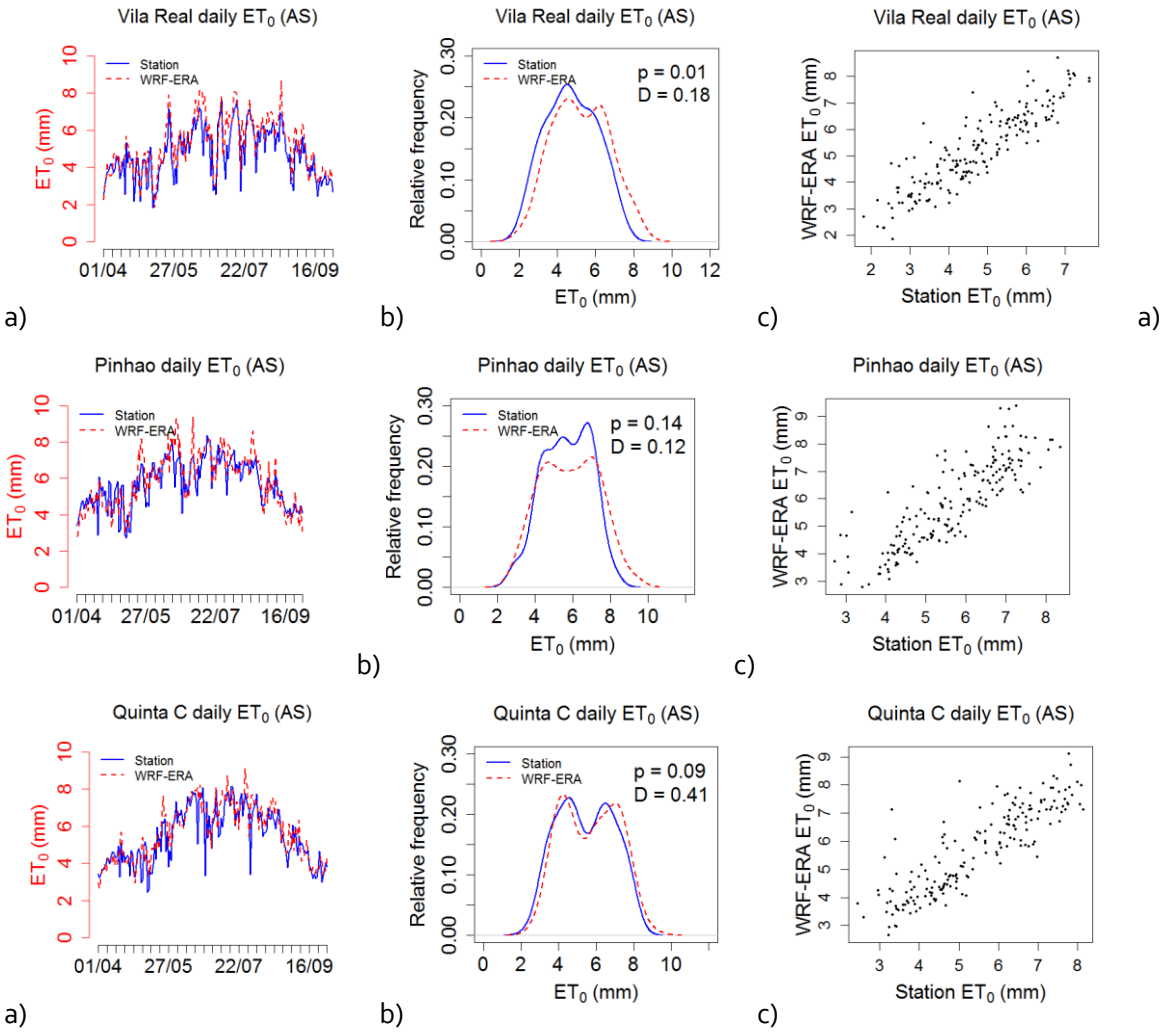

Figure C-1. Time series, b) density plots and d) scatter plots for ET_0.

Table C-2. Validation statistics for daily *ET_0* (April-September 2017 period).

Daily simulations	Field mean	CORR	BIAS	RMSE	MAE	MAPE (%)	SD Ratio
Vila Real ET_0 (mm)	4.78	0.89	0.48	0.81	0.62	14.5%	1.08
Pinhao ET_0 (mm)	5.70	0.85	0.16	0.82	0.63	11.9%	1.20
Quinta C ET_0 (mm)	5.44	0.86	0.22	0.80	0.58	11.9%	1.02

- ***CLRTAP and Touriga Nacional DO3SE parameters and functions***

Figures C-2 and C-3show the evolution of stomatal conductance (gs_{H2O}) and its controlling factors at Quinta A (Baixo Corgo) and Quinta B (Cima Corgo). As it was already illustrated for Quinta C (Douro Superior) in the main manuscript, temperature exerts the main control during the day early in July whereas the vpd factor does so in August in the DO3SE CLRAP parametrization. The DO3SE TN parametrization show a similar hourly pattern for both the

temperature and the vapour pressure factor but the leaf water potential factor, which is not included in the DO3SE CLRTAP parametrization, exerts a much greater limit to stomatal conductance, which increases through the summer. A stronger control on stomatal conductance from the leaf water potential factor is also observed at the eastern, drier sites.

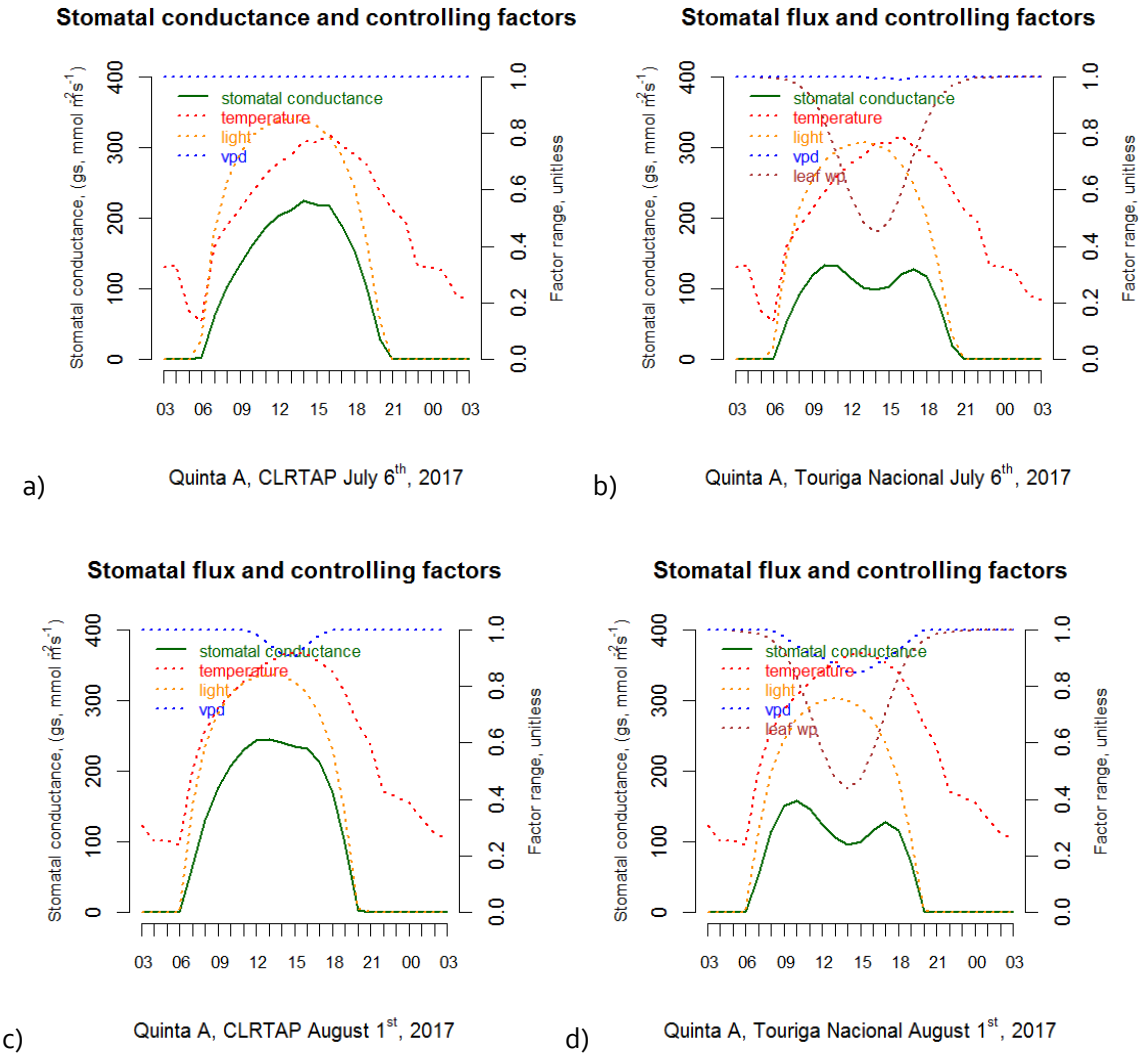

Figure C-2. Evolution of stomatal conductance and environmental control factors on July 6th and August 1st 2017 at Quinta da A (Baixo Corgo subregion).

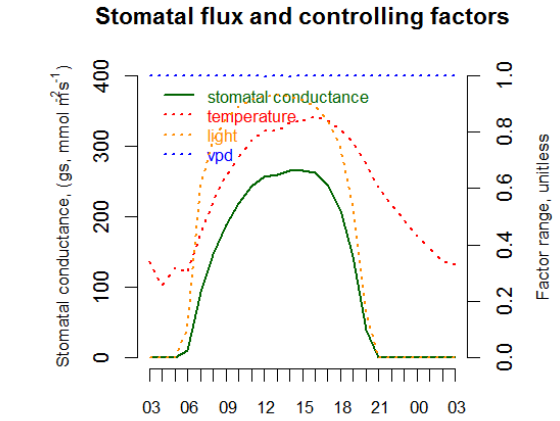

a) Quinta B, CLRTAP July 6th, 2017

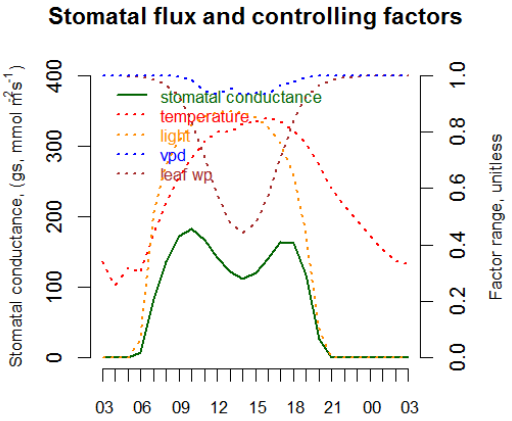

b) Quinta B, Touriga Nacional July 6th, 2017

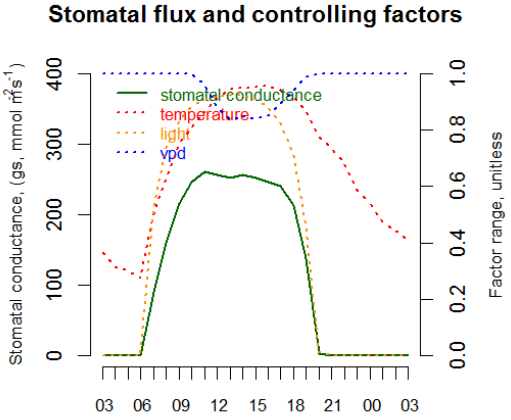

c) Quinta B, CLRTAP August 1st, 2017

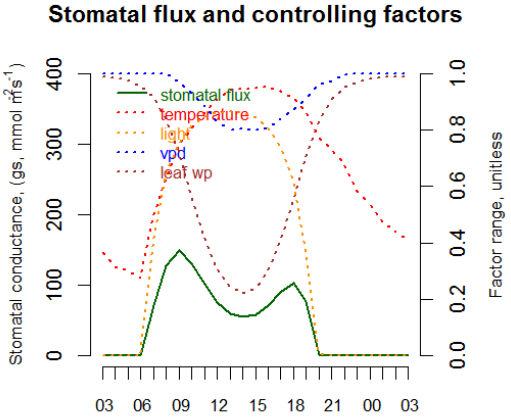

d) Quinta B, Touriga Nacional August 1st, 2017

Figure C-3. Evolution of stomatal conductance and environmental control factors on July 6th and August 1st 2017 at Quinta B (Cima Corgo subregion).